
Separations and Reactions in Organic Supramolecular Chemistry

Editorial Board

Founding Editor

J.-M. Lehn, Collège de France, Chimie des Interactions Moléculaires, 11 Place Marcelin Berthelot, 75005 Paris, France

Editors

C.J. Burrows, Office 3152 HEB, Department of Chemistry, University of Utah, 315 S. 1400 East, RM Dock, Salt Lake City, UT 84112, Utah, USA

G.R. Desiraju, University of Hyderabad, School of Chemistry, Hyderabad 500046, India

A.D. Hamilton, Yale University, Department of Chemistry, New Haven, CT 06520, USA

D. Hilvert, Laboratorium für Organische Chemie, ETH Zentrum, Universitätsstrasse 16, 8092 Zürich, Switzerland

D.N. Reinhoudt, University of Twente, Faculty of Chemical Technology, P.O. Box 217, NL-7500 AE Enschede, The Netherlands

J.-P. Sauvage, Université Louis Pasteur, Institut le Bel, 4 Rue Blaise Pascal, F-67070 Strasbourg, France

Former Editors

J.-P. Behr, Faculté de Pharmacie. Université Louis Pasteur, Strasbourg, B.P. 24, F-67401 Illkirch, France

T. Kunitake, Kyushu University, Faculty of Engineering. Hakozaki, Fukuoka 812, Japan

Separations and Reactions in Organic Supramolecular Chemistry

*Perspectives in Supramolecular
Chemistry*
Volume 8

EDITED BY

FUMIO TODA

Okayama University of Science, Japan

AND

ROGER BISHOP

University of New South Wales, Sydney, Australia



John Wiley & Sons, Ltd

Copyright © 2004

John Wiley & Sons Ltd, The Atrium, Southern Gate, Chichester,
West Sussex PO19 8SQ, England

Telephone (+44) 1243 779777

Email (for orders and customer service enquiries): cs-books@wiley.co.uk

Visit our Home Page on www.wileyurope.com or www.wiley.com

All Rights Reserved. No part of this publication may be reproduced, stored in a retrieval system or transmitted in any form or by any means, electronic, mechanical, photocopying, recording, scanning or otherwise, except under the terms of the Copyright, Designs and Patents Act 1988 or under the terms of a licence issued by the Copyright Licensing Agency Ltd, 90 Tottenham Court Road, London W1T 4LP, UK, without the permission in writing of the Publisher. Requests to the Publisher should be addressed to the Permissions Department, John Wiley & Sons Ltd, The Atrium, Southern Gate, Chichester, West Sussex PO19 8SQ, England, or emailed to permreq@wiley.co.uk, or faxed to (+44) 1243 770620.

This publication is designed to provide accurate and authoritative information in regard to the subject matter covered. It is sold on the understanding that the Publisher is not engaged in rendering professional services. If professional advice or other expert assistance is required, the services of a competent professional should be sought.

Other Wiley Editorial Offices

John Wiley & Sons Inc., 111 River Street, Hoboken, NJ 07030, USA

Jossey-Bass, 989 Market Street, San Francisco, CA 94103-1741, USA

Wiley-VCH Verlag GmbH, Boschstr. 12, D-69469 Weinheim, Germany

John Wiley & Sons Australia Ltd, 33 Park Road, Milton, Queensland 4064, Australia

John Wiley & Sons (Asia) Pte Ltd, 2 Clementi Loop #02-01, Jin Xing Distripark, Singapore 129809

John Wiley & Sons Canada Ltd, 22 Worcester Road, Etobicoke, Ontario, Canada M9W 1L1

Wiley also publishes its books in a variety of electronic formats. Some content that appears in print may not be available in electronic books.

Library of Congress Cataloging-in-Publication Data

Separations and reactions in organic supramolecular chemistry / edited
by Fumio Toda and Roger Bishop.

p. cm. – (Perspectives in supramolecular chemistry ; v. 8)

Includes bibliographical references and indexes.

ISBN 0-470-85448-0 (cloth : alk. paper)

1. Supramolecular chemistry. 2. Chromatographic analysis. 3.

Chemical reactions. I. Toda, Fumio. II. Bishop, Roger. III. Series.

QD878 .S47 2004

547'.1226 – dc22

2003020628

British Library Cataloguing in Publication Data

A catalogue record for this book is available from the British Library

ISBN 0-470-85448-0

Typeset in 10/12pt Times by Laserwords Private Limited, Chennai, India

Printed and bound in Great Britain by Antony Rowe Ltd, Chippenham, Wiltshire

This book is printed on acid-free paper responsibly manufactured from sustainable forestry in which at least two trees are planted for each one used for paper production.

Contents

Contributors	vii
Preface	ix
1 Inclusion Complexation as a Tool in Resolution of Racemates and Separation of Isomers Zofia Urbanczyk-Lipkowska and Fumio Toda	1
2 Enantiomer Ordering and Separation During Molecular Inclusion Roger Bishop	33
3 Molecular Recognition of Crystalline Dipeptides and Its Application to Separation Katsuyuki Ogura and Motohiro Akazome	61
4 Separation of Isomers and Enantiomers by Bile Acid Derivatives Mikiji Miyata, Nungruethai Yoswathananont, Kazunori Nakano and Kazuki Sada	87
5 Physicochemical Studies of Separation of Isomers by Supramolecular Systems Luigi R. Nassimbeni	123

6	Regioselective Synthesis of Fullerene Derivatives and Separation of Isomers of the Higher Fullerenes	137
	L. Echegoyen, M. A. Herranz, F. Diederich and C. Thilgen	
7	Selective Reactions in Inclusion Crystals	173
	Zofia Urbanczyk-Lipkowska and Fumio Toda	
8	Supramolecular Control of Reactivity in the Solid State Using Linear Templates	185
	Leonard R. MacGillivray	
9	Development of a New Biocide as an Inclusion Complex	205
	Minoru Yagi, Ayako Sekikawa and Tetsuya Aoki	
	Cumulative Author Index	221
	Cumulative Title Index	227
	Index	231

Contributors

Motohiro Akazome, Department of Materials Technology, Faculty of Engineering, Chiba University, 1-33 Yayoicho, Inageku, Chiba 263–8522, Japan

Tetsuya Aoki, Kurita Water Industries Ltd, 4-7 Nishi-Shinjuku, 3-Chome, Shinjuku-ku, Tokyo 160–8383, Japan

Roger Bishop, School of Chemical Sciences, University of New South Wales, UNSW Sydney NSW 2052, Australia

François Diederich, Laboratorium für Organische Chemie, ETH-Hönggerberg, Wolfgang-Pauli-Strasse 10, CH-8093 Zürich, Switzerland

Luis Echegoyen, Department of Chemistry, Clemson University, 219 Hunter Laboratories, Clemson, SC 29634-0973, USA

M A Herranz, Department of Chemistry, Clemson University, 219 Hunter Laboratories, Clemson, SC 29634-0973, USA

Leonard R MacGillivray, Department of Chemistry, University of Iowa, 323B Chemistry Building, Iowa City, IA 52242-1294, USA

Mikiji Miyata, Department of Material and Life Science, Graduate School of Engineering, Osaka University, 2-1 Yamadaoka, Suita, Osaka 565–0871, Japan

Kazunori Nakano, Nagoya Municipal Industrial Research Institute, 3-4-41, Rokuban, Atsuta-ku, Nagoya 456-0058, Japan

Luigi R Nassimbeni, Department of Chemistry, University of Cape Town, Rondebosch 7701, South Africa

Katsuyuki Ogura, Department of Materials Technology, Faculty of Engineering, Chiba University, 1-33 Yayoicho, Inageku, Chiba 263–8522, Japan

Kazuki Sada, Department of Chemistry and Biochemistry, Graduate School of Engineering, Kyushu University, 6-10-1 Hakozaki, Higashi-ku, Fukuoka 812–8581, Japan

Ayako Sekikawa, Kurita Water Industries Ltd, 4-7 Nishi-Shinjuku, 3-Chome, Shinjuku-ku, Tokyo 160–8383, Japan

C Thilgen, Laboratorium für Organische Chemie, ETH-Hönggerberg, Wolfgang-Pauli-Strasse 10, CH-8093 Zürich, Switzerland

Fumio Toda, Department of Chemistry, Okayama University of Science, Ridaycho 1-1, Okayama, 700-0005, Japan

Zofia Urbanczyk-Lipkowska, Institute of Organic Chemistry, Polish Academy of Sciences, Kasprzaka Str. 44/52, Warsaw, Poland

Minoru Yagi, Kurita Water Industries Ltd, 4-7 Nishi-Shinjuku, 3-Chome, Shinjuku-ku, Tokyo 160–8383, Japan

Nungruethai Yoswathananont, Department of Material and Life Science, Graduate School of Engineering, Osaka University, 2-1 Yamadaoka, Suita, Osaka 565–0871, Japan

Preface

Classical organic chemistry largely involves making new molecules by means of structural changes involving strong attractive forces (covalent and ionic bonds), and concomitant studies (structure, reactivity, spectroscopy, applications) of the pure substances thereby produced. Supramolecular chemistry, on the other hand, involves the relationships between molecules that result from weak noncovalent bonding forces. This modern science currently is expanding rapidly in many different exciting directions. A number of excellent books have been written in recent years, covering the general scope of supramolecular chemistry, but less attention has been given to specific areas of application that are developing within this new field. In this volume we therefore present a selection of topics, written by experts in these fields, dealing with aspects of separation and reaction that are specific to supramolecular chemistry.

Fumio Toda
Okayama

Roger Bishop
Sydney

May 2003

Chapter 1

Inclusion Complexation as a Tool in Resolution of Racemates and Separation of Isomers

ZOFIA URBANCZYK-LIPKOWSKA

*Institute of Organic Chemistry, Polish Academy of Sciences, 01-224
Warsaw, Poland*

FUMIO TODA

*Department of Chemistry, Okayama University of Science, Okayama
700-0005, Japan*

1 INTRODUCTION

Molecular chirality is one of the most intriguing phenomena on Earth. It originated with the evolution of simple achiral molecules into more complex ones, and, as a result, the structure and functions of biological systems are controlled by direct recognition between chiral molecules. The physical and biological properties of various man-made materials depend on their chirality, and careful control of chirality at the molecular and supramolecular level is important for their performance. Recently, an increased demand for enantiopure materials has led to the intensive development of strategies to the selective introduction of new chiral centres into molecules. In contemporary synthesis, apart from using chiral starting materials (amino acid derivatives, carbohydrates, etc.), the creation of chiral centres via biocatalysis or asymmetrical synthesis is commonly used. Nevertheless, the resolution of racemates is still necessary in order to prepare optically

pure chiral auxiliaries and to purify products of low enantiomeric excess. Another significant problem is the resolution of low-molecular-weight isomeric products obtained in the laboratory or on a commercial scale. Both approaches require a careful design strategy based on understanding intermolecular interactions at the supramolecular level.

This chapter reviews recent methodologies for the effective resolution of racemates and mixtures of isomers, applying the inclusion complexation technique.

2 DEFINITIONS

Chirality is a property of nonidentity of an object with its mirror image. Therefore, a chiral object may exist in two enantiomorphous forms that are mirror images of one another. This means that both a chiral single object and collections of chiral objects should not contain symmetry elements such as mirror planes, centres of symmetry, as well as complex elements of symmetry containing one of the latter. All objects that contain such symmetry elements are *achiral*. At the molecular level, the lack of the above symmetry elements in a molecule means that it is *chiral* and can exist in two forms, called *enantiomers*, that are mirror images of one another. It is well appreciated that the relationship between *enantiomorphous forms* resembles that between the left and right hands. On a macroscopic level, a collection of *homochiral* molecules, or even a collection of *heterochiral* molecules containing an excess of one enantiomeric form and whose composition is defined by its enantiomeric purity p or its enantiomeric excess, ee , is called an *enantiomer*. One physical property that is inherently connected with chirality is *optical activity*, i.e. the ability to rotate plane-polarized light— α_D . Two enantiomers exhibit the same absolute value, but opposite signs, of rotation. Another property that may differentiate two enantiomers is the presence of hemihedral faces in their monocrystals. Except for their interactions with polarized light and their different crystal habits, enantiomers have identical physical properties (melting or boiling points, solubility, chromatographic behaviour, etc.).

An equimolar mixture of two enantiomers is called a *racemate*. The separation of two enantiomers that constitute a racemate is called *optical resolution* or *resolution*. Their crystalline forms best characterize types of racemates. A *racemic mixture* is a crystal where two enantiomers are present in equal amounts. A *conglomerate* is a case where each enantiomer has its own crystalline form. Sometimes their crystals have so-called hemihedral faces, which differentiate left and right crystals. For over a hundred years, crystallization processes have been used for the separation and purification of isomers and optical resolution, both in the laboratory and on an industrial scale.

Various methodologies can be applied for resolving racemates, depending on their type. The most useful method for separating racemates that crystallize as a collection of enantiomorphous left and right crystals (a conglomerate) is preferential crystallization (or crystallization by entrainment). It involves alternate

stereoselective crystallization of a single enantiomer out of a conglomerate and, after each filtration, recycling the mother liquor in order to crystallize the other enantiomer. Since the reason why, and under which conditions only *c.* 10% of racemates crystallize spontaneously as conglomerates is unknown, this method is of limited use. However, the method could be enhanced by a phenomenon called stirred crystallization, in which the resolution rate is enhanced due to secondary nucleation caused by stirring or by introduction of an amount of chiral impurities sufficient to catalyse the reaction [1,2]. In the latter method, selective chiral recognition between chiral impurities and one of the enantiomeric forms of the conglomerate may result in the transient crystallization of the opposite enantiomer [3,4].

The conventional way to obtain homochiral products in the laboratory is by diastereo-isomeric crystallization. Louis Pasteur developed this method back in 1853 [5]. He demonstrated that one could resolve racemic tartaric acid into ‘non-superposable right and left bodies’ by co-crystallization with an optically active amine. Basically, the general strategy involves the conversion of mixtures of enantiomers into a pair of diastereoisomeric derivatives that can be further separated by fractional crystallization. This is possible because although enantiomers have identical physical properties (melting or boiling points, solubility, chromatographic behaviour, etc.), apart from their interactions with polarized light, the properties of the diastereoisomers may differ significantly. This method involves the formation of a crystalline acid–base pair with an optically active resolving agent, mostly of natural origin. In their book *Enantiomers, racemates and resolutions*, Jacques and Collet listed over 200 of the most representative compounds used for optical resolution [6]. However, one disadvantage of this method is the fact that every natural compound used as chiral auxiliary has only one enantiomeric form, and another is that the technique becomes more expensive when it is scaled up for commercial applications. This is because, in order to make the technique industrially feasible, it requires versatile, cheap, chiral host compounds that are able to form diastereoisomeric inclusion complexes with vast groups of compounds.

Another way to obtain pure enantiomers is the separation of racemates through preparative chromatography on chiral stationary phases. In fact, the most significant developments over the last 20 years have been the application of GLC and HPLC techniques to the effective resolution of enantiomeric mixtures and to determining the enantiomeric ratio [7,8].

Several new techniques or significant improvements of the known techniques with the application of a recent technology are worth mentioning. These are the use of capillary electrophoresis [9], and the design of tailor-made polymers [10].

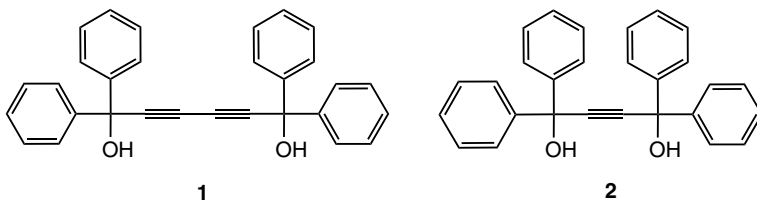
3 INCLUSION PHENOMENA

The classic, chiral auxiliaries used in the optical resolution process were natural acidic or basic compounds, able to form crystalline organic salts preferentially

with one enantiomer of the resolved species. Typically, they formed molecular complexes by proton transfer from acid to amine. Electrostatic interactions, intermolecular hydrogen bonds and other much weaker interactions like dispersive or van der Waals' forces assembled such diastereoisomeric pairs in crystals. With advances in supramolecular chemistry, knowledge of the formation of molecular complexes turned attention to inclusion phenomena [11]. Inclusion compounds are formed by the noncovalent insertion of *guest* molecules into the *host* lattice during the crystallization process. Several factors, such as topographic complementarity, hydrophobic effects, van der Waals' and dispersive forces, as well as much stronger ionic- and hydrogen-bond interactions, play a key role in the molecular recognition between two molecules forming an inclusion complex. This technique allows resolution of both racemic compounds and conglomerates. However, if the industrial application of optical resolution methods is being considered, it is very important to design new, versatile chiral compounds that can be prepared in both enantiomeric forms, and can recognize enantio- or diastereoselective organic guests. Of particular interest are those that can be obtained from cheap natural sources.

4 THE MOLECULAR BASIS OF INCLUSION COMPLEXATION

Although, at that time, the term 'supramolecular chemistry' had not yet been coined, the practical potential for inclusion complexation for acetylene alcohol guests **1** and **2** was recognized back in 1968 [12]. Spectroscopic studies showed that **1** and **2** formed molecular complexes with numerous hydrogen-bond donors and acceptors, i.e. ketones, aldehydes, esters, ethers, amides, amines nitriles, sulfoxides and sulfides. Additionally, **1** formed 1:1 complexes with several π -donors, such as derivatives of cyclohexene, phenylacetylene, benzene, toluene, etc. The complexation process investigated by IR spectrometry revealed the presence of OH absorption bands at lower frequencies than those for uncomplexed **1** and **2** [12]. These data, followed by X-ray studies, confirmed that the formation of intermolecular hydrogen bonds is the driving force for the creation of complexes [13].



However, differences in the host to guest ratio and the inability to form aggregates with all guests suggested that—apart from strong H-bond formation—the

shape and size of cavities, the electrostatic interactions and the π - π compatibility were also important factors affecting recognition events. Further X-ray studies confirmed the complex nature of molecular recognition [14]. It was assumed that the primary reason for the complexing ability of these molecules was the steric hindrance of the diphenylhydroxymethyl moiety, which prevented dimerization of the bulky host molecules via formation of intermolecular $\text{OH}\cdots\text{OH}$ hydrogen bonds. Therefore, small organic guest molecules could be included in the crystal, with the formation of hydrogen-bonded host-guest aggregates. This principle has been used to design new classes of chiral host compounds, where the diphenylhydroxymethyl moiety was a necessary building block. In the early 1980s, numerous new diols and polyols with steric hindrance around hydroxyl groups were synthesized from tartaric acid by Seebach *et al.* (so-called taddols) and were used as chiral auxiliaries in stereoselective synthesis, as catalysts in the preparation of new materials, and as chiral selectors [15]. Independently, in Japan, Toda *et al.* designed various types of new chiral host compounds for the extensive study of nonsolvent processes such as enantioselective organic solid-state reactions and the optical resolution of low-molecular-weight racemic compounds. For each new group of chiral hosts, NMR, UV, FTIR and X-ray crystallographic methods were used to study the structures of the above compounds, in solution and in the solid state, and their numerous molecular complexes [16].

Some of the first, and most versatile hosts are compounds **3a-c**, which can be prepared from optically active tartaric acid. It has been found that they work as chiral selectors in solution [17], and in a powdered state [18]. In the crystal structure of the free host compound (*R,R*)-(-)-*trans*-bis(hydroxydiphenylmethyl)-1,4-dioxaspiro[4.5]decane (**3c**), only one hydroxyl group is intramolecularly hydrogen bonded (Figure 1). As long as no suitable guest molecules are present, the other OH-group remains unbonded in both media.

Since the observed $\text{O}\cdots\text{H}$ distances and $\text{OH}\cdots\text{O}$ angles are in the range 1.60–1.62 Å and 165–175°, respectively, formation of this intramolecular H-bond is energetically favourable. The other OH group is free. The same situation is observed in solution, where two OH bands: one for hydrogen-bonded and the other for free hydroxyl groups, were found in the FTIR spectra [19]. It appears that a hydroxy group that is not involved in intramolecular hydrogen bonding shows a strong tendency for interactions with guest molecules that act as hydrogen-bond donors or acceptors. It is interesting that—in contrast to enantiomerically pure compounds—racemates and *meso* forms of such diols often form dimers in the crystals. These compounds have been used as versatile resolving agents with high complexation potential when applied to mixtures of isomers and racemates [17].

In a typical resolution procedure, two equivalents of a racemic compound and one equivalent of a chiral host dissolved in an ‘inert’ solvent (toluene, benzene or hexane) are left to crystallize. The resulting crystalline product is an inclusion compound with a typical host:guest ratio of 1:1 or 2:1. The guest compound

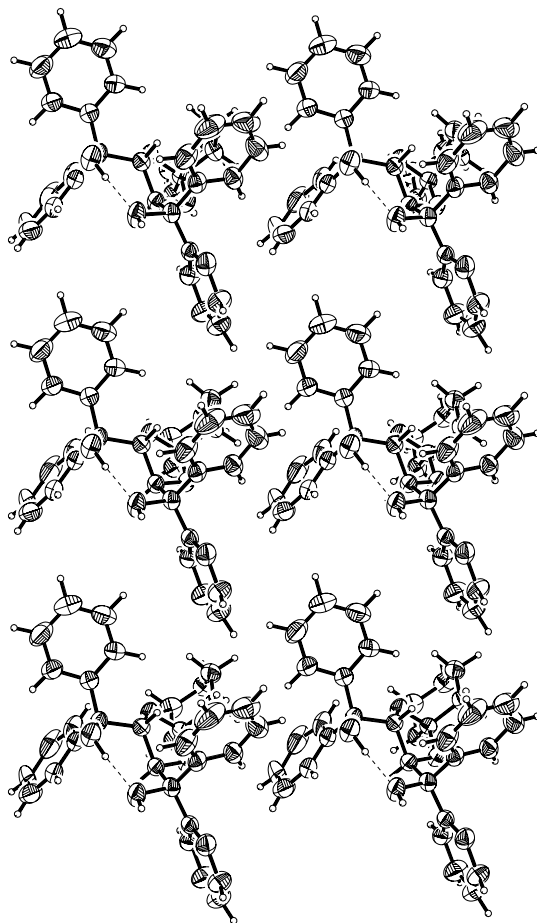


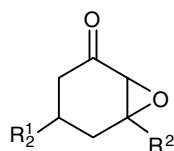
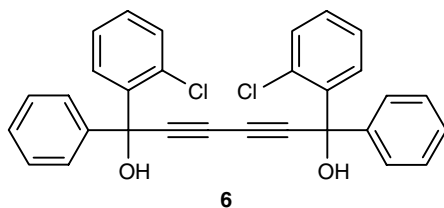
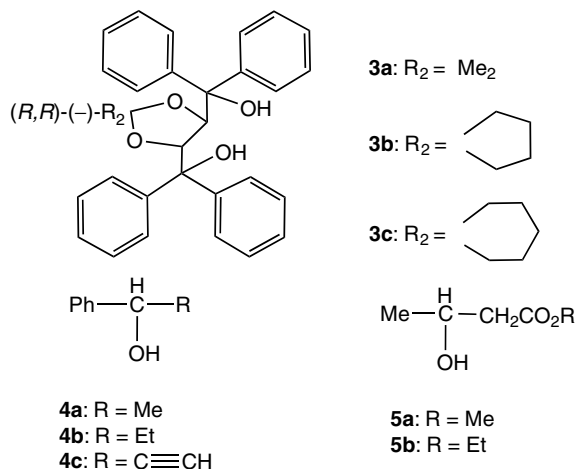
Figure 1 Crystal structure of *(R,R)*-(-)-*trans*-bis(hydroxydiphenylmethyl)-1,4-dioxaspiro[4.5]decane **3c** (courtesy of B. Szczesna).

can be removed from the complex by heating the solid compound *in vacuo*. The opposite enantiomer is left in solution. Inclusion compounds can also be formed by the insertion of guest molecules into channels created by the crystal structure of the host. In such a case, a stirred suspension of the host in hexane or water is added to a racemic mixture of a guest. After filtration of the solid compound, the pure enantiomeric guest is distilled off *in vacuo*.

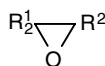
4.1 Optical Resolution of Alcohols and Epoxides

Another variation of the enantioselective inclusion complexation procedure leading to optical resolution is the application of powdered host compounds in the

form of a suspension [20]. Chiral hosts **3a–c** are not soluble in hexane and water, and therefore they have been used in suspension in order to resolve oily racemic alcohols **4a–c** and **5a–b**.



- 7a:** $R^1 = \text{H}, R^2 = \text{Me}$
7b: $R^1 = R^2 = \text{H}$
7c: $R^1 = R^2 = \text{Me}$

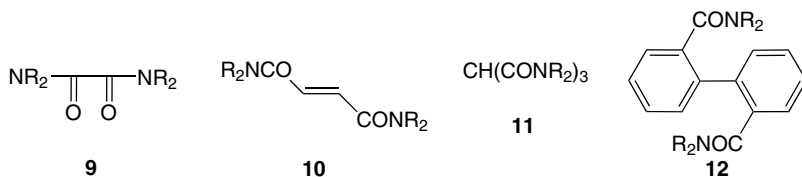


- 8a:** $R^1 = \text{Et}, R^2 = \text{CO}_2\text{Et}$
8b: $R^1 = \text{Me}, R^2 = \text{CO}_2\text{Et}$
8c: $R^1 = \text{Me}, R^2 = \text{CO}_2\text{Me}$
8d: $R^1 = \text{H}, R^2 = \text{Ph}$

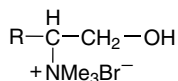
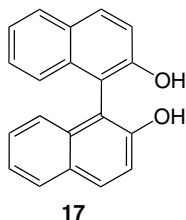
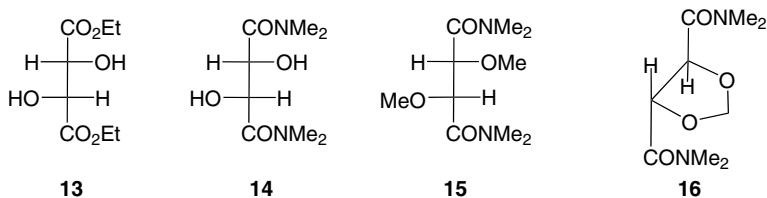
For example, when a suspension of powdered optically active host **3a** was mixed with racemic 1-phenylethanol (**4a**) in a 1:1 molar ratio and stirred at room temperature for 6 h, a 2:1 inclusion complex was formed. When the filtered solid complex was heated *in vacuo*, it gave (–)-**4a** (95% ee, 85% yield). For the host compounds **3a–c**, approximately the same ee (78–99.9%) and high yield (75–93%) could be achieved in the resolution of alcohols of the **4** and **5** series in water and hexane. It has been found that introducing

N-hexadecyltrimethylammonium bromide as a surfactant helped to prevent coagulation of the two substrates in aqueous suspension. It is interesting that, although bulky but small molecules of epoxides (**8**) easily penetrated the void space in crystals of **3b–c** and underwent optical resolution, compounds **5a–b** (with long aliphatic chains) and **7b** did not form inclusion compounds. The application of suspension conditions resulted in a very efficient optical resolution, sometimes better than that achieved by the classic formation of complexes by recrystallization of host and guest from a common solvent. For comparison, optical resolution of **4c** by co-crystallization with the host **6** after two recrystallizations gave the crude product at 100% ee but only 35% yield [21], in comparison with 57% and 85%, respectively, in hexane and water suspension [20].

Among the different types of compounds whose complexation properties have been studied are various amides: linear oxoamide **9** [22], fumaramide **10** [23,24] and methanetricarboxamide **11** [25], biphenyl derivatives **12** [26], and derivatives of tartaric acid **13–16**, that can also be prepared in an optically active form [27]. The above-mentioned chiral hosts have been found to form inclusion complexes with chiral guests **17** and **18**. Molecular recognition between chiral hosts and



R = *i*Pr, C₆H₆



- 18a**: R = Me
18b: R = *i*Pr
18c: R = Bu^{*i*}
18d: R = Bu^{*s*}

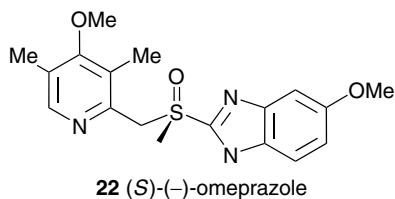
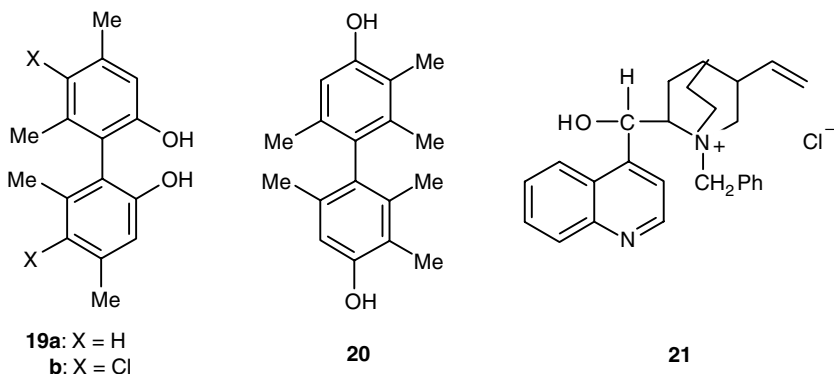
17–18 is enantioselective, and this technique has been used for optical resolution of their racemates. For example, when a solution of (*R,R*)-(+)-**15** in benzene was kept at room temperature with a hexane solution of *rac*-**17**, after 12 h it produced colourless prismatic crystals of a 1:1 inclusion complex of (+)-**15** and (–)-**17**. The crude product recrystallized from benzene was chromatographed on silica gel, using benzene as a solvent, to give (*S*)-(–)-**17** with 100 % ee and 72 % yield. The (*R*)-(+)-**17** was obtained in 100 % ee and 59 % yield by co-crystallization of the filtrate with (*S,S*)-(–)-**15** and subsequent chromatography of the deposited crystals using the above-mentioned conditions. The number of possible chiral auxiliaries is effectively unlimited. Recently, the new chiral host compounds **18a–d** have been obtained from amino acids, which resolved *rac*-**17** very efficiently [28].

4.2 Resolution of Bi-aryl Compounds

Optical resolution of biphenyl and binaphthyl derivatives is of particular interest in contemporary chemistry. Both families of compounds serve as a source of chiral catalysts used in asymmetrical synthesis [29–31], chiral shift reagents [32] or chiral host compounds for the optical resolution of various racemic guests. The classic preparative method for obtaining optically active **17** describes the formation of diastereoisomeric salts of cyclic binaphthylphosphoric acid with cinchonine, and subsequent reaction with POCl₃ followed by hydrolysis [33,34]. Recently, optically active 1,1'-binaphthyl-2,2'-diols have been synthesized by the oxidative coupling of 2-naphthols using *Camelia sinensis* cell culture as a catalytic system [35]. The inclusion complexation method used with such a system does not require application of preparative chemistry or expensive natural resolution agents. Moreover, both enantiomers of **17** can be obtained easily using this method.

Optically active **19a** was previously obtained by inclusion complexation with *N*-benzylcinchonidium chloride **21** [36]. Compound **21** was also a very efficient resolving agent for *rac*-**17** [37]. Crystal structure analysis of a (1:1) complex of **21** and selectively included (+)-**17** showed that the molecular aggregate was associated by formation of a Cl[–] ···HO hydrogen bond. Racemic compound **20** could be efficiently resolved only by complexation with (*R,R*)-(–)-*trans*-2,3-bis(hydroxydiphenylmethyl)-1,4-dioxaspiro[4.4]nonane **3b**. A crude inclusion complex of 1:1 stoichiometry of **3b** was formed selectively with (+)-**20** in a 2:1 mixture of dibutyl ether/hexane. One recrystallization from the above combination of solvents gave a 34 % yield of the pure complex. Optically active (+)-**20** was obtained by dissolving the complex in 10 % NaOH, followed by acidification with HCl and then recrystallization. The optical purity determined by HPLC (Chiralpack As) was >99.9 %. As far as we know, this is the only report of the resolution of 4,4'-dihydroxybiphenyl derivatives. Conversely, an inclusion

complexation technique using a chiral form of **17** has been reported recently as a very efficient method for the resolution of the important pharmaceutical compound omeprazole (**22**), with an ee of over 99% for both (*S*)-(-)- and (*R*)-(+)-enantiomers [38].



Data from the literature show that even if new convenient preparative methods are being developed for the resolution of 1,1'-binaphthyl-2,2'-diol (**17**) via a phosphite using (-)-menthol as a resolving agent [39], the inclusion complexation method can still compete with these, owing to its simplicity, efficiency, and low cost.

4.3 Resolution of P-Chiral Phosphorus Compounds

Among the preparative methods used for obtaining P-chiral phosphorus compounds, there are procedures involving the use of optically pure auxiliaries like (-)-menthol [40], (-)-ephedrin [41,42], or more recently, the kinetic resolution of 1-hydroxymethylalkylphenylphosphine oxides using *Pseudomonas* or *Candida antarctica* lipases [43]. It has been found that some [(alkyl-substituted)arene] phosphinates and phosphine oxides can also be resolved efficiently by inclusion complexation with optically active 2,2'-dihydroxy-1,1'-binaphthyl (**17**) [44].

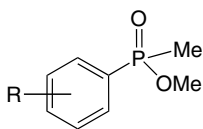
The resolution process however, depends on place of substitution at the benzene ring and on bulkiness of the alkyl residue. Compounds **23** and **26** could not be

Table 1 Optical resolution of compounds **22–25** with (–)-**17** (from ref. 44).

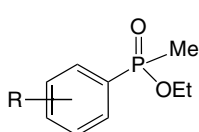
1:1 complex	Enantiomer	ee (%)	Yield (%)
(–)- 17 and 22a	(+)- 22a	100	12
22b	(+)- 22b	100	47
22c	(+)- 22c	100	31
22d	(+)- 22d	100	32
24a	(+)- 24a ^a	>10 %	20
24b	Complex decomposition	–	–
25a	(–)- 25b	100	60
25b	No resolution	–	–
25c	(–)- 25c	100	33
25d	No resolution	–	–

^a(+)-**20a** was obtained after four recrystallizations followed by decomposition.

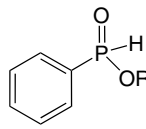
resolved using this method. Among the *o*-, *m*-, and *p*-isomers of **22** and **25**, resolution of the *m*-derivatives was best, reaching the yields and ee shown in Table 1. The optical resolution procedure involved formation of 1:1 co-crystals between (–)-**17** and **22a–d**, **24a–b**, and **25a–d** from benzene solution. Twofold recrystallization gave pure crystalline complexes. These were resolved by column chromatography on silica gel using benzene as an eluent, with the yields shown in Table 1. Similarly, the filtrate was treated with a benzene solution of (+)-**17** and the crystalline 1:1 complexes thus obtained were chromatographed on silica gel (benzene).



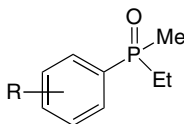
22a: R = H
b: R = *o*-Me
c: R = *m*-Me
d: R = *p*-Me



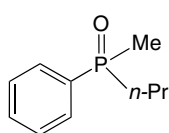
23



24a: R = Me
b: R = Et



25a: R = H
b: R = *o*-Me
c: R = *m*-Me
d: R = *p*-Me



26

The resolution studies have been followed by thorough analysis of X-ray structures of the two isomeric complexes formed by both enantiomers of **17** with

(+)-**22a**. In both structures, oxygen atoms from phosphine oxides in (+)-**22a** were hydrogen bonded with two OH-groups of the neighbouring molecules of binaphthyl. However, in the case of the 1:1 complex of (+)-**17** with (+)-**22a**, the packing pattern was less efficient, resulting in less-dense packing. Similar efficiencies of the optical resolution of alkylaryl-substituted sulfoxides [45,46] and selenoxides [47] have been reported previously.

4.4 Resolution By New Dimeric Hosts Containing 1,4-Diol Units

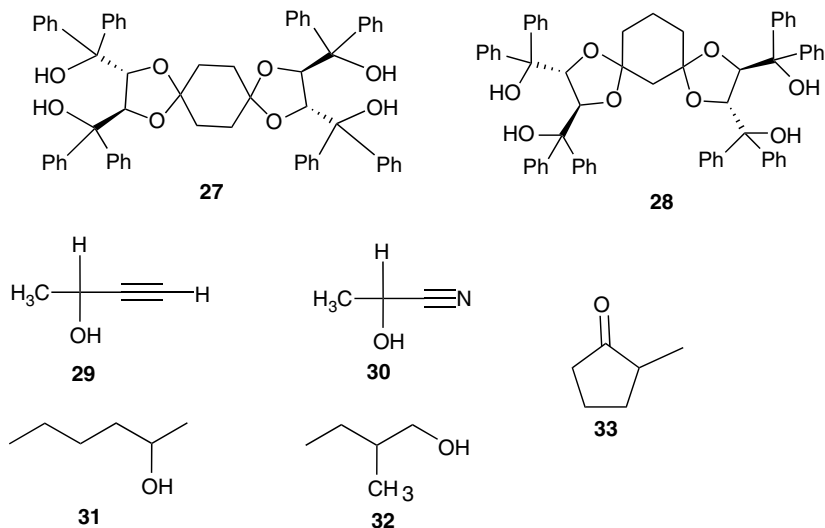
Recently, dimeric hosts containing two 1,4-diol units—**27** and **28**, possessing large hydrophobic areas on both sides of cyclohexane ring, have been designed [48]. A dual action of these hosts might be expected during the molecular recognition process, hydrogen-bond formation with guests bearing groups being hydrogen bond donors or acceptors and enclathration of hydrophobic guests. Table 2 shows that a variety of organic molecules can be accommodated in crystals of hosts **27** and **28**. Host compound **27** has been found to be extremely efficient in the resolution of small chiral alcohols that could not be resolved by the monomeric compound **3c**. The role of multiple recognition sites on the complexing properties of these new host compounds, and their role in chiral discrimination processes, were studied in the solid state using X-ray diffraction methods.

For example, when powdered host **27** was mixed with volatile *rac*-but-3-yn-2-ol (**29**) and left for 24 h, a 1:1 inclusion complex with (+)-**29** was formed. The alcohol can be removed from the complex by heating *in vacuo* yielding **29** of 59 % ee and 77 % yield. A second complexation, followed by distillation *in vacuo*, gave (+)-**29** of 99 % ee and 28 % yield. The best resolution of *rac*-**29** reported to date was by enzymatic esterification, and gave chiral alcohol at 70 % ee and 31 % yield [49]. Host **27** could be used for optical resolution of *rac*-2-hexanol

Table 2 Complexing properties and host:guest ratio for **27** and **28** in comparison with **3c** (from ref. 48).

Guest	3c	27	28
MeOH	1:1	1:2	1:1
Acetone	2:1	1:2	1:1
Cyclopentanone	2:1	1:1	1:1
Ethyl acetate	— ^a	1:1	1:1
γ-Butyrolactone	1:1	1:2	1:1
THF	1:1	1:2	2:1
DMF	1:1	1:2	1:1
DMSO	2:1	1:1	1:1
Toluene	— ^a	1:1	1:1
Cyclohexane	— ^a	1:1	— ^a

^aNo complex was formed.



(31) and *rac*-2-methyl-1-butanol (**32**), after two complexation–distillation steps giving optically pure (+)-**31** and (–)-**32** in 34 % and 5 % yields, respectively. An attempt at optical resolution of 2-methylcyclopentanone (**33**) was less efficient, and although a 1:1 inclusion complex was formed easily, the distilled alcohol gave only 15 % ee.

The X-ray structure of the 1:1 complex of (*R,R,R,R*)-(–)-**27** and (–)-**33** (see Figure 2) shows that the host compound can interact with guests, or via hydrogen-bond formation, or by inclusion of less-polar molecules into the hydrophobic cavity. In the case of (*R*)-(–)-**33**, the carbonyl group of the guest is hydrogen bonded by the OH group of the host and its hydrophobic part fits the hydrophobic cavity of the second host molecule. The same pattern was found in the case of the 1:2 complex of (–)-**27** with amphiphilic (–)-**32**, where two recognition sites worked cooperatively, binding selectively two molecules of (–)-**32**. Hydrophobic cavities contain the lipophilic portion of an alcohol molecule (Figure 3). As a result of (1:2) stoichiometry, no host-to-host hydrogen bonds were found in the latter crystal structure.

4.4.1 Chiral discrimination in the competitive environment of a solvent

Interesting, solvent-dependent chiral discrimination properties have been observed for chiral host **28** [48]. In the absence of toluene, compound **28** forms a 1:2 crystalline complex with *rac*-cyanohydrin (**30**). When both **28** and *rac*-**30** were dissolved in toluene, the crystalline product contained **28** and (+)-**30** and toluene in 1:1:1 ratio. One recrystallization of the complex from toluene gave crystals which upon heating *in vacuo* gave (+)-**30** at 100 % ee and 24 % yield.

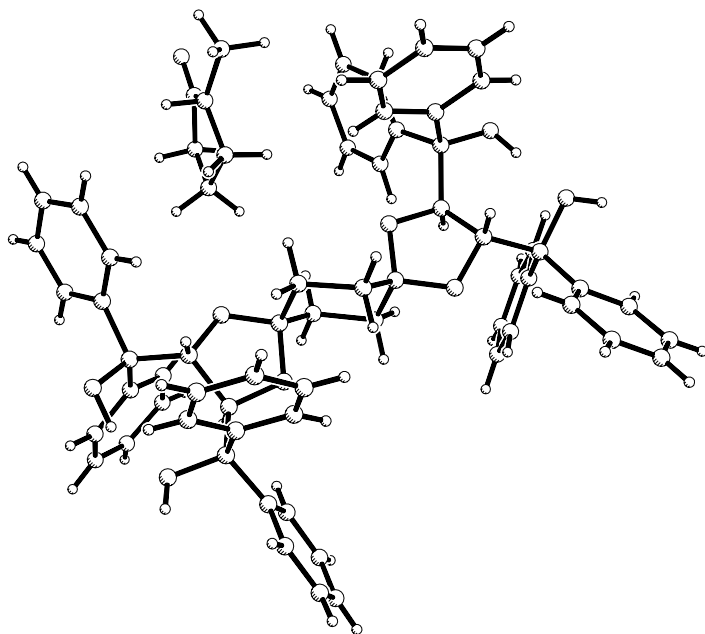


Figure 2 Molecular recognition pattern found in the crystal of the 1:1 complex of (*R,R,R,R*)-(-)-27 and (-)-33. Reprinted with permission from ref. 48. © 2000, Wiley-VCH Verlag GmbH.

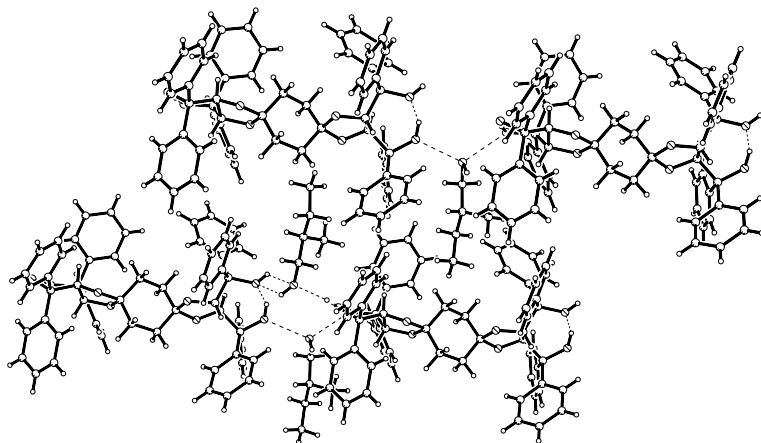


Figure 3 Crystal structure of the 1:2 complex of (-)-27 and (-)-32. Reprinted with permission from ref. 48. © 2000, Wiley-VCH Verlag GmbH.

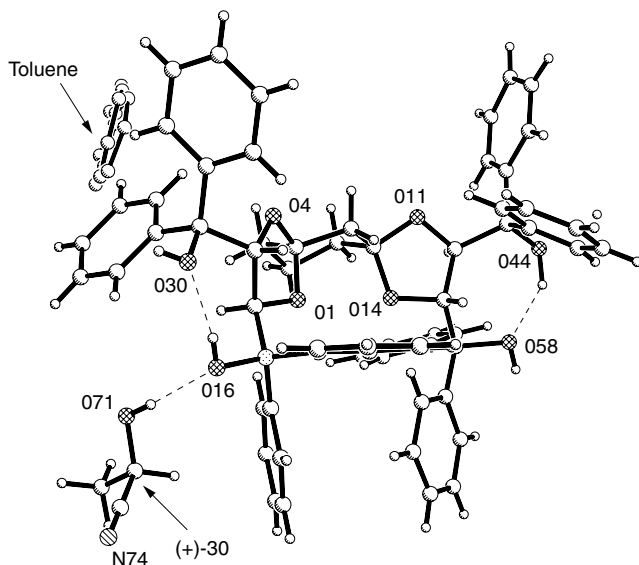
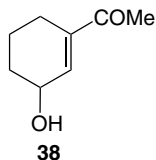
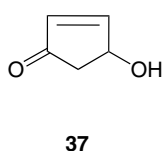
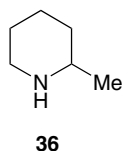
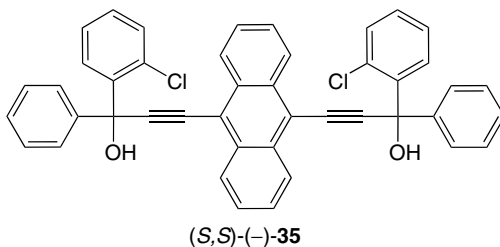
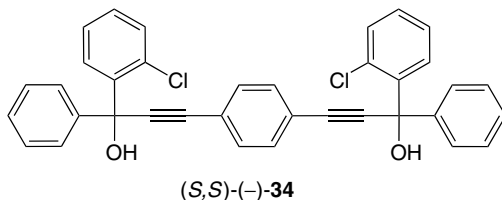
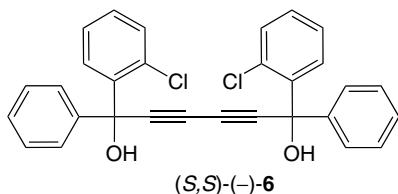


Figure 4 Molecular recognition pattern found in a 1:1:1 complex of (R,R,R) -(-)-**28** with (-)-**30** and toluene. One enantiomer of cyanohydrine is bound to the enantioselective binding site of the host. The disordered toluene molecule fits well into the hydrophobic cavity. Reprinted with permission from ref. 48. © 2000, Wiley-VCH Verlag GmbH.

According to X-ray studies, the host **28** has two recognition mechanisms: enantioselective binding via hydrogen-bond formation with hindered hydroxyl groups, and nonselective enclathration into hydrophobic cavities formed in the crystals by numerous phenyl rings. As can be seen in Figures 3 and 4, the same enantiomer of the cyanohydrin is hydrogen-bonded to the alcohol OH group, regardless of whether the complex is formed from the enantiomerically pure or racemic **30**. Phenyl groups can fit into the crystal forming cavities, of the host which can unselectively bind disordered toluene molecules as in the (1:1:1) complex of **28** and toluene (Figure 4) or a molecule of the second enantiomer of **30** ((+)-**30** giving a 1:2 complex of **28** with racemic **30**; Figure 5). Solvent-dependent chiral discrimination properties have been found previously, during optical resolution of *rac*-2-methylpiperidine (**36**) by the host **35**. Hosts of the same chirality included (R) -(-)-**36** in the presence of toluene, and (S) -(+)-**36** in the presence of methanol [50]. X-ray structural analysis of these two crystals revealed that MeOH and (S) -(+)-**36** molecules compete for the free proton of the host. Finally, both of them are included in the host lattice via hydrogen bonding in a 1:1:1 ratio. Toluene molecules under the same conditions are repelled and only (-)-**36** forms a 1:1 inclusion complex with the host. Similarly, in toluene, the host (S,S) -(-)-**34** formed a crystalline 1:2 complex with (+)-4-hydroxycyclopent-2-enone, (+)-**37**. This high host:guest ratio allowed separation of (+)-**37** at 38 % ee but in 72 % yield.



When complexation was carried out in MeOH, a 1:1:1 complex of the host, (-)-**37** and MeOH was formed. Distillation *in vacuo* gave (-)-**37** in 42% ee and 44% yield. In the case of complexes formed by the host **28**, the large hydrophobic void space can competitively include a disordered toluene molecule or (-)-cyanohydrin [48]. (S,S)-(-)-**6**, which in the solid state forms much smaller hydrophobic cavities, could not resolve *rac*-**36** in either solvent. Under the same conditions, however, it successfully resolved *rac* 3-acetylcyclohex-2-enol, **38**, forming 1:2 complexes in both solvents. From these (+)-**38** was obtained in 40% ee and 86% yield, and 66% ee and 79% yield, respectively, from toluene and MeOH solutions. The above cases suggest that each of the hosts (**28**, **34** and **35**) contains two recognition sites—one enantioselective, located around sterically hindered OH groups, and the other nonspecific, and located in the hydrophobic cavity. If molecules of one enantiomer and a solvent compete for the enantioselective recognition site (with H-bond formation), the enantioselectivity of the host

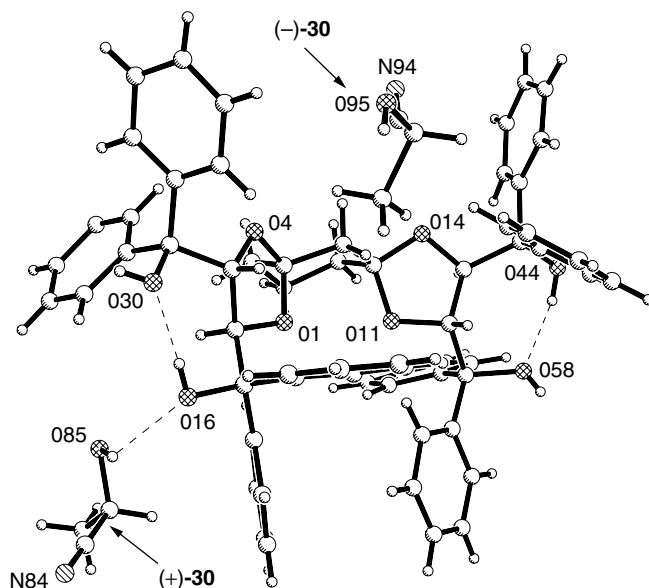
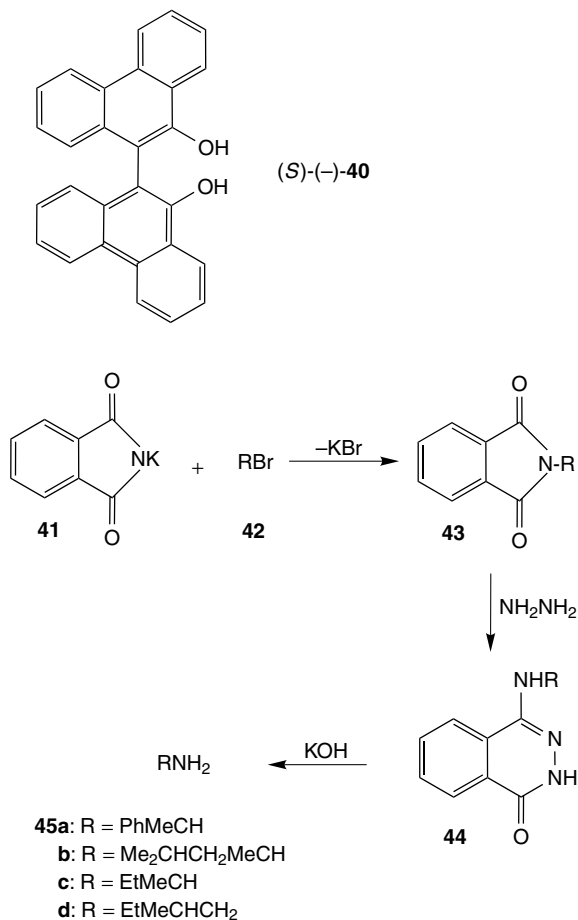


Figure 5 Molecular recognition pattern found in a 1:2 complex between (*R,R,R,R*)-(-)-**28** and *rac* **30**, formed in the absence of toluene. One enantiomer of the cyanohydrine is bound to the enantioselective binding site of the host. The second enantiomer fills the hydrophobic cavity. Reprinted with permission from ref. 48. © 2000, Wiley-VCH Verlag GmbH.

may be changed with a change of solvent. When molecules of one enantiomer and a solvent compete for a space in the nonspecific cavity, they are interchangeable with one another in the crystal cavity, and the enantioselectivity of the host is retained.

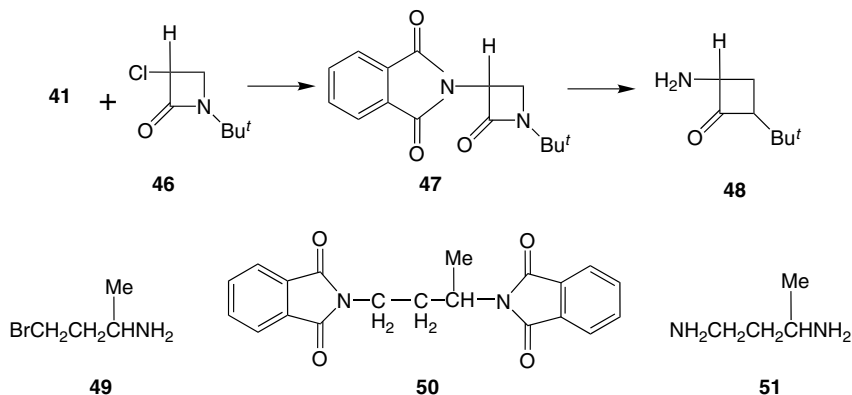
4.5 The Optical Resolution of Reaction Intermediates by Inclusion Complexation

The enantioselective complexation technique can also be applied as one step in the reaction sequence, providing chiral substrates for the next step. We will now discuss the example of Gabriel synthesis between potassium phthalimide **41** and alkyl bromide **42**, which leads to optically active amines (Scheme 1) [51]. Instead of the complicated preparation of chiral alkyl bromides (halides), imides (**43**), which are reaction intermediates, have been resolved. Upon treatment with hydrazine and KOH, these gave optically active amines. The chiral host (*S,S*)-(-)-**6** or the chiral biaryl host (*S*)-(-)-**40** was used for the effective resolution of the intermediates **43**. Racemic mixtures **43a–d** were resolved by complex formation with the host (*S,S*)-(-)-**6** in a mixture of diethyl ether and light petroleum.



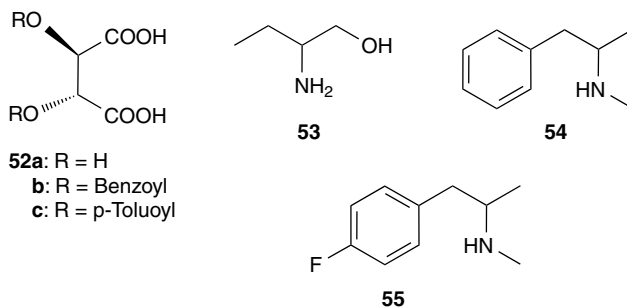
For example (+)-**43a** was obtained after two purifications at 55 % ee and 10 % yield. Treatment of (+)-**43a** with hydrazine and KOH gave (+)-**45a** at 55 % ee and 40 % yield. The chiral host (S) -(-)-**40** has been found to be extremely effective as a chiral selector towards comparatively bulky molecules of the phthalimide formed from 1-*tert*-butyl-3-chloro-azetidin-2-one, **47**. A crystalline inclusion complex of 1:1 stoichiometry was formed between one mole of (S) -(-)-**40** and two moles of *rac*-**47** dissolved in benzene/hexane 1:1 solution. After one recrystallization, the complex was chromatographed on silica gel, and the crystalline product was treated with hydrazine. Optically pure (-)-3-amino-1-*tert*-butyl-azetidin-2-one (-)-**47**, was obtained at 100 % ee and 44 % yield [51]. Primary diamines, like 1,3-dibromobutane (**49**), can undergo a similar reaction with potassium phthalimide, yielding diphtalimide, **50**. The complexation process between *rac*-diphtalimide **50** and host (S,S) -(-)-**6** gave a 1:1 complex containing (-)-**50**

and (*S,S*)-(-)-**6** at 100 % ee and 42 % yield. Subsequent decomposition of the complex with hydrazine and KOH gave optically pure (-)-**51** at 100 % ee and 50 % yield.



4.6 Optical Resolution with Application of Mixtures of Resolving Agents

Recently, several new findings have been reported in the area of optical resolution methodology. It has been found that the enantiomeric excess of some separation processes does not correlate linearly with the optical purity of the resolving agents. The so-called ‘Dutch method’, shows, that if the resolving agent belongs to the homologous series, then it is worthwhile trying to accomplish resolution using all the compounds in the series [52]. Applying a mixture of resolving agents, even if they do not show individually good resolving properties, may significantly enhance the effectiveness of enantiomer separation by fractional crystallization. This method has also been found to work in the case of liquid racemates [53]. Elevated yields and enantiomeric enhancement, ee, have been observed in some cases of racemic amines **53–55** resolved with the appropriate mixtures of tartaric acid derivatives **52a–c**. Moreover, this technique could be

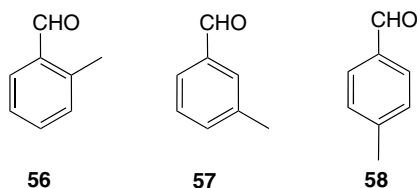


of industrial importance. Although the two above methods are quite new empirical observations with no theoretical explanations, they are assumed to have a common supramolecular background.

5 ISOMER SEPARATION

Inclusion phenomena employing organic hosts with high potency complexation can also be successfully used for the resolution of technical mixtures of isomers. The basic property that qualifies a group of compounds as good selectors is the presence of proton-donors and/or proton-acceptors within the molecule, and the ability, during crystallization, to form host frameworks containing layers, channels and various other types of cavities. On the other hand, the host structure has to be flexible enough to accommodate a variety of guests. Several techniques are commonly used in evaluating the complexing abilities of the host and for selecting the best complexor. The competitive experiments can be performed in parallel [54], or in a so-called cocktail [55] fashion. They are based on assumption that the complex will be preferentially formed with the best guest compound. The thermodynamic and kinetic parameters of the host–guest complexation process can be studied using various techniques, including NMR, fluorescence and UV-titration, differential scanning calorimetry, thermogravimetry, etc. These results are usually discussed from the viewpoints of size and shape complementarity, the induced-fit concept, and cooperation between several types of weak noncovalent interactions. Therefore, X-ray diffractometry remains one of the best tools to give an insight into the solid-state structure of the hosts and their supramolecular complexes. The above studies show that, within certain host types, binding constants towards isomeric compounds can be enthalpy- or entropy-driven, and can depend on the solvent used and the ratio of the concentrations of the isomeric guests [56–58].

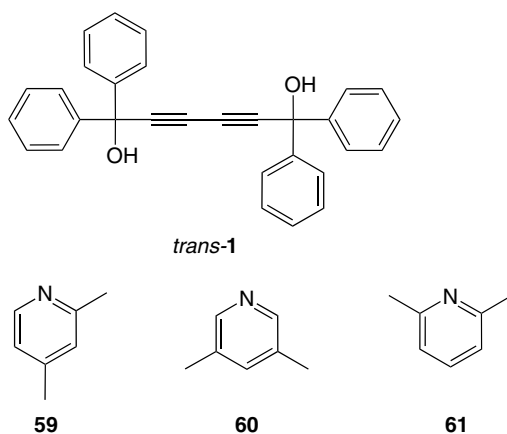
One of the first examples is the use of achiral 1,1,6,6-tetraphenylhexa-2,4-diyne-1,6-diol (**1**) for resolution of a mixture of *o*-, *m*- and *p*-methylbenzaldehydes (**56**–**58**). It showed that an inclusion complex at a 1:1 ratio was formed selectively with the *p*-isomer **58**. The complexant was effectively separated from the complex by heating *in vacuo*, and *p*-methylbenzaldehyde was obtained at 100 % purity and 96 % yield [59].



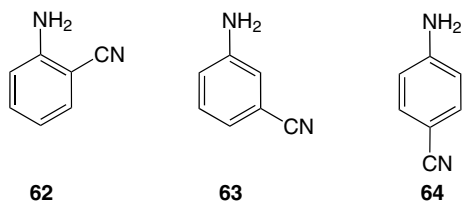
The *o*-isomer **56** was distilled off from the remaining filtrate at 99 % purity and 90 % yield. The above processes are solvent-dependent, and therefore polar

solvents like water and less polar ones, such as benzene, toluene or a mixture of ether-light benzene, etc., should be tried in every individual case. It was observed that selectivity of complexation could be changed drastically by changing the solvent [57]. The purity of the obtained guest can be significantly improved by repeating the crystallization several times.

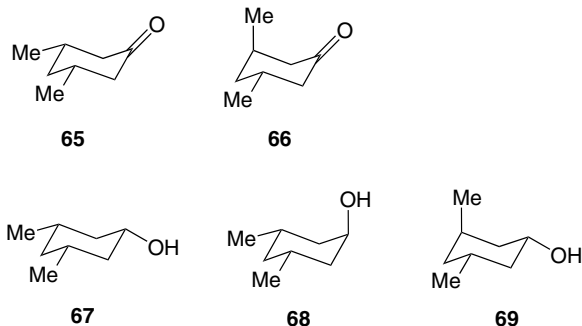
The host compound **17** has been used for separation of alcohols or NaOH from aqueous solution [60]. One interesting application of inclusion complexation is the separation of natural compounds from natural sources, e.g. caffeine from tea leaves and nicotine from tobacco leaves – making this technique industrially feasible [61]. Similarly, host **1** was used for the separation of mono- and disubstituted naphthalenes [62]. More complete information about selectivity rules involving host **1** and isomeric 2,4-, 3,5- and 2,6-lutidines (**59–61**) was obtained in competition experiments carried out between pairs of guest compounds [63]. In these experiments, a small quantity of the host was added to 11 vials in which the molar fractions of the two isomeric complexors were varied from 0 to 1. The resulting crystalline product was analysed by gas chromatography to determine the composition of the guest compounds. The experiments were repeated for all three combinations of guests. The crystal structures of three inclusion complexes formed with the isomeric guests were analysed independently from this. For each crystal structure the lattice energy was calculated, using the atom–atom potential with coefficients given by Gavezzotti [64] and the hydrogen-bonding potential according to Vedani and Dunitz [65]. The results show that 3,5-lutidine (**60**) is selectively included in the host lattice in the presence of **59**. Competition between **59** and **61** is concentration dependent; 2,6-lutidine (**61**) is favoured when its molar fraction exceeds 0.2. Under the same conditions, **60** is favoured over **61**. In crystal structures, host **1** is always hydrogen bonded to two guest molecules. The lattice energy calculations agree with the complexation preferences.



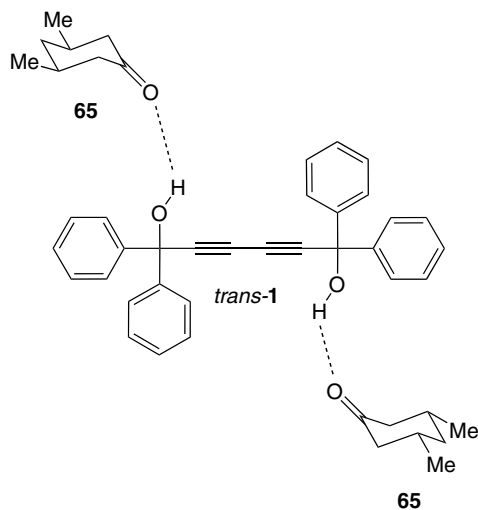
Similarly, competition experiments on the aminobenzonitrile isomers **62–64** showed **62** > **63** > **64** preferences towards host **1** [66]. In this case, complexing selectivity was also concentration dependent. Lattice energy calculations performed for the crystallographically obtained models agreed well with the results of the competition experiments. Additionally, when there were no pronounced selectivity differences, both hosts were included in the host framework.



The versatility of host **1** allows discrimination not only between isomeric planar, aromatic compounds but also between quite bulky derivatives of cyclohexane. For example, host **1** will include selectively the diequatorial isomer of 3,5-dimethylcyclohexanone (**65**), but not **66** or isomer **67** from a mixture of **67–69** [67].

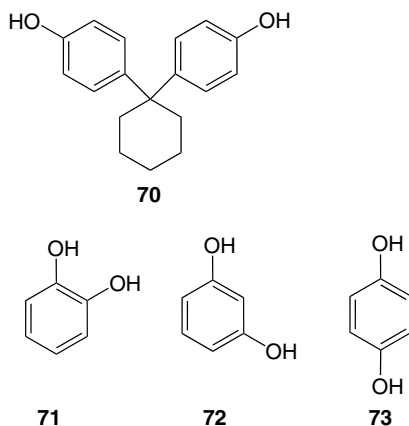


It can be seen from the X-ray structure of the 1:2 complex of **1** and **65** that the two hydroxyls of the hosts are hydrogen-bond donors for the two carbonyl groups of the guest. The crystal is a collection of trimeric aggregates bound via two intermolecular hydrogen bonds (Scheme 1). In the case of a 1:2 complex of **1** and **67**, two guest molecules donate their H-atoms and form intermolecular hydrogen bonds. In both cases, the isomers that were included into the host framework were those with smaller space-demands. Due to the elongated structure of these guests, hydrogen bonds formed with a sterically constrained host were more energetically favourable.



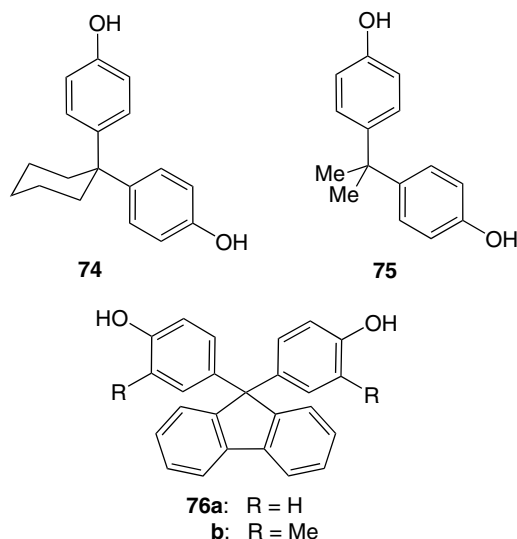
Scheme 1

Recently, an interesting example of the resolution of isomeric benzenediols **71**–**73** by the host **70**, performed in solution under solvent-free conditions has been reported [68]. Although in aqueous solution the *para*-isomer was strongly favoured by a suspension of powdered **70**, no complexation occurred when **70** and **73** were ground together.



Most of the isomeric guests are achiral compounds, and therefore achiral hosts with variable properties are effective enough to selectively form a molecular complex with one of these hosts. 2,2'-Dihydroxy-1,1'-binaphthyl **17**, has been found to

form inclusion complexes of various geometries with air- and moisture-sensitive alkali-metal hydroxides [60]. This organic–inorganic hybrid forms crystals with large hydrated domains made up by several water molecules (six to eight). This technique will allow separation of these hydroxides from aqueous solution. Small variations in the chemical structure of a host can change its complexing selectivity. This is observed in the case of the two hosts **74** and **75**. Whereas the latter selectively recognizes *p*-cresol and easily forms a 1:1 complex from benzene, under the same conditions the former selectively forms a 1:1 complex with *m*-cresol [69].

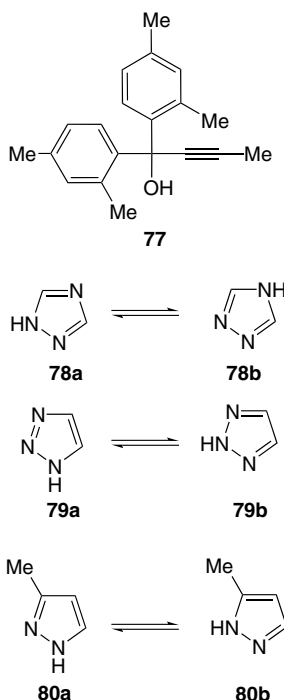


Further modification of **74** by introducing a bulky fluorene residue gave two compounds: **76a** and **76b** [70]. Of particular interest is host **76b**, which forms inclusion complexes with volatile guests such as MeOH, Me₂CO, MeCN, DMSO, and DMF, as well as with low-boiling-point dimethyl (bp –25 °C) and diethyl ethers (bp 35 °C). This makes it possible to store these complexes at room temperature, for easy release on heating. X-ray studies have shown markedly different construction of the host framework. Its versatility was studied using DSC measurements. It appears that the 1:1 complex of **76b** with MeCN decomposes at 95 °C, releasing a MeCN molecule (endothermic peak), then rearranges itself at 130 °C (exothermic peak), and finally melts at 225 °C.

The above examples show that resolution of isomeric mixtures is possible both in solution and under solvent-free conditions. The resolution process is driven by multicentre recognition events in which solvent molecules play an important role.

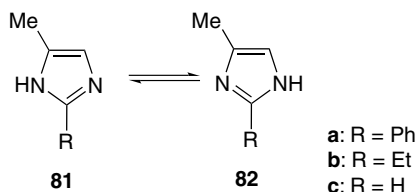
6 STABILIZATION OF TAUTOMERIC FORMS BY INCLUSION COMPLEXATION

The problem of tautomeric equilibria is of general interest, because it concerns the isomeric situation in natural systems like the nucleic acid pairs in DNA and RNA, ligand–receptor interactions, and, in general, the reactivity of organic compounds [71]. This problem has been approached both experimentally in solution by ^1H NMR and UV spectroscopy, in the gas phase, as well as theoretically by conventional *ab initio* Hartree–Fock and density functional theory (DFT) calculations [72,73]. It has been found that, due to specific noncovalent interactions during the inclusion complexation process, a particular tautomer can be selected or even generated during crystallization [74]. For example, host **77** is extremely efficient at differentiating between tautomers of 1,2,4-triazole-**78** (a 1:1 complex between **77** and **78a**) and 1,2,3-triazole-**79** (a 1:1 complex between **77** and **79a**), whereas both tautomers of methyl 3(5)-methylpyrazole-**80** have been included into the 1:1:1 complex with host **77** [75,76].



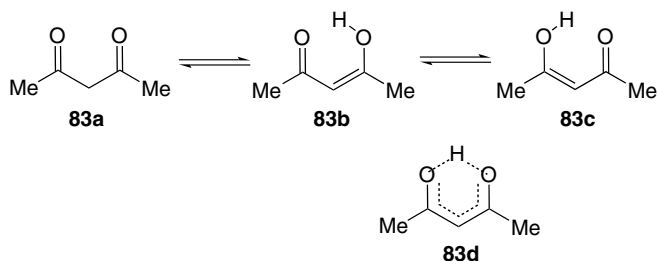
Modifications of the tautomeric equilibrium and therefore the pK_a value, through hydrogen-bond formation and the electrostatic solvation effects of imidazole, are

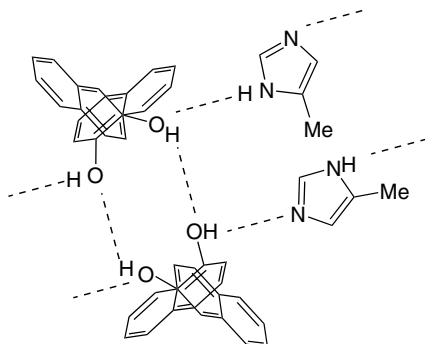
fundamental for explaining the mechanism of several biological processes involving histidine residues. As molecular recognition is solvent and host specific, co-crystallization of 2-ethyl-5-methylimidazole **81** and 2-ethyl-4-methylimidazole **82** with two other hosts—binaphthyl **17** and versatile host **1**—was attempted. In this case, recrystallization of **81b** and **1** from diethyl ether gave a 2:1:1 complex of **81b** and **17** and a solvent molecule [77].



The tautomer **82c** of 3-methylimidazole, however, was found in the 1:1 complex with *rac*-**17**. X-ray structure analysis of the above inclusion complex showed that molecules of **82c** act as hydrogen-bond donors and acceptors between two dimeric assemblies of binaphthyl molecules (Scheme 2). Methyl groups are located in the vicinity of the dimeric host. However, steric hindrance of this methyl group is less important for the energetics of crystal construction than formation of two hydrogen bonds.

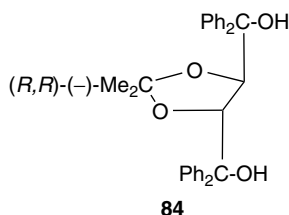
The keto–enol equilibrium of the 1,3-diketones has been the subject of intensive studies using various physical techniques and theoretical calculations [78–80]. Recently, X-ray crystal analysis of acetylacetone (**83**) was carried out at 110 K, and it was found that it exists as an equilibrium mixture of the two enol forms **83b** and **83c** [81]. Room-temperature studies show an acetylacetone molecule with the enolic H-atom centrally positioned, which can be attributed to the dynamically averaged structure **83d**. Application of a crystal engineering technique showed that a 1:1 inclusion complex of **83** can be formed with 1,1'-binaphthyl-2,2'-dicarboxylic acid in which the enol form is stabilized by a notably short intramolecular hydrogen bond [82].





Scheme 2

Another example is the 1:1:1 complex of acetylacetone with the host **74** and a water molecule in which again the enol form was observed. In the case of the 2:2 complex of acetylacetone with (*R,R*)-(-)-*trans*-4,5-bis(hydroxydiphenylmethyl)-2,2'-dimethyl-1,3-dioxacyclopentane **84**; however, a crystal measured at room temperature showed a disordered enolic proton, i.e. the presence of two enol forms. The same complex measured at 100 K revealed the pure enol form for both symmetrically independent molecules of acetylacetone [83]. The geometry of the enolic molecules resembled that obtained by gas-phase electron diffraction studies at room temperature [84].



The above examples show that proton transfer resulting in keto-enol tautomerism cannot be studied separately from the environment. The equilibrium between keto and enol forms, both in solution and in the solid state is a derivative of numerous noncovalent interactions that can stabilize a particular isomer. In this context, host-guest chemistry can shed more light towards understanding of the proton-transfer mechanism in biological systems.

7 CONCLUSIONS

Recent interest in the preparation of enantiopure compounds both in the laboratory and on an industrial scale has created the need for new synthetic methodologies

and efficient resolution processes. In particular, the optical resolution process is currently one of the most frequently investigated. The examples presented show that supramolecular concepts of host–guest chemistry with application to solid-state techniques could be used for designing new chiral host molecules. One of the characteristic features of these chiral host compounds is the property of optical resolution of a wide range of racemic guests. The resolution process is accomplished by the formation of inclusion complexes selectively with one enantiomer of the resolved compound, followed by chemical decomposition of the complex, distillation under low pressure, or fractional distillation. Complex formation is driven mostly by construction of the hydrogen-bonding network between host and guest molecules in the solid state. There is experimental evidence that protonic solvents may strongly influence chiral selection. Investigation of the resolution process showed unexpectedly that, for the designed host compounds, chiral resolution is efficient also in the solid state or in suspension media, giving optical purity around 100% and good yields. The rapid movement of guest molecules within the solid-state structure of the host is of particular interest. The chiral recognition process depends on the solid-state host structure, the character of the solvent used and the guest topography. Although the effective optical resolution of a new class of compounds is a matter of trial and error, there are already several versatile chiral host compounds that can be tried first. There is continuous need to design new, chiral host compounds capable of efficiently resolving racemates and isomeric mixtures of higher molecular weight compounds. As it has been shown, the chemistry of inclusion compounds also offers the opportunity of isomer separation and the generation of particular keto-enol isomers. From this perspective, it is reasonable to look for new types of versatile synthons, allowing both strong hydrogen bonding and enclathration opportunities.

REFERENCES

1. D. K. Kontepudi, K. L. Bullock, J. A. Digits, J. K. Hall and J. S. Miller, *J. Am. Chem. Soc.*, **1993**, *115*, 10211.
2. J. M. McBride and R. L. Carter, *Angew. Chem. Int. Ed. Engl.*, **1991**, *30*, 293.
3. L. Addadi, S. Weinstein, E. Gati, I. Weissbuch and M. Lahav, *J. Am. Chem. Soc.*, **1982**, *104*, 4610.
4. L. Addadi, Z. Berkovitch-Yellin, N. Domb, E. Gati, M. Lahav and L. Leiserovitz, *Nature (London)*, **1982**, *296*, 21.
5. L. Pasteur, *Leçons de Chimie professées en 1860*, Société Chimique de Paris, **1861**, 25.
6. J. Jacques and A. Collet, 'Enantiomers, Racemates and Resolutions', Wiley, New York, **1981**.
7. P. Piras, C. Roussel and J. Pierrot-Sanders, *J. Chromatogr. A*, **2001**, *906*, 443.
8. J. Haginaka, *Trends Glycosci. Glycotechnol.*, **1997**, *9*, 399.
9. A. Rizzi, *Electrophoresis*, **2001**, *22*, 3079.

10. D. Zbaida, M. Lahav, K. Drauz, G. Knaup and M. Kottenhahn, *Tetrahedron Asymm.*, **2000**, *56*, 6645.
11. Solid-State Supramolecular Chemistry: Crystal Engineering, Vol. 6, in *Comprehensive Supramolecular Chemistry*, ed. J. L. Atwood, J. E. D. Davies, D. D. MacNicol, F. Vögtle, Pergamon Oxford, **1996**
12. F. Toda and K. Akagi, *Tetrahedron Lett.*, **1968**, 3695.
13. F. Toda, D. L. Ward and H. Hart, *Tetrahedron Lett.*, **1981**, *22*, 3865.
14. F. Toda, K. Tanaka, Y. Wong and G.-H. Lee, *Chem. Lett.*, **1986**, 109.
15. D. Seebach, A. K. Beck and A. Heckel, *Angew. Chem., Int. Ed.* **2001**, *40*, 92, and references cited therein.
16. F. Toda, in *Advances in Supramol. Chem.*, **1992**, *2*, 149.
17. F. Toda, in *Advances in Supramol. Chem.*, ed. G. W. Gokel, **1995**, JAI Press, London, *2*, 141.
18. F. Toda, K. Tanaka and A. Seikawa, *J. Chem. Soc., Chem. Commun.*, **1987**, 279.
19. G. Kaupp, J. Schmeyers, F. Toda and H. Koshima, *J. Phys. Org. Chem.*, **1996**, *29*, 137.
20. F. Toda and Y. Tohi, *J. Chem. Soc., Chem. Commun.*, **1993**, 1238.
21. K. Tanaka and F. Toda, **1983**, *J. Chem. Soc., Chem. Commun.*, 1513.
22. F. Toda, K. Tanaka and T. C. W. Mak, *Chem. Lett.*, **1985**, 195.
23. F. Toda, K. Tanaka and T. C. W. Mak, *Chem. Lett.*, **1986**, 113.
24. F. Toda, K. Tanaka and T. C. W. Mak, *Chem. Lett.*, **1986**, 1909.
25. F. Toda, M. Khan and T. C. W. Mak, *Chem. Lett.*, **1985**, 1867.
26. F. Toda, A. Kai, Y. Tagami and T. C. W. Mak, *Chem. Lett.*, **1987**, 1393.
27. F. Toda, K. Tanaka, L. Nassimbeni and M. Niven, *Chem. Lett.*, **1988**, 1371.
28. F. Toda and K. Tanaka, *J. Chem. Soc., Chem. Commun.*, **1997**, 1087.
29. R. Noyori, I. Tomio, Y. Tanimoto and M. Nishizawa, *J. Am. Chem. Soc.*, **1984**, *106*, 6709.
30. D. Seebach, A. K. Beck, A. Roggo and A. Wonnacott, *Chem. Ber.*, **1985**, *118*, 3673.
31. B. M. Trost and D. J. Murphy, *Organometall.*, **1985**, *4*, 1143.
32. (a) F. Toda, K. Mori and J. Okada, *Chem. Lett.*, **1988**, 131; (b) F. Toda, K. Mori and A. Sato, *Bull. Chem. Soc. Jpn.*, **1988**, *61*, 4167.
33. E. B. Kyba, K. Koga, L. R. Sousa, M. G. Siegel and D. J. Cram, *J. Am. Chem. Soc.*, **1973**, *95*, 2692.
34. J. Jacques, C. Fouguey and R. Viterbo, *Tetrahedron Lett.*, **1971**, 4617.
35. M. Takemoto, Y. Suzuki and K. Tanaka, *Tetrahedron Lett.*, **2002**, *43*, 8499.
36. K. Tanaka, A. Moriyama and F. Toda, *J. Chem. Soc., Perkin Trans. 1*, **1996**, 603.
37. K. Tanaka, T. Okada and F. Toda, *Angew. Chem. Int. Ed. Engl.*, **1993**, *32*, 1147.
38. J. G. Deng, Y. X. Chi, F. M. Fu, X. Cui, K. B. Yu, J. Zhu and Y. Z. Jiang, *Tetrahedron Asymm.*, **2000**, *11*, 1729.
39. J. X. Cai, Z. H. Zhou, K. Y. Li, C. H. Yeung and C. C. Tang, *Chin. Chem. Lett.*, **2002**, *13*, 617.
40. O. Korpium, R. A. Levis, J. Chickos and K. J. Mislow, *J. Am. Chem. Soc.*, **1968**, *90*, 4842.
41. D. B. Cooper, C. R. Hall, J. M. Harrison and D. T. Inch, *J. Chem. Soc.*, **1977**, 1969.
42. C. R. Hall, D. T. Inch and I. W. Lawson, *Tetrahedron Lett.*, **1979**, 2729.
43. K. Shioji, Y. Ueno, Y. Kurauchi and K. Okuma, *Tetrahedron Lett.*, **2001**, *42*, 6569.
44. F. Toda, K. Mori, Z. Stein and I. Goldberg, *J. Org. Chem.*, **1988**, *53*, 308.

45. F. Toda, K. Tanaka and S. Nagamatsu, *Tetrahedron*, **1984**, 25, 4929.
46. F. Toda, K. Tanaka and T. C. W. Mak, *Chem. Lett.*, **1984**, 2085.
47. F. Toda and K. Mori, *J. Chem. Soc., Chem. Commun.*, **1986**, 1357.
48. K. Tanaka, Sh. Honke, Z. Urbanczyk-Lipkowska and F. Toda, *Eur. J. Org. Chem.*, **2000**, 3171.
49. M. Schudok and G. Kretzschmar, *Tetrahedron Lett.*, **1997**, 38, 387–388.
50. F. Toda, K. Tanaka, I. Miyahara, S. Akutsu and K. Hirotsu, *J. Chem. Soc., Chem. Commun.*, **1994**, 1795.
51. F. Toda, S. Soda and I. Goldberg, *J. Chem. Soc., Perkin Trans. 1*, **1993**, 2357.
52. T. Vries, H. Wynberg, E. van Echten, J. Koek, W. ten Hoeve, R. M. Kellog, J. Broxtermann *et al.*, *Angew. Chem. Int. Ed.*, **1998**, 37, 2349.
53. I. Markovits, G. Egri and E. Fogassy, *Chirality*, **2002**, 14, 674.
54. G. Kemperman, R. de Gelder, F. J. Dommerholt, P. C. Raemakers-Franken, A. J. H. Klunder and B. Zwanenburg, *J. Chem. Soc., Perkin Trans. 2*, **2000**, 1425.
55. K. Sada, K. Yoshikawa and M. Miyata, *Chem. Commun.*, **1998**, 1763.
56. Y. Liu, C. C. You, Y. Chen, T. Wada and Y. Inoue, *J. Org. Chem.*, **1999**, 64, 7781.
57. G. J. Kemperman, R. de Gelder, F. J. Dommerholt, P. C. Raemakers-Franken, A. J. H. Klunder and B. Zwanenburg, *Eur. J. Org. Chem.*, **2001**, 19, 3641.
58. Y. Liu, Y. Chen, B. Li, T. Wada and Y. Inoue, *Chem. Eur. J.*, **2001**, 7, 2528
59. F. Toda, *Top. Curr. Chem.*, **1987**, 140, 43.
60. F. Toda, K. Tanaka, M. C. Wong and T. C. W. Mak, *Chem. Lett.*, **1987**, 2069.
61. M. Segawa, K. Mori and F. Toda, *Chem. Lett.*, **1988**, 1755.
62. F. Toda, K. Tanaka and A. Sekikawa, *J. Chem. Soc., Chem. Commun.*, **1987**, 279.
63. M. R. Caira, L. R. Nassimbeni, F. Toda and D. Vujovic, *J. Chem. Soc. Perkin Trans 2*, **1999**, 2681.
64. A. Gavezzotti, *Crystallogr. Rev.*, **1998**, 7, 5.
65. A. Vedani and J. D. Dunitz, *J. Am. Chem. Soc.*, **1985**, 107, 7653.
66. M. R. Caira, L. R. Nassimbeni, F. Toda and D. Vujovic, *J. Am. Chem. Soc.*, **2000**, 122, 9367.
67. F. Toda, K. Tanaka and A. Kai, *Chem. Lett.*, **1988**, 1375.
68. M. R. Caira, A. Horne, L. R. Nassimbeni and F. Toda, *J. Chem. Soc., Perkin Trans. 2*, **1977**, 1717.
69. F. Toda, K. Tanaka, T. Hoyoda and T. C. W. Mak, *Chem. Lett.*, **1988**, 107.
70. F. Toda, S. Hirano, S. Toyota, M. Kato, Y. Sugio and T. Hachiya, *CrystEngComm*, **2002**, 4, 171.
71. E. Iglesias, *J. Org. Chem.*, **2000**, 65, 6583.
72. V. Barone, M. Cossi and J. Tomasi, *J. Comput. Chem.*, **1998**, 19, 404.
73. G. Bakalarski, P. Grochowski, J. S. Kwiatkowski, B. Lesyng and J. Leszczynski, *Chem. Phys.*, **1996**, 204, 301.
74. F. Toda, *CrystEngComm*, **2002**, 4, 215.
75. F. Toda, K. Tanaka, J. Elguero, L. Nassimbeni and M. Niven, *Chem. Lett.*, **1987**, 2317.
76. F. Toda, *Top. Curr. Chem.*, **1987**, 1061.
77. M. Yagi, S. Hirano, S. Toyota, M. Kato and F. Toda, *CrystEngComm*, **2002**, 4, 143.
78. J. Emsley, *Struct. Bonding*, **1984**, 57, 147.
79. Z. Rappoport, *The Chemistry of Enols*, J Wiley, **1990**.

80. A. J. Villa, C. M. Lagier and A. C. Olivieri, *J. Chem. Soc., Perkin Trans. 2*, **1990**, 1615.
81. R. Boese, M. Y. Antipin, D. Blaeser and K. A. Lysenko, *J. Phys. Chem. B*, **1998**, *102*, 8654.
82. O. Gallardo, I. Csoregh and E. Weber, *J. Chem. Crystallogr.*, **1995**, *25*, 769.
83. Z. Urbanczyk-Lipkowska, K. Yoshizawa, S. Toyota and F. Toda, *CrystEngComm*, **2003**, *5*, 114.
84. K. Iijima, A. Ohnogi and S. Shibata, *J. Mol. Struct.*, **1987**, *156*, 111.

Chapter 2

Enantiomer Ordering and Separation During Molecular Inclusion

ROGER BISHOP

*School of Chemical Sciences, University of New South Wales, UNSW Sydney
NSW 2052, UNSW SYDNEY NSW 2052, Australia*

1 INTRODUCTION

The formation of lattice inclusion compounds has long been regarded as a fascinating area of chemistry. In the early days it was a rare and unpredictable phenomenon that was difficult to explain [1,2]. Nowadays, although such behaviour is more familiar and better understood, it still carries with it an air of mystery.

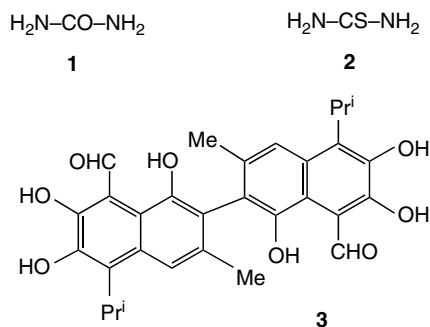
Molecular inclusion is now known to involve factors such as the size and shape of the various component molecules or ions, their complementarity, intermolecular forces of attraction and repulsion, directional forces and properties, and supramolecular synthons [3], all of which make their contribution to the overall lattice energy.

A further consideration is the chirality (handedness) of both the individual components and the resulting molecular assembly. This important aspect is the subject of this chapter. Although the role of chirality has been discussed with respect to individual examples, I believe that this is the first occasion where this particular property has been reviewed with reference to clathrate behaviour in

general. Due to the enormous scope of modern inclusion chemistry, this article is selective and deals only with representative cases, in particular examples encountered during our own work. I hope, however, that this account will set the scene for wider and more thorough discussion.

2 ACHIRAL AND ATROPISOMERIC HOST MOLECULES

A number of well-known host molecules have achiral molecular structures. In other words, the atoms of these molecules are, or may formally be, arranged in space such that a plane of symmetry or a centre of symmetry is present. At first sight, this group of compounds may appear to be irrelevant to a discussion on chirality, but this is far from being so.



Achiral objects can be assembled into chiral solid-state structures, and this is frequently the case for urea **1** when it encloses guests. Other compounds adopt a chiral conformation in solution and therefore may ultimately produce either chiral or achiral host structures. On the other hand, thiourea **2** forms an inclusion lattice that is achiral. This arrangement is nonetheless very effective in enclosing guest molecules.

Further compounds, such as gossypol **3**, normally exist as atropisomers due to steric crowding effects. Hence, it is possible to prepare the compound in a homochiral state, provided that the experimental temperature is not raised sufficiently to overcome the restricted rotation energy barrier. If this does occur, then the outcome is a racemic mixture of (+)- and (-)-isomers.

2.1 Formation of Chiral Inclusion Structures

The best-known example of an achiral molecule forming a chiral inclusion structure is that of the hexagonal urea tubulate [4] lattice (Figure 1). Helical assembly

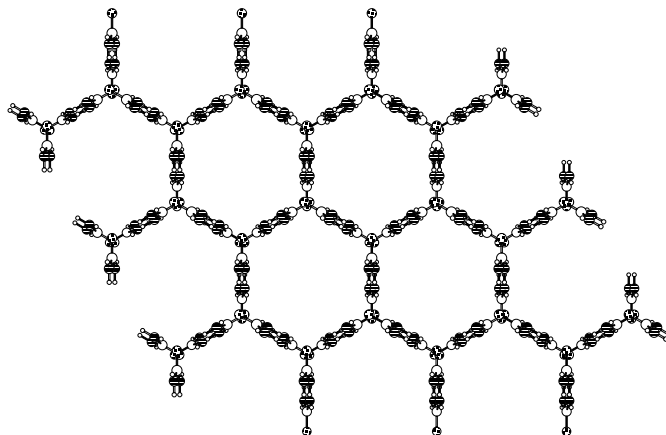


Figure 1 Projection in the ab plane of the host lattice of a typical urea tubulate inclusion structure in space group $P6_122$ with the guest molecules omitted. Atom designators: O stippling, N horizontal hatching, C and H unshaded.

of urea **1** molecules leads to formation of chiral crystals in the space group $P6_122$ (and its enantiomorph $P6_322$) [5–7]. In some cases, these hexagonal inclusion compounds undergo reversible conversion into a low-temperature form in chiral space group $P2_12_12_1$. This change results from the guest molecules adopting preferred orientations in the tubes, with concomitant deformation of the walls [8].

Under normal circumstances, and using an achiral or homochiral guest, a 1:1 mixture of (+)- and (–)-urea inclusion crystals will form [9,10]. If the guest is racemic, on the other hand, then the four compounds (+)-host/(+)-guest, (+)-host/(–)-guest, (–)-host/(+)-guest, and (–)-host/(–)-guest all can be produced. It is for this reason that chirally pure inclusion hosts are simpler to use in guest resolution experiments [11–13].

To employ urea successfully as a resolving agent for racemic guests, it therefore is necessary to induce preferential formation of one of the chiral host forms. This can be achieved through seeding, crystallisation on a chiral surface, or crystallisation with chiral co-solutes such as sugars. The diastereomeric pair produced, for example (+)-host/(+)-guest and (+)-host/(–)-guest, then can be separated and the resolved guest recovered. Repetition of the process several times can result in excellent resolution, and separation does not depend on specific functional group types. For example, (+)-2-chlorooctane has been obtained in 95.6% purity [14].

2.2 Formation of Achiral Inclusion Structures

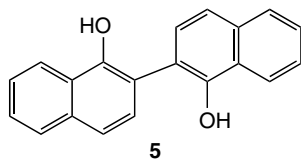
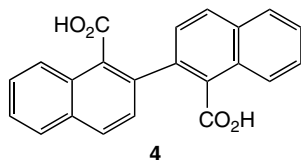
Like urea, thiourea **2** also forms tubulate inclusion compounds with a rather similar cross-sectional topology [15]. However, the tubes are now differently

shaped and wider. Whereas the urea tubes have a roughly uniform diameter (c. 5.5–5.8 Å) along their tube axis, the thiourea tubes (c. 5.8–7.1 Å diameter) contain large bulges and therefore are able to accommodate much larger guests. Thiourea tubulate crystals normally form in space group $R\bar{3}c$ and therefore are achiral. Thus, unlike urea, the thiourea tubes cannot be used for chiral separations, chiral polymerisation reactions [16,17], and related experiments.

2.3 Hosts Exhibiting Atropisomerism

Gossypol is a natural product isolated from the cotton plant, and has the binaphthyl structure **3**. Its molecular structure is formally achiral in the sense that it can be drawn with a plane and a centre of symmetry. However, in practice, this arrangement is an energy maximum (conformational transition state) due to crowding between the methyl and hydroxy substituents flanking the bond between the two identical binaphthyl subunits. This results in restricted rotation at laboratory temperatures. Hence, gossypol exhibits atropisomerism, and can exist either as a racemic mixture of both enantiomers or in the chirally pure form. Racemic gossypol is a versatile host molecule, and over 100 inclusion compounds have been reported. In contrast, however, enantiomerically pure samples of gossypol usually give crystals whose quality is inadequate for X-ray analysis [18].

Other well-known molecules that similarly exist as chiral scissor-like C_2 -symmetrical structures, are the diacid **4** and the bis(naphthol) **5**. Both of these substances are potent inclusion hosts. However, racemic **4** shows greater inclusion potential than the resolved material, while both racemic and resolved samples of **5** have rich inclusion chemistry [19,20].



3 RACEMIC MIXTURES OF CHIRAL HOST MOLECULES

Chiral molecules are frequently synthesised as a 1:1 mixture of both enantiomers (a racemic mixture), and the most common occurrence on crystallisation is

formation of a lattice containing both these enantiomers. Less commonly, a conglomerate is produced instead. In this instance, the two enantiomeric molecules separate completely, and a 1:1 mixture of chirally pure (+)- and (–)-crystals is produced [9,10].

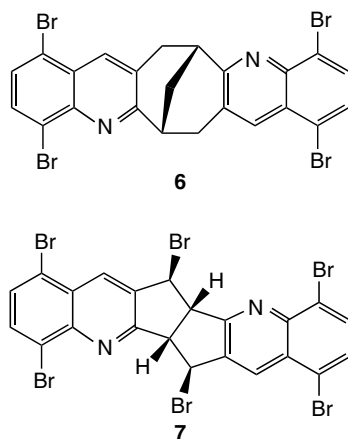
A related phenomenon can also occur when the crystal lattice packing is chiral. This intrinsic handedness can result in formation of a 1:1 mixture of enantiomeric crystals. In this case, although there has been self-resolution into (+)- and (–)-crystals, both molecular enantiomers remain unseparated in each crystal. The fundamental distinction is that a conglomerate single crystal contains only one molecular enantiomer and therefore would be optically active in solution, while, for the latter, a single crystal contains both molecular enantiomers and its solution would be optically inactive.

These various possibilities are examined here in the context of lattice inclusion compounds.

3.1 Formation of Unresolved Inclusion Structures

3.1.1 Centrosymmetric enantiomer ordering

Recently, we have been investigating the chemistry of a series of racemic diquinoline compounds that form lattice inclusion hosts. The solid-state structures of these involve only rather weak intermolecular attractions. A number of these hosts assemble by means of centrosymmetric supramolecular synthons, and therefore their enantiomer separation is limited in the solid state.



For example, the racemic tetrabromide **6** invariably forms inclusion compounds with a staircase structure. Each host molecule contributes one of its aromatic

wings as a staircase step, while the second aromatic wing acts as a staircase surround. The guest molecules occupy interstitial channels between the parallel infinite staircases, as illustrated in Figure 2 for the inclusion compound with benzene [21].

The dominant supramolecular synthon present in these compounds is the pi-halogen dimer (PHD) interaction [22]. This efficient packing motif results from two inversion-related host molecules packing such that one bromine atom from each is situated in the cleft of its V-shaped partner (Figure 3), in addition to aromatic *endo*, *endo*-facial interaction.

The series of inclusion compounds formed by **6** differ in the details of their staircase construction and guest inclusion, but their common feature is the PHD interaction involving pairs of opposite enantiomers. Between these step pairs, however, there may be a twofold axis or no symmetry at all. In some examples, such as **(6)**₄·(benzene), there are two independent molecules (A and B) in the asymmetric unit. The staircase structure now contains both A–A* and B–B* PHD interactions (where * indicates the enantiomer of opposite handedness), as illustrated in Figure 4.

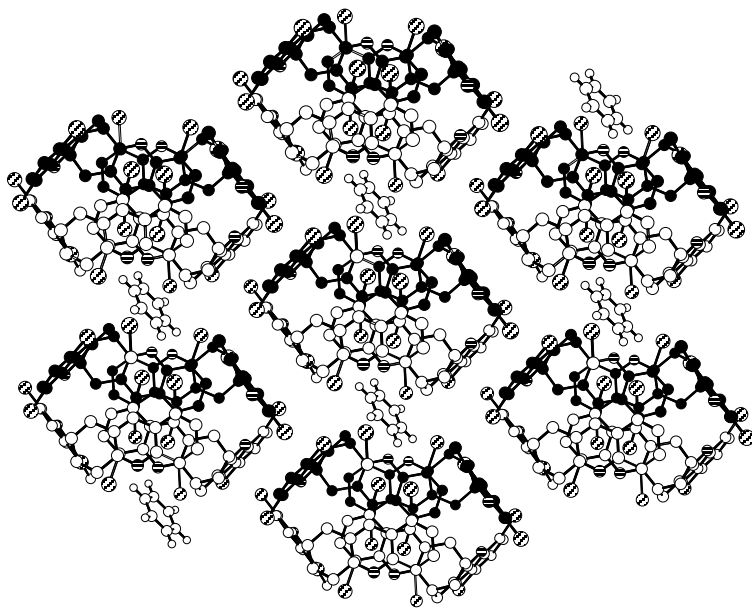


Figure 2 Projection in the *ac* plane of the inclusion compound **(6)**₄·(benzene) showing several host molecular staircases (hexagonal projection). The guest molecules occupy interstitial channels between these staircases. Host hydrogen atoms are omitted for clarity. In this figure, and subsequent ones, the opposite enantiomers are indicated by white or black carbon atoms, and the atom designators N (horizontal hatching) and Br (diagonal hatching), are used.

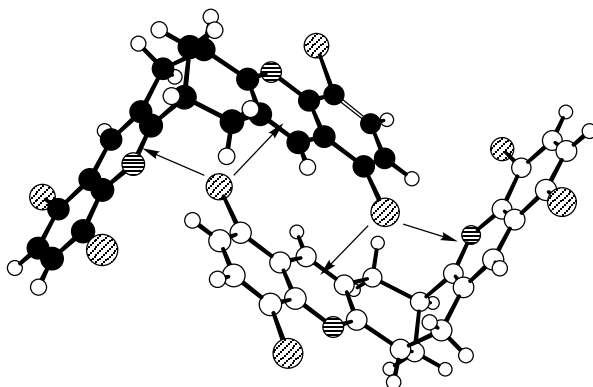


Figure 3 A centrosymmetric PHD interaction present in the structure of $(\mathbf{6})_4 \cdot (\text{benzene})$, with the arrows indicating the four $\pi \cdots \text{Br}$ interactions present in this *endo*, *endo*-facial motif.

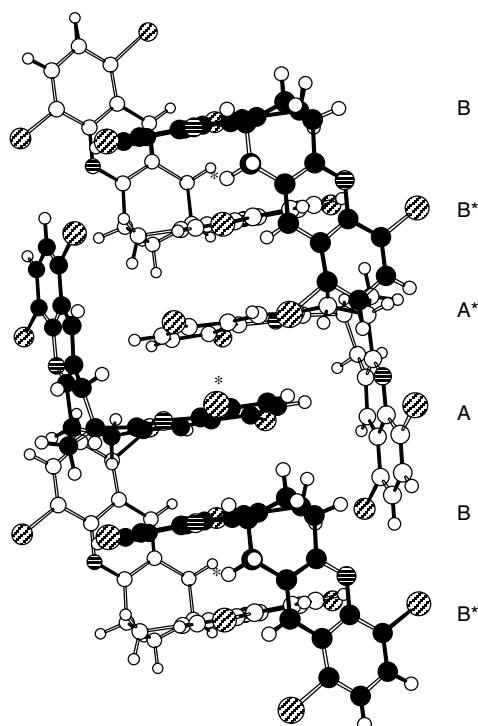


Figure 4 Side view of a molecular staircase along *b* in the compound $(\mathbf{6})_4 \cdot (\text{benzene})$. Two types of centrosymmetric PHD interactions, involving the independent host molecules A–A* and B–B*, are present in this particular case. Centres of symmetry are designated by * symbols in the middle of the PHD interactions.

Solvent-free samples of the hexabromide **7** crystallise with the molecules arranged in layers, and large numbers of Br...Br attractions holding the layers together [23]. Each layer is constructed from parallel chains of **7** molecules, linked by aromatic edge-face (EF) and both offset *exo*, *exo*- and *endo*, *endo*-facial OFF interactions [24,25]. Enantiomer ordering in this structure is simple. The (+)- and (-)-enantiomers alternate along each chain and are associated by means of the centrosymmetric OFF interactions (Figure 5).

In crystalline **7** there is only poor interaction between the parallel chains, and it is this property that results in its special inclusion behaviour. The only guests included are small aromatic hydrocarbons, and these usually give a host:guest ratio of 1:1. Incorporation of the guests between the parallel chains increases the OFF and EF attractions within the layers, with concomitant reduction of the Br...Br interactions between layers.

In the benzene inclusion compound, each host-host *exo*, *exo*-facial interaction switches to a centrosymmetric PHD interaction. Effectively, a small mutual rotation converts one OFF and two EF interactions of the host dimer into four aryl π ...Br interactions. This change allows the smaller benzene guest to become incorporated between the layers, as well as within them (Figure 6). The resulting inclusion compound, $(\mathbf{7})_2 \cdot (\text{benzene})_3$, has even more aromatic interactions and therefore has the lowest energy of the series. Throughout this series of structures, the host enantiomer ordering remains unchanged.

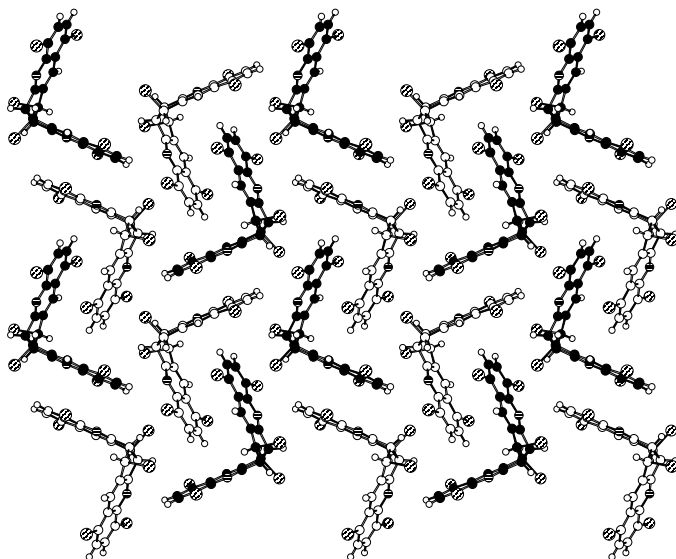


Figure 5 View of one layer of the structure of solvent-free **7**, close to the *bc* plane, showing the parallel chains of molecules running vertically (along *b*). These are linked by means of OFF and EF interactions.

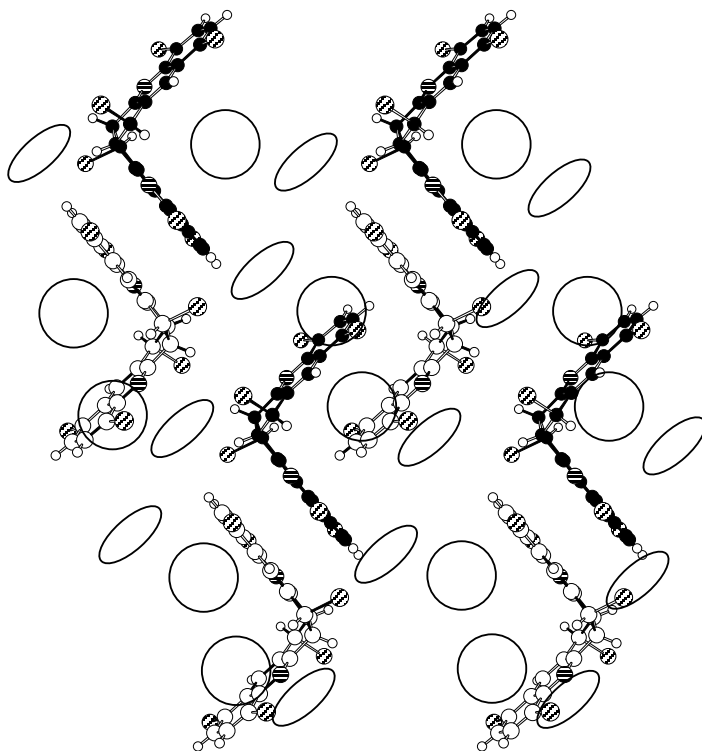
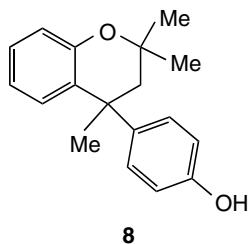


Figure 6 View of one layer of $(7)_2 \cdot (\text{benzene})_3$, showing the relative orientations of the benzene guests edge-on within the host layers (ellipses) and in-plane between the layers (circles). The host molecules within the vertical chains are now linked by means of PHD interactions.



Dianin's compound **8** is a famous example of a lattice inclusion host from the early days of inclusion chemistry [26,27]. It is usually prepared as the racemate and forms inclusion compounds with many guests in space group $R\bar{3}$. Six molecules of **8** assemble by means of their phenolic groups into a near-planar hydrogen-bonded $(-\text{O}-\text{H})_6$ cycle, with alternate molecules being orientated up

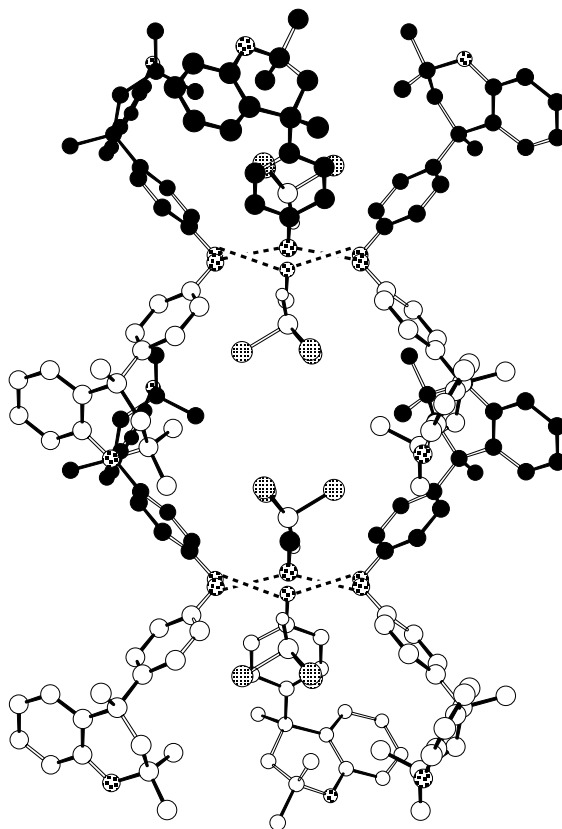


Figure 7 The structure formed when Dianin's compound **8** is crystallised from chloroform. Each cage is closed at the top and bottom by (O–H)₆ cycles of hydrogen bonds (dashed lines). In this figure, the front and back molecules of **8** have been removed to reveal the two chloroform guest molecules occupying the central cage. Oxygen atoms are indicated by heavy stippling, chlorines by light stippling, and all host hydrogens are omitted for clarity.

and down around the ring. The aromatic groups of neighbouring assemblies intermesh to generate cages that surround the guests (Figure 7) [28]. Each cage is about 10.9 Å long and has a hourglass-shaped internal cavity (maximum and minimum diameters 7.1 and 4.1 Å, respectively).

The enantiomer ordering in the Dianin inclusion compounds is simple, with the opposite enantiomers (R and R*) alternating around each (–O–H)₆ cycle (Figure 8). Mundane though it appears, this centrosymmetric arrangement is actually critical for success. Resolved samples of Dianin's compound no longer show inclusion behaviour, do not form (–O–H)₆ cycles, and pack entirely differently in space group $P2_12_12_1$ [29].

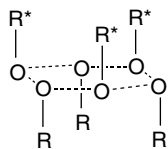
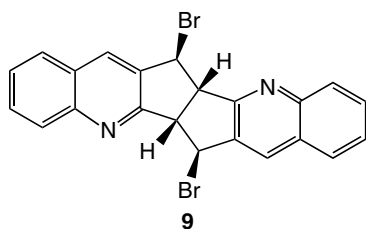


Figure 8 A diagrammatic simplification of the solid state (O–H)₆ hydrogen-bonding motif formed by racemic samples of Dianin’s compound. The opposite enantiomers R and R* alternate around the (O–H)₆ cycle to create a centrosymmetric hydrogen-bonded motif.

3.1.2 Significant enantiomer separation

Many other crystallisations result in compounds that still contain both enantiomers, but where considerable separation or ordering of these has occurred. In other words, significant regions of local chirality can be present in the solid, but these are counterbalanced by equivalent regions of the opposite handedness.



One example is the racemic dibromide **9**, where two host molecules invariably wrap around a guest molecule to form a penannular unit [30]. The *exo*-faces of these units associate through aromatic offset face–face (OFF) attractions to form layers of guest-containing molecular pens, and the layers associate by means of two types of double C–H \cdots N interactions. One of these is a bifurcated arrangement Ar–H \cdots N \cdots aliphatic H–CBr–, and the other is an eight-membered double Ar–H \cdots N cycle. Figure 9 illustrates one layer, and Figure 10 the interlayer association, for the case of (**9**)₂·(CH₃–CCl₃).

Both C–H \cdots N motifs operate edge–edge, and between opposite enantiomers of **9**. The molecules of **9** within each layer may be enantiomerically pure (as for this case), or may be a mixture of enantiomers (as for the trifluoromethylbenzene compound, Section 3.3). However, in all cases, the layers stack edge–edge, with the double C–H \cdots N weak hydrogen bonds [31] operating only between opposite enantiomers of the host molecules.

When racemic diol **10** is crystallised from small solvents, an extraordinary type of inclusion compound is formed. These compounds, (**10**)₄·(guest), have a unit cell in space group *I4₁/acd* containing 32 molecules of the host diol and

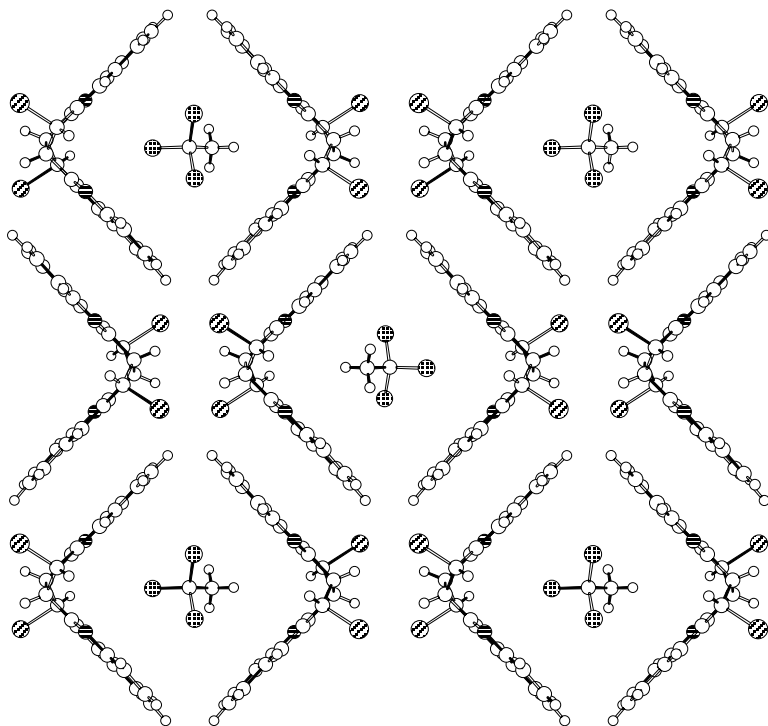
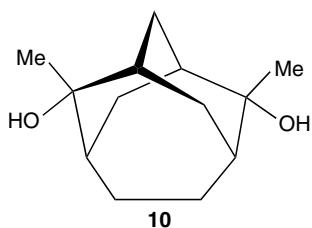


Figure 9 A projection in the *ab* plane of one layer of molecular pens in the inclusion compound $(\mathbf{9})_2 \cdot (\text{CH}_3\text{-CCl}_3)$. All the host molecules in a given layer have the same chirality, and neighbouring pens associate by means of aromatic OFF interactions.



8 of the guest. The crystal superlattice is built from two identical, but inversion related, interpenetrating sublattices [32]. Small, rugby ball-shaped cavities are formed where the two sublattices interpenetrate, and these spaces contain the guest molecules.

Each sublattice of this ellipsoidal clathrate structure contains both diol **10** enantiomers. However, interpenetration creates fourfold screw axes of both handedness. Only one diol enantiomer participates in the 4_1 axes, and only the other

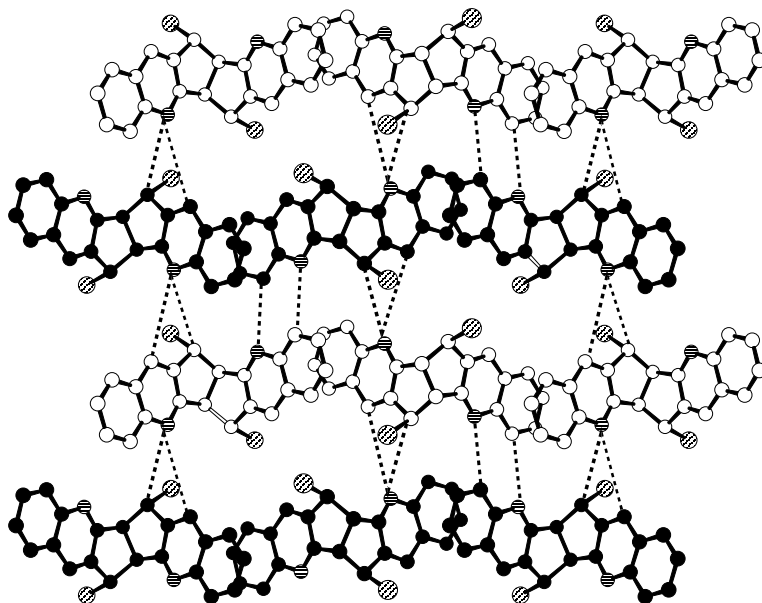


Figure 10 The two types of edge–edge C–H...N interactions (dashed lines) present between four layers of molecular pens in the structure $(\mathbf{9})_2 \cdot (\text{CH}_3\text{-CCl}_3)$. These interactions all operate between opposite enantiomers of the host. Hydrogen atoms are omitted for clarity.

enantiomer in the 4_3 axes. Figure 11 shows six adjacent fourfold screw axes, projected in the ab plane. Between these axes lie constricted channels that contain the guest cavities. Alternate cavities along the channel are orthogonal (Figure 12). Once again, this achiral lattice contains large regions with local homochirality, and it shows a remarkable degree of enantiomer ordering within its structure.

Another case of major enantiomer separation occurs when helical tubuland diols (Section 3.2.1) are crystallised with small phenol molecules and intimately hydrogen bonded co-crystals are produced. A typical example is $(\mathbf{11}) \cdot (p\text{-chlorophenol})$ [33]. The major supramolecular synthon is H–O...H–O...H–O... hydrogen bonding with eclipsed stacks of the participating molecules surrounding a pseudo-threefold screw axis (Figure 13). This chiral motif involves molecules of p -chlorophenol and only one of the enantiomers of **11**.

Propagation of the lattice through similar use of the second diol hydroxy groups creates a layer. Hence, the crystal structure of $(\mathbf{11}) \cdot (p\text{-chlorophenol})$ comprises a series of parallel layers, each of which is chiral. The net structure, however, is achiral because adjacent layers are of opposite handedness (Figure 14).

An analogous structure is produced when the helical tubuland diol **12** forms a 1:1 co-crystalline adduct with methanol (Figure 15). The lattice, as before, comprises stacked layers of alternating chirality, but overall is an achiral structure [34].

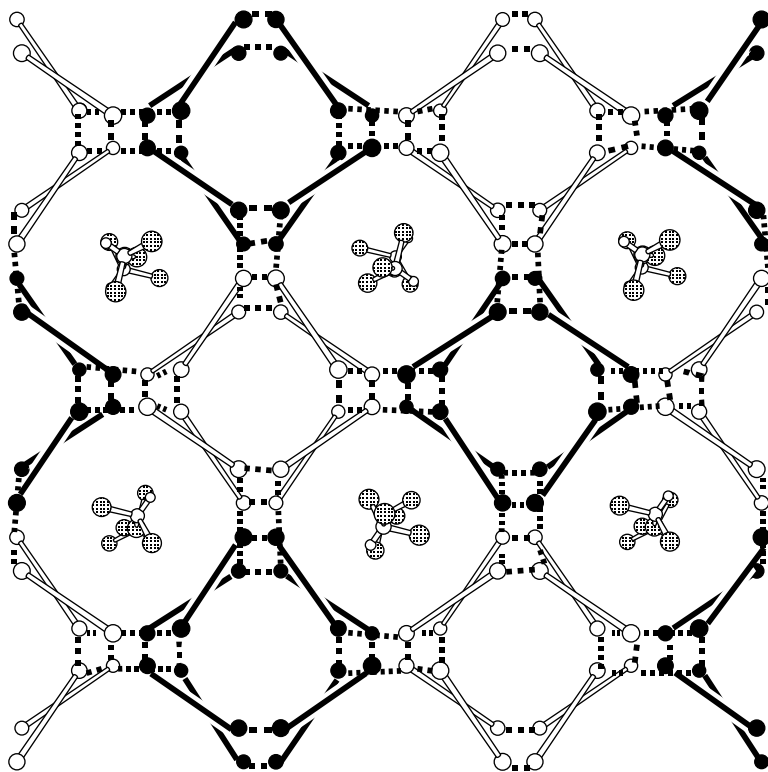
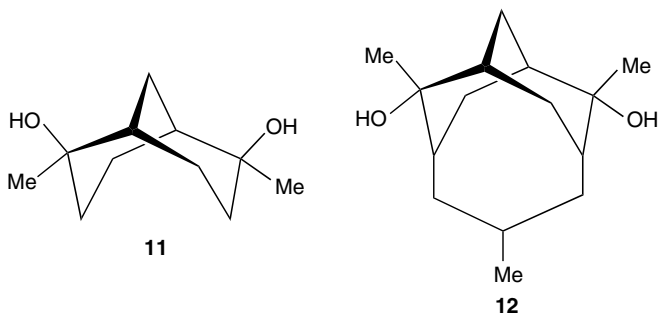


Figure 11 Diagrammatic representation of the ellipsoidal clathrate compound $(\mathbf{10})_4 \cdot (\text{chloroform})$ projected in the ab plane. The black and white coding indicates the host enantiomers. Diol molecules are represented as two oxygen atoms (solid spheres) joined by their carbocyclic framework (solid rod). Dashed lines represent the hydroxy hydrogen bonds. The three 4_1 screw axes involve only one enantiomer of $\mathbf{10}$ (surrounded by white rods), and the three 4_3 screw axes the other (black rods). Each ellipsoidal clathrate cage site is, however, centrosymmetric.



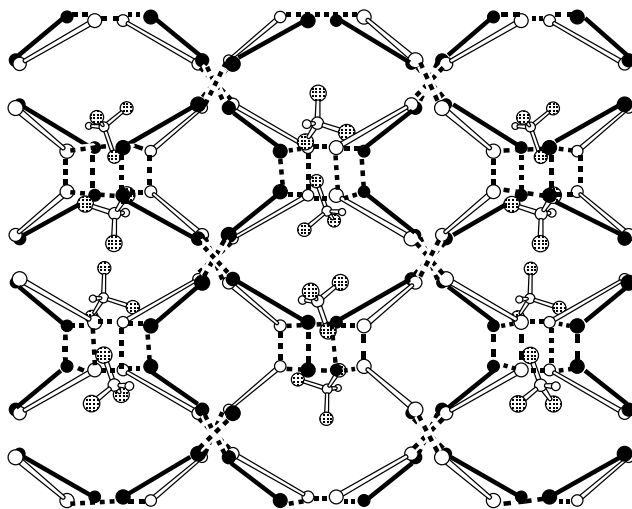


Figure 12 A similar representation of $(10)_4 \cdot (\text{chloroform})$ but projected on to the ac plane. The ellipsoidal cavities that make up the vertical columns are alternately orthogonal.

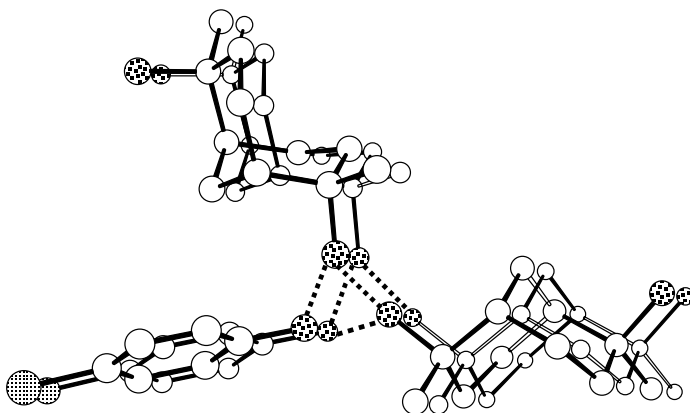


Figure 13 The pseudo-threefold screw arrangement of diol and p -chlorophenol molecules in the structure $(11) \cdot (p\text{-chlorophenol})$. Hydrogen atoms are omitted for clarity, and the hydrogen bonding is designated by dashed lines.

3.2 Self-resolution of Enantiomeric Molecules

3.2.1 Enantiomeric self-resolution on crystallisation

The helical tubuland (HT) diols are a group of alicyclic dialcohols that show characteristic crystallisation behaviour [32,35]. When a racemic sample is crystallised, then enantiomeric self-resolution occurs, yielding a conglomerate of (+)- and

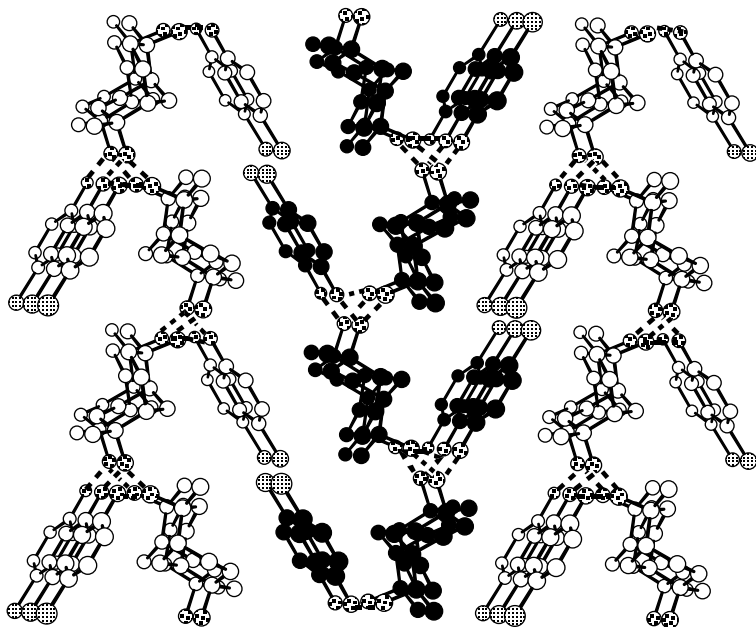


Figure 14 Part of the $(11) \cdot (p\text{-chlorophenol})$ structure projected in the bc plane, showing three parallel layers edge-on and with their hydrogen atoms omitted. The alternating handedness of adjacent layers is apparent.

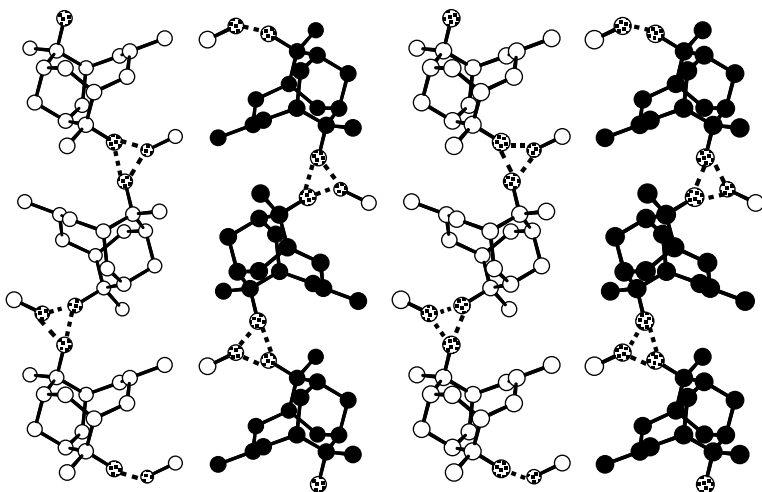


Figure 15 The $(12) \cdot (\text{methanol})$ structure projected in the bc plane and showing the parallel layers of opposite chirality. Hydrogen atoms are omitted for clarity.

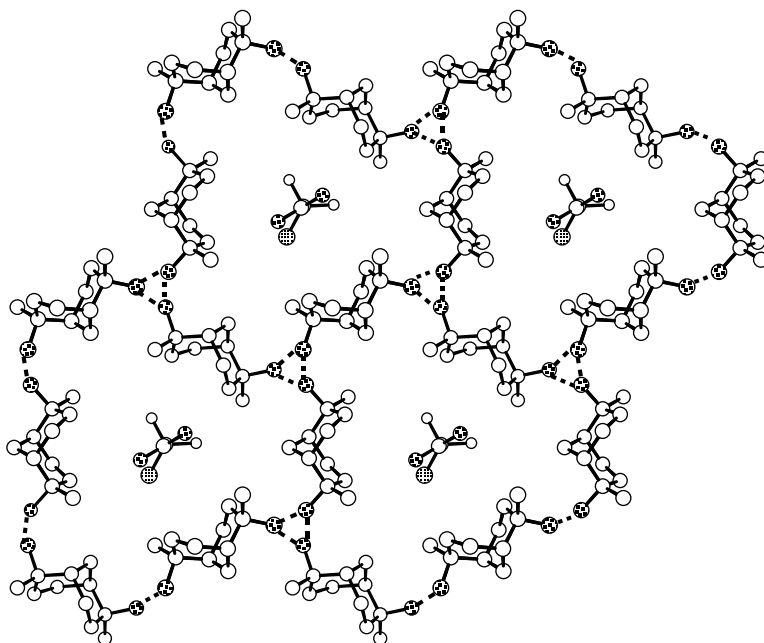


Figure 16 Projection in the *ab* plane of the helical tubulate structure of $(\mathbf{11})_3 \cdot (\text{chloroacetic acid})_{1,2}$ with all host hydrogen atoms omitted. The chloroacetic acid guest molecules trapped within the tubes are present as centrosymmetric hydrogen-bonded dimers.

(–)-diol crystals in space groups $P3_121$ and $P3_221$. The hydrogen-bonded network lattice contains parallel tubes filled with guest molecules (Figure 16).

The supramolecular synthon underpinning formation of the helical tubulate host lattice is $\text{H-O} \cdots \text{H-O} \cdots \text{H-O} \cdots$ hydrogen bonding surrounding a threefold screw axis (Figure 17). This arrangement is remarkably resilient for diol **11**, and still forms in the presence of many polar guests (such as chloroacetic acid, ethanol and dimethyl sulfoxide) capable of hydrogen bonding [36]. These guests are trapped within the tubes as helical tubulate inclusion compounds, unlike the co-crystalline cases discussed earlier.

New examples of this diol family can be designed using well-defined symmetry and structure rules. At present, 12 HT diols are known, spanning a wide range of tube cross-sectional areas. The HT diols are arguably the record holders for exhibiting reliable conglomerate formation through spontaneous self-resolution of their enantiomers [37].

An even more startling case of self-resolution was observed when a mixture of diols **12** and **13** was crystallised from toluene solution, and the helical tubulate $(\mathbf{12})_2 \cdot (\mathbf{13}) \cdot (\text{toluene})$ was produced (Figure 18) [38]. Specific, stoichiometric and chiral combination of three components occurs from the solution of the five

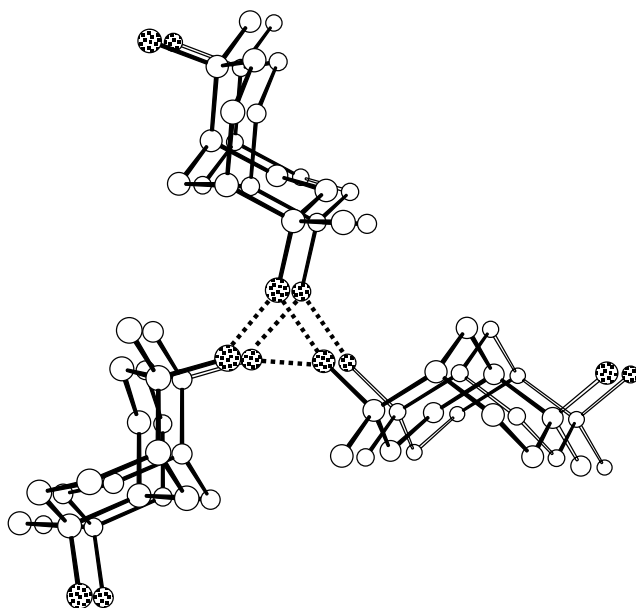
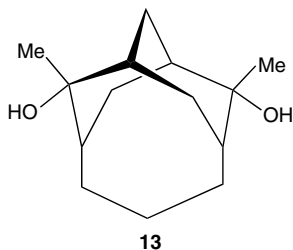


Figure 17 The hydrogen-bonded supramolecular synthon present in all helical tubulate inclusion compounds formed by diol **11** (and its family of hosts). The molecules hydrogen bond together $\text{O-H}\cdots\text{O-H}\cdots\text{O-H}\cdots$ to form the threefold screw axis structure illustrated. Identical arrangements subtended by the second diol hydroxy groups give rise to the chiral tubular lattice structure shown in Figure 16. Hydrogen atoms are omitted for clarity.

substances (+)-**(12)**, (–)-**(12)**, (+)-**(13)**, (–)-**(13)** and toluene during this self-assembly process. Formation of this product involves two simultaneous self-resolution processes, the combination of (+)-diols yielding half the crystals and the combination of (–)-diols the other half. The toluene guests fit snugly in the host tubes, which show a cross-sectional area between those observed for pure **12** and pure **13** (Figure 19). The included solvent molecule clearly plays a significant role as a template controlling formation of this material.

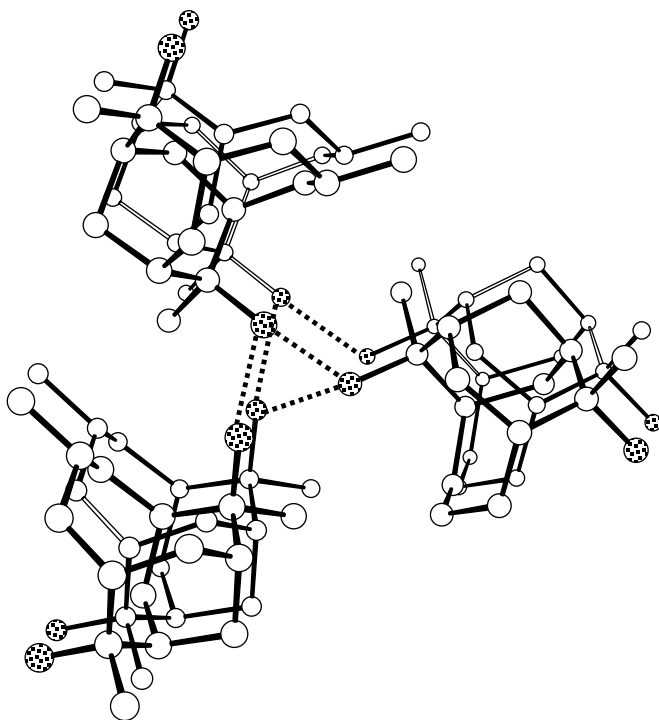


Figure 18 The hydrogen-bonded supramolecular synthon present in the helical tubulate compound $(\mathbf{12})_2 \cdot (\mathbf{13}) \cdot (\text{toluene})$. Hydrogen atoms are omitted for clarity.

3.2.2 Enantiomeric self-resolution through guest complexation

The crystallisation solvent can also play a more obvious role in enantiomer ordering and the type of crystal lattice produced [39]. For example, the fluorinated diol **14** showed no indication of inclusion properties when crystallised from a variety of solvents. The X-ray structure of a crystal ($P2_1/c$) grown from benzene solution confirmed this, and revealed a layer structure. Hydroxy groups from four different molecules associate to form $(-\text{OH})_4$ cycles where each group participates in one donor and one acceptor hydrogen bond. Four further $(-\text{OH})_4$ cycles are subtended from the second diol hydroxy groups, and so on, to build up corrugated layers of hydrogen-bonded molecules that stack through dispersion forces (Figure 20). This structure is unremarkable except that considerable enantiomer ordering has taken place, such that each layer is chirally pure. Adjacent layers contain the opposite enantiomer of **14**.

Even greater enantiomer ordering occurs if **14** is crystallised from dimethyl sulfoxide (DMSO), because the compound $(\mathbf{14})_2 \cdot (\text{DMSO})$ is produced. This material, in space group $P2_12_12_1$, is a conglomerate where each crystal contains

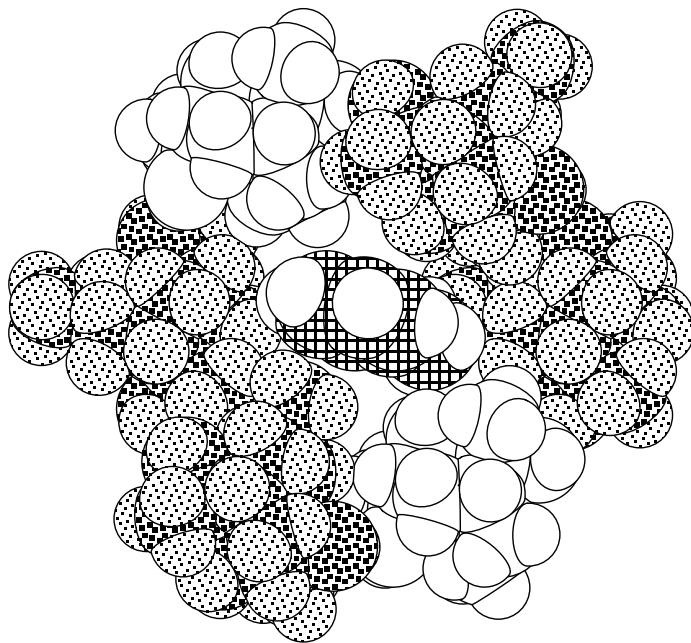
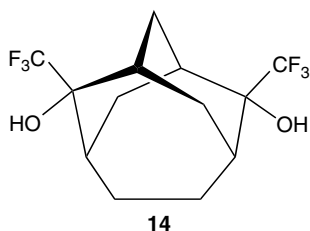


Figure 19 Space-filling projection view in the *ab* plane of just one tube of the solid inclusion compound $(\mathbf{12})_2 \cdot (\mathbf{13}) \cdot (\text{toluene})$. The atoms of diol $\mathbf{13}$ are unmarked, while those of diol $\mathbf{12}$ and the guest are highlighted.



only one enantiomer of **14**. In this structure, parallel strands of diol molecules are hydrogen-bonded $\text{H}-\text{O} \cdots \text{H}-\text{O} \cdots \text{H}-\text{O}$. Dimethyl sulfoxide molecules cross-link pairs of strands, by accepting one hydrogen bond donor $\text{O}-\text{H} \cdots \text{O}=\text{S}$ from each strand, to produce series of ribbons along *a*. Multiple $\text{C}-\text{F} \cdots \text{H}-\text{CH}_2-\text{SO}$ interactions link the strands and ribbons (Figure 21).

Enantiomeric self-resolution through complexation with a hydrogen-bonding guest solvent has interesting potential as a means of separation. Unfortunately, little prediction of new examples seems possible with our current level of understanding.

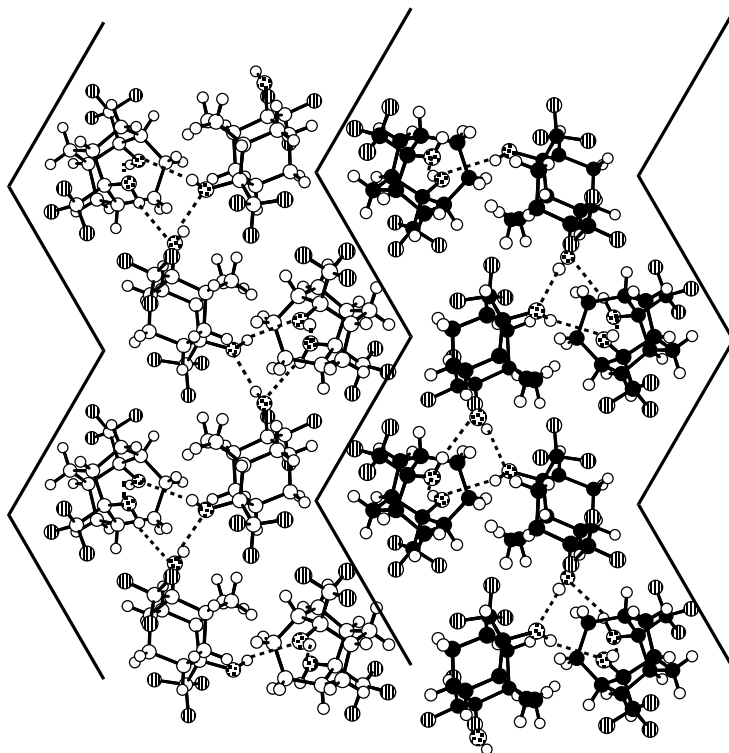


Figure 20 The crystal structure of pure diol **14** projected in the *bc* plane, and showing an edge-on view of two corrugated hydrogen-bonded layers. Each layer in the compound is built from enantiomerically pure molecules, but adjacent layers have opposite handedness. Fluorine atoms are designated by vertical hatching.

3.3 Self-resolution of Enantiomeric Crystals Containing Both Enantiomeric Molecules

As explained earlier (Section 3), a 1:1 mixture of (+)- and (–)-crystals may also be obtained where self-resolution of the molecular enantiomers has not taken place. This occurs because the crystallisation process generates a lattice that is itself handed. Two examples of this phenomenon are presented here.

Crystallisation of racemic **9** from a variety of solvents results in penannular inclusion compounds where two molecules of the host wrap round one of the guest [30]. The resulting molecular pens assemble as layers by means of aryl offset face–face (OFF) interactions (Section 3.1.2). The crystal space groups observed are usually $P2_1/c$, and sometimes $C2/c$.

However, when $\text{CF}_3\text{-C}_6\text{H}_5$ is used as solvent, the inclusion compound $(\mathbf{9})_2 \cdot (\text{CF}_3\text{-C}_6\text{H}_5)$ is produced in the chiral space group $P2_12_12_1$ [30]. Two independent

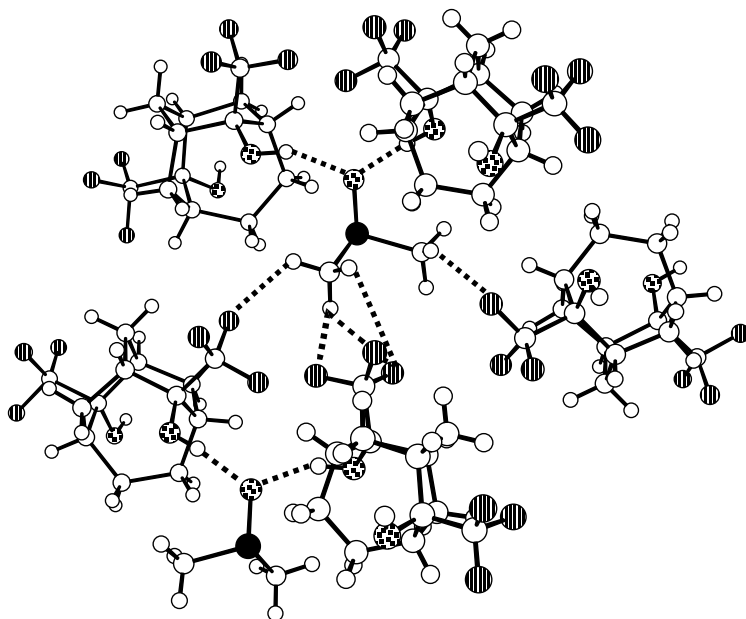


Figure 21 Part of the crystal structure of $(\mathbf{14})_2 \cdot (\text{DMSO})$ projected in the ab plane, showing the $\text{O}-\text{H} \cdots \text{O}=\text{S}$ and $\text{C}-\text{F} \cdots \text{H}-\text{CH}_2-\text{SO}$ interactions (dashed lines) present between the two components. Atom designators: O heavy stippling, S black, and F vertical hatching.

host molecules (A and B) are involved. In (+)-crystals only A and B* molecules are present, while in (–)-crystals only A* and B crystals are present (where * indicates molecules of the opposite handedness). Hence, the enantiomeric nature of the crystals produced does not result from self-resolution of the host molecular enantiomers A and B. In a sense, however, the host combinations A/B* and A*/B are resolved during crystal formation. The resulting arrangement of molecular pens is illustrated in Figure 22.

Although the layers in the trifluoromethylbenzene compound are constructed differently to those in $(\mathbf{9})_2 \cdot (\text{CH}_3-\text{CCl}_3)$ (Section 3.1.2), the network of double edge–edge $\text{C}-\text{H} \cdots \text{N}$ interactions present between the layers (Figure 23) is remarkably similar. Once again, the same two types of double edge–edge $\text{C}-\text{H} \cdots \text{N}$ attractions operate between the opposite host enantiomers.

Crystallisation of racemic **15** from either chloroform or 1,1,2,2-tetrachloroethane yields achiral inclusion compounds that contain both host enantiomers. In contrast, when **15** is crystallised from tetrahydrofuran (THF), a mixture of (+)- and (–)- crystals is produced in space group $P2_12_12_1$ [40]. Once again, chirality arises from the lattice structure rather than from self-resolution of the host enantiomers.

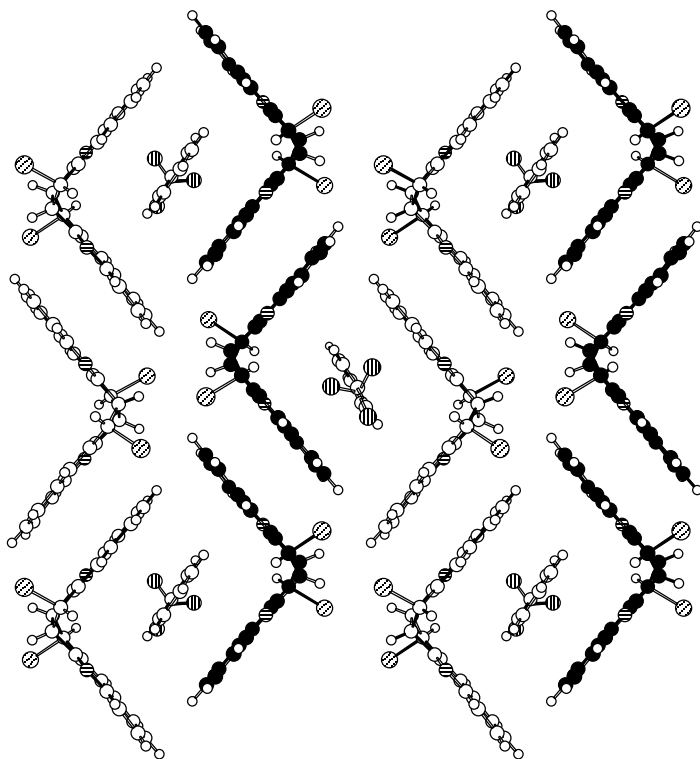
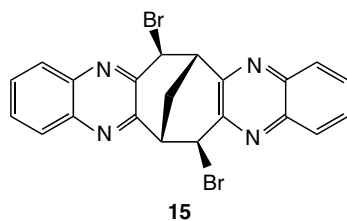


Figure 22 Part of the structure of $(\mathbf{9})_2 \cdot (\text{CF}_3\text{-C}_6\text{H}_5)$ showing a projection in the bc plane of one layer of molecular pens and their guests. In one type of enantiomeric crystal the pens involve A and B* host molecules, whereas in the second type only A* and B hosts are present.



In $(\mathbf{15})_2 \cdot (\text{THF})$ double C-H \cdots N interactions again play an important role in linking opposite enantiomers of the host. In this structure, only one of the aromatic wings is involved in these double interactions. Both edges of this wing, however, participate by subtending one edge-edge aryl C-H \cdots N and one edge-edge aliphatic BrC-H \cdots N interaction. The values of these interactions are different

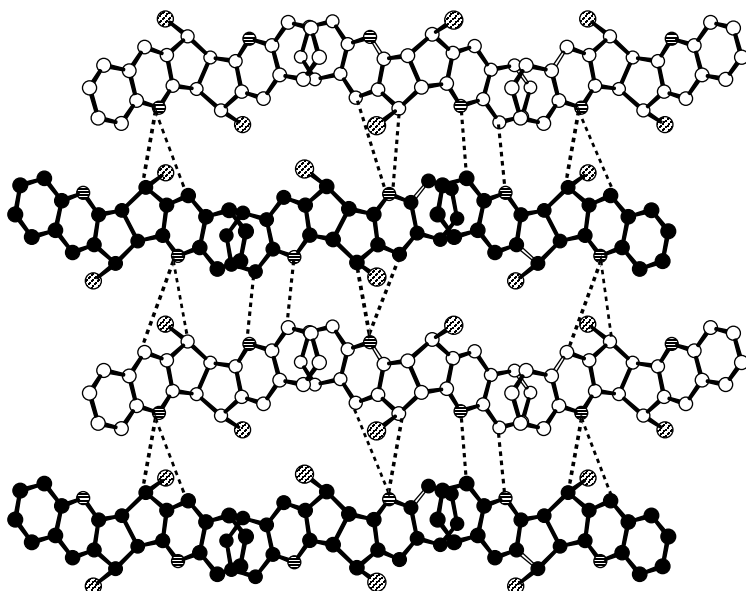


Figure 23 The bifurcated Ar-H...N... aliphatic H-CBr- and eight-membered double Ar-H...N cyclic interactions present between host layers in the structure of $(\mathbf{9})_2 \cdot (\text{CF}_3\text{-C}_6\text{H}_5)$.

on the two edges of the host and it is this asymmetry that generates the chiral lattice. Once again the enantiomeric crystals contain A/B* or A*/B combinations of the host molecule.

The overall lattice structure contains slightly kinked, but unobstructed, parallel tubes, and so $(\mathbf{15})_2 \cdot (\text{THF})$ is a compound of the tubulate type. The THF guest molecules can occupy two alternate disorder positions within a tube, one only of these being illustrated in Figure 24.

4 ENANTIOMERICALLY PURE HOST MOLECULES

Several prominent types of host molecule, such as the steroidal bile acids and the cyclodextrins, are chiral natural products that are available as pure enantiomers. Chemical modification of these parent compounds provides an easy route to the preparation of large numbers of further homochiral substances. Since all these materials are present as one pure enantiomer, it automatically follows that their crystalline inclusion compounds must have chiral lattice structures. It is not currently possible to investigate racemic versions of these compounds, but the examples discussed previously in this chapter indicate that very different behaviour could result.

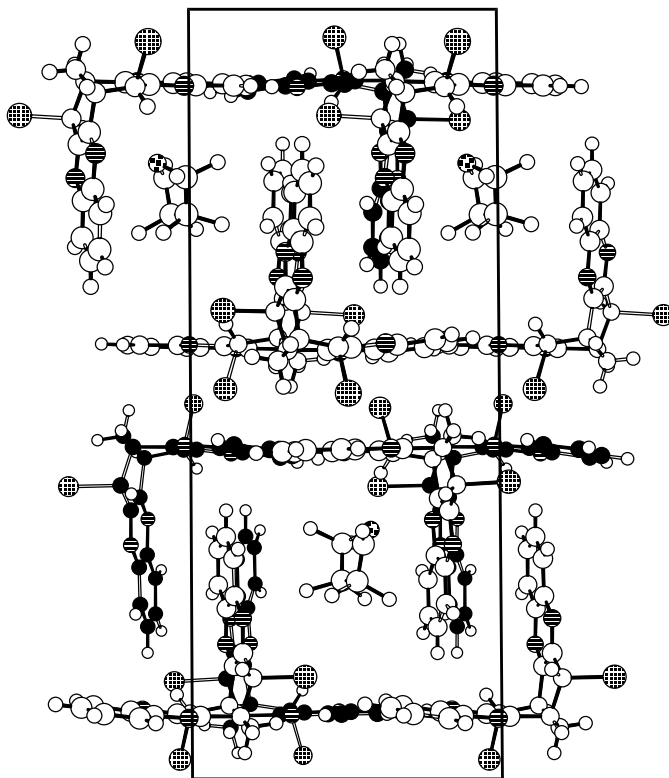


Figure 24 Part of the structure of $(\mathbf{15})_2 \cdot (\text{THF})$ projected in the ac plane, showing end-on views of three guest-containing tubes and the nature of the enantiomeric host molecules involved in the tube wall construction.

4.1 Synthesis of Chirally Pure Hosts

In the case of known racemic host systems, enantiomeric resolution or chiral synthesis can provide samples of the pure (+)- and/or (–)-compound. There is no guarantee that the chirally pure material will behave in a similar manner to the racemic mixture, or even that it will still show inclusion behaviour. Pre-resolution has, however, recently been demonstrated to play an important role in inclusion chemistry.

The racemic alicyclic diol **10** can form two types of lattice inclusion compounds on crystallisation, ellipsoidal clathrates (Section 3.1.2) or helical tubulates (Section 3.2.1). Small guests give the former, and large guests give the latter, lattice.

The ellipsoidal clathrate structure contains both enantiomers, whereas the helical tubulate structure contains only one. It follows, therefore, that a sample of

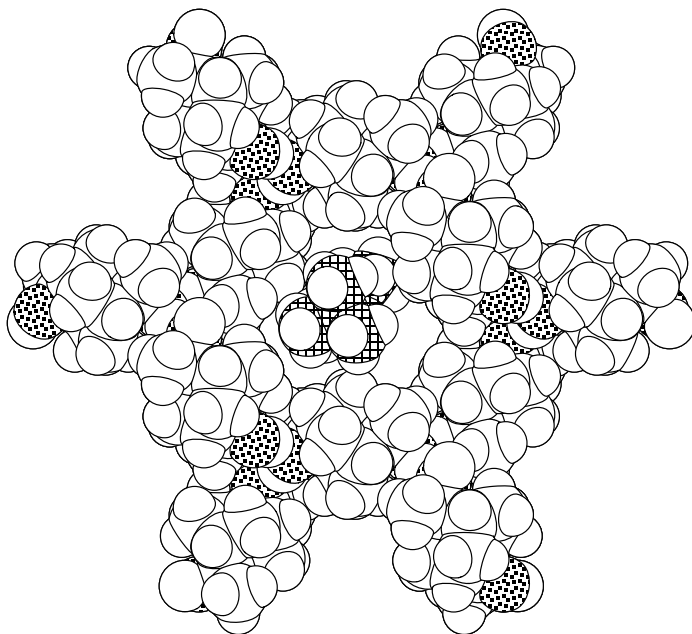


Figure 25 A projection in the *ab* plane of just one tube of the $(\mathbf{10})_3 \cdot (t\text{-butylcyclohexane})_{0.75}$ helical tubulate structure, showing the large guest molecule contained therein.

resolved diol **10** cannot give the ellipsoidal clathrate structure. The pure enantiomer might fail to include, or perhaps yield a third type of inclusion structure, but it actually now produces helical tubulate compounds with small guests. Hence, the ellipsoidal clathrate compound $(\mathbf{10})_4 \cdot (\text{cyclohexane})$ gives way to helical tubulate $(\mathbf{10})_3 \cdot (\text{cyclohexane})_{1.5}$ if the diol used is pre-resolved [41].

These results show that there can be considerable advantages in using pre-resolved samples of a chiral host, rather than just relying on self-resolution and conglomerate formation. An additional discovery revealed that some larger solvents excluded by racemic **10**, were now included when resolved **10** was used. Thus, mesitylene (1,3,5-trimethylbenzene) and *t*-butylcyclohexane (see Figure 25) both form helical tubulate inclusion compounds with pre-resolved **10**, but not with racemic **10** when a different guest-free structure is obtained.

5 CONCLUSIONS

This short account demonstrates that chirality is a key factor in determining whether, or not, molecular inclusion will occur. It cannot be ignored in any crystal engineering design. Unfortunately, with our present level of understanding, prediction is currently at a low level. The examples discussed, however, give

pointers that at least some compounds have requirements and outcomes that can be recognised. For example, the diquinoline hosts like to interact by means of various centrosymmetric arrangements and therefore racemic material is obligatory. In contrast, the helical tubuland diols usually prefer to self-resolve and form conglomerates. Thus, it can be advantageous to use enantiomerically pure compounds in this instance.

ACKNOWLEDGEMENTS

I wish to thank Dr Marcia Scudder for preparing the crystallographic figures used to illustrate this account, and the Australian Research Council for financial support of my inclusion chemistry and crystal engineering research over recent years.

REFERENCES

1. H. M. Powell, in *Inclusion Compounds, Vol. 1*, eds J. L. Atwood, J. E. D. Davies and D. D. MacNicol, Academic Press, London, **1984**, Ch. 1, pp. 1–28.
2. J. E. D. Davies, W. Kemula, H. M. Powell and N. O. Smith, *J. Incl. Phenom.*, **1983**, *1*, 3–44.
3. G. R. Desiraju, *Angew. Chem., Int. Ed. Engl.*, **1995**, *34*, 2311–2327.
4. E. Weber and H.-P. Josel, *J. Inclusion Phenom.*, **1983**, *1*, 79–85.
5. K. Takemoto and N. Sonoda, in *Inclusion Compounds, Vol. 2*, eds J. L. Atwood, J. E. D. Davies and D. D. MacNicol, Academic Press, London, **1984**, Ch. 2, pp. 47–67.
6. R. Bishop and I. G. Dance, *Top. Curr. Chem.*, **1988**, *149*, 137–188.
7. M. D. Hollingsworth and K. D. M. Harris, in *Comprehensive Supramolecular Chemistry, Vol. 6*, eds D. D. MacNicol, F. Toda and R. Bishop, Pergamon Press, Oxford, **1996**, Ch. 7, pp. 177–237.
8. Y. Chatani, Y. Taki and H. Tadokoro, *Acta Crystallogr., Sect. B*, **1977**, *33*, 309–311.
9. J. Jacques, A. Collet and S. H. Wilen, *Enantiomers, Racemates, and Resolutions*, Wiley, New York, **1981**.
10. A. Collet, M.-J. Brienne and J. Jacques, *Chem. Rev.*, **1980**, *80*, 218–230.
11. D. Worsch and F. Vögtle, *Top. Curr. Chem.*, **1987**, *140*, 21–41.
12. I. Goldberg, in *Inclusion Compounds, Vol. 4*, eds J. L. Atwood, J. E. D. Davies and D. D. MacNicol, Oxford University Press, Oxford, **1991**, Ch. 10, pp. 406–447.
13. R. Arad-Yellin, B. S. Green, M. Knossow and G. Tsoucaris, in *Inclusion Compounds Vol. 3*, eds J. L. Atwood, J. E. D. Davies and D. D. MacNicol, Academic Press, London, **1984**, Ch. 9, pp. 263–295.
14. W. Schlenk, *Justus Liebigs Ann. Chem.*, **1973**, 1145–1209.
15. L. C. Fetterley, in *Non-Stoichiometric Compounds*, ed L. Mandelcorn, Academic Press, New York, **1964**, pp. 491–567.
16. M. Farina, in *Inclusion Compounds, Vol. 3*, eds J. L. Atwood, J. E. D. Davies and D. D. MacNicol, Academic Press, London, **1984**, Ch. 10, pp. 297–329.

17. M. Miyata, in *Comprehensive Supramolecular Chemistry*, Vol. 10, ed D. N. Reinhoudt, Pergamon, Oxford, **1996**, Ch. 19, pp. 557–582.
18. M. Gdaniec, B. T. Ibragimov and S. A. Talipov, in *Comprehensive Supramolecular Chemistry*, Vol. 6, eds D. D. MacNicol, F. Toda and R. Bishop, Pergamon, Oxford, **1996**, Ch. 5, pp. 117–145.
19. E. Weber, in *Inclusion Compounds*, Vol. 4, eds J. L. Atwood, J. E. D. Davies and D. D. MacNicol, Oxford University Press, Oxford, **1991**, Ch. 5, pp. 188–262.
20. E. Weber, in *Comprehensive Supramolecular Chemistry*, Vol. 6, eds D. D. MacNicol, F. Toda and R. Bishop, Pergamon, Oxford, **1996**, Ch. 17, pp. 535–592.
21. A. N. M. M. Rahman, R. Bishop, D. C. Craig, C. E. Marjo and M. L. Scudder, *Cryst. Growth Des.*, **2002**, 2, 421–426.
22. A. N. M. M. Rahman, R. Bishop, D. C. Craig and M. L. Scudder, *CrystEngComm*, **2002**, 4(84), 510–513.
23. A. N. M. M. Rahman, R. Bishop, D. C. Craig and M. L. Scudder, *Org. Biomol. Chem.*, **2003**, 1, 1435–1441.
24. G. R. Desiraju and A. Gavezzotti, *Acta Crystallogr., Sect. B*, **1989**, 45, 473–482.
25. C. A. Hunter, K. R. Lawson, J. Perkins and C. J. Urch, *J. Chem. Soc., Perkin Trans. 2*, **2001**, 651–669.
26. D. D. MacNicol, J. J. McKendrick and D. R. Wilson, *Chem. Soc. Rev.*, **1978**, 7, 65–87.
27. D. D. MacNicol, in *Inclusion Compounds*, Vol. 2, eds J. L. Atwood, J. E. D. Davies and D. D. MacNicol, Academic Press, London, **1984**, Ch. 1, pp. 1–45.
28. J. L. Flippen, J. Karle and I. L. Karle, *J. Am. Chem. Soc.*, **1970**, 92, 3749–3755.
29. B. J. Brienne and J. Jacques, *Tetrahedron Lett.*, **1975**, 2349–2352.
30. A. N. M. M. Rahman, R. Bishop, D. C. Craig and M. L. Scudder, *Eur. J. Org. Chem.*, **2003**, 72–81.
31. G. R. Desiraju and T. Steiner, *The Weak Hydrogen Bond in Structural Chemistry and Biology*, Oxford University Press, Oxford, **1999**.
32. R. Bishop, in *Comprehensive Supramolecular Chemistry*, Vol. 6, eds D. D. MacNicol, F. Toda and R. Bishop, Pergamon, Oxford, **1996**, Ch. 4, pp. 85–115.
33. A. T. Ung, R. Bishop, D. C. Craig, I. G. Dance and M. L. Scudder, *Chem. Mater.*, **1994**, 6, 1269–1281.
34. W. Yue, R. Bishop, D. C. Craig and M. L. Scudder, *CrystEngComm*, **2002**, 4(98), 591–595.
35. A. T. Ung, D. Gizachew, R. Bishop, M. L. Scudder, I. G. Dance and D. C. Craig, *J. Am. Chem. Soc.*, **1995**, 117, 8745–8756.
36. R. Bishop, D. C. Craig, K. D. M. Harris, Y. Hishikawa, A. Kawamura and M. L. Scudder, paper in preparation.
37. A. Nangia, *Curr. Opin. Solid State Mater. Sci.*, **2001**, 5, 115–122.
38. W. Yue, R. Bishop, M. L. Scudder and D. C. Craig, *Chem. Lett.*, **1998**, 803–804.
39. R. Bishop, G. A. Downing, D. C. Craig and M. L. Scudder, *J. Inclusion Phenom. Mol. Rec. Chem.*, **1998**, 31, 145–160.
40. C. E. Marjo, R. Bishop, D. C. Craig and M. L. Scudder, *Eur. J. Org. Chem.*, **2001**, 863–873.
41. S. F. Alshahateet, R. Bishop, D. C. Craig and M. L. Scudder, *CrystEngComm*, **2002**, 4(8), 42–45.

Chapter 3

Molecular Recognition of Crystalline Dipeptides and Its Application to Separation

KATSUYUKI OGURA AND MOTOHIRO AKAZOME

*Department of Materials Technology, Faculty of Engineering, Chiba University,
1-33 Yayoicho, Inageku, Chiba 263-8522, Japan*

1 INTRODUCTION

The chemistry of inclusion crystals has a long history. In the early days, investigations were made of the way in which host molecules include appropriate guest molecules as they crystallize [1]. Early examples of inclusion crystals included urea and bile acids. Over time, many types of host molecules, such as axel-type diols, cholic acid, deoxycholic acid, tartaric acid derivatives, binaphthols and resorcinol derivatives have been developed. Crystal engineering to design and control the crystal packing arrangement has emerged as one of the most active fields in chemistry, but no general theory is yet available to systematically predict how a given molecule will pack in the solid state [2,3]. In order to solve this problem, many kinds of organic host molecules that construct a three-dimensional rigid network or two-dimensional framework in a crystal have been designed to include guest molecules [4,5]. However, there are only a few reports available on the organic host molecules used to form a precise two-dimensional network (sheet structure) followed by the inclusion of a guest molecule [6]. Ward and

his co-workers developed pillared two-dimensional hydrogen-bonded networks comprising guanidinium ions and disulfonate ions, in which the disulfonate ions act as pillars that connect opposing hydrogen-bonded sheets with adjustable porosity [7].

In 1990 [8], we found that a simple dipeptide, (*R*)-phenylglycyl-(*R*)-phenylglycine (**1**) (Figure 1), forms an inclusion crystal with a sheet structure, as depicted in Figure 2. Enantiomerically pure isopropyl phenyl sulfoxide is included in the cavity between the sheets. This finding is very interesting from the viewpoint of asymmetric recognition of a chiral guest by a simple peptide. One of its most useful applications is optical resolution, i.e. using the diastereomeric interaction that results from the inclusion of a racemic guest substance into the molecular cavity or crystal lattice of a chiral host.

Prior to our current investigations, we studied the structure of the dipeptide molecules that make up proteins. Based on the data supplied by the Cambridge database, the dipeptides were shown to adopt many types of arrangement mode in their crystalline state [9]. Furthermore, it was shown that water, methanol,

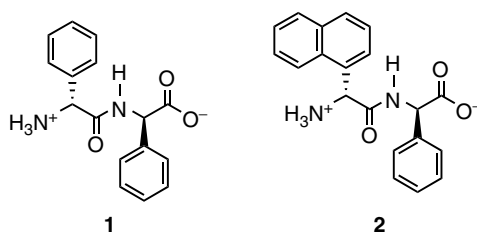


Figure 1 Dipeptide hosts.

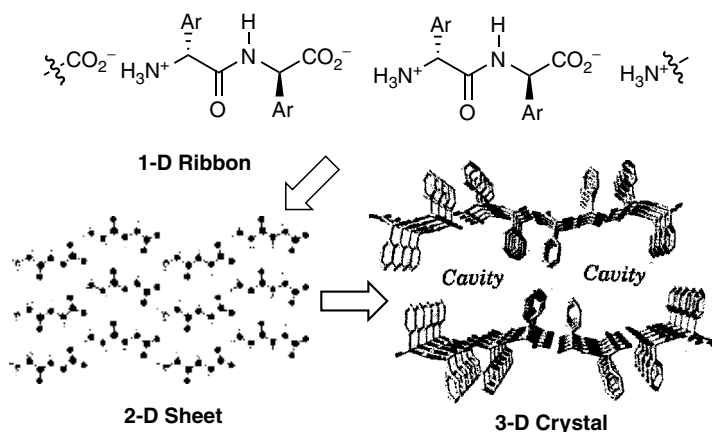


Figure 2 Assembly of dipeptides to form a three-dimensional structure.

dimethyl sulfoxide, etc. were included by crystalline dipeptides, but their phenomena have not been investigated systematically [10]. Here, we would like to survey the diverse types of molecular recognition of (*R*)-arylglycyl-(*R*)-phenylglycines (**1**; aryl = phenyl or 1-naphthyl), together with their application to the optical resolution of alkyl aryl sulfoxides and the optical separation of poly(ethylene glycols) (PEGs) by their molecular weight.

2 THE DIVERSE TYPES OF SHEET STRUCTURE USED IN THE MOLECULAR RECOGNITION OF CRYSTALLINE (*R*)-ARYLGLYCYL-(*R*)-PHENYLGLYCINE

From the standpoint of the structures that they form within proteins, the crystal structures of oligopeptides have been investigated and classified into α -helices, β -sheets and β -turns [11]. However, the assembly and orientation modes of oligopeptides depend so much on their primary structures that it is extremely difficult to control their secondary structures. In order to force them to aggregate in parallel or antiparallel β -sheets, molecular scaffolds have been employed as a useful tool to orientate hydrogen bonding between the peptide backbones [12]. Since it is well known that, in usual inclusion compounds, the arrangement of host molecules can be altered by host–guest interactions [4], our attention focused on whether the β -sheet structures of dipeptides can be controlled by the guest molecules that are accommodated in their voids.

As mentioned above, (*R*)-phenylglycyl-(*R*)-phenylglycine (**1**) molecules self-assemble to form a layer structure, and (*S*)-isopropyl phenyl sulfoxide molecules are stereospecifically included in the void between the layers [8]. The inclusion compound of the sulfoxide was obtained by recrystallization of **1** in the presence of the sulfoxide (see below). X-ray crystal analysis (Figure 3) shows that the dipeptide molecules are arranged in a parallel β -sheet-like structure which is constructed by ionic pairing of the carboxyl and amino groups via a hydrogen-bonding network: one terminal COO^- bridges two NH_3^+ of adjacent dipeptides, and the NH_3^+ also binds two adjacent COO^- groups. The phenyl groups are placed perpendicular to the sheet. The neighboring two phenyl rings are stacked with the aid of the edge-to-face interaction, to form a wall [13]. Interestingly, typical intermolecular hydrogen bonding among amide groups, which is essential to the formation of oligopeptide crystals [11], did not contribute to the formation of parallel β -sheets. The dipeptide backbones of the parallel mode are aligned with an interchain spacing of 5.51 Å, which corresponds with the length of the *c*-axis. The value is larger than the interchain spacings of general parallel β -sheet structures (4.85 Å; ideally, 4.90–5.08 Å observed) [12].

The sulfoxide molecules are accommodated in the void between the layers via three-point interaction: hydrogen bonding between NH_3^+ and the sulfinyl group, the ‘tilted T’-shaped interaction between two phenyl groups [14], and the CH/π

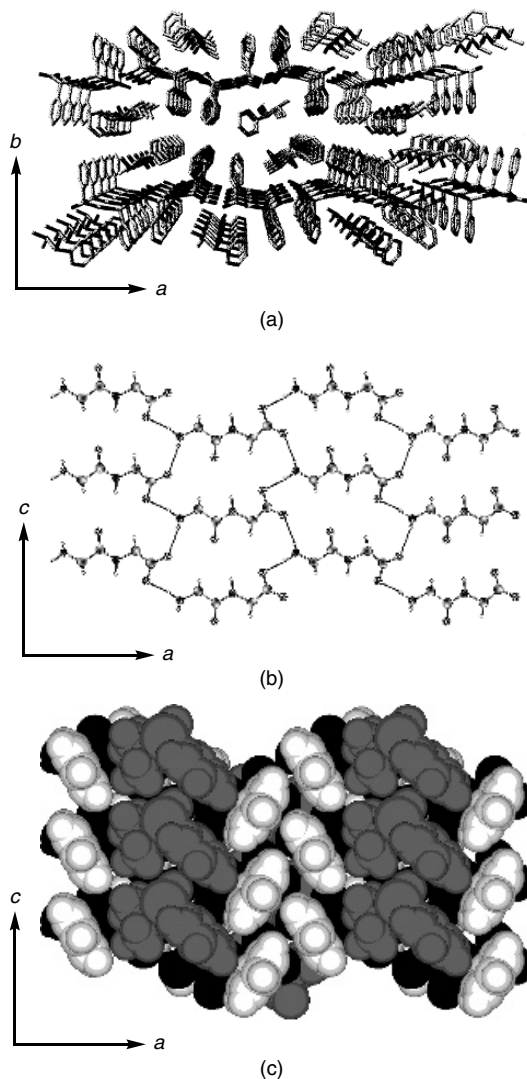


Figure 3 Inclusion compound of (*S*)-isopropyl phenyl sulfoxide by **1**: (a) perspective view of crystals; (b) sheet structure of **1**; (c) CPK model. For clarity, phenyl groups of **1** and guest are unshaded and gray, respectively.

interaction of the phenyl and isopropyl groups [15]. In proteins, π - π interactions on their side chains have already been investigated to reveal the importance of the edge-to-face interaction between the two benzene rings [13].

A sheet structure was formed in THF-included crystals of (*R*)-(1-naphthyl)glycyl-(*R*)-phenylglycine (**2**) [16]. The THF-included compound of **2** formed on

crystallization of **2** from a mixed solvent of tetrahydrofuran (THF) and methanol. The sheet structure (Figure 4) of the THF-included crystals is analogous to that of the above sulfoxide-included compounds of **1**. THF molecules were linked to the NH_3^+ of the dipeptides via hydrogen bonding, and accommodated in the void between the walls of the naphthyl and phenyl groups. In addition, the diethyl ether-included compound of **2** showed a similar sheet structure.

When allylic alcohols were used as a guest molecule instead of ethers (THF and diethyl ether), the arrangement of the dipeptide molecules was changed to an antiparallel β -sheet-like structure [16]. By crystallization from methanol–methallyl alcohol, we obtained a single crystal of an inclusion compound, which consisted of **2**, methanol, and methallyl alcohol. The X-ray structure shows an antiparallel mode where two kinds of dipeptide ribbon structures are bound to one another by multiple hydrogen bonding (Figure 5). Both of the dipeptide ribbons adopt a zigzag form,

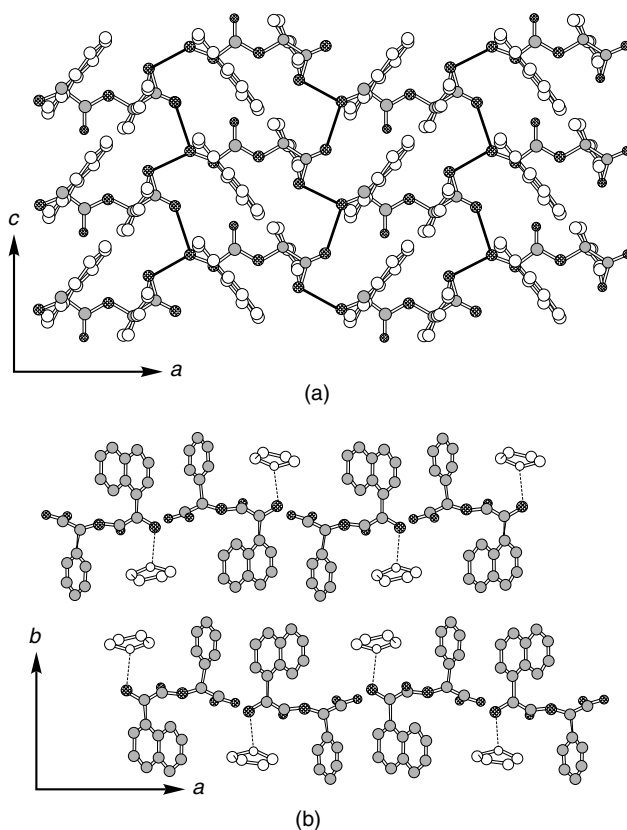


Figure 4 Parallel β -sheet-like structure of the THF-included compound of **2**. To improve clarity, all hydrogen atoms are omitted. (a) ac plane. THF is omitted, and the naphthyl and phenyl groups are unshaded. (b) ab plane. The carbons of THF are unshaded.

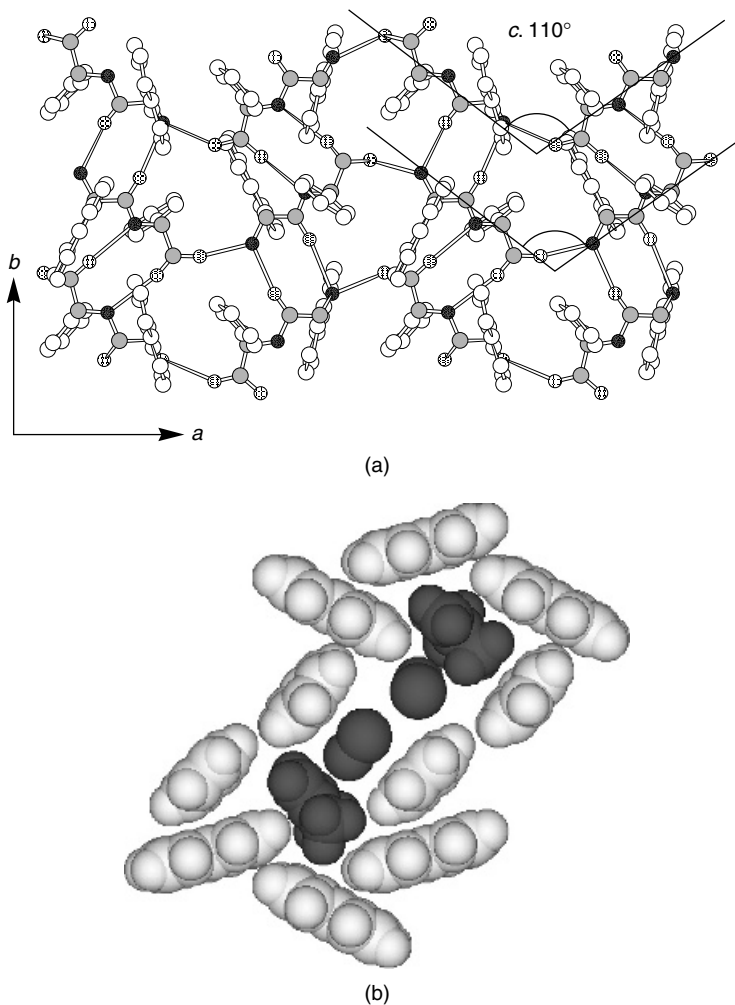


Figure 5 Antiparallel β -sheet-like structure of **2** including methallyl alcohol and methanol. (a) ab plane. To improve clarity, guest molecules are omitted, and the naphthyl and phenyl groups are unshaded. (b) Guests (dark gray) in the pocket-type void surrounded by naphthyl and phenyl groups (unshaded).

with a binding angle of *c.* 110° . The spacings of the ionic pair ($\text{COO}^- \cdots \text{NH}_3^+$) are 2.68 and 2.71 Å, and the four hydrogen bonding distances between the two peptide ribbons are 2.82, 2.83, 2.86 and 2.94 Å. Thus, four additional hydrogen bonds play an important role in the antiparallel mode. This is in sharp contrast to the parallel mode. Methanol and methallyl alcohol exist as two guest molecules

in pocket-type cavities surrounded by naphthyl and phenyl groups that stand perpendicular to the sheet. In addition, an inclusion compound of 2-propen-1-ol (allyl alcohol) was also obtained, and single-crystal X-ray crystallography confirmed that it exhibits the same antiparallel mode.

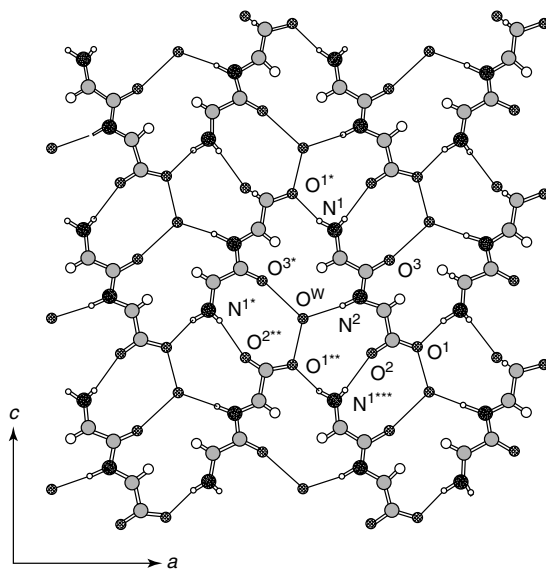
Thus, (*R*)-(1-naphthyl)glycyl-(*R*)-phenylglycine (**2**) was shown to have the ability to optionally form 'parallel or antiparallel' β -sheet-like structures with the included molecules, ethers or allylic alcohols. This is regarded as a prototype of the way in which guest molecules control β -sheet structures.

In proteins, the internal water not only fills the structural cavities, but is necessary to stabilize the three-dimensional folding, especially the α -helix [17]. This is achieved by hydrogen bonding to unsatisfied donor or acceptor sites or by mediating charges. During our investigation, it was found that water promotes the crystallization of **2** to construct a new type of 'water-buried sheet' and give inclusion crystals [18]. The 'water-buried' inclusion crystals with diethyl ether or 1,2-dimethoxyethane (DME) were prepared by crystallization from a solution of **2** and the ether (more than 2 mol. equiv. to **2**) in aqueous methanol (MeOH:H₂O = 3:1). The typical crystal structure of **2**·DME·H₂O is shown in Figure 6. The formation of salts between the amino and carboxyl groups of **2** contributes to the linkage of the dipeptide molecules (N¹...O^{1*} and N^{1***}...O²; 2.71 and 2.73 Å, respectively) to form a sheet structure along the *a*-*c* axis (Figure 6). The dipeptides are arranged into a zigzag motif by salt formation along to the *a* and *c* axis. A water molecule (O^w) was effectively bridged by three hydrogen bonds between three dipeptides (O^{3*}...O^w, O^{1**}...O^w, and N²...O^w, 2.72, 2.72 and 2.83 Å, respectively) to fill the vacancy in the dipeptide sheet.

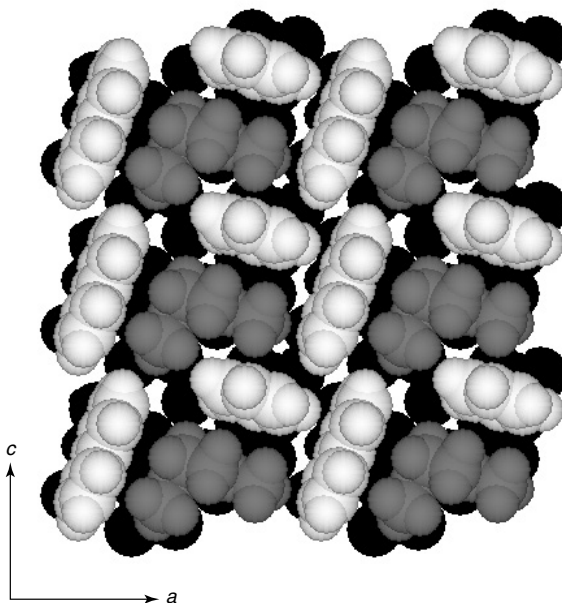
Between the layer structures, the oxygen atoms of DME are anchored to the NH₃⁺ of the dipeptide via three-centered hydrogen bonding. The inclusion cavity of **2**·DME·H₂O is shown in Figure 6. The naphthyl and phenyl groups of **2** stand perpendicular to the sheet to form an L-shaped cavity. This zero-dimensional pocket is surrounded by three naphthyl and two phenyl groups, which stack at almost right angles in a T-shaped mode [14].

Similarly, other ethers, such as 1-methoxy-2-methylthioethane, 1-methoxypropane, 1,2-dimethoxypropane and 1,3-dimethoxypropane, form water-buried inclusion crystals. In these inclusion crystals, the arrangement of **2** molecules is similar to that of **2**·DME·H₂O. All of these inclusion crystals are found to form a zero-dimensional L-shaped cavity. In these cavities, the size of the guest molecules is restricted. However, tetrahydrofuran did not give rise to the formation of water-buried inclusion crystals, but preferentially formed inclusion crystals whose channel cavity contained no water [16].

As mentioned in the next section, bulky α -hydroxy esters form an 'extended antiparallel' sheet in their inclusion crystals of **2**. The various types of the inclusion crystals of **2** are summarized in Figure 7.



(a)



(b)

Figure 6 (a) The sheet structure of dipeptide backbones of the inclusion compound ($2 \cdot \text{DME} \cdot \text{H}_2\text{O}$) (ac plane). (b) The CPK model of packing in the inclusion compound (ac plane). The naphthyl and phenyl groups of **2** are unshaded, and DME gray, respectively.

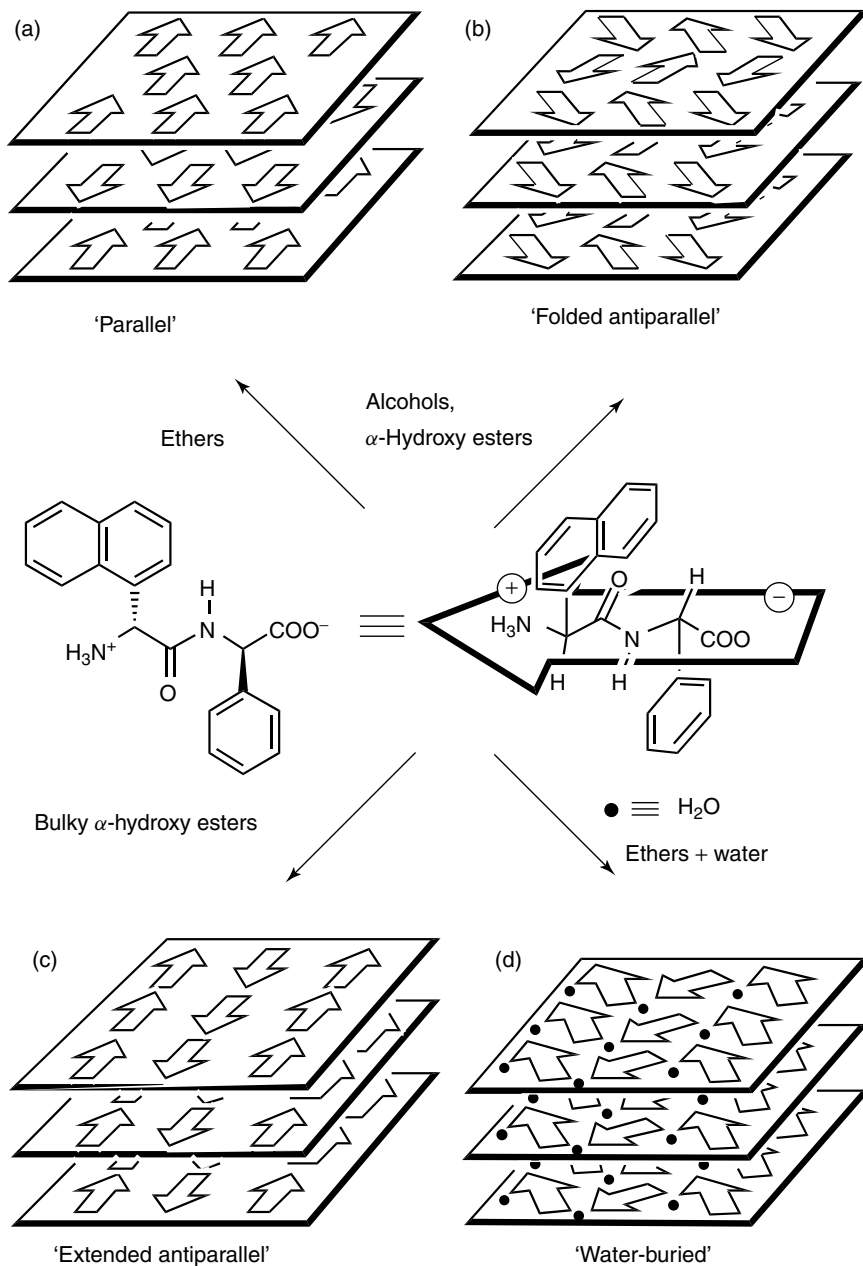


Figure 7 Structural variation in inclusion compounds of 2.

3 CHIRAL RECOGNITION OF α -HYDROXY ESTERS

As mentioned above, the dipeptide (**2**) molecules form a ‘parallel’ or ‘antiparallel’ β -sheet-like structure according to the type of guest molecule, i.e. an ether or an alcohol, respectively [16]. Interestingly, the pocket-type cavity surrounded by naphthyl and phenyl groups appears in the ‘antiparallel’ mode. Since the pocket-type cavity in the antiparallel mode of **2** is chiral, we investigated its asymmetric recognition of chiral α -hydroxy esters [19], which have two functional groups, allowing synergistic hydrogen bonding.

By crystallization of a mixture of the dipeptide (**2**) and racemic methyl lactate from methanol, asymmetric recognition occurred to give an inclusion compound that contains the (*S*)-form of methyl lactate in 89 % ee [20]. X-ray crystallographic study of the inclusion compound was able to elucidate that the dipeptide molecules

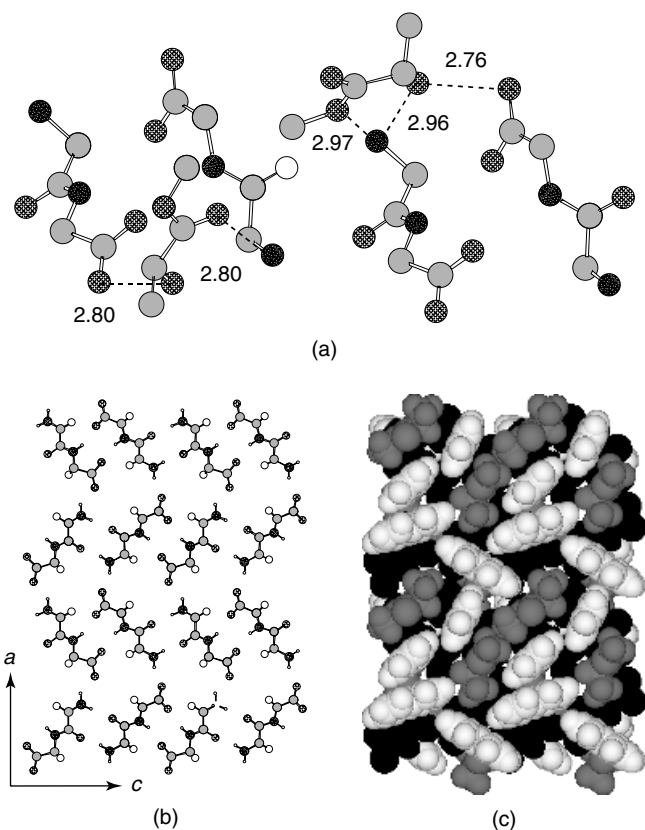


Figure 8 Inclusion compound of (*S*)-methyl lactate and **2**. (a) Host–guest hydrogen bonding (Å). (b) Sheet structure of dipeptide backbone. (c) Packing (CPK model) of the inclusion compound.

are arranged in a 'folded antiparallel' β -sheet-like structure to accommodate the α -hydroxy ester in the pocket-type cavity surrounded by naphthyl and phenyl groups on the sheet (Figure 8).

In a similar manner, (*S*)-ethyl lactate and -(*S*)-dihydro-3-hydroxy-4,4-dimethyl-2(3*H*)-furanone were included with high enantioselectivity. The pocket-type cavities of these inclusion crystals are similar to each other, as shown in Figure 9.

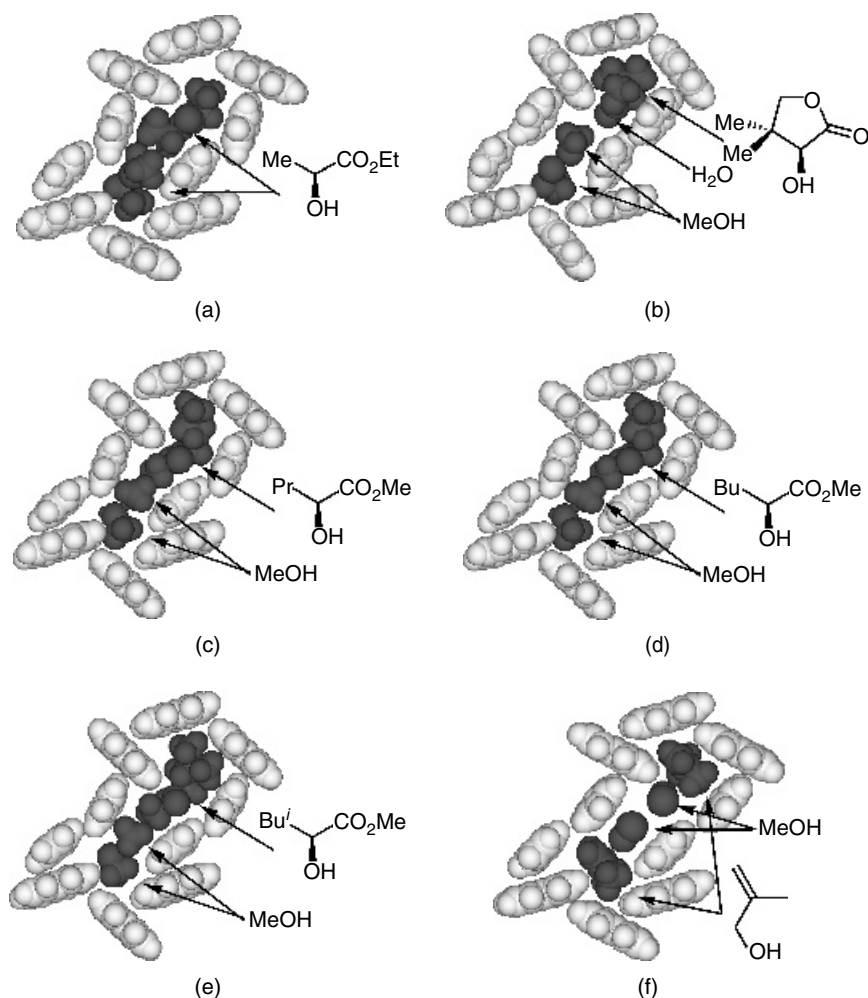


Figure 9 Cavities of the inclusion compounds (a) 2-(*S*)-ethyl lactate (1:1), (b) 2-(*S*)-dihydro-3-hydroxy-4,4-dimethyl-2(3*H*)-furanone·MeOH·H₂O (2:1:2:1), (c) 2-(*S*)-methyl α -hydroxypentanoate·MeOH (2:1:2), (d) 2-(*S*)-methyl α -hydroxyhexanoate·MeOH (2:1:2), (e) 2-(*S*)-methyl α -hydroxy- γ -methylpentanoate·MeOH, (f) 2-methylallyl alcohol·MeOH (1:1:1).

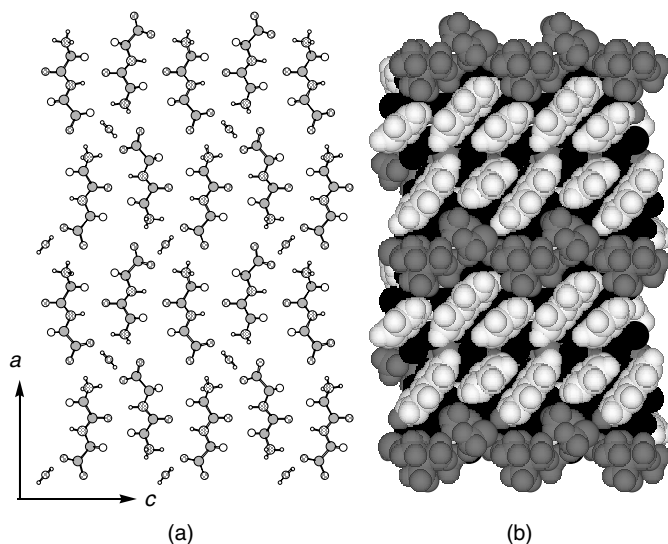


Figure 10 2·(*S*)-methyl α -hydroxy- β,β -dimethylbutyrate·MeOH·H₂O (2:1:2:1). (a) Sheet structure of dipeptide backbone. (b) Packing (CPK model) of the inclusion compound.

When the bulkier methyl α -hydroxy- β,β -dimethylbutyrate was used as a guest molecule, the arrangement of dipeptide molecules changed to an ‘extended antiparallel’ mode, where the naphthyl and phenyl groups are arranged in a ‘parallel stacked and displaced’ mode and a channel-type cavity is constructed (Figure 10). The guest molecules were accommodated via hydrogen bonding in the channel-type cavity with high enantioselectivity of the (*S*)-form (82 % ee). In the case of methyl α -hydroxy- β -methylbutyrate, the optically pure (*S*)-enantiomer formed the dipeptide sheet with the ‘folded antiparallel’ structure by co-crystallization with **2**, while the ‘extended antiparallel’ structure appeared in the inclusion of racemic methyl α -hydroxy- β -methylbutyrate.

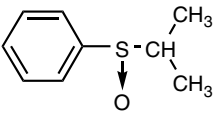
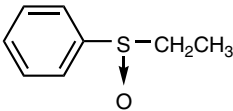
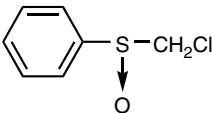
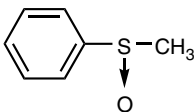
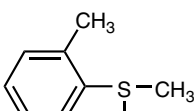
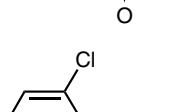
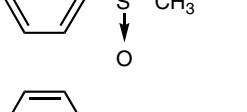
Thus, the arrangement of the host (**2**) molecules in the inclusion compound is governed by the size or shape of α -hydroxy esters (guest) to form optional sheet structures with adjustable cavities for highly enantiomeric inclusion.

4 CHIRAL RECOGNITION OF SULFOXIDES

As mentioned in Section 2, isopropyl phenyl sulfoxide was included in the crystals of **1** with a high enantioselectivity of its (*S*)-form. Generally, the inclusion compound of a sulfoxide was prepared by two methods: (1) insoluble **1** was simply stirred in the presence of an alkyl phenyl sulfoxide and water (Method A: ‘sorption’) and (2) **1** was recrystallized in the presence of the sulfoxide (Method B:

'crystallization') [8,21]. The results are summarized in Table 1, which shows enantioselectivity and efficiency for the included alkyl phenyl sulfoxides. The efficiency means mole percentage of the guest molecule to **1** molecule in the inclusion compound.

Table 1 Enantioselective inclusion of sulfoxides by crystalline **1**.

Entry	Sulfoxide	A (sorption)		B (crystallization)	
		ee (%)	Ef. ^a (%)	ee (%)	Ef. ^a (%)
1		86(<i>S</i>)	100	87(<i>S</i>)	100
2		Not included		91(<i>S</i>)	95
3		Not included		Not included	
4		92(<i>R</i>)	95	93(<i>R</i>)	100
5		92(<i>R</i>)	54	94(<i>R</i>)	98
6		48(<i>R</i>)	100	99(<i>R</i>)	97
7		Rac. ^b	100	Rac. ^b	100

^aEf. is an abbreviation of 'efficiency'. Efficiency means mol. % of guest based on **1** in the inclusion compound.

^bRac. means that the enantioselectivity is less than 10%.

Using Methods A and B, isopropyl phenyl sulfoxide was included in crystalline **1** with high (*S*)-enantioselectivity (86 % and 87 % ee, respectively). Ethyl phenyl sulfoxide formed no inclusion compound by Method A, but the inclusion compound of its (*S*)-enantiomer was obtained by Method B. *tert*-Butyl phenyl sulfoxide was recognized with high (*S*)-enantioselectivity only by Method B. The inclusion crystal of (*S*)-ethyl phenyl sulfoxide is isostructural with that of (*S*)-isopropyl phenyl sulfoxide (Figure 3). As mentioned above, (*S*)-ethyl phenyl sulfoxide was not included by Method A. Method A does not involve crystallization (unlike Method B) and a strong interaction between sulfoxide molecules and the crystals of **1** is required in order to complete the inclusion via Method A. However, the lack of one methyl group may make enthalpy (interaction with the inclusion cavity) and entropy disadvantageous in crystal packing, resulting in no inclusion of ethyl phenyl sulfoxide via Method A.

It is noteworthy that the behaviour of methyl phenyl sulfoxide in the inclusion of crystalline **1** is in sharp contrast with that of the above-mentioned alkyl phenyl sulfoxides; Methyl phenyl sulfoxide was absorbed into crystalline **1** using Methods A and B to give the inclusion compound with high (*R*)-enantioselectivity (92 % and 93 % ee, respectively) [21]. Hence, the question is why (*R*)-methyl phenyl sulfoxide is included in crystalline **1**. Since a good-quality single crystal could not be obtained for the (*R*)-methyl phenyl sulfoxide inclusion compound, we designed a new guest molecule, bis[2-(methylsulfinyl)benzyl] ether, that has two methyl phenyl sulfoxide units linked by a $-\text{CH}_2\text{OCH}_2-$ bridge.

Consideration using a CPK molecular model suggested that the designed disulfoxide is large enough to spread over two continuous cavities between the layers of **1**. This may make it easier for the inclusion compound of the disulfoxide to crystallize. Fortunately, single crystals of good quality were obtained by Method B. As expected, the disulfoxide molecules were intercalated between two layers of **1**. From a perspective side view (Figure 11b) and a top view (Figure 11c) of its crystal structure, the following distinct features became apparent: the layer structure is the same as that of the inclusion compound of (*S*)-isopropyl phenyl sulfoxide, *except for the phenyl–phenyl stacking mode*. The phenyl groups on the dipeptide layer change their conformation from the ‘tilted T’-shaped mode to ‘parallel stacking and displaced’ mode [14]. The (*R*)-(methylsulfinyl)phenyl moiety interacted with two phenyl groups of the layer. One interaction is ‘T’-mode phenyl–phenyl stacking [14], and a CH/ π interaction [15] operates between methyl and phenyl groups. For the interaction with phenyl groups, the methyl group that binds directly to a highly polarized sulfinyl group seems to have an advantage over the corresponding ethyl group in terms of entropy and enthalpy. In fact, strong CH/ π interaction was observed between a benzene ring and the methyl group on a cationic nitrogen [22]. The same inclusion mode was also observed in the inclusion crystals of (*R*)-2-chlorophenyl methyl sulfoxide, as shown in Figure 12.

Thus, the shape of the sulfoxide guest was shown to induce conformational change of the phenyl groups on the dipeptide layer (Figure 13). This behaviour, which is analogous to induced-fit phenomena at the active site of enzymes, seems to be based on the allosteric character of the crystalline dipeptide host.

It should be noted that benzyl methyl sulfoxide was included without the recognition of its chirality (entry 7 in Table 1) [23]. Using single-crystal X-ray analyses

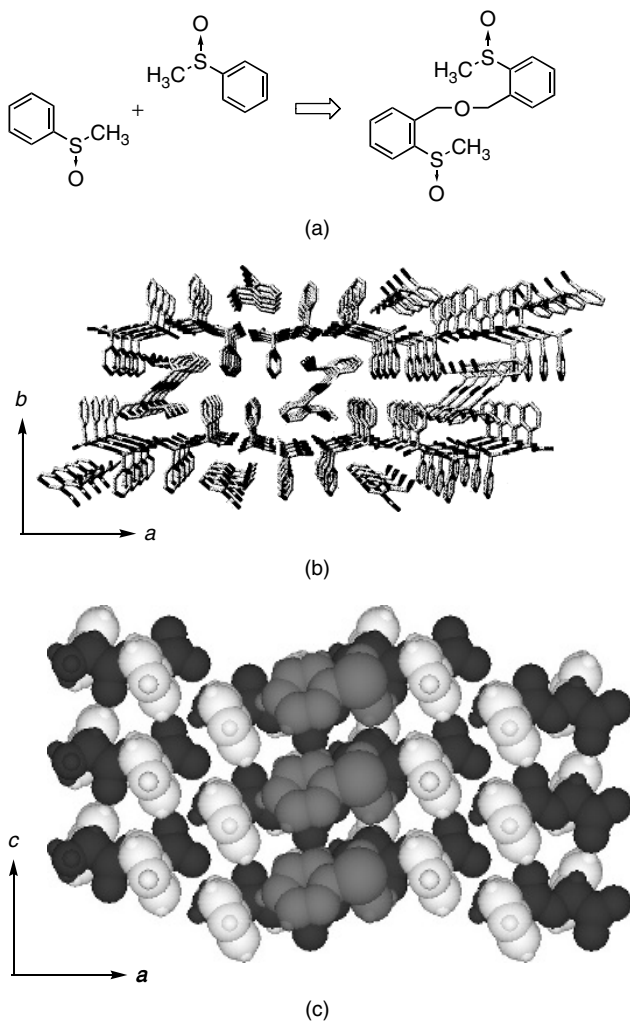


Figure 11 (a) Design of a new guest linking two methyl phenyl sulfoxide molecules; (b) Perspective views from *ab* plane of the inclusion compound of **1**; (c) top view of CPK model from *ac* plane of the inclusion compound of **1** (the half of the guest molecule is shown). For clarity, phenyl groups of **1** and guest are unshaded and gray, respectively.

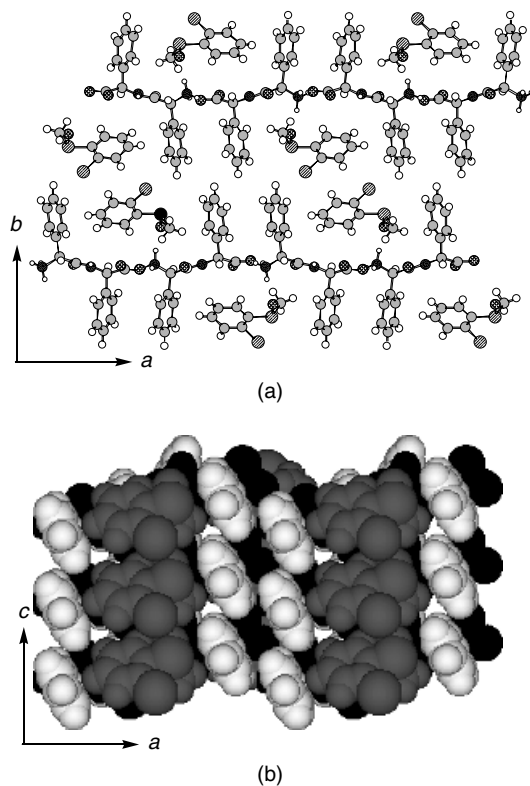


Figure 12 Inclusion compound of (*R*)-2-chlorophenyl methyl sulfoxide by **1**. (a) Layer structure. (b) Packing (CPK model) of the inclusion compound. For clarity, phenyl groups of **1** and guest are unshaded and gray, respectively.

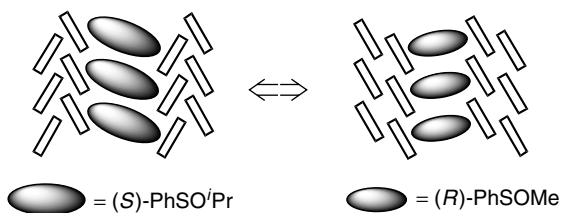


Figure 13 Conformational change of phenyl groups of **1**, depending on the guest size.

of this inclusion compound, it was elucidated that the molecules of **1** form a layer structure similar to that of the above-mentioned alkyl phenyl sulfoxide-inclusion crystals, and the sulfoxides are included between these layers. There are two different recognition cavities on the upper side for its *S* enantiomer and on the lower side for its *R* enantiomer. The upper side cavity can be illustrated by motif A,

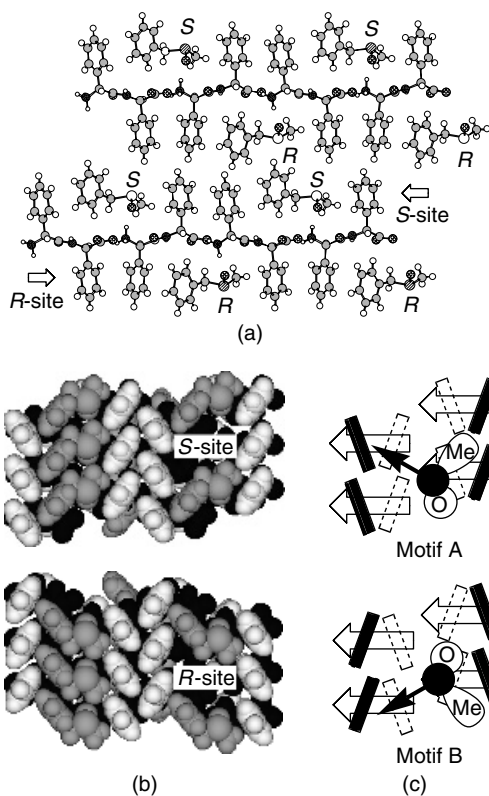


Figure 14 Inclusion compound of benzyl methyl sulfoxide by **1**. (a) Layer structure. (b) Packing (CPK model) and schematic representation of both recognition sites. For clarity, phenyl groups of **1** and guest are unshaded and gray, respectively.

and the lower side one by motif B in Figure 14. These cavities are just like a mirror images of each other in shape. In these cases, (*R*)- and (*S*)-benzyl methyl sulfoxides directed the methyl group and benzyl groups to the C-terminal phenyl group and to the *N*-terminal phenyl group, respectively. This arrangement makes the phenyl groups of **1** and benzyl methyl sulfoxide pack tightly in the usual herringbone motif [24]. The relative position between the ammonium proton and the C-terminal phenyl group in one molecule of the dipeptide determined which is included, its (*S*)-enantiomer or (*R*)-enantiomer.

5 INCLUSION OF ETHERS

In Section 2, it was revealed that (*R*)-(1-naphthyl)glycyl-(*R*)-phenylglycine (**2**) forms inclusion compounds with ethers (tetrahydrofuran and diethyl ether). X-ray crystallographic study showed that the dipeptide has the ability to form a ‘parallel’

β -sheet-like structure. It is worthy of note that (*R*)-phenylglycyl-(*R*)-phenylglycine (**1**) also forms an inclusion compound with THF or ether. These crystals have the similar parallel β -sheet-like structure, but they are so unstable that the included ether molecules escape from the crystal lattice at room temperature to give the original crystals of **1**.

We also found the inclusion of 1,2-dimethoxyethane and its derivatives (guests) between the layers in crystalline dipeptide (**1** or **2**), as summarized in Table 2 [25].

Packing views of the crystal structures for the DME- and *o*-dimethoxybenzene-included compounds of **2** are illustrated in Figure 15. The inclusion compounds have the same layer structure, where the dipeptide molecules were arranged to adopt a parallel β -sheet-like structure. The neighboring naphthyl and phenyl rings stacked with one another with the aid of edge-to-face interactions, to form a wall on the layer [13,14]. The benzene rings of the *o*-dimethoxybenzene molecules effectively stacked between the wall of the naphthyl and phenyl groups (Figure 15b). As can be seen in the figure, the guest molecules act as pillars to change the layer distance according to their length.

Consideration of the CPK model also implies that the channel cavity of **1** is wider than that of **2** [21]. The channel cavity of **2** expands at one side, with the

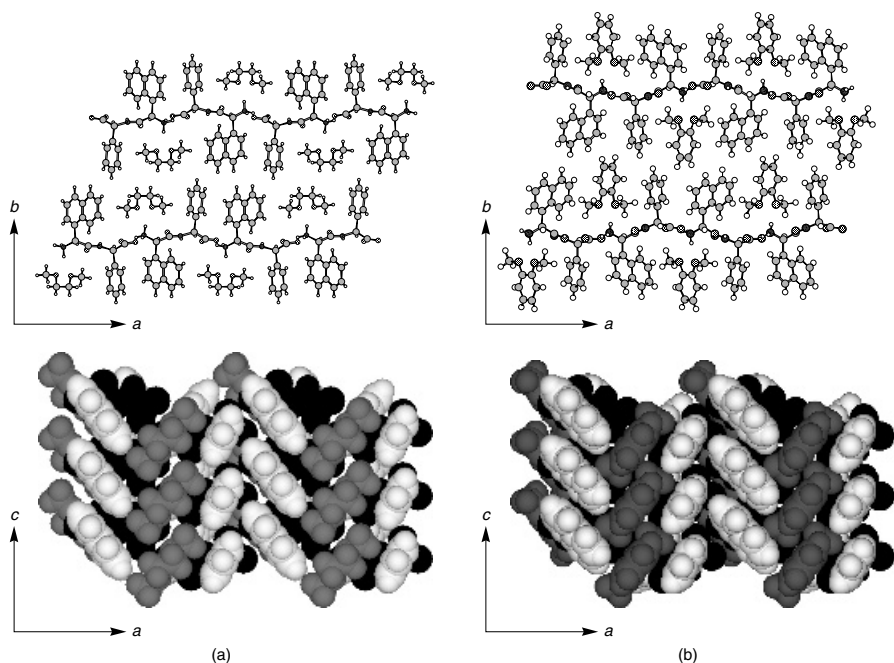
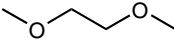
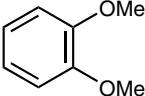
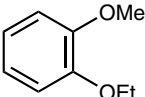
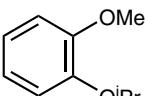
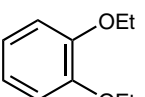
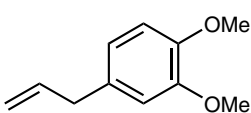
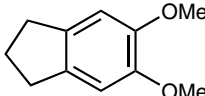


Figure 15 Inclusion compounds of 1,2-dimethoxyethane (a) and *o*-dimethoxybenzene (b) by **2**. Layer structure and packing (CPK model) of these inclusion compounds. For clarity, phenyl groups of **2** and guest are unshaded and gray, respectively.

Table 2 Inclusion of ethers by crystallization of dipeptides.

Entry	Guest	1		2	
		Ef. ^a (%)	LD ^b (Å)	Ef. ^a (%)	LD ^b (Å)
1		100	11.8	100	12.1
2		98	13.5	100	13.7
3		83	13.4	78	13.8
4		42	13.4	Not included	
5		Not included		Not included	
6		94	15.2	90	15.2
7		78	15.7	88	15.0

^aEf. means the ratio (mol. %) of the guest based on the dipeptide in the inclusion compound.

^bLD means the layer distance measured by PXRD.

^cCrystals released the guest during isolation.

replacement of a naphthyl group by a phenyl group, to include a larger guest molecule. In fact, **1** more easily formed an inclusion compound with 1-ethoxy-2-methoxybenzene and 1-isopropoxy-2-methoxybenzene than did **2** (entries 2–4 in Table 2). Since another side of the cavity always terminates at the phenyl group, it is reasonably rationalized that 1,2-diethoxybenzene is not included. It is likely that the substituents at the 4- and/or 5-positions of 1,2-dimethoxybenzene do not hinder the inclusion. As expected, 4-allyl-1,2-dimethoxybenzene and 5,6-dimethoxyindan formed the corresponding inclusion compounds with high efficiency. It is noteworthy that the interlayer distances increased in these inclusion

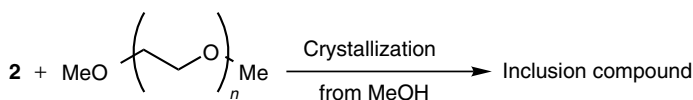
compounds. Thus, the interlayer distance of inclusion compounds is changeable and adjustable, depending on the size of the guest.

6 INCLUSION OF POLY(ETHYLENE GLYCOL)S AND THEIR DIMETHYL ETHERS

In the DME-included compound of **2**, DME molecules are regularly arranged in the one-dimensional channel. By intermolecular linkage of the terminal methyl groups of DME, the arranged DME molecules can be regarded as the dimethyl ether of poly(ethylene glycol)s (PEG). Hence, we investigated whether **2** molecules form an inclusion compound of an oligo(ethylene glycol) dimethyl ether ($\text{CH}_3\text{O}-(\text{CH}_2\text{CH}_2\text{O})_n-\text{CH}_3$; PEG DM(n)) [26]. The illustration in Table 3 shows that the calculated molar ratios can be estimated according to an equation $(n + 1)/2$, in which n is the number of the ethyleneoxy unit.

Ten kinds of PEG DM ($n = 1-7, 9, 12$ and 20) were selected as guest molecules. Fortunately, the inclusion compound was obtained from **2** and all of the selected PEG DM(n) by co-crystallization from methanol. As summarized

Table 3 Inclusion of poly(ethylene glycol) dimethyl ethers by the dipeptide (**2**).



Guest	Calculated H/G ^a	Observed H/G ^b	LD ^c	
$n = 1$	1.00	1.00	12.1	
$n = 2$	1.50	1.56	12.2	
$n = 3$	2.00	1.92	12.2	
$n = 4$	2.50	2.50	12.2	
$n = 5$	3.00	3.10	12.0	
$n = 6$	3.50	3.15	12.3	
$n = 7$	4.00	3.80	12.1	
$n = 9$	5.00	5.00	12.3	
$n = 12$	6.50	6.40	12.1	
$n = 20$	10.50	10.50	12.1	

^aCalculated values of the host/guest ratio.

^bThe host/guest ratio determined by NMR.

^cThe layer distance measured by PXRD.

in Table 3, PEG DE(*n*) molecules were efficiently included in the crystal lattice of **2**. Actually, the observed ratios were proportional to the length of the polymer chain and comparable with the calculated ratios.

In their PXRD patterns, all of these inclusion compounds showed a strong diffraction peak at a lower 2θ angle. Irrespective of the length of the included oligomers, the strong peaks appear in the range 12.0–12.3 Å. Notably, these values are the same as the interlayer distance of the inclusion compound of **2** and DME. Therefore, it is suggested that oligo(ethylene glycol) dimethyl ethers are accommodated in the channel constructed by **2** molecules. When hepta(ethylene glycol) dimethyl ether (PEG DM(7)) was used as the guest molecule, we obtained a single crystal suitable for X-ray crystallographic analysis at 173 K. By regarding a series of the guest molecules in the channel as the repeating of a $-\text{C}-\text{C}-\text{O}-\text{C}-\text{C}-\text{O}-$ moiety, their conformation could be resolved and refined isotropically.

A herringbone motif of naphthyl and phenyl groups forms the wall of the one-dimensional channel, and the PEG DM(7) molecules are accommodated in the channel via hydrogen bonding ($\text{O}\cdots\text{N}$ distance: 2.98 Å). The conformation of PEG DM(7) was found to be $\text{G}^+\text{TG}^-\text{G}^+\text{TG}^-$, where T, G^+ and G^- denote *trans*, right-handed *gauche*, and left-handed *gauche* conformations, respectively (Figure 16b). A similar conformation of a PEG chain was observed in a PEG– HgCl_2 as shown in Figure 16c [27]. Thus, the included PEGs adopt a conformation that not only conforms to the spatial restriction of the inclusion channel, but also to the requirements of the above-mentioned hydrogen bonding. It should be noted that the ethyleneoxy unit seems to be essential for the inclusion in the one-dimensional channel, because no tris(trimethylene glycol) dimethyl ether ($\text{CH}_3\text{O}(\text{CH}_2\text{CH}_2\text{CH}_2\text{O})_3\text{CH}_3$) was included at all.

The dipeptide (**2**) formed an inclusion compound with such alcoholic guests as allyl alcohols and α -hydroxy esters. In these cases, the one-dimensional channel was not constructed, but a zero-dimensional pocket-type cavity was formed [20]. Therefore, it is doubtful whether poly(ethylene glycol)s (PEGs) are included in the crystal lattice of **2**. Indeed, tri(ethylene glycol), tetra(ethylene glycol) and tri(ethylene glycol) monomethyl ether did not form the corresponding inclusion crystals. A thought occurred to us: if the poly(ethylene glycol)s (PEG(M_n)) are fairly long, then their terminal hydroxy groups might have little influence over the present inclusion. Hence, we tried to form an inclusion compound from PEGs with high molecular weight. PEGs with a molecular weight of 400–20 000 succeeded in forming the corresponding inclusion compounds. The ratios of **2**: PEG correspond well with the values calculated by the equation $(n + 1)/2$ (see later). The layer distances of these inclusion compounds, which were assigned by their PXRD analysis, are in the range of 12.0–12.1 Å. These facts supported the observation that the present inclusion compounds have a layer structure similar to that of the DME inclusion compound.

We were also interested in the possibility that a mixture of PEGs with various molecular weights might be fractionated by inclusion into **2** crystals. Preliminarily,

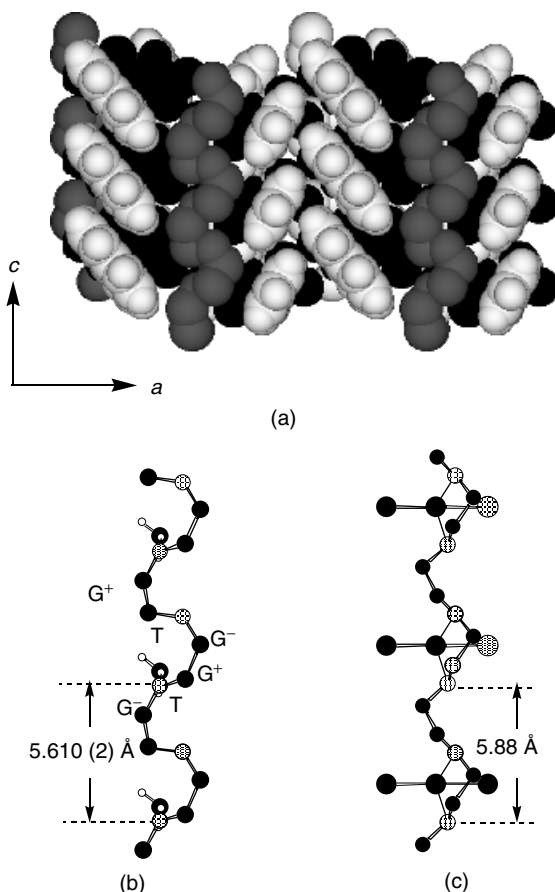


Figure 16 (a) Inclusion compound of $\text{MeO}(\text{CH}_2\text{CH}_2\text{O})_7\text{Me}$ by **2**. The guest molecule was resolved as a PEG. (b) Conformation of PEG in the channel. (c) PEG– HgCl_2 complex.

we investigated the fractionation of PEG DM(4) and PEG DM(12). After a mixture (82.0 mg) of PEG DM(4) and PEG DM(12) (49:51, wt/wt) was dissolved in methanol containing **2**, the resulting solution was allowed to stand at room temperature. After about one week, the deposited crystals were collected by filtration. The ratio of PEG DM(4):PEG DM(12) in the crystals was determined by GPC to be 14:86 (the total amount of PEG DM(4) and PEG DM(12) = 20.2 mg). In a similar manner, PEGs with a broad distribution of molecular weight were fractionated. The PEG mixtures was prepared by mixing commercially available PEGs. Sample A is a 1:1 mixture of commercial PEG #1000 and PEG #20 000. Sample B is a 1:1:1 mixture of PEG #600, PEG #1000, and PEG #1,500. In the case of Sample A, the ratio of the included PEGs #1000 and #20 000 was 35:65, while that of the non-included ones was 56:44. The favorable inclusion of a PEG with a higher

molecular weight was also observed in the inclusion of Sample B, as summarized in Figure 17.

Since analogous phenomena were reported in the formation of urea–poly(tetrahydrofuran) inclusion compounds [28,29], it seems to be generally conclusive that, in the crystallization process, the inclusion of a polymer with higher molecular weight is more favored. This is reasonably explained in terms of entropic advantage: inversely speaking, the inclusion of a polymer with a higher molecular weight involves a smaller entropy loss.

7 SUMMARY

We have described the molecular recognition of various guests using (*R*)-phenylglycyl-(*R*)-phenylglycine (**1**) and (*R*)-(1-naphthyl)glycyl-(*R*)-phenylglycine (**2**)

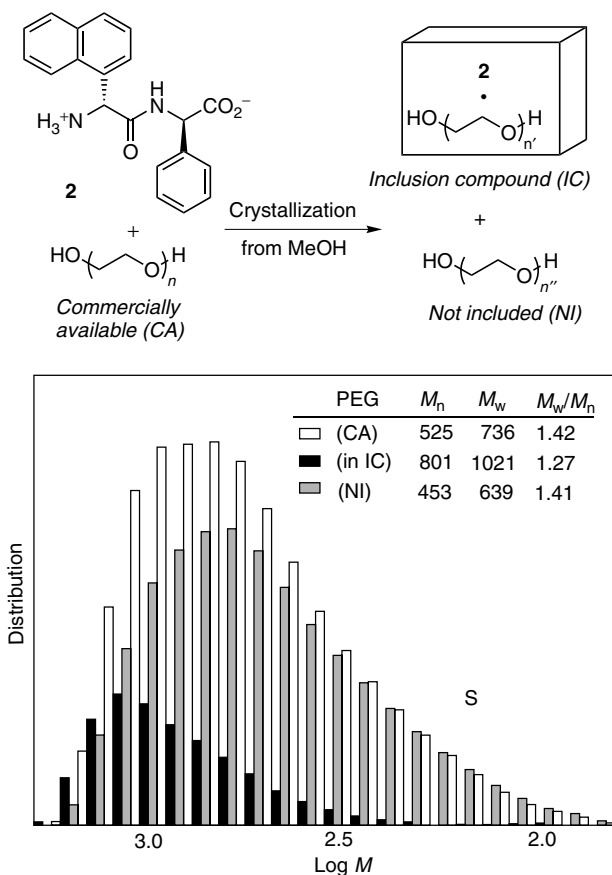


Figure 17 Molecular weight distribution: the polymer employed (white), the included polymer (black), and the non-included polymer (gray).

to form inclusion crystals. Their crystal structures vary according to the functionalities and the size of the guest. Since these dipeptides have a straight glycyglycine backbone, a two-dimensional layer is generally constructed by intermolecular salt formation between the COOH and NH₂ groups. Guest molecules are included between the layers via host–guest interactions such as hydrogen bonding, aromatic–aromatic interaction and CH/π interaction. α-hydroxy esters and sulfoxides were included with high enantioselectivity in the chiral cavities. Motifs of dipeptide aggregation depend on the type of guest: sulfoxide and ether guests assemble the dipeptide molecules in parallel, whereas α-hydroxy esters arrange them in antiparallel. It was demonstrated that these simple dipeptide hosts change their conformation according to the shape of the guest. This seems like a flexible model for the recognition of substrates by enzymes. Interestingly, the peptides recognized poly(ethylene glycol)s, which penetrated through the crystal lattice. Longer polymers were preferably recognized and the inclusion crystals became more thermally stable.

REFERENCES

1. Comprehensive Supramolecular Chemistry, eds D. D. MacNicol, F. Toda and R. Bishop, Elsevier Science, Oxford, 1996, Vol. 6.
2. (a) G. R. Desiraju, *Crystal Engineering: the Design of Organic Solids*, Elsevier, New York (1989); (b) J. C. MacDonald and G. M. Whitesides, *Chem. Rev.*, **94**, 94 (1994); (c) J. S. Moore and S. Lee, *Chem. Ind.*, **1994**, 556 (1994); (d) V. A. Russell, M. C. Etter, and M. D. Ward, *J. Am. Chem. Soc.*, **116**, 1941 (1994); (e) S. Hanessian, M. Simard and S. Roelens, *J. Am. Chem. Soc.*, **117**, 7630 (1995); (f) J. D. Hartgerink, J. R. Granja, R. A. Milligan and M. R. Ghadiri, *J. Am. Chem. Soc.*, **118**, 43 (1996); (g) A. Zafar, J. Yang, S. J. Geib and A. D. Hamilton, *Tetrahedron Lett.*, **37**, 2327 (1996); (h) F. D. Lewis, J.-S. Yang and C. L. Stern, *J. Am. Chem. Soc.*, **118**, 12029 (1996); (i) S. Coe, J. J. Kane, T. L. Nguyen, L. M. Toledo, E. Wininger, F. W. Fowler and J. W. Lauher, *J. Am. Chem. Soc.*, **119**, 86 (1997).
3. (a) A. Gavezzotti, *J. Am. Chem. Soc.*, **113**, 4622 (1991); (b) A. Gavezzotti and G. Filippini, *J. Am. Chem. Soc.*, **118**, 7153 (1996).
4. *Molecular Inclusion and Molecular Recognition – Clathrates I and II*, ed. E. Weber, Springer-Verlag, Berlin–Heidelberg (1987) and (1988), Vols 140 and 149.
5. (a) Y. Aoyama, K. Endo, K. Kobayashi and H. Masuda, *Supramolecular Chem.*, **4**, 229 (1995); (b) S. V. Kolotuchin, E. E. Fenlon, S. R. Wilson, C. J. Loweth and S. C. Zimmerman, *Angew. Chem., Int. Ed. Engl.*, **34**, 2654 (1995); (c) D. Su, X. Wang, M. Simard and J. D. Wuest, *Supramolecular Chem.*, **6**, 171 (1995); (d) A. T. Ung, D. Gizachew, R. Bishop, M. L. Scudder, I. G. Dance and D. C. Craig, *J. Am. Chem. Soc.*, **117**, 8745 (1995); (e) P. Brunet, M. Simard and J. D. Wuest, *J. Am. Chem. Soc.*, **119**, 2737 (1997); (f) K. Endo, T. Koike, T. Sawaki, O. Hayashida, H. Masuda and Y. Aoyama, *J. Am. Chem. Soc.*, **119**, 4117 (1997).
6. O. M. Yaghi, C. E. Davis, G. Li and H. Li, *Nature*, **378**, 703 (1995).
7. V. A. Russell, C. C. Evans, W. Li and M. D. Ward, *Science*, **276**, 575 (1997).

8. K. Ogura, T. Uchida, M. Noguchi, M. Minoguchi, A. Murata, M. Fujita and K. Ogata, *Tetrahedron Lett.*, **31**, 3331 (1990).
9. (a) C. G. Suresh, M. Vijayan, *Int. J. Peptide Protein Res.*, **26**, 311 (1985); (b) C. H. Görbitz, M. C. Etter, *Int. J. Peptide Protein Res.*, **39**, 93 (1992).
10. (a) C. H. Görbitz, *Acta Cryst.*, **C53**, 736 (1997); (b) C. H. Görbitz, *Acta Cryst.*, **C55**, 670 (1999); (c) C. H. Görbitz, *Acta Cryst.*, **C55**, 2171 (1999); (d) C. H. Görbitz and E. Torgersen, *Acta Cryst.*, **B55**, 104 (1999); (e) S. M. Mitra, L. Govindasamy and E. Subramanian, *Acta Cryst.*, **C53**, 2871 (1996).
11. T. Ashida, I. Tanaka and Y. Yamane, *Int. J. Protein Res.*, **17**, 322 (1981).
12. (a) K. Y. Tsang, H. Diaz, N. Graciani, and J. W. Kelly, *J. Am. Chem. Soc.*, **116**, 3988 (1994); (b) S. R. LaBrenz and J. W. Kelly, *J. Am. Chem. Soc.*, **117**, 1655 (1995); (c) J. P. Schneider and J. W. Kelly, *J. Am. Chem. Soc.*, **117**, 2533 (1995); (d) J. P. Schneider and J. W. Kelly, *Chem. Rev.*, **95**, 2169 (1995); (e) J. S. Nowick, E. M. Smith and G. Noronha, *J. Org. Chem.*, **60**, 7386 (1995); (f) J. S. Nowick, S. Mahrus, E. M. Smith and J. W. Ziller, *J. Am. Chem. Soc.*, **118**, 1066 (1996); (g) J. S. Nowick, D. L. Holmes, G. Mackin, G. Noronha, A. J. Shaka and E. M. Smith, *J. Am. Chem. Soc.*, **118**, 2764 (1996).
13. (a) S. K. Burley and G. A. Petsko, *Science*, **229**, 23 (1985); (b) R. O. Gould, A. M. Gray, P. Taylor and M. D. Walkinshaw, *J. Am. Chem. Soc.*, **107**, 5921 (1985); (c) S. K. Burley and G. A. Petsko, *J. Am. Chem. Soc.*, **108**, 7995 (1986); (d) C. A. Hunter and J. K. M. Sanders, *J. Am. Chem. Soc.*, **112**, 5525 (1990); (e) A. P. Bisson, F. J. Carver, C. A. Hunter and J. P. Waltho, *J. Am. Chem. Soc.*, **116**, 10292 (1994).
14. (a) W. L. Jorgensen and D. L. Severance, *J. Am. Chem. Soc.*, **112**, 4768 (1990); (b) S. Tsuzuki, K. Honda, T. Uchimura, M. Mikami and K. Tanabe, *J. Am. Chem. Soc.*, **124**, 104 (2002).
15. For a review of CH/ π interactions, see: M. Nishio, Y. Umezawa, M. Hirota, and Y. Takeuchi, *Tetrahedron*, **51**, 8665 (1995) and references therein.
16. M. Akazome, A. Sumikawa, R. Sonobe and K. Ogura, *Chem. Lett.*, **1996**, 995 (1996).
17. (a) M. Sundaralingam and Y. C. Sekharudu, *Science*, **244**, 1333 (1989); (b) R. Parthasarathy, S. Chaturvedi and K. Go, *Proc. Natl. Acad. Sci. USA*, **87**, 871 (1990).
18. M. Akazome, T. Takahashi, R. Sonobe, and K. Ogura, *Tetrahedron*, **58**, 8857 (2002).
19. There are a few reports for enantiomeric inclusion of hydroxy esters by other crystalline hosts, see: (a) F. Cramer and W. Dietsche, *Chem. Ber.*, **92**, 378 (1959); (b) F. Toda and Y. Tohi, *J. Chem. Soc., Chem. Commun.*, **1993**, 1238 (1993); (c) F. Toda and K. Tanaka, *Tetrahedron Lett.*, **29**, 1807 (1988); (d) F. Toda, A. Sato, K. Tanaka and T. C. W. Mak, *Chem. Lett.*, 781 (1988); (e) A. Mravik, Z. Böcskei, Z. Katona, I. Markovits and E. Fogassy, *Angew. Chem., Int. Ed. Engl.*, **36**, 1534 (1997).
20. M. Akazome, T. Takahashi and K. Ogura, *J. Org. Chem.*, **64**, 2293 (1999).
21. M. Akazome, M. Noguchi, O. Tanaka, A. Sumikawa, T. Uchida and K. Ogura, *Tetrahedron*, **53**, 8315 (1997).
22. D. A. Dougherty, *Science*, **271**, 163 (1997).
23. M. Akazome, Y. Ueno, H. Ooiso and K. Ogura, *J. Org. Chem.*, **65**, 68 (2000).
24. (a) J. A. Swift, R. Pal and J. M. McBride, *J. Am. Chem. Soc.*, **120**, 96 (1998); (b) G. R. Desiraju and A. Gavezzotti, *J. Chem. Soc., Chem. Commun.* **1989**, 621 (1989); (c) A. Gavezzotti, *Chem. Phys. Lett.*, **161**, 67 (1989).

25. M. Akazome, Y. Yanagita, R. Sonobe and K. Ogura, *Bull. Chem. Soc. Jpn.*, **70**, 2823 (1997).
26. M. Akazome, T. Takahashi, R. Sonobe and K. Ogura, *Supramolecular Chem.*, **13**, 109 (2001).
27. M. Yokoyama, H. Ishihara, R. Iwamoto and H. Tadokoro, *Macromolecules*, **2**, 184 (1969).
28. A. Chenite and F. Brisse, *Macromolecules*, **25**, 776 (1992).
29. G. Schmidt, V. Enkelmann, U. Westphal, M. Dröscher and G. Wegner, *Colloid Polym. Sci.*, **263**, 120 (1985).

Chapter 4

Separation of Isomers and Enantiomers by Bile Acid Derivatives

NUNGRUETHAI YOSWATHANANONT AND MIKIJI MIYATA

Department of Material and Life Science, Graduate School of Engineering, Osaka University, 2-1 Yamadaoka, Suita, Osaka 565-0871, Japan

KAZUNORI NAKANO

Nagoya Municipal Industrial Research Institute, 3-4-41, Rokuban, Atsuta-ku, Nagoya 456-0058, Japan

KAZUKI SADA

Department of Chemistry and Biochemistry, Graduate School of Engineering, Kyushu University, 6-10-1 Hakozaki, Higashi-ku, Fukuoka 812-8581, Japan

1 INTRODUCTION

Extensive systematic work over the past decade has established that bile acid derivatives have the ability to form crystalline inclusion compounds with various organic substances [1]. The accumulated data tell us two notable things. One is that their inclusion behavior varies from one case to another. The other is that their crystals consist of host-inherent or guest-dependent assemblies with different molecular arrangements and hydrogen-bonding networks. These facts force us to direct our attention to separation engineering accompanied by crystallization and

intercalation processes. This article will first describe the inclusion behavior of bile acid derivatives, and then the separation of isomers and enantiomers.

It is well known that bile acids are produced in the liver of vertebrates for digestion and absorption of fats and fat-soluble vitamins. Starting from isoprene, a series of biochemical reactions yield a key compound, cholesterol, which is converted to primary bile acids, such as cholic acid (CA), deoxycholic acid (DCA), chenodeoxycholic acid (CDCA) and lithocholic acid (LCA). Hereafter the abbreviations of bile acid derivatives can be seen by consulting Table 1 and Figure 1.

DCA is the first bile acid whose inclusion ability was confirmed in the crystalline state. During the last century many research groups dealt with the inclusion compounds of DCA with various guest molecules, such as aliphatic, aromatic and alicyclic hydrocarbons, alcohols, ketones, fatty acids, esters, ethers, nitriles, peroxides and amines, and so on [2]. In 1972, Craven and DeTitta first reported the exact crystal structure of DCA with acetic acid [3]. Subsequent crystallographic studies made clear that most of DCA inclusion crystals have bilayer

Table 1 Bile acid derivatives and their abbreviations, as used in this article (see also Figure 1).

R ₁	R ₄	n	R ₂ = α -H, R ₃ = α -OH	R ₂ = α -OH, R ₃ = α -OH
α -OH	COOH	1	Deoxycholic acid (DCA)	Cholic acid (CA)
α -OH	CONH ₂	1	Deoxycholamide (DCAM)	Cholamide (CAM)
α -OH	CH ₂ OH	1	3 α ,12 α ,24-Trihydroxy-5 β -cholane (DCAtriol)	3 α ,7 α ,12 α ,24-Tetrahydroxy-5 β -cholane(CATetraol)
α -OH	COOCH ₃	1	Methyl deoxycholate (MDC)	Methyl cholate (MC)
α -OH	COOH	0	Nordeoxycholic acid (NDCA)	Norcholic acid (NCA)
α -OH	COOH	3	Bishomodeoxycholic acid (BHDCA)	Bishomocholic acid (BHCA)
β -OH	COOH	1	3-Epideoxycholic acid (3EDCA)	3-Epicholic acid (3ECA)
R ₁	R ₄	n	R ₂ = α -OH, R ₃ = α -H	R ₂ = α -H, R ₃ = α -H
α -OH	COOH	1	Chenodeoxycholic acid (CDCA)	Lithocholic acid (LCA)
α -OH	CONH ₂	1	Chenodeoxycholamide (CDCAM)	Lithocholamide (LCAM)
α -OH	CH ₂ OH	1	3 α ,7 α ,24-Trihydroxy-5 β -cholane (CDCAtriol)	3 α ,24-dihydroxy-5 β -cholane(LCAdiol)
α -OH	COOCH ₃	1	Methyl chenodeoxycholate (MDCD)	Methyl lithocholate (LMC)
α -OH	COOH	0	Norchenodeoxycholic acid (NCDCA)	Norlithocholic acid (NLCA)
α -OH	COOH	3	Bishomochenodeoxcholic acid (BHCDC)	Bishomolithocholic acid (BHLCA)
β -OH	COOH	1	3-Epichenodeoxycholic acid (3ECDCA)	3-Epilithocholic acid (3ELCA)

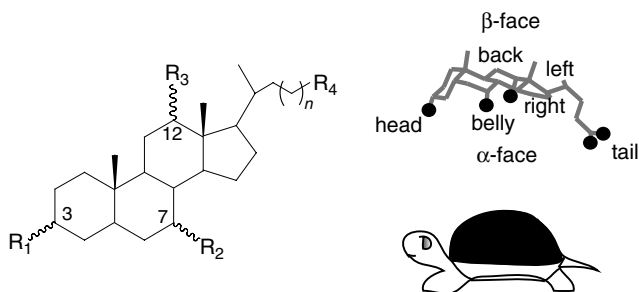


Figure 1 Schematic representation of the facially amphiphilic and asymmetric structure of a bile acid, a skeletal structure which can be likened to the body of a turtle.

structures, where the guest molecules are included in the channels composed of DCA molecules. In the mid-1980s, Giglio compiled an overview of the compounds to give a significant insight into flexible bilayer structures [4].

In contrast to DCA, there were no detailed reports on the inclusion abilities of its related compounds. There are only a few descriptions of apocholic acid [5] (ACA, see later, in Figure 5) with a very similar bilayer structure to DCA. In 1986, Miyata and Miki *et al.* discovered lots of inclusion compounds of CA with the similar bilayer structures [6]. On the other hand, it took a long time to determine the hexagonal crystal structures of CDCA inclusion compounds, and LCA exhibits no inclusion abilities as yet. In this way, it was confirmed that an increase or decrease of only one atom brings about completely different inclusion behaviors and crystal structures. This fascinating fact has given us adequate and continuous motivation to investigate the inclusion compounds of bile acid derivatives.

2 CHARACTERISTIC STRUCTURES OF BILE ACID DERIVATIVES

2.1 Unique Molecular Structures

Bile acid derivatives have unique molecular structures. As shown in Figure 1, they are composed of large, rigid, facial skeletons as well as small, flexible, axial side-chains. The many chiral carbon atoms create facially amphiphilic and asymmetric structures. The hydroxyl groups on the skeletons are directed toward the steroidal α -face to form a hydrophilic side, while the methyl groups are drawn towards the β -face to form a lipophilic side. The facially asymmetric structure enables us to distinguish the three axes of the skeletons. First, we will designate the hydrophilic and lipophilic sides as the *belly* and the *back*, respectively. Second, we will separate the small side-chain as the *tail*, and the reverse part of the skeleton as the *head*. And third, we will discriminate the hydroxyl groups at the carbon 7 and 12 positions as *left* and *right*, respectively.

2.2 Modification of the Molecular Structures and Inclusion Behavior

Bile acids can be modified to many derivatives due to their unique molecular structures, as listed in Table 1. First, we can convert the functional groups at the side-chains from carboxylic acid to amide, alcohol, ester, and so on. Second, we can change the length of the side-chains by decreasing or increasing their methylene number. Third, we can regulate the direction of the hydroxyl groups of the skeletons at the axial or equatorial positions.

We have researched the inclusion abilities of bile acid derivatives by using more than one hundred organic compounds as guest candidates. The inclusion phenomena vary from one case to another, indicating that subtle changes in molecular structures induce alteration in their molecular assemblies. In fact, X-ray diffraction studies prove that the steroidal hosts form various assemblies such as monolayers, bilayers, helical tubes, and so on, as shown in Figure 2. Therefore, systematic investigation of inclusion crystals of bile acid derivatives is expected to reveal a relationship between their molecular structures, assemblies and inclusion behavior.

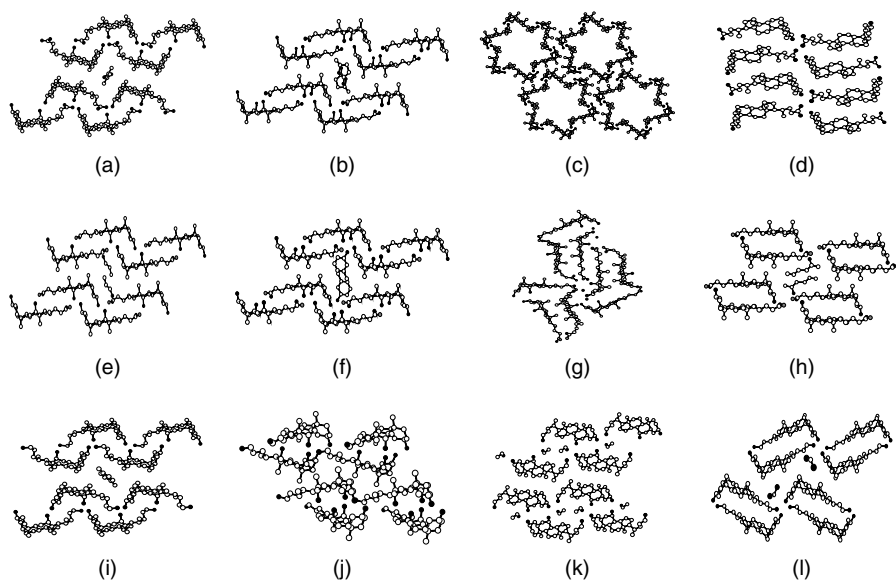


Figure 2 Crystal structures of (a) DCA with acetone, (b) CA with γ -valerolactone, (c) hexagonal crystal of CDCA, (d) guest-free crystal of LCA, (e) DCAM with 1-propanol, (f) CAM with *m*-cresol, (g) CDCAM with water, (h) LCAM with 2-hexanol, (i) DCAtriol with *p*-xylene, (j) guest-free crystal of CATetraol, (k) CDCAtriol with ethanol, and (l) LCAdiol with dichloromethane.

2.3 Assembly Process

Bile acid derivatives are assembled via weak noncovalent bonds such as van der Waals' forces and hydrogen bonds (Figure 3). One example of the assembly process is as follows. The host molecules are connected by multiple hydrogen-bonding groups to construct two-dimensional sheets with various hydrogen-bonding networks. Such sheets stack together in various ways, via van der Waals' forces, to yield different bilayer structures. This process produces various asymmetric combinations. For example, we can distinguish two types of molecular arrangements, parallel and antiparallel, in the case of the *head* and *tail* direction. These two arrangements theoretically combine together on both the hydrophilic and lipophilic sides to yield four types of arrangement, as shown in Figure 4(a). Most of the DCA inclusion crystals have a parallel arrangement on the hydrophilic side, but an antiparallel arrangement on the lipophilic side (Figure 4(b)). Table 2 lists a classification of the molecular arrangements in the bilayers.

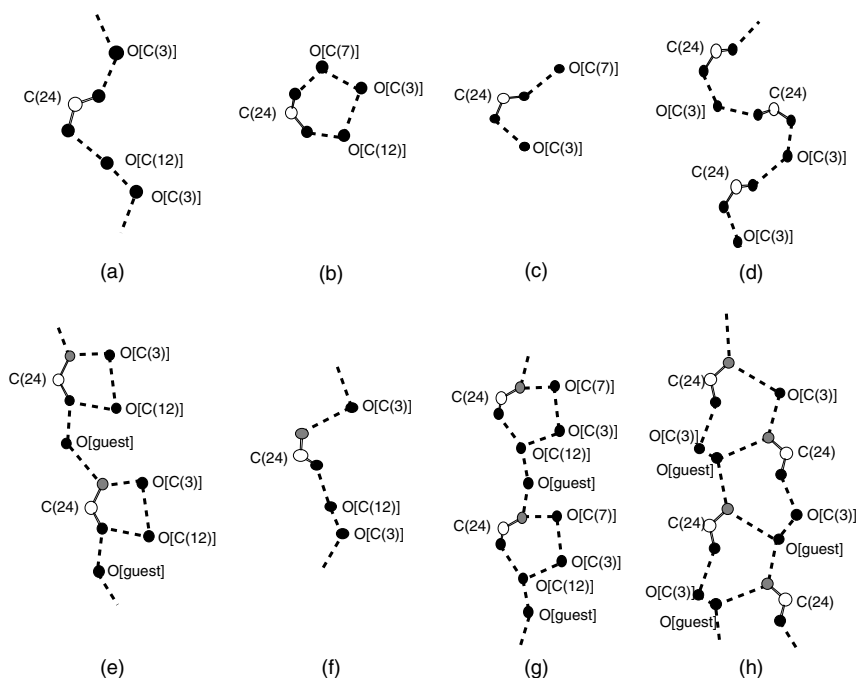


Figure 3 Hydrogen-bonding networks of (a) DCA, (b) CA, (c) CDCA, (d) LCA and (e) DCAM with a hydrogen-bonding guest, (f) DCAM with a non-hydrogen-bonding guest, (g) CAM and (h) LCAM. Carbon, nitrogen and oxygen atoms are represented by open, shaded, and filled circles, respectively.

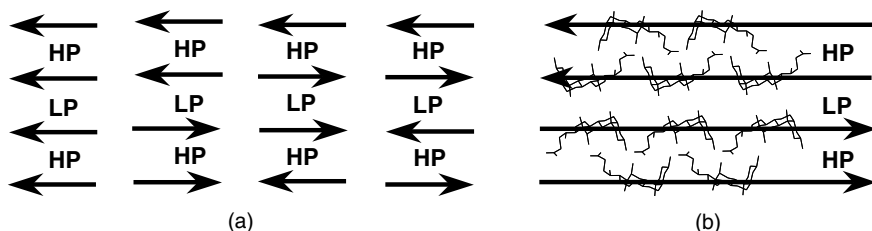


Figure 4 Schematic representation of molecular arrangements in a *head-to-tail* direction: (a) four different arrangements in the bilayers by a combination of the hydrophilic side (HP) and the lipophilic side (LP). (b) A bilayer with a parallel arrangement on HP sides and antiparallel on LP. The arrows indicate the direction from the *tail* to the *head*.

Table 2 Classification of molecular arrangements in asymmetric bilayers composed of steroidal molecules.

Type	Hydrophilic site	Lipophilic site	Host (guest)
1	Parallel	Parallel	DCatriol (benzene)
2	Parallel	Antiparallel	DCA (<i>p</i> -xylene) DCatriol (<i>p</i> -xylene)
3	Antiparallel	Parallel	CA (<i>m</i> -chloroaniline)
4	Antiparallel	Antiparallel	CA (benzene) CAM (1,4-dioxane)

3 INCLUSION COMPOUNDS OF BILE ACID DERIVATIVES

3.1 Acid Derivatives

DCA, one of the classical hosts, is known to form crystalline inclusion compounds with a wide range of organic substances. Most of the DCA inclusion crystals belong to the orthorhombic system, and have cumulated bilayer structures with channels (Figure 2(a)). The host molecules are arranged in a *head-to-tail* arrangement via a helical hydrogen-bonding network (Figure 3(a)). The side-chain adopts only the *gauche* conformation. Only a small selection of the inclusion compounds are shown in Table 3. ACA has slightly larger channels than DCA. Figures 5(a) and (b) show the molecular structure and the crystal structure of ACA, respectively. It is noteworthy that small alcohols are not included in the DCA and ACA channels.

Mylius, in 1887 [7] was the first to report that CA will include some alcohols. One hundred years later Johnson and Schaefer found that it possessed a crossing type of crystal structure [8], whereas Miki *et al.* discovered a bilayer structure [6b]. Extensive studies made it clear that CA forms various host frameworks to include a wide variety of organic guest compounds. For example, small

Table 3 Formation of the inclusion compounds of bile acid derivatives with their host-guest ratios.

Guest (G ₁)	DCA H:G ₁	CA H:G ₁	CDCA H:G ₁	LCA H:G ₁	NDCA H:G ₁ :G ₂ ^d	NCA H:G ₁ :G ₂ ^d	NCDCA H:G ₁	NLCA H:G ₁	DCAM H:G ₁ :G ₂ ^d	CAM H:G ₁ :G ₂ ^d
Methanol	NC ^b	1:1	NC	NC	W ^c	1:1	1:1	1:1	1:1	1:1
Ethanol	NC	1:1	NC	NC	1:1	1:1	1:1	1:1	1:1	1:1
1-Propanol	NC	1:1	NC	NC	1:1	2:1	1:1	2:1	1:1	1:1
2-Propanol	1:1	1:1	NC	NC	1:1	2:1:1	2:1	2:1	1:1	1:1
1-Butanol	NC	GF ^d	NC	NC	2:1:1	2:1	2:1	W	1:1	1:1
2-Butanol	NC	GF	NC	NC	1:1	NC	2:1	2:1	1:1	1:1
Acetone	1:1	GF	NC	NC	2:1	2:1:1	2:1	2:1	1:1:1	NC
Ethylene glycol	NC	1:1	NC	NC	W	1:1	1:1	2:1	NC	1:1:1
Acetophenone	1:1	1:1	NC	NC	2:1	2:3	GF	2:1	NC	1:1

^aG₂ = water.^bNC = not crystallized.^cW = water-included crystal.^dGF = guest-free crystal.

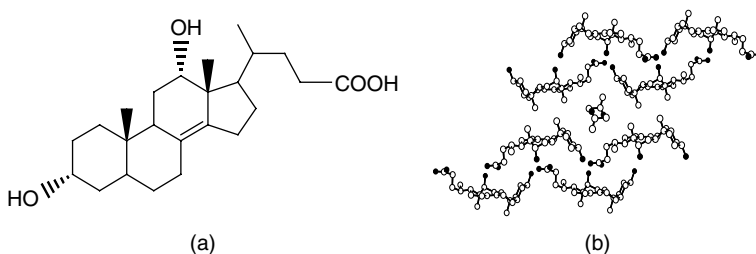


Figure 5 (a) Molecular structure of ACA and (b) crystal structure of ACA with acetone.

alcohols such as methanol, ethanol and propanol, are included in the crossing structure, while aromatic compounds are included in the bilayer structure (Table 3). The host molecules are arranged in an antiparallel fashion on the both hydrophilic and the lipophilic sides, as shown in Figure 2(b). The bilayer structure forms a cyclic hydrogen-bonding network between four hydrogen-bonding groups of four different host molecules (Figure 3(b)). The versatile enclathration of CA comes from isomerization of the host frameworks on the basis of layer sliding on the lipophilic sides and conformational changes in the side-chains.

Only a few reports [9–11] are concerned with inclusion compounds of CDCA, as compared with many papers on those of DCA and CA. CDCA forms guest-free crystals (monoclinic $P2_1$) [9a], as well as inclusion crystals with helical assemblies (hexagonal $P6_5$) [9b, 10]. Figure 2(c) shows the latter hexagonal structure, in which various guest compounds are included into a large channel. Figure 3(c) shows a helical hydrogen bonding network. Recently, large crystals were obtained from the gel state, leading to a study of intercalation and polymerization in CDCA channels while retaining a crystalline state [11].

LCA does not seem to include any organic guests (Table 3). In fact, we also failed to obtain inclusion compounds by recrystallization from over 100 organic compounds. Only two structures, guest-free (Figure 2(d)) and hydrate crystals, have been found [12]. Figure 3(d) shows the spiral hydrogen network of the guest-free crystal.

3.2 Amide Derivatives

A great change in inclusion ability was observed after replacing the carboxyl group by an amide group at the side-chain. Thus, an additional hydrogen-bond donor acts as a hook to catch a guest molecule with a hydrogen-bond acceptor, allowing bile amide hosts to include many aliphatic alcohols – in contrast to the original bile acids.

DCAM includes various types of organic compounds and does not give guest-free crystals at all (Table 3) [13]. There are several host frameworks which

depend on the type of guest. For example, Figure 2(e) illustrates a framework for the case of small alcohols. It has a bilayer structure where the host molecules are arranged in an antiparallel fashion both on the hydrophilic and lipophilic sides, as in the case of CA. The hydroxyl groups of the guest molecules insert into cyclic hydrogen-bonding networks (Figure 3(e)). Large alcohols or aromatic compounds lead to a different bilayer structure: a parallel mode on the hydrophilic side and an antiparallel mode on the lipophilic side, with a helical hydrogen-bonding network (Figure 3(f)), as in the case of DCA (Figure 3(a)).

CAM forms the same bilayer structure (Figure 2(f)) as CA, leading to the same steric dimensions of the host channels [14]. However, their inclusion abilities are completely different (Table 3). Thus, CAM prefer polar guests involving hydrogen-bonding groups and does not include non-polar guests. This tendency is opposite to that of CA, and arises from hydrogen-bond hooks on the wall of the channels. For example, CAM forms stable inclusion crystals with a wide range of alcohols, from methanol to decanol. The hydroxyl groups of the guest molecules are linked between two cyclic hydrogen-bonding networks among the host molecules, as depicted in Figure 3(g).

CDCAM does not yield inclusion crystals with organic guest molecules, but does hydrate crystals, as shown in Figure 2(g). In contrast, LCAM constructs a bilayer structure with channels for including various organic molecules, as shown in Figure 2(h) [15]. LCAM tends to include aliphatic alcohols involving over five carbon atoms, while it does not include small alcohols, such as methanol, ethanol and propanol. LCAM forms flexible molecular assemblies, due to the sliding of the bilayer as well as the conformational change of the side-chain. The transformation of the carboxyl to the amide group accompanies a change in the hydrogen-bonding network from the helical to ladder type, as shown in Figure 3(h).

3.3 Alcohol Derivatives

DCatriol prefers nonpolar guests such as aromatic compounds, but does not prefer polar guests such as alcohols [16]. The inclusion crystals of DCatriol with many guests have a parallel arrangement on the hydrophilic side and an antiparallel one on the lipophilic side, as shown in Figure 2(i). The helical hydrogen-bonding network of DCatriol is similar to that of DCA. However, in the benzene clathrate, the host molecules are arranged in a parallel fashion on both the hydrophilic and the lipophilic sides. On the other hand, CATetraol does not include organic guests at all and gives only guest-free crystals [17], as shown in Figure 2(j). Figure 2(k) shows a bilayer structure of CDCatriol, which is completely different from a tubular structure of CDCA (Figure 2(c)). Small alcohols are included in the hydrophilic sides of the bilayers. LCAdiol forms inclusion crystals only with small guests (Figure 2(l)).

3.4 Ester Derivatives

Esterification of the carboxylic acid decreases the number of hydrogen-bond donor groups at the steroidal side-chain, leading to a reduction in their inclusion abilities. MDC includes only methanol and does not form a bilayer structure [18]. MC includes only small polar guests [19]. The inclusion compounds of MC with small nitriles have the same crystal structure as that of CA with acetonitrile. Although there are no channels on the lipophilic sides, the guest molecules are held in the cavities between the pleated bilayers without host–guest hydrogen bonds. However, when the alcoholic guests are included, the side chains of the host molecules are pushed toward the lipophilic face. The hydroxyl groups of alcoholic guests are inserted in the helical hydrogen-bonding networks. On the other hand, MCDC and MLC do not seem to include any organic compounds.

3.5 Other Derivatives

3.5.1 Norbile acids

Norbile acids (NDCA, NCA, NCDCA and NLCA) have side-chain length one methylene unit shorter than the original bile acids. They form inclusion crystals with various organic substances (Table 3) [20]. Shortening of the side-chain length brings about a change in the orientation of the carboxyl group, to deform the hydrogen-bonding modes. Figure 6 shows the crystal structures and hydrogen-bonding networks of four norbile acids with acetone. It can be seen that they have

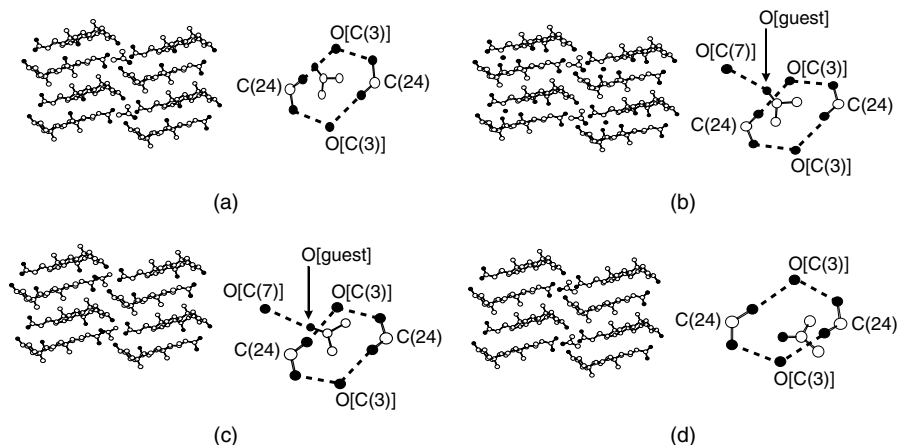


Figure 6 Crystal structures of norbile acids with acetone, together with hydrogen-bonding networks of (a) NDCA, (b) NCA, (c) NCDCA and (d) NLCA.

all the same bilayer structures with cage-like cavities. Their cyclic hydrogen-bonding networks are formed between two hydroxyl groups at the 3-position and two carboxyl groups at the side-chains, from four different host molecules. As shown in Table 3, NLCA and NCDCA include a wide range of organic substances, as compared with the lack of inclusion ability shown by the original LCA and CDCA.

3.5.2 *Bishomobile acids*

BHCA has two extra methylene units in its side chain, as compared with CA. It has been reported to form inclusion compounds with various guests [21] in a 1:1 host-to-guest ratio. X-ray crystallographic studies reveal that BHCA have two kinds of host frameworks: bilayer and crossing structures, like CA. Figure 7(a) shows the former host framework with 1-methylnaphthalene, and proves that the elongation of the side-chain of CA gives rise to the expansion of the host cavity. On the other hand, the latter host framework was employed with smaller compounds, such as nitriles and alcohols, as shown in Figure 7(b). In contrast to BHCA, the other bishomobile acids do not tend to include any guest molecules, and yield only guest-free crystals.

3.5.3 *3-Epibile acids*

3-Epibile acids are produced by directional change of the hydroxyl groups at the 3-position, from α to β . 3EDCA tends to include only hydrophilic guests such as alcohols and lactones [22], while DCA forms inclusion crystals with a wide range of organic compounds, except for alcohols. It can be seen from Figure 7(c) that 3EDCA molecules arrange in an antiparallel fashion on both the hydrophilic and lipophilic sides, creating cyclic hydrogen-bonding networks. 3ECA also produces inclusion crystals with various aliphatic alcohols. Figure 7(d) shows a crystal structure of 3ECA with 2-pentanol, which is very similar to the bilayer structure of CA. 3ECA forms a cyclic hydrogen-bonding network, as in the case of 3EDCA. The alcoholic guest is inserted between the 3- and 12-positioned hydroxy groups, as shown in Figures 7(c) and (d).

3.5.4 *Salt derivatives*

Bile acids, which have carboxylic acid groups at their side-chains, form salts with various amines. Salts of DCA and CA with various primary amines [23] show bilayer structures with a one-dimensional ladder hydrogen-bonding network. These salts act as host compounds and will include small alcohols.

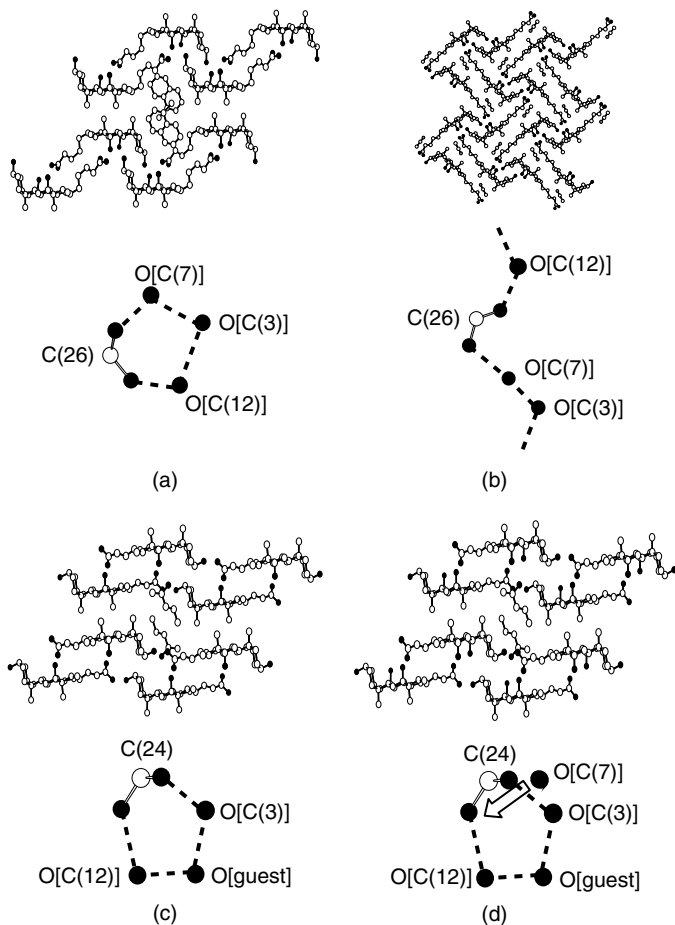


Figure 7 Crystal structures and hydrogen-bonding networks of BHCA: (a) bilayer structure, (b) crossing structure, and epibile acids with 2-pentanol, (c) 3EDCA, and (d) 3ECA.

4 INCLUSION MECHANISM OF BILE ACID DERIVATIVES

4.1 Polymorphism of Bile Acid Derivatives

4.1.1 Polymorphic crystals with different guests

Most of the bile acid derivatives exhibit guest-dependent polymorphism. The typical host is CA, which forms at least 12 host frameworks, depending on guest sizes and shapes, as shown in Figure 8. Most organic guests form bilayer structures, which can be further classified into several subtypes on the

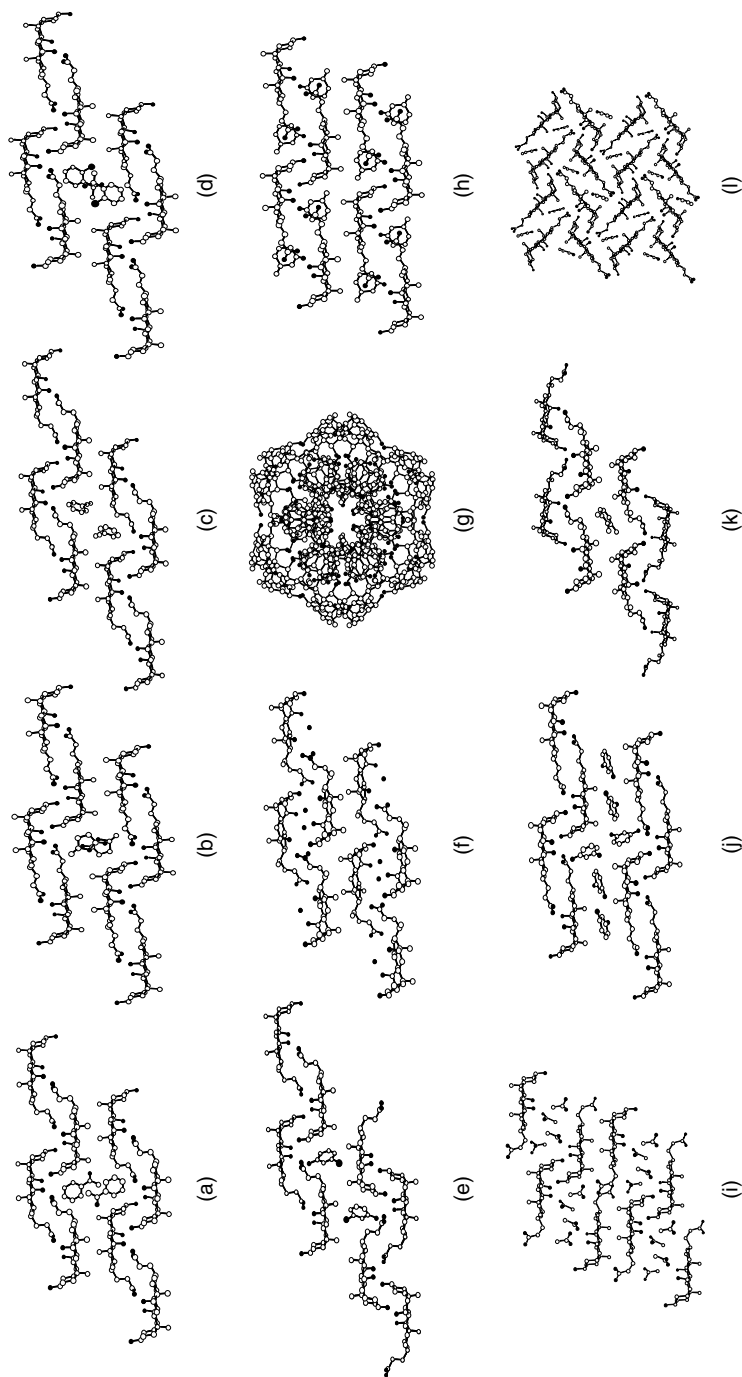


Figure 8 Guest-dependent polymorphism in CA inclusion crystals with (a) acetophenone, (b) γ -valerolactone, (c) ethynylbenzene, (d) 2-fluoropropiophenone, (e) *m*-chloroaniline, (f) water (Form I), (g) water (Form II), (h) 3-methylcyclohexanone, (i) acetic acid, (j) *m*-fluoroaniline, (k) 1,2,3-trimethylbenzene, and (l) acrylonitrile. Hydrogen atoms are omitted for clarity. Carbon, nitrogen and oxygen atoms are represented by open, gray and filled circles, respectively.

basis of the side-chain conformation and the interdigitation on the lipophilic layer [24]. Figures 8(a) to (d) show four subtypes; αG , αT , βG , and βT [24d]. *m*-Chloroaniline [24e] gives a parallel orientation of the CA molecules in the lipophilic layers and antiparallel in the hydrophilic layers (Figure 8(e)), while the other common guests give antiparallel orientation in both layers. Water molecules yield two different host frameworks as bilayer (Figure 8(f)) and hexagonal (Figure 8(g)) types [25]. Only 3-methylcyclohexanone gives the unique monoclinic *C2* crystal with larger host cavities (Figure 8(h)) [39b]. Acetic acid provides a bilayer structure in which the side-chain of the host molecules leans towards the lipophilic faces (Figure 8(i)) [26a]. A sandwich-type host framework with a two-dimensional inclusion cavity is formed by *m*-fluoroaniline, which is inserted into the lipophilic side of the bilayer in addition to the usual cavities (Figure 8(j)) [24b]. Trisubstituted-benzene guests are included in the DCA type (Figure 8(k)) [24c]. Small organic guests such as carboxylic acids, alcohols, nitriles and nitro compounds are included in the crossing structure (Figure 8(l)).

4.1.2 Polymorphic crystals with identical guests

4.1.2.1 Real polymorphism

Polymorphism in crystalline materials has been well documented. Most of the organic compounds have a chance to form their crystal packing with different molecular arrangements as well as with different conformations. This phenomenon is called crystal structure polymorphism and has attracted much attention for controlling the physical properties of crystals in the pharmaceutical and dye industries. Systematic investigation clarified that CA forms polymorphic inclusion crystals with acrylonitrile (Figures 9(a) and (b)) and methacrylonitrile (Figures 9(c) and 9(d)) [26a,b]. They have the same 1:1 host–guest ratios but different host frameworks (crossing and bilayer types). The formation of different polymorphs is influenced by recrystallization conditions such as the type of solvent, the temperature and the concentration of the guest in the feed solution. Moreover, conformational polymorphism is observed in 1:1 inclusion crystals of CA with ethyl acetate [26c]. Form I belongs to the monoclinic $P2_1$ system (Figure 9(e)), while Form II is triclinic $P1$ (Figure 9(f)). The side-chain adopts *gauche* and *trans* conformations in Forms I and II, respectively. The conformational differences in the side-chain affect the hydrogen-bonding networks, as well as the shape of the host channels. On the other hand, the polymorphs of CA with *o*-xylene have apparently different bilayer structures at a 2:1 host–guest ratio; Form I has an antiparallel stacking in the lipophilic layer and parallel stacking in the hydrophilic layer, while Form II has antiparallel stacking in both layers [24c].

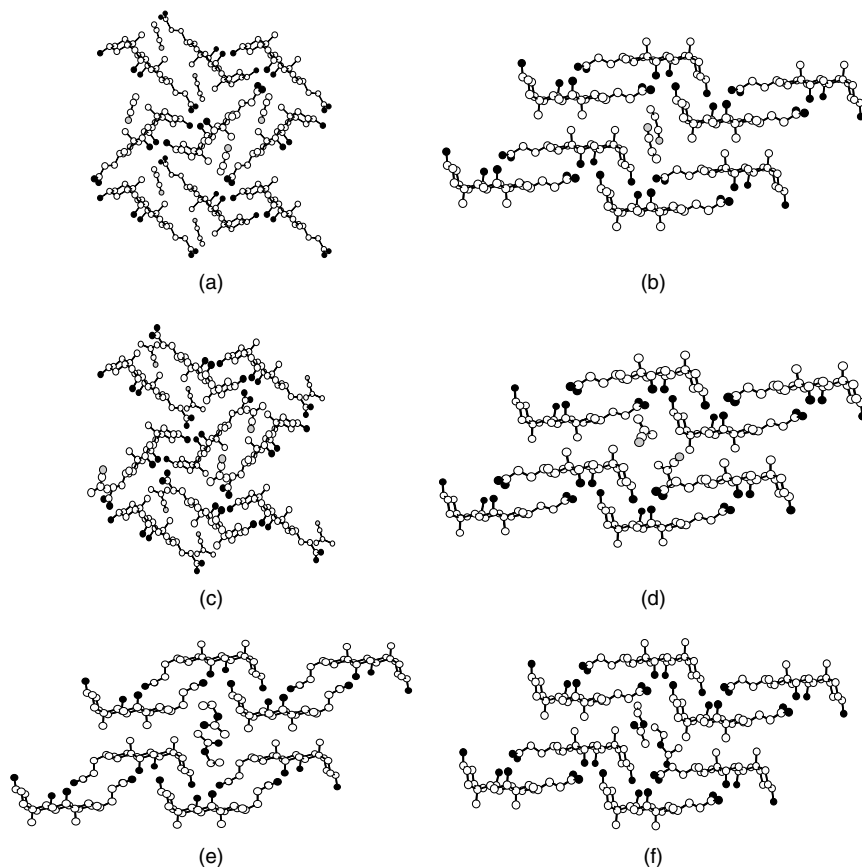


Figure 9 Molecular packing diagrams of CA with (1) acrylonitrile: (a) a crossing structure and (b) a bilayer structure; with (2) methacrylonitrile: (c) a crossing structure, and (d) a bilayer structure; and (3) with ethyl acetate: (e) Form I and (f) Form II. Hydrogen atoms are omitted for clarity. Carbon, nitrogen, and oxygen atoms are represented by open, gray and filled circles, respectively.

4.1.2.2 Pseudopolymorphism

Pseudopolymorphism is a term used to define the different crystal structures in which molecules of solvation differ in the species or in the stoichiometries to host molecules. Bile acid derivatives form pseudopolymorphs in different molar ratios of host and guest. Figures 10(a) and (b) show two polymorphs of CA with acetic acid [26a]. Direct recrystallization from acetic acid yielded 1:1 inclusion crystals (Figure 10(a)) that show a crossing structure with helical hydrogen bonding networks involving the carboxyl groups of the guest molecules. On the other hand, using cyclohexane as a third component yielded 1:2 inclusion crystals

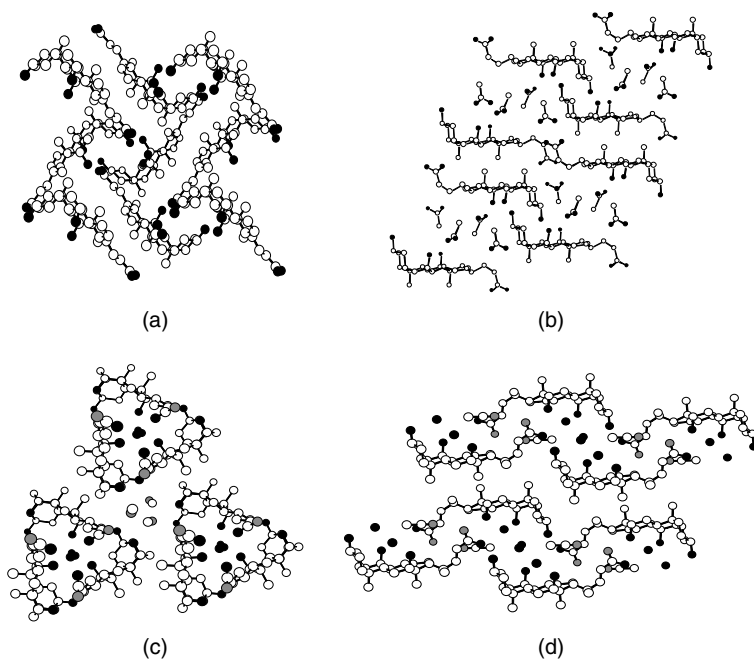


Figure 10 Crystal structures of CA with acetic acid: (a) 1:1 crossing structure and (b) 1:2 bilayer structure. Crystal structures of CAM with acetonitrile and water: (c) 1:1:1 triangular structure and (d) 1:1:2 bilayer structure. Open, gray and filled circles represent carbon, nitrogen and oxygen atoms, respectively. Hydrogen atoms are omitted for clarity.

with a bilayer structure (Figure 10(b)). The side-chain of the host molecule leans towards the lipophilic face, resulting in two types of cyclic hydrogen-bonding networks. One is the typical cyclic motif and the other is a carboxylic acid dimer motif. CAM also shows pseudopolymorphism when including acetonitrile and water [27]. The two polymorphs have different molar ratios and molecular assembly modes, as depicted in Figures 10(c) and (d). One polymorph (Form I) shows a triangular structure at a 1:1:1 molar ratio of CAM:acetonitrile:water. Form II gave a bilayer structure at 1:1:2 molar ratio. Water molecules support the formation of flexible host frameworks in the presence of acetonitrile.

4.2 Packing Coefficients of Host Cavities (PC_{cavity})

4.2.1 Definition of packing coefficients of host cavities (PC_{cavity})

The key and lock mechanism is widely accepted as a principle of molecular recognition. This concept is based on steric and electronic complementarity between

concave host cavities and convex guest compounds. The compounds that are complementary to the host cavities are included in the host frameworks, while otherwise do not act as guest compounds to give guest-free crystals or no crystalline mass. In particular, the size of included components plays an important role for the guest recognition in the host frameworks. Recently, Rebek introduced the term ‘packing coefficient’ – the ratio of the guest volume to the host volume – for his encapsulated host compounds in solution [28]. Using this concept, we have introduced the term packing coefficient of host cavity (*PCcavity*) as the parameter to define the size fit of the guest molecules in the host cavities for the inclusion crystals. *PCcavity* can be calculated from the following equation:

$$PCcavity = \frac{V_g \times Z_g}{V_c} \times 100$$

where V_g and Z_g refer to the volume of the guest molecule and the number of guest molecules in the unit cell, while V_c is the volume of the host cavity. Advances in X-ray crystallographic analyses and computation software for visualization of crystal structures are an advantage when studying the molecular unit in detail.

4.2.2 *PCcavity in the inclusion compounds of CA with aromatic guests*

The inclusion crystals of CA with monosubstituted benzenes [24d] were systematically investigated, and all of them were found to have bilayer structures with one-dimensional molecular channels. Table 4 shows values of their *PCcavity*, which was calculated from the free volumes of the host cavities and the molecular volumes of the guest compound in the unit cell, using the Cerius² software package [29] with the Free Volume program [30]. This is the first application of *PCcavity* to organic lattice inclusion compounds. *PCcavity* tends to increase with increasing guest volumes within the same host frameworks, indicating that the volumes of the host cavities are less sensitive than those of the guest molecules. The optimal values of *PCcavity* are in the range of 55–70%. This value is much larger than those of the encapsulated host compounds (46–64%) [28], and intermediate between the packing coefficients of the liquid state (44–56%) [28] and the crystalline state (66–77%) [31], as shown in Figure 11.

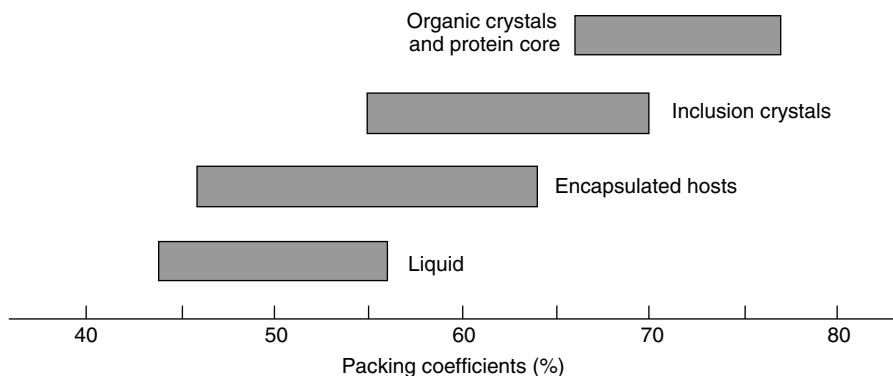
Guest molecules with *PCcavity* out of this range give rise to isomerization of the host frameworks or changes in the host-to-guest ratios, due to steric misfitting. In addition, *PCcavity* can be used as parameter for estimating the change of the host framework as well as the host:guest ratio, and also for screening guest molecules with the expected host frameworks. However, this range of *PCcavity* (55–70%) refers to inclusion crystals without host–guest hydrogen bonds, because most of the guest compounds are included in CA host cavities only by van der Waals’ forces. Therefore, the *PCcavity* of the host–guest crystals with

Table 4 Molecular volume of guests (V_g), host cavity (V_c) and PC_{cavity} in the inclusion compounds of CA with monosubstituted benzenes.

Guest	V_g (\AA^3)	V_c (\AA^3) ^a	PC_{cavity} (%) ^b
Benzene	83.4	298.1	56.0
Fluorobenzene	88.4	319.2	55.4
Aniline	95.8	336.0	57.0
Chlorobenzene	97.5	327.6	58.0
Toluene	100.8	334.5	60.3
Bromobenzene	101.8	318.9	63.8
Benzaldehyde	104.0	331.0	62.8
Iodobenzene	107.9	351.6	61.4
Nitrobenzene	109.6	326.4	67.2
Anisole	110.4	332.0	66.5
Styrene	111.2	345.7	64.3
Benzyl chloride	114.5	370.1	61.9
Ethylbenzene	117.7	386.1	61.0
Benzyl bromide	119.1	400.4	59.5
Acetophenone	120.9	344.9	70.1
Allylbenzene	127.9	393.9	64.9
Phenetol	128.1	389.2	65.8
Phenyl acetate	131.0	399.4	65.6

^a V_c is the volume of the cavity in the unit cell calculated with a 0.7 Å radius probe.

^b PC_{cavity} is the packing coefficient of the guest components in the host cavity.

**Figure 11** Packing coefficients in various states: organic crystals, protein cores, inclusion crystals, encapsulated hosts and the liquid state.

specific host–guest interactions such as hydrogen bonds, π – π interactions, and so on, should be expanding the range of *PCcavity*.

4.2.3 *PCcavity* in the inclusion compounds of CAM with aliphatic alcohol guests

As described earlier, CAM is effective at forming inclusion crystals with various aliphatic alcohols. X-ray crystallographic studies revealed that CAM and CA form the same host frameworks with similar host cavities. However, CAM includes guest compounds by host–guest hydrogen bonds, while CA does so by van der Waals' forces. Calculation of *PCcavity* in a system of CAM clathrates should indicate the effect of host–guest hydrogen bonds on the packing of the guest molecules in the host cavities.

Table 5 shows the molecular volume of aliphatic alcohol guests with *PCcavity*, whose values are in the range 50–75%. This range is wider than those of CA (55–70%), suggesting that the hydrogen bonds between host and guest molecules support the incorporation of guest molecules whose molecular volumes do not fit the host cavities. Therefore, a host that can form a host cavity with a hydrogen-bond hook is expected to have a wide inclusion ability.

Table 5 Molecular volume of guests (V_g), host cavity (V_c) and *PCcavity* in the inclusion compounds of CAM with aliphatic alcohols.

Guest	V_g (\AA^3)	V_c (\AA^3) ^a	<i>PCcavity</i> (%) ^b
Methanol	38.9	434.2	71.7
Ethanol	55.6	387.4	57.4
1-Propanol	73.4	274.3	53.5
2-Propanol	73.1	288.5	50.7
1-Butanol	91.1	316.3	57.6
<i>iso</i> -Butanol	90.3	300.3	60.1
<i>tert</i> -Butanol	89.5	362.6	49.4
1-Pentanol	108.4	328.1	66.1
1-Hexanol	126.2	366.1	68.9
4-Methyl-1-pentanol	125.5	336.4	74.6
1-Heptanol	144.0	404.3	71.2
1-Octanol	161.8	229.8	70.4
1-Nonanol	179.6	312.5	57.5
1-Decanol	196.7	358.0	55.0

^a V_c is the volume of the cavity in the unit cell calculated with a 0.7 \AA radius probe.

^b *PCcavity* is the packing coefficient of the guest components in the host cavity.

4.3 Guest Exchanges by Recrystallization and Intercalation

Inclusion crystals of bile acid derivatives can be obtained by direct recrystallization of host and liquid guests. When the guests do not have enough solubility for a host, the third component or the solvent were used. In the case of solid guests, solvents were used as well. The solvent should not form inclusion compounds with the host, and should not interact with host and guest compounds.

Intercalation phenomena have been long known in inorganic chemistry, for example with clay, graphite, and zeolites. However, Miyata *et al.* are the first to prove intercalation occurs in the organic crystal of CA [32a]. CA can absorb or exchange guest molecules by changing the host framework types, while retaining the crystalline state. Powder X-ray diffraction has provided valuable data for continuing investigation of the intercalation mechanism. Further study has made it clear that intercalation phenomena are not specific only to CA, but also to NDCA and the other bile acid hosts.

Another intercalation was observed in the inclusion crystals of CA with *n*-propylbenzene [32c]. Heat treatment of a 1:1 molar ratio of CA with *n*-propylbenzene gave intermediate inclusion crystals with the same guests at 2:1 stoichiometry. Comparison of both crystal structures by powder X-ray diffraction indicated that the bilayers slide past each other on the lipophilic sides by *ca.* 4.5 Å in the horizontal direction. The 2:1 crystals can be returned to the original crystal (1:1) by soaking them in the liquid *n*-propylbenzene, and the bilayer can slide back to the initial position without changing to the amorphous state.

5 SEPARATION OF ISOMERS BY BILE ACID DERIVATIVES

5.1 Competitive Recrystallizations Using CA

5.1.1 Method and evaluation of selectivities

Inclusion compounds of CA with hydrocarbons and esters were obtained easily by using 1-butanol as a solvent in the following way. A host solution was prepared by dissolving CA (130 mg) in 1-butanol (0.4 ml), while prescribed amounts (10 mmol) of two guest compounds were mixed to make a guest solution [24a]. After mixing both solutions, the resulting feed solution was allowed to settle overnight at 20 °C to attain crystallization equilibrium. On the other hand, in the case of carboxylic acid as a guest, CA (500 mg) was directly dissolved in the warmed guest liquids (10 mmol each) because CA is highly soluble in them. The resulting inclusion crystals were filtered and allowed to stand in air for some time, to remove the adhering solvent and guests on the crystal surface. Amounts of the guests incorporated within the crystals were determined by gas chromatography with an MS detector after dissolving the crystals in methanol and/or by X-ray crystallography for a single crystal.

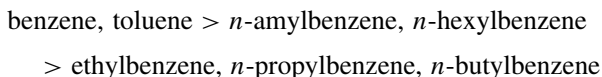
The experiments described here were carried out on guest mixtures under guest-rich conditions, i.e. crystallization was attained from solutions containing excess amounts of the two guests. The separation factor (SF) was defined and simplified under the present condition that the molar concentration of each guest was the same and much higher than that of the host, as follows:

$$\text{SF} = ([A]_{\text{cry}}/[A]_{\text{sol}})/([B]_{\text{cry}}/[B]_{\text{sol}}) = [A]_{\text{cry}}/[B]_{\text{cry}}$$

where the subscripts cry and sol denote the crystal and solution phases, respectively.

5.1.2 Competitive recrystallizations

Table 6 shows competitive recrystallization of CA with various compounds. Entries 1–21 are concerned with selectivity among *n*-alkylbenzenes from benzene to *n*-hexylbenzene [33]. The separation factors for all the binary systems of benzene and the other *n*-alkylbenzenes were more than unity, indicating that benzene is preferentially incorporated in the CA crystals. The selectivity increased with an increase in the number of the methylene groups in the guest molecules, and the separation factor became as high as 7.6 for *n*-butylbenzenes but then, a further increase reduced the separation factors. A similar trend can be seen in mixtures of toluene, and the highest separation factor of 15.1 was obtained from a mixture of toluene and *n*-propylbenzene. Moreover, *n*-amylbenzene and *n*-hexylbenzene are favorably included in CA as compared with the other three (ethylbenzene, *n*-propylbenzene, and *n*-butylbenzene). The following combinations gave no or less selective enclathrations ($0.75 < \text{SF} < 1.5$); benzene + toluene, ethylbenzene + *n*-propylbenzene, ethylbenzene + *n*-butylbenzene, and *n*-amylbenzene + *n*-hexylbenzene (entry 1, 12, 13 and 21). From the results, the order of inclusion in CA is (from more favorable to less favorable) as follows:



This order shows that the size of the guest molecules seems to be important for selective enclathration of CA, although the order is not in proportion to the molecular size.

Entry 22–24 shows competitive recrystallization from 1:1 mixtures of xylene isomers [34]. In contrast to mono-alkylbenzenes, *m*-xylene and *p*-xylene were exclusively included in CA cavities from mixtures of *o*- and *m*-xylene, *o*- and *p*-xylene, respectively, i.e. *o*-xylene acts as a solvent and is not included in the CA host cavity at all. Recrystallization from a 1:1 mixture of *m*-xylene and *p*-xylene yielded a crystal that included both guest components in a similar guest ratio

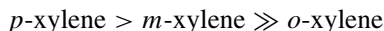
Table 6 Competitive recrystallizations of CA with various compounds^a.

Entry	Guest A	Guest B	$\frac{[A]_{\text{cry}}}{([A]_{\text{cry}} + [B]_{\text{cry}})}$ (%)	$\frac{[B]_{\text{cry}}}{([A]_{\text{cry}} + [B]_{\text{cry}})}$ (%)	SF (reciprocal value) ^b
1	Benzene	Toluene	54	46	1.2
2	Benzene	Ethylbenzene	81	19	4.3
3	Benzene	<i>n</i> -propylbenzene	84	16	5.3
4	Benzene	<i>n</i> -butylbenzene	88	12	7.6
5	Benzene	<i>n</i> -amylbenzene	80	20	4.0
6	Benzene	<i>n</i> -hexylbenzene	72	28	2.6
7	Toluene	Ethylbenzene	81	19	4.4
8	Toluene	<i>n</i> -propylbenzene	94	6	15.1
9	Toluene	<i>n</i> -butylbenzene	91	9	9.6
10	Toluene	<i>n</i> -amylbenzene	82	18	4.7
11	Toluene	<i>n</i> -hexylbenzene	78	22	3.5
12	Ethylbenzene	<i>n</i> -propylbenzene	59	41	1.4
13	Ethylbenzene	<i>n</i> -butylbenzene	48	52	0.91 (1.1)
14	Ethylbenzene	<i>n</i> -amylbenzene	32	68	0.48 (2.1)
15	Ethylbenzene	<i>n</i> -hexylbenzene	43	57	0.75 (1.3)
16	<i>n</i> -propylbenzene	<i>n</i> -butylbenzene	30	70	0.43 (2.3)
17	<i>n</i> -propylbenzene	<i>n</i> -amylbenzene	13	87	0.15 (6.7)
18	<i>n</i> -propylbenzene	<i>n</i> -hexylbenzene	14	86	0.16 (6.1)
19	<i>n</i> -butylbenzene	<i>n</i> -amylbenzene	26	74	0.35 (2.8)
20	<i>n</i> -butylbenzene	<i>n</i> -hexylbenzene	33	67	0.50 (2.0)
21	<i>n</i> -amylbenzene	<i>n</i> -hexylbenzene	55	45	1.1
22	<i>o</i> -xylene	<i>m</i> -xylene	0	ca. 100	–
23	<i>o</i> -xylene	<i>p</i> -xylene	0	ca. 100	–
24	<i>m</i> -xylene	<i>p</i> -xylene	38	62	0.61 (1.6)
25	Benzene	Cyclohexane	85	15	5.7
26	Cyclohexene	Cyclohexane	76	24	3.2
27	Allyl acetate	<i>n</i> -propyl acetate	77	23	3.3
28	Methyl methacrylate	Methyl isobutyrate	86	14	6.1
29	Isopropenyl acetate	Isopropyl acetate	69	31	2.2
30	2-pentenoic acid	<i>n</i> -pentanoic acid	19	81	0.23 (4.3)
31	3-pentenoic acid	<i>n</i> -pentanoic acid	68	32	2.1

^aAmounts of the guests incorporated within the crystal of entries 1–21 and 25–31 were determined by gas chromatography and entries 22–24 by single X-ray crystallography.

^bReciprocal values, i.e. values of $[B]_{\text{cry}}/[A]_{\text{cry}}$.

(SF = 0.61(1.6)). A 1:1:1 mixture of all isomers also yielded a mixture of *m*-xylene and *p*-xylene. The order of inclusion in CA is as follows:



This selectivity indicates that CA can include a single component exclusively from binary mixtures with recognition of molecular shapes.

Entries 25–31 show the results for the separation of saturated and unsaturated compounds. Although these compounds have similar molecular structures, the unsaturated compounds, except for the case of entry 30, were found to

be preferentially crystallized with CA over the corresponding saturated ones; e.g. the amount of methyl methacrylate incorporated in the crystal is more than six times of that of methyl isobutyrate. The order of inclusion in CA can be described as follows: unsaturated compounds > saturated compounds. These results indicate a possibility of separating compounds with similar size and shape by using CA.

5.2 Mechanism of Selective Enclathration of CA

5.2.1 Monosubstituted benzenes

In order to reveal the mechanism of selective enclathration, the crystal structures of CA with pure monosubstituted benzenes were investigated. Table 7 summarizes the lattice parameters, the types of host framework, the host–guest molar ratios and *PCcavity* [33]. They all have bilayer structures, which are classified into three types of host framework, αG , αT , and βT , based on the differences in the interdigitation style and in the steroidal side-chain conformations, as already described in Section 4.1.1. Small guest molecules (benzene, toluene, ethylbenzene and *n*-propylbenzene) are included at 1:1 host–guest ratios, and guests with more than ten carbons (*n*-butylbenzene, *n*-amylbenzene, and *n*-hexylbenzene) are included at 2:1. Namely, CA inclusion crystals with seven monosubstituted benzenes are classified into four types, 1:1 αG , 1:1 βT , 2:1 αG , and 2:1 αT , based on the host frameworks and host–guest ratios.

The selectivities for the guest compounds by enclathration seem to be dependent on the four types. The order of preference is given below:

$$1:1 \alpha G > 2:1 \alpha G > 1:1 \beta T \text{ or } 2:1 \alpha T$$

Table 7 Lattice parameters, host framework type, host:guest ratio, and *PCcavity* for inclusion compounds of CA.

Guest	Space group	<i>a</i> (Å)	<i>b</i> (Å)	<i>c</i> (Å)	β (°)	<i>V</i> (Å ³)	Host framework	Host:guest ratio	<i>PCcavity</i> (%)
Benzene	<i>P</i> 2 ₁	13.63	8.04	14.08	114.3	1406	αG	1:1	56
Toluene	<i>P</i> 2 ₁	13.74	8.04	14.01	114.1	1421	αG	1:1	60
Ethylbenzene	<i>P</i> 2 ₁	12.41	7.83	16.28	111.8	1469	βT	1:1	61
<i>n</i> -propylbenzene	<i>P</i> 2 ₁	12.07	7.84	16.25	109.8	1447	βT	1:1	70
<i>n</i> -butylbenzene	<i>P</i> 2 ₁	12.78	7.90	14.12	105.5	1375	αT	2:1	52
<i>n</i> -amylbenzene	<i>P</i> 2 ₁	14.11	7.87	25.13	96.8	2774	αG	2:1	54
<i>n</i> -hexylbenzene	<i>P</i> 2 ₁	14.07	7.91	25.12	96.7	2779	αG	2:1	60
<i>o</i> -xylene (Form I)	<i>P</i> 2 ₁	7.52	25.61	13.83	91.0	2261	<i>DCA</i>	2:1	47
<i>o</i> -xylene (Form II)	<i>P</i> 2 ₁	12.33	7.92	14.33	105.0	1351	αT	2:1	41
<i>m</i> -xylene	<i>P</i> 2 ₁	12.08	8.17	15.97	109.3	1487	βT	1:1	58
<i>p</i> -xylene	<i>P</i> 2 ₁	13.58	8.30	14.24	114.5	1462	αG	1:1	65
Methyl methacrylate	<i>P</i> 2 ₁	12.94	8.05	14.67	113.9	1397	αG	1:1	68

This order indicates that the αG -type host framework is more favorable than the other two *trans*-types (βT or αT), and the 1:1 αG type is more favorable than 2:1 αG . In addition, this order agrees with the fact that less-selective enclathrations (entry 1, 12 and 21) were observed when they construct the same host frameworks at the same host–guest ratios in a single-component system. For example, both benzene and toluene can be included in the same 1:1 αG type. In the same way, less-selective enclathrations were also observed in the cases of ethylbenzene vs. *n*-propylbenzene (1:1 βT) and *n*-amylbenzene vs. *n*-hexylbenzene (2:1 αG).

In order to clarify the factors affecting selective inclusion, we compared *PCcavity*, the packing coefficient of the host cavity described in Chapter 4.2, as shown in Table 7. The values were in the range of 52–70 %, indicating that all the aromatic guest molecules are sufficiently large to give stable inclusion compounds. The order of *PCcavity* (*n*-propylbenzene > toluene, ethylbenzene, *n*-hexylbenzene > benzene, *n*-butylbenzene, *n*-amylbenzene) has no correlation with that of the selectivities, indicating that *PCcavity* does not sufficiently explain the guest selectivities in this case. From the results, shape complementarity should play an important role.

Figure 12 illustrates typical cross-sections of host cavities sliced parallel to the axis of the one-dimensional host cavity at a height that shows the cross-sections surrounded by the side-chains. The host cavity of the αG type has a square groove accommodating the phenyl ring of the guest molecule (Figures 12(a) and (d)), while those of the *trans* type frameworks have triangular ones (Figures 12(b) and (c)). These figures illustrate that the αG type has host cavities which should be more appropriate for the phenyl ring than the αT and βT type. From the results, the αG type is predominantly formed from the guest mixtures. The host–guest ratios also play an important role in shape fitting. For the case of the αG type framework, the guest compounds that give inclusion crystals at 1:1 ratios are included more efficiently than those at 2:1. In the former, every square groove of the host cavities along the twofold screw axis is occupied by the phenyl ring of the guest compounds, while, in the latter, half of them are accommodated by the alkyl group. The shape complementarity between a groove and a guest molecule appears to cause the dependence of the selectivity on the four types of CA crystals.

5.2.2 Xylene isomers

The inclusion crystals of CA with *m*-xylene or *p*-xylene has a unique bilayer structure, while those of CA with *o*-xylene show the two polymorphic structures described above. The lattice parameters, the type of host framework, the host–guest molar ratios and *PCcavity* are shown in Table 7 [34].

Two polymorphs of CA with *o*-xylene have 2:1 DCA and 2:1 αT types, and both have apparently lower values of *PCcavity* than the other CA crystals. On the

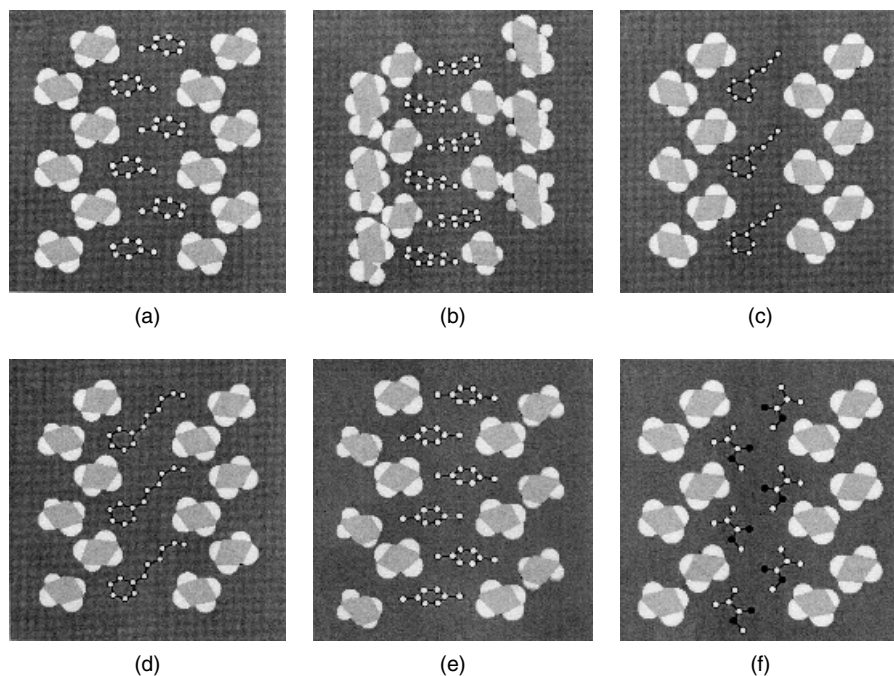


Figure 12 Cross-sections of CA host channels sliced parallel to the direction of the channel (carbon and hydrogen atoms are represented by gray and white, respectively) with arrays of included guest molecules (hydrogen atoms are omitted for clarity, and carbon and oxygen atoms are represented by open and filled circles, respectively). (a) toluene, (b) *n*-propylbenzene, (c) *n*-butylbenzene, (d) *n*-hexylbenzene, (e) *p*-xylene, and (f) methyl methacrylate.

other hand, *m*-xylene and *p*-xylene give 1:1 βT and 1:1 αG type host frameworks, respectively, and their values of *PC* cavity lie in the normal range. The difference in the *PC* cavity indicates the stability of the inclusion crystals, and results in the exclusion of *o*-xylene. That is, *m*-xylene and *p*-xylene were exclusively included from mixtures of *o*- and *m*-xylene, *o*- and *p*-xylene, respectively.

In contrast, recrystallization from a 1:1 mixture of *m*-xylene and *p*-xylene yielded a crystal that included both of the guest components. From the viewpoint of CA crystal type (1:1 βT v. 1:1 αG type), this selectivity ($SF = 0.61(1.6)$) is lower than that for *n*-alkylbenzenes: the values of *SF* are more than 4.3 in the case of the 1:1 αG v. 1:1 βT type (entries 2, 3, 7 and 8). The difference in the selectivity is due to shape fitting between a square groove of the αG framework and a moiety of the guest molecule. As shown in Figure 12(e), *p*-xylene molecules lie with their molecular long axis approximately perpendicular to the channel, and a phenyl ring of the *p*-xylene molecule fits in the center of the channel and a methyl group in the square groove. On the other hand, inclusion

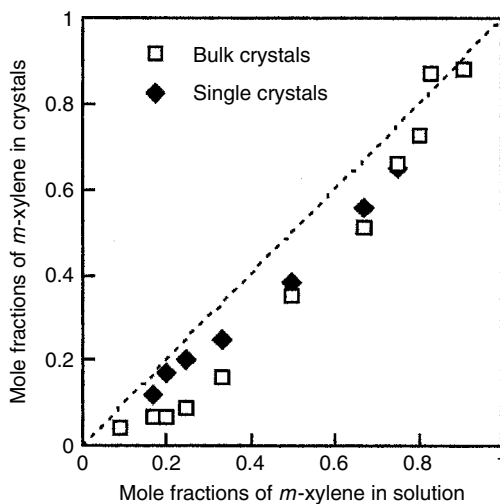


Figure 13 Mole fractions of *m*-xylene in single crystals and in bulk crystals are plotted against those of the starting mixed solvents of *m*-xylene and *p*-xylene.

crystals of benzene and toluene fit snugly between the square groove and the phenyl ring of the guest molecules. Therefore the fact that moieties of the guest molecules are accommodated in the cavity grooves is an important influence on the selectivity.

Then we further investigated the guest selectivities from the mixtures at various mixed ratios. The ratios between *m*-xylene and *p*-xylene in the single crystals are evaluated by refinement of the occupancy parameters of both isomers, but this time in bulk crystals by gas chromatography. Figure 13 illustrates plots of mole fraction of *m*-xylene in single crystals *v.* the feed ratios, as well as those in the bulk crystals. It is noteworthy that the guest ratios in the single crystals are in a good agreement with those in the bulk crystals, and they are similar to those of the recrystallization mixtures. This indicates that both *m*-xylene and *p*-xylene are included in the same cavity and that the bulk crystals consist of homogeneous single crystals.

5.2.3 Other compounds

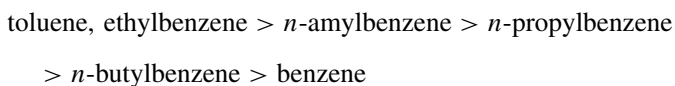
The preference of unsaturated compounds over saturated compounds can also be understood in terms of the fit of the guest moiety in the cavity groove, while not all of the crystal structures of CA with guest molecules of entries 25–31

have been analyzed. Crystals of CA with methyl methacrylate have the 1:1 αG type structure. The lattice parameters and other data are summarized in Table 7. Figure 12(f) shows the typical cross-sections of the host cavities with arrays of methyl methacrylate, where $-C=C-$ double-bond moieties of the molecules are accommodated in the square grooves. Similar arrangements in *gauche* type cavities, except for the case of carboxylic acids, may be achieved by unsaturated compounds. On the other hand, in the case of saturated compounds, methyl and/or methylene units can be accommodated in the cavity grooves. The double bond moiety will be more appropriate for the square groove than saturated compounds, and this leads to the selective enclathration of unsaturated compounds.

In contrast to the results (entries 25–29 and 31), saturated *n*-pentanoic acid is preferentially incorporated in CA cavities as compared with 2-pentenoic acid. This implies that the separation depends not only on the space effect of the cavities but also on host–guest hydrogen-bond interaction, which is observed in the inclusion crystals of CA with acetic acid [26a]. This indicates that the separation mechanism of protic compounds cannot be understood only in the terms of the fit between the host cavity and guest molecule.

5.3 Selective Enclathration Using Other Bile Acids

Table 8 shows the results for the separation of monosubstituted benzenes using DCA as the host. In the binary systems containing benzene, benzene was excluded from the DCA crystal, with the resulting separation factors less than unity. This makes a complete contrast to the previous results with CA. Two guests, toluene and ethylbenzene, were preferentially included in the DCA crystal. The order of preferential inclusion in DCA can be described as follows:



This selectivity is completely different from that in the case of CA as host. The difference between the two hosts is ascribed to the different shapes of their cavities. Figure 14 shows typical cross-sections of host cavities with arrays of *o*-xylene, where the guest molecules are arrayed in cavities that do not possess grooves. In the case of CA, the grooves play an important role in selective enclathration, while the DCA cavity has no grooves. This means that the mechanism of separation differs between the CA and the DCA hosts.

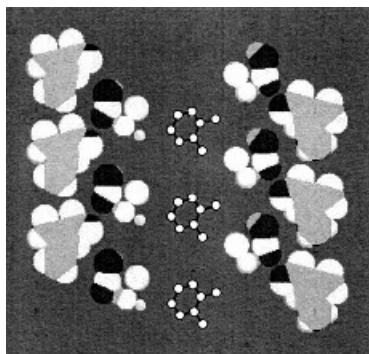


Figure 14 Cross-section of a DCA host channel sliced parallel to the direction of the channel (carbon, hydrogen and oxygen atoms are represented by gray, white and black, respectively) with arrays of *o*-xylene (hydrogen atoms are omitted for clarity, and carbon atoms are represented by open circles).

Table 8 Competitive recrystallizations of DCA with monosubstituted benzenes^a.

Entry	Guest A	Guest B	$\frac{[A]_{\text{cry}}}{([A]_{\text{cry}} + [B]_{\text{cry}})}$ (%)	$\frac{[B]_{\text{cry}}}{([A]_{\text{cry}} + [B]_{\text{cry}})}$ (%)	SF ^b (reciprocal of value)
1	Benzene	Toluene	15	85	0.18 (5.7)
2	Benzene	Ethylbenzene	16	84	0.19 (5.3)
3	Benzene	<i>n</i> -propylbenzene	28	72	0.40 (2.6)
4	Benzene	<i>n</i> -butylbenzene	29	71	0.40 (2.4)
5	Benzene	<i>n</i> -amylbenzene	31	69	0.46 (2.2)
6	Toluene	Ethylbenzene	48	52	0.92 (1.1)
7	Toluene	<i>n</i> -propylbenzene	87	13	6.6
8	Toluene	<i>n</i> -butylbenzene	94	6	14.6
9	Toluene	<i>n</i> -amylbenzene	86	14	6.0
10	Ethylbenzene	<i>n</i> -propylbenzene	87	13	7.0
11	Ethylbenzene	<i>n</i> -butylbenzene	88	12	7.3
12	Ethylbenzene	<i>n</i> -amylbenzene	68	32	2.1
13	<i>n</i> -propylbenzene	<i>n</i> -butylbenzene	38	62	0.61 (1.6)
14	<i>n</i> -propylbenzene	<i>n</i> -butylbenzene	20	80	0.25 (4.0)
15	<i>n</i> -butylbenzene	<i>n</i> -amylbenzene	25	75	0.33 (3.0)

^aAmounts of guests incorporated within the crystal were determined by gas chromatography.

^bReciprocal values, i.e. values of $[B]_{\text{cry}}/[A]_{\text{cry}}$.

6 SEPARATION OF ENANTIOMERS BY BILE ACID DERIVATIVES

6.1 Optical Resolution of Enantiomers

6.1.1 Aliphatic alcohols

The ability of bile acid derivatives to include various alcohols differs greatly, as is partly shown in Table 3. It can be seen that DCA does not include any

Table 9 Enantioresolution of aliphatic secondary alcohols, CH(OH)(CH₃)R, by inclusion method using CAM, LCAM and NDCA.

Entry	R	CAM		LCAM		NDCA	
		ee%	Predominant configuration	ee%	Predominant configuration	ee%	Predominant configuration
1	Et	17	<i>S</i>	–	–	8	<i>R</i>
2	<i>i</i> -Pr	20	<i>R</i>	<1	<i>S</i>	11	<i>S</i>
3	<i>n</i> -Pr	30	<i>R</i>	13	<i>R</i>	6	<i>S</i>
4	<i>t</i> -Bu	18	<i>R</i>	28	<i>R</i>	15	<i>R</i>
5	<i>n</i> -Bu	13	<i>R</i>	33	<i>R</i>	3	<i>R</i>
6	<i>i</i> -Bu	56	<i>R</i>	–	–	47	<i>S</i>

small alcohols, but CA includes only methanol, ethanol and propanol. On the other hand, amide derivatives include lots of aliphatic alcohols. As a result, optical resolution of the alcohols has been performed by using the latter amide hosts. Table 9 shows the result of optical resolution with CAM [35]. Various secondary alcohols, such as 2-butanol, 2-pentanol, 2-hexanol, etc., were employed for the resolution, using the recrystallization method. It can be seen that CAM prefers (*R*)-isomers to (*S*)-isomers, and that the efficiency depends on the size and shape of the alkyl groups of the alcohols. Furthermore, Table 9 shows the results for the case of LCAM, which includes aliphatic alcohols involving more than four carbon atoms [36]. (*R*)-isomers of secondary alcohols were predominantly included, rather than (*S*)-isomers. In the case of 2,3-dimethyl-3-pentanol, the enantiomer excess value is over 50 %, which is the highest value among the alcohols employed.

NDCA was used for optical resolution of the secondary alcohols [37]. The predominant configuration is dependent on the size and shape of the guest components. The enantioselectivity amounted to a maximum of 47 % ee for the case of 4-methyl-2-pentanol. 3ECA and 3EDCA form inclusion compounds with aliphatic alcohols, as described in the previous section. 3ECA displays an efficient chiral recognition for aliphatic alcohols. For example, (*R*)-isomers of 2-butanol and 2-pentanol are included more preferentially than the corresponding (*S*)-isomers. Moreover, recognition of two different chiral carbons was achieved by using 3-methyl-2-pentanol. Its (2*R*, 3*S*)-isomer is selectively included from its four isomers. In addition, 3EDCA exhibits a chiral recognition ability similar to 3ECA.

6.1.2 Lactones, cyclic ketones and epoxides

Although much work has been devoted to examination of a wide range of DCA inclusion compounds, an efficient enantioresolution has not yet been achieved. This is because DCA channels have only small pockets on the walls of the

channels. In contrast, CA has large pockets where substituents at chiral carbon are included. For example, CA serves as the host compound for enantioresolution of lactones with four- to six-membered rings [38]. Enantiomeric excess values were in the range of 20% to 50% for these lactones. Two stages of recrystallization increase the value to a maximum of 80–90%. Cyclic ketones as well as epoxides with phenyl rings were effectively resolved by using CA [39a]. For example, (1*S*, 2*S*)-(–)-1,2-epoxy-1,2-diphenylethane was resolved in an enantiomeric excess of 95%. Out of the other bile acid derivatives, dehydrocholic acid is known to be an effective host [39b,c]. This acid was employed for the enantioresolution of several alkyl aryl sulfoxides and many cyclic amides to give the highest values of 99% and 64%, respectively.

6.1.3 Attachment of chiral conformers in cavities

An interesting phenomenon whereby achiral compounds occupy chiral cavities has been reported. Steroidal host compounds give rise to the attachment of definite chiral conformations of achiral compounds within cavities, making it possible to observe solid-state circular dichroism spectra. Gdaniec and Polonski reported this type of property for the inclusion compounds of DCA and CA with various aromatic ketones [40a] and benzil [40c]. Furthermore, it is possible for the selected conformers to maintain their chiral state temporarily in solution. That is, soon after the inclusion compounds are dissolved, the chirality may be retained for some time. *N*-Nitrosopiperidines were found to display this type of dynamic chiral recognition in DCA and CA inclusion compounds [40b]. In this case, one can observe the decay of the circular dichroism signal after dissolution of these inclusion compounds in methanol.

6.2 Chiral Recognition Mechanism

6.2.1 Steric visualization of inclusion spaces

Visual observations help us to understand the molecular recognition mechanism in the cavities of the inclusion compounds from a steric viewpoint. Since the host components constitute a wall, they serve as a vessel where the guest components are accommodated. X-ray crystallographic data are used for obtaining steric views by computer simulation and tomography, enabling us to visualize and interpret the interaction among the host and guest molecules through weak noncovalent bonds, such as hydrogen bonds, van der Waals' forces and so on. This research resulted in valuable information about chiral recognition in steroidal inclusion compounds. For example, Figures 12 and 14 illustrate cross-sectional views of a channel in a CA inclusion compound. It can be seen that there is a pocket or a groove on the channel wall where part of the guest molecule is inserted.

6.2.2 Four-location model for chiral recognition

Enantioresolution studies using bile acid derivatives have been widely undertaken, as described in Section 6.1. In most of the cases, however, the resulting enantioselectivities are not as efficient as we expected. This fact conflicts with the following two observations. One is that X-ray crystallographic analyses by means of automatic software revealed the existence of one enantiomer in a cavity. The other is that tomographic views of the guest molecules in the channels give definite locations for the positions of the three substituent groups at a chiral carbon atom in appearance. These results indicate that the recognition mechanism involved in enantioresolution remains unclear.

Recently, Mesecar and Koshland have proposed that a four-location model is reasonable for explaining chiral recognition in some proteins [41]. This report prompts us to apply this model to conventional inclusion compounds. Thus, the three-point attachment model has been accepted so far for enantioselective complexation, as depicted in Figure 15(a). This model is based on pinpointing the three locations (A, B and C) of a guest component on the surface of a host component (A', B' and C'). This surface may be deformed relative to the planar one in the following way. The surface is concave, so that the substituents at a chiral carbon attach to the wall of the dip. The shallow dip accommodates one enantiomer on the basis of the three-point attachment model (Figure 15(b)), but the steep dip accommodates both the enantiomers (Figure 15(c)). Such a deformation will reach a maximum in the case of a channel (Figure 15(d)), where both can be included.

In this way, this model is applicable to channel-type inclusion compounds of steroidal hosts. In order to prove this hypothesis, detailed analyses of electron density maps have been performed in the case of an inclusion compound of NDCA with 3-methyl-2-butanol [37]. Figure 16 shows a schematic view of the guest molecule included and a cross-section of an electron density map. It can be seen that the hydroxyl, isopropyl groups and chiral carbon are fixed, while the methyl carbon is disordered. On the other hand, in the case of 3-methyl-2-butanol in LCAM channels, the chiral carbon is disordered, while the other groups are fixed. We can conclude from these results that effective recognition of the remaining hydrogen atom is indispensable for discriminating the chiral molecule in the channel.

6.2.3 Hierarchical structures generated by chiral molecules

The chiral steroidal molecules associate together through noncovalent bonds to form chiral assemblies. Representative forms are two-dimensional sheets and one-dimensional helices, which are further combined in various ways. For example, the chiral layers of DCA stack together in a parallel fashion on the hydrophilic

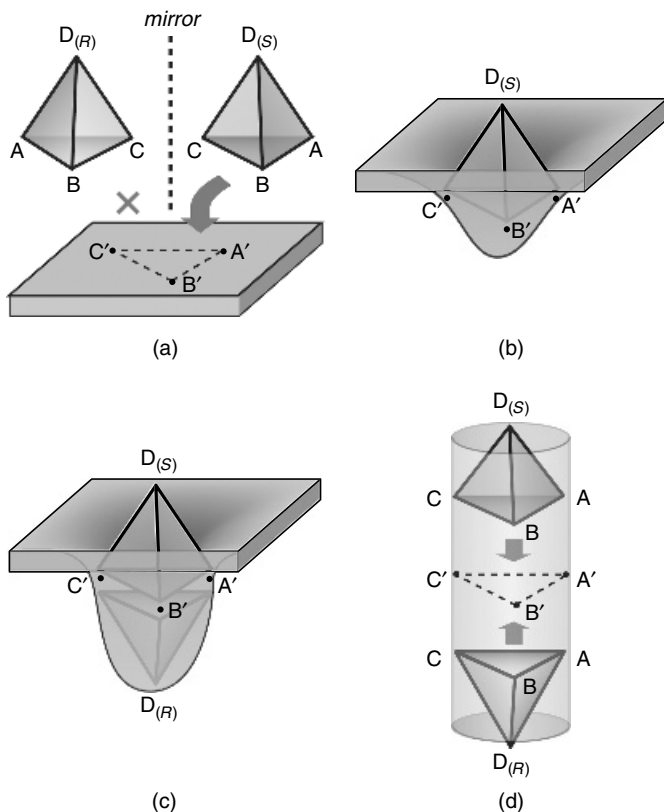


Figure 15 Deformation of the surface for chiral recognition. (a) A three-point attachment model for enantioresolution on the surface; (b) a surface with a shallow dip; (c) a surface with a steep dip; and (d) a channel in the extreme case, caused by deformation.

side and antiparallel on the lipophilic side. In the latter case, there are several helices with different directionality and amphiphilicity. For example, CDCA has a left-handed helix with an inner hydrophilic core and an outer lipophilic surface. Moreover, these assemblies often have chiral cavities where guest molecules can be included. In other words, the assemblies function as chiral molecular vessels which can include chiral guest components. In this manner, various chiral assemblies are produced, starting from the chiral molecules.

Such research into the assemblies of chiral steroidal compounds gave us a chance to think about the hierarchical structure of materials in the universe [42]. We have the simple idea that the atoms combine together through stronger covalent bonds to yield molecules which serve as information carriers, and that the molecules combine together through noncovalent bonds to yield molecular assemblies which serve to express the information. Chiral carbon chains

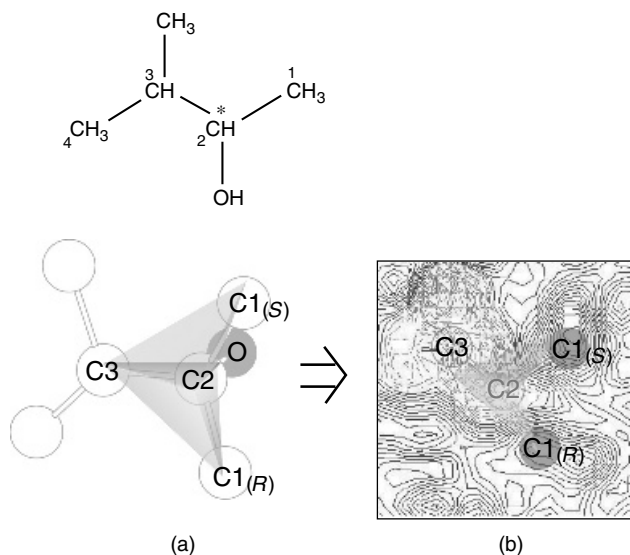


Figure 16 Chiral recognition based on a four-location model in the case of 3-methyl-2-butanol. (a) Two enantiomeric alcohol molecules in the channel of NDCA; (b) an electron density map of the alcohol on a plane composed of C1, C2 and C3 carbons.

are the most suitable information carriers, because the chains make chiral self-assembled architectures, such as crystals and proteins, which accompany the host–guest recognition process. Therefore, chiral recognition may be considered to be indispensable for the expression of the molecular information. In this way, it is considered that steroidal molecules, which are composed of chiral chains with about 20 carbon atoms, would have to possess a significant amount of information, and that this information is expressed as dynamic association processes through noncovalent bonds.

7 CONCLUSION

We have shown that bile acid derivatives have diverse inclusion abilities according to their molecular structures. It is fascinating that modification of only one atom of the molecules bring about slight or drastic changes in the inclusion behaviors followed by changes in the crystal structures. Such changes come from various combinations among multiple and discrete hydrogen-bonding groups. This indicates that simple molecular design enables us to find a host suitable for separating each mixture of various organic compounds. In particular, when we regard the steroidal hosts as sequential and chiral carbon chains, the design is attributed to diverse changes in the sequence, in other words, molecular information, as in the case of proteins and nucleic acids.

REFERENCES

1. (a) Miyata, M.; Sada, K. 'Deoxycholic Acid and Related Hosts' in '*Comprehensive Supramolecular Chemistry*' eds MacNicol, D. D.; Toda, F.; Bishop, R. Pergamon, Oxford, **1996**, Vol. 6, pp. 147–176; (b) Miyata, M.; Sada, K.; Miyake, Y. in '*Organized Assemblies in Chemical Analysis*', ed. Hinze, W., JAI Press, Greenwich, **2000**, Vol. 2, Chap. 7, pp. 205–228. (c) Miyata, M., Sada, K.; Yoswathananont, N. in '*Encyclopedia of Supramolecular Chemistry*', ed. Atwood, J. L., Marcel Dekker, New York, in press.
2. Herndon, W. C. *J. Chem. Educ.*, **1967**, *44*, 724.
3. Craven, B. M.; DeTitta, G. T. *J. Chem. Soc., Chem. Commun.*, **1972**, 530.
4. Giglio, E. in '*Inclusion Compounds*' eds Atwood, J. L.; Davies, J. E. D.; MacNicol, D. D., Academic Press, London, **1984**, Vol. 2, pp. 207–229.
5. (a) Rheinboldt, H.; Flume, E.; König, O. *Z. Physiol. Chem.*, **1929**, *180*, 180. (b) Popovitz-Biro, R.; Tang, C. P.; Chang, H. C.; Lahav, M.; Leiserowitz, L. *J. Am. Chem. Soc.*, **1985**, *107*, 4043.
6. (a) Miyata, M.; Shibakami, M.; Goonewardena, W.; Takemoto, K. *Chem. Lett.*, **1987**, 605. (b) Miki, K.; Masui, A.; Kasai, N.; Miyata, M.; Shibakami, M.; Takemoto, K. *J. Am. Chem. Soc.* **1988**, *110*, 6594.
7. Mylius, F. *Chem. Ber.*, **1887**, *20*, 1968.
8. Johnson, P. L.; Schaefer, J. P. *Acta Crystallogr., Sect. B.* **1972**, *28*, 3083.
9. (a) Lindley, P. F.; Mahmound, M. M.; Watson, F. E.; Jones, W. A. *Acta Crystallogr., Sect. B.* **1980**, *36*, 1893. (b) Rizkallah, P. J.; Harding, M. M.; Lindley, P. F.; Aigner, A.; Bauer, A. *Acta Crystallogr., Sect. B.* **1990**, *46*, 262.
10. Sluis, P.; Schouten, A.; Kanters, J. A. *Acta Crystallogr., Sect. C.* **1990**, *46*, 2165.
11. Chikada, M.; Sada, K.; Miyata, M. *Polym. J.*, **1999**, *31*, 1061.
12. Arora, S. K.; Germain, G.; Declercq, J. P. *Acta Crystallogr., Sect. B.* **1976**, *32*, 415.
13. Sada, K.; Kondo, T.; Miyata, M. *Supramol. Chem.*, **1995**, *5*, 189.
14. (a) Sada, K.; Kondo, T.; Miyata, M.; Tamada, T.; Miki, K. *J. Chem. Soc. Chem. Commun.*, **1993**, 753. (b) Sada, K.; Kondo, T.; Miyata, M. *Chem. Mater.*, **1994**, *6*, 1103. (c) Sada, K.; Kondo, T.; Ushioda, M.; Matsuura, Y.; Nakano, K.; Miyata, M.; Miki, K. *Bull. Chem. Soc. Jpn.*, **1998**, *71*, 1931.
15. (a) Hishikawa, Y.; Aoki, Y.; Sada, K.; Miyata, M. *Chem. Lett.*, **1998**, 1289. (b) Aoki, Y.; Hishikawa, Y.; Sada, K.; Miyata, M. *Enantiomer*, **2000**, *5*, 95.
16. Sada, K.; Matsuo, A.; Miyata, M. *Chem. Lett.*, **1995**, 877.
17. Sada, K.; Kondo, T.; Yasuda, Y.; Miyata, M.; Miki, K. *Chem. Lett.*, **1994**, 727.
18. Miki, K.; Masui, A.; Kasai, N.; Miyata, M.; Goonewardena, W.; Shibakami, M.; Takemoto, K. *Acta Crystallogr., Sect. C.* **1989**, *45*, 79.
19. (a) Miyata, M.; Goonewardena, W.; Shibakami, M.; Takemoto, K.; Masui, A.; Miki, K.; Kasai, N. *J. Chem. Soc., Chem. Commun.*, **1987**, 1140. (b) Miki, K.; Masui, A.; Kasai, N.; Shibakami, M.; Takemoto, K.; Miyata, M. *Acta Crystallogr., Sect. C.* **1992**, *48*, 503. (c) Goonewardena, W.; Miyata, M.; Takemoto, K. *Polym. J.*, **1993**, *25*, 731. (d) Scott, J. L. *J. Chem. Soc. Perkin Trans. 2*, **1995**, 495.
20. (a) Sada, K.; Sugahara, M.; Nakahata, Y.; Yasuda, Y.; Nishio, A.; Miyata, M. *Chem. Lett.*, **1998**, 31. (b) Sugahara, M.; Sada, K.; Miyata, M. *Chem. Commun.*, **1999**, 293.

21. Sada, K.; Sugahara, M.; Kato, K.; Miyata, M. *J. Am. Chem. Soc.*, **2001**, *123*, 4386.
22. Miyata, M.; Sada, K.; Miyake, Y. *Mol. Cryst. Liq. Cryst.*, **1998**, *313*, 173.
23. (a) Sada, K.; Maeda, T.; Miyata, M. *Chem. Lett.*, **1996**, 837. (b) Sada, K.; Shiomi, N.; Miyata, M. *J. Am. Chem. Soc.*, **1998**, *120*, 10543.
24. (a) Nakano, K.; Sada, K.; Miyata, M. *Chem. Lett.*, **1994**, 137. (b) Shibakami, M.; Sekiya, A.; *J. Chem. Soc., Chem. Commun.*, **1994**, 29. (c) Nakano, K.; Sada, K.; Miyata, M. *J. Chem. Soc. Chem. Commun.*, **1995**, 953. (d) Nakano, K.; Sada, K.; Kurozumi, Y.; Miyata, M. *Chem. Eur. J.* **2001**, *7*, 209. (e) Yoswathananont, N.; Chirachanchai, S.; Tashiro, K.; Nakano, K.; Sada, K.; Miyata, M. *CrystEngComm.*, **2001**, *3*, 74.
25. (a) Lessinger, L. *Cryst. Struct. Commun.*, **1982**, *11*, 1787. (b) Lessinger, L.; Low, B. W. *J. Cryst. Spectrosc. Res.*, **1993**, *23*, 85.
26. (a) Nakano, K.; Sada, K.; Miyata, M. *Chem. Commun.*, **1996**, 989. (b) Nakano, K.; Tani, K.; Sada, K.; Miyata, M. *Progr. Colloid. Polym. Sci.*, **1997**, *106*, 249. (c) Nakano, K.; Katsuta, M.; Sada, K.; Miyata, M. *CrystEngComm.*, **2001**, *3*, 44.
27. Yoswathananont, N.; Kita, H.; Tohnai, N.; Sada, K.; Miyata, M. *Chem. Lett.*, **2002**, *12*, 1234.
28. Mecozzi, S.; Rebek Jr, J. *Chem. Eur. J.*, **1998**, *4*, 1016.
29. Cerius², Molecular Simulation Software; Molecular Simulation Inc.
30. Voorintholt, R.; Kusters, M. T.; Vegter, G.; Vriend, G.; Hol, W. G. J. *J. Mol. Graphics*, **1989**, *7*, 243.
31. (a) Kitaigorodskii, A. I. *Molecular Crystals and Molecules*, Academic Press, New York, **1973**. (b) Desiraju, G. R. *Crystal Engineering: the Design of Organic Solids*, Elsevier, New York, **1989**. (c) Gavezzotti, A. *Acc. Chem. Res.* **1994**, *27*, 309.
32. (a) Miyata, M.; Shibakami, M.; Chirachanchai, S.; Takemoto, K.; Kasai, N.; Miki, K. *Nature*, **1990**, *343*, 446. (b) Shibakami, M.; Tamura, M.; Sekiya, A. *J. Am. Chem. Soc.*, **1995**, *117*, 4499. (c) Nakano, K.; Sada, K.; Miyata, M. *Mol. Cryst. Liq. Cryst.*, **1996**, *276*, 129.
33. Yoswathananont, N.; Sada, K.; Miyata, M.; Akita, S.; Nakano, K. *Org. Biomol. Chem.*, **2003**, *1*, 210.
34. Nakano, K.; Mochizuki, E.; Yasui, N.; Morioka, K.; Yamauchi, Y.; Kanehisa, N.; Kai, Y.; Yoswathananont, N.; Tohnai, N.; Sada, K.; Miyata, M. *Eur. J. Org. Chem.*, **2003**, 2428.
35. Sada, K.; Kondo, T.; Miyata, M. *Tetrahedron: Asymmetry*, **1995**, *6*, 2655.
36. Aoki, Y.; Hishikawa, Y.; Sada, K.; Miyata, M. *Enantiomer*, **2000**, *5*, 95.
37. Kato, K.; Aoki, Y.; Sugahara, M.; Tohnai, N.; Sada, K.; Miyata, M. *Chirality*, **2003**, *15*, 53.
38. (a) Miyata, M.; Shibakami, M.; Takemoto, K. *J. Chem. Soc., Chem. Commun.* **1988**, 655. (b) Miki, K.; Kasai, N.; Shibakami, M.; Takemoto, K.; Miyata, M. *J. Chem. Soc., Chem. Commun.* **1991**, 1757. (c) Sada, K.; Nakano, K.; Hirayama, K.; Miyata, M.; Sasaki, S.; Takemoto, K.; Kasai, N.; Kato, K.; Shigesato, M.; Miki, K. *Supramol. Chem.*, **2001**, *13*, 35.
39. (a) Bortolini, O.; Fantin, G.; Fogagnolo, M.; Medici, A.; Pedrini, P. *Chem. Lett.*, **2000**, 1246. (b) Bertolasi, V.; Bortolini, O.; Fogagnolo, M.; Fantin, G.; Pedrini, P.

- Tetrahedron: Asymmetry*, **2001**, *12*, 1479. (c) Bortolini, O.; Fogagnolo, M.; Fantin, G.; Medici, A. *Chem. Lett.*, **2003**, 206.
40. (a) Gdanice, M.; Polonski, T. *J. Am. Chem. Soc.*, **1998**, *120*, 7353. (b) Gdanice, M.; Milewska, M.; Polonski, T. *Angew. Chem. Int. Ed.*, **1999**, *38*, 392. (c) Polonski, T.; Szyszyng, M.; Gdanice, M.; Nowak, E.; Herman, A. *Tetrahedron: Asymmetry*, **2001**, *12*, 797.
41. Mesecar, A.; Koshland, D. *Nature*, **2000**, *403*, 614.
42. Miyata, M. in '*New Macromolecular Architecture and Functions*', eds Kamachi, M.; Nakamura, A., Springer-Verlag, Berlin, **1996**, pp. 21–30.

Chapter 5

Physicochemical Studies of Separation of Isomers by Supramolecular Systems

LUIGI R. NASSIMBENI

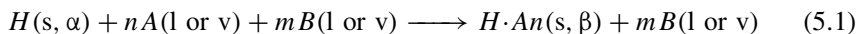
Department of Chemistry, University of Cape Town, Rondebosch, 7701, South Africa

1 INTRODUCTION

The separation of a particular component from a mixture may be carried out by exploiting differences in physical properties. The most common techniques: distillation, crystallisation and liquid–liquid extraction, rely on differences in vapour pressure or solubility of the components. In the case of molecular isomers, however, their physical properties are often similar, rendering traditional separation techniques inefficient or unusable. For example, if one considers the isomers ethylbenzene, *para*-, *meta*- and *ortho*-xylene, their normal boiling points are 136.2 °C, 138.4 °C, 139.1 °C and 144.4 °C, making their separation by distillation impracticable. Thus, the method of selective inclusion becomes an attractive possibility.

There are essentially two approaches: one may employ a traditionally porous material such as inorganic zeolite, in which the framework remains essentially unchanged during the absorption and desorption of the various guest molecules, and whose selectivity is governed by the channel patterns and dimensions [1–3]. Alternatively, one may utilise organic or metal–organic compounds as hosts, and

the separation process may then be represented by the equation:



Here H represents the host molecule in its nonporous α -phase, the apohost, which, when placed in contact with a mixture of guests A and B , which can be liquid or vapour, selects A and forms a solid inclusion compound $H \cdot An$, the β -phase, while excluding guests B .

This approach depends on the process of molecular recognition, which is based on the complementarity of the molecular shapes of the host and guest, and is shown schematically in Figure 1.

If the host were to display perfect selectivity, the process outlined in Equation (1) need only be carried out once, the solid inclusion compound filtered, guest A released by gentle warming, and the host H would be recycled. This seldom occurs in practice, and one has to perform carefully designed competition experiments in order to establish the selectivity profile of a given host.

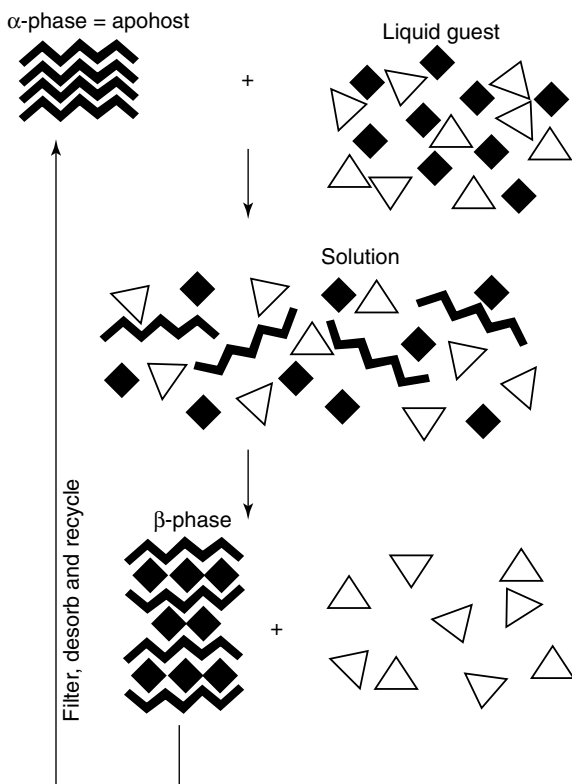


Figure 1 Schematic diagram of selective inclusion.

It is noteworthy that, in general, the host framework does not retain its β , porous phase upon guest release, but collapses to the structure of the apohost – the α -phase. There are a few exceptions, in which the host behaves as a zeolite retaining its structural integrity [4–6], and a copper-containing porous open-framework structure has been reported which also withstands partial chemical modification while maintaining its structure [7].

2 COMPETITION EXPERIMENTS

A typical procedure for a competition experiment between two guests A and B is to set up 11 vials with mixtures of the two guests, varying their mole fraction from 0 to 1. The host is added and allowed to dissolve. Care should be taken to keep the guests in excess, and conventionally the total guest:host ratio is 20:1. The inclusion compounds are allowed to crystallise, filtered, and both the mother liquor and guest content of the crystals are analysed by a suitable technique such as gas chromatography or NMR spectroscopy. In general, three kinds of selectivity curves arise, as shown in Figure 2. X_A is the mole fraction of guest A in the liquid mixture, and Z_A that of the guest entrapped in the crystal. The diagonal line, 'a', represents zero selectivity, curve 'b' occurs when A is preferentially

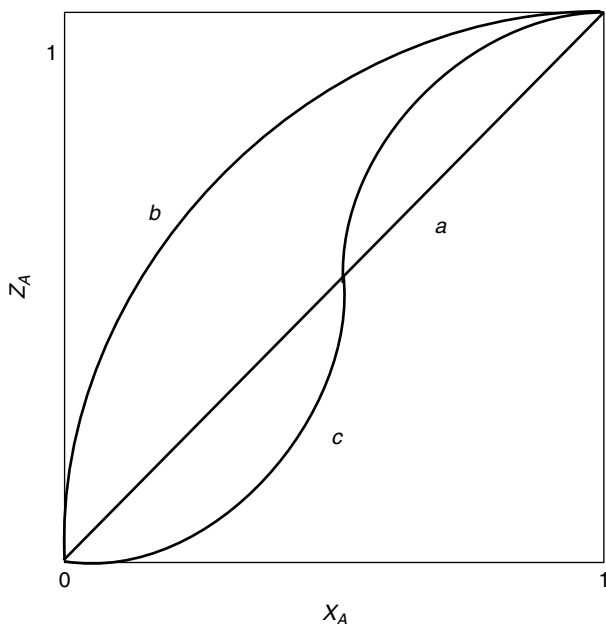


Figure 2 Two-component selectivity curves obtained from competition experiments.

enclathrated over B for the whole concentration range, while curve 'c' results when the selectivity is concentration dependent.

The method can be extended to the analysis of the competition for three guests simultaneously. The results are displayed on an equilateral triangle in which each apex represents a pure guest. Various situations arise, depending on the relative affinities of the chosen host for guest A , B and C . Following Pivovar *et al.*, [8] we may define a selectivity coefficient:

$$K_{A:B} = (K_{B:A})^{-1} = Z_A/Z_B^* X_B/X_A$$

$$(X_A + X_B = 1)$$

In Figure 3 we show the result which obtains when the host selectivity is $A > B > C$ in which $K_{A:B} = 50$, $K_{B:C} = 5$ and $K_{A:C} = 2$. The results of the three-component competitions are difficult to predict with precision, because of the mutually synergistic effects of the three guests.

However, an equimolar sample starting at the centre of the triangle would move approximately as indicated in Figure 3. Results of this kind were obtained in the selectivity experiments carried out with the host 1,1-bis(4-hydroxyphenyl)cyclohexane with the isomers of benzenediol [9], picoline [10] and lutidine [11].

When the selectivity for a pair of guests is concentration dependent, this will be reflected in the three component experiment. In Figure 4 we show the case in which the selectivity of the host $A > B$ with $K_{A:B} = 5$, $B \approx C$ with $K_{B:C} \approx 1$, and $A:C$ is concentration dependent. In this case, samples of the three-component mixture will give a split result which is dependent on their initial concentrations. This outcome occurred in the selectivity by the host 1,1,6,6-tetraphenylhexa-2,4-diyne-1,6-diol of mixtures of lutidines [12], and the host dinaphthol with

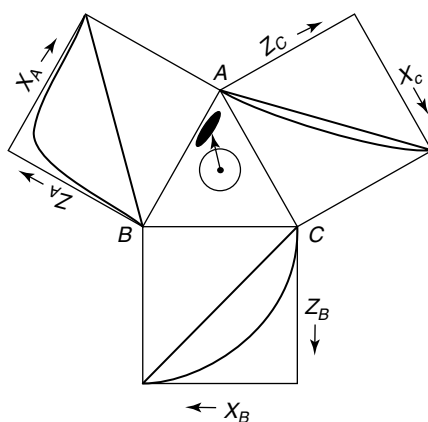


Figure 3 Selectivity profiles for three guests A , B and C with $K_{A:B} = 50$, $K_{B:C} = 5$, and $K_{A:C} = 2$.

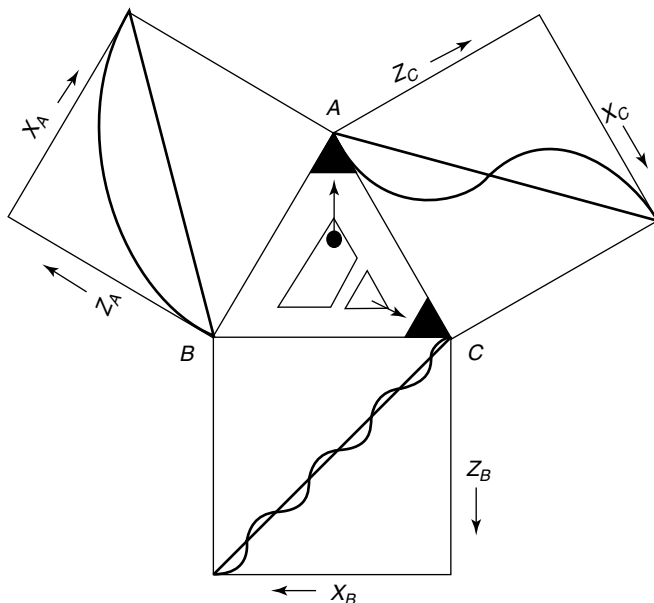


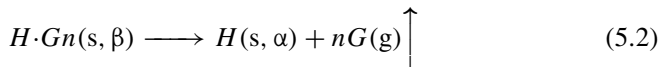
Figure 4 Selectivity profiles for three guests A, B and C with $K_{A:B} = 5$, $K_{B:C} \approx 1$ and A:C concentration dependent.

xylydines [13]. In such situations the sampling methodology of the original mixtures has to be carefully considered.

We have also carried out four-component competition experiments, in which the host 1,1-bis(4-hydroxyphenyl)cyclohexane was employed to separate a mixture of methanol, ethanol, isopropanol and *n*-butanol. In this case the pure components were represented by the apices of a regular tetrahedron, and the 12 starting mixtures were such that they represented an icosahedron embedded in the tetrahedron. The selectivity showed that isopropanol was enriched in all cases [14].

3 THERMAL STABILITY AND LATTICE ENERGIES

Thermal gravimetry (TG) and differential scanning calorimetry (DSC) are useful techniques in the analysis of inclusion compounds. If we consider the desolvation of a host–guest compound with a volatile guest:



the TG curve will yield an accurate value of *n*, the guest/host ratio, and the area under the endotherm is a measure of the enthalpy of the guest-release reaction. This is shown in Figure 5.

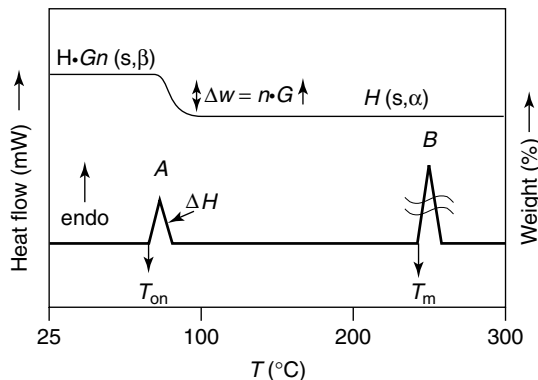


Figure 5 TGA and DSC traces for a one-step desolvation reaction.

It should be noted that the experimental ΔH is not a direct measure of the host–guest interactions, but is a complex quantity incorporating the desorption of the guest, the evaporation (sublimation) of the guest, the shrinkage of the β -host structure to the empty β_0 structure, and the collapse and rearrangement of the β_0 phase to the nonporous α -phase of the apohost [15,16]. Nevertheless, when comparing the desorption of a series of inclusion compounds with the same host and guests of similar shape and physical properties, and which all revert to the same α -phase, the ΔH of desorption is a fair approximation of the host–guest interactions. The measured ΔH of the guest-release reaction may then be regarded as the relative stability of the inclusion compound. We have also noted that the difference between the onset temperature T_{on} and the normal boiling point of the guest, T_b , is an indicator of the thermal stability of the host–guest system under study. In the case where the guest is a high-boiling liquid or a low-melting solid, the DSC may not show a separate endotherm for the host melt, but would give rise to a single endotherm representing the dissolution of the host in the liquid guest.

A quantitative measure of thermal stability is the lattice energy of the compound. This may be evaluated by the method of atom–atom potentials using the refined atomic positions derived from accurate crystal structure determinations. One may employ force fields of the type:

$$V(r) = a \exp(-br) - c/r^6$$

where r is the interaction distance and a , b and c are the coefficients given by Gavezzotti [17]. It is important to incorporate a suitable hydrogen-bonding potential, and we employ that of Vedani and Dunitz [18], which is formulated as:

$$V(\text{H-bond}) = (A/R^{12} - C/R^{10}) \cos^2 \theta$$

where R is the distance between the donor hydrogen and the acceptor atom, θ is the donor-H...acceptor angle and the $\cos^2 \theta$ term is the energy penalty paid by the bond in order to take nonlinearity into account.

We have investigated several systems where the selectivity of the host for a particular guest correlates with thermal stability parameters and lattice energy. Thus, for the host 1,1,6,6-tetraphenylhexa-2,4-diyne-1,6-diol which forms inclusion compounds with lutidines, the selectivity (lattice energy) is in the order 3,5-lutidine ($-452.5 \text{ kJ mol}^{-1}$) > 2,6-lutidine ($-441.4 \text{ kJ mol}^{-1}$) > 2,4 lutidine ($-320.8 \text{ kJ mol}^{-1}$) [12]. An interesting case arose with the inclusion compounds of this same host with isomers of aminobenzonitrile (ABN) [19]. The DSC traces only gave rise to a single endotherm due to dissolution of the host in the liquefied aminobenzonitriles, and the onset-melt temperatures ($T_{\text{on}} - T_{\text{m}}$), ΔH values and lattice energies all correlated with the competition experiments in solution, which showed the selectivity to be 2ABN > 3ABN > 4ABN. This is illustrated in Figure 6.

Remarkably, we obtained the same selectivity results by direct solid–solid reactions, and this enabled us to carry out the displacement reaction whereby we grew the inclusion compound H·2 (3ABN) from solution and ground the crystals with 2ABN:



This is the expected product, because it has the more negative lattice energy. We checked our hypothesis by attempting the reverse reaction, but the product was identical to the starting material:



showing that guest displacement had not taken place.

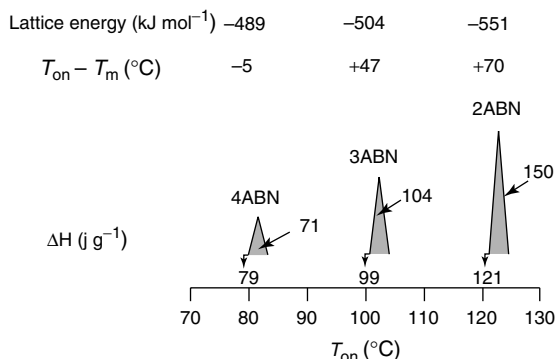
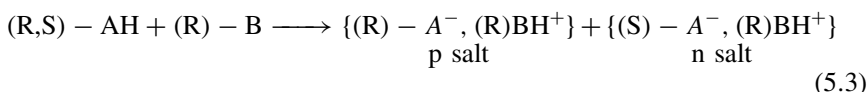


Figure 6 Host = 1,1,6,6-tetraphenylhexa-2,4-diyne-1,6-diol. Guest = 4-, 3- and 2-aminobenzonitrile. Correlation between lattice energies ($T_{\text{on}} - T_{\text{m}}$) and ΔH of guest release.

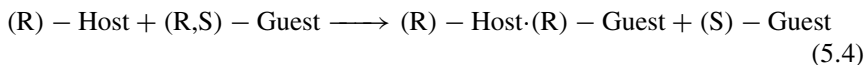
There are several cases, however, where the most negative lattice energy does not correspond with the preferred guest in a competition experiment. We attribute this to imprecise force-field parameters and kinetic effects which may be controlling the nucleation step in crystal formation [20].

4 ENANTIOMERIC RESOLUTION

A special case of host-guest inclusion is the resolution of a racemic mixture of chiral guests. This has important implications for the pharmaceutical industry, where the production of enantiomerically pure drugs has recently become increasingly important. A common method of chiral resolution is via the formation and separation of diastereomers. For example, a racemic acid AH may be treated with a chiral base B [21]:



The method relies on the p and n salts having different solubilities, and they must not form solid solutions or double salts. The more insoluble salt is filtered and the purified acid recovered by adding mineral acid. This method of chiral resolution is well established, and lists of resolving agents for many classes of racemic compounds are available [22]. Inclusion chemistry may be employed for the same purpose by preparing host-guest compounds with a chiral host:



In the above equation, we presuppose a higher degree of molecular recognition between the (R) - Host and (R) - Guest than between the (R) - Host and (S) - Guest ($K_{(R)-H \cdot (R)-G} \gg K_{(R)-H \cdot (S)-G}$). This is illustrated schematically in Figure 7.

The process is seldom, however, completely efficient, and the procedure may require several cycles in order to obtain the desired results. This is illustrated in a McCabe-Thiele type plot in Figure 8, which shows a system in which $K_{(R)-H \cdot (R)-G} = 10$. Starting with a racemic mixture we may obtain the (R) - Guest in 99% purity in two crystallisation/filtration steps.

The design of host compounds for optical resolution has received much attention. Toda [23,24] has reviewed the subject, and has used a number of novel techniques to effect efficient optical separation. He has demonstrated the possibility of resolving a racemic oil by stirring in a water suspension of a chiral host [25], and has applied fractional distillation techniques at different temperatures to separate a variety of racemic guests in the presence of chiral hosts [26]. An overview of the industrial applications and production of optically active materials is given in the book 'Chirality in Industry' [27].

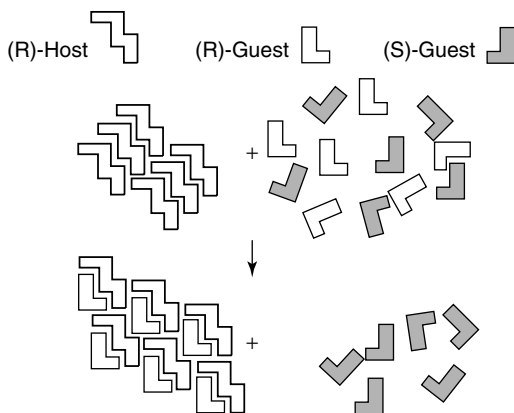


Figure 7 Schematic diagram of chiral resolution.

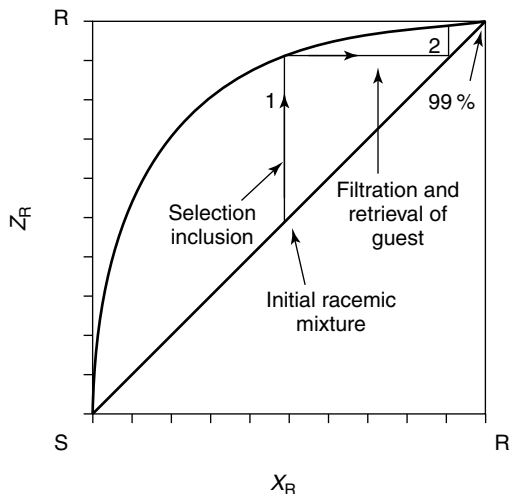


Figure 8 Two-step enrichment of racemic mixture to yield 99% pure (R)-guest.

5 SYSTEMS WITH MIXED GUESTS

An interesting area for further investigation lies in the field of inclusion compounds which contain different guests. In cases where the selectivity curve is concentration dependent, crystals that occur in the sharply vertical portion of the curve often give rise to a solid solution of the guests incorporated in the host structure (Figure 9).

This occurred in the competition experiment with the host 1,1-bis(4-hydroxyphenyl)cyclohexane and the guests 2,3-xyleneol and 3,5-xyleneol [28].

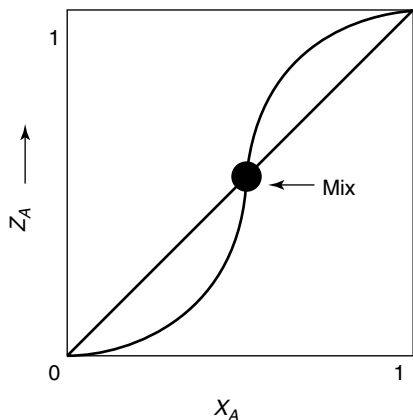


Figure 9 Mixed-guest crystal from concentration-dependent competition experiment.

The structures of the inclusion compounds $H \cdot 2, 3$ -xyleneol and $H \cdot 3, 5$ -xyleneol are isostructural with respect to the host atom positions, and the guests are located at the same site in the structures. We grew a large crystal of the host with the mixed guests, $H \cdot \text{MIX}$, which we cut into three portions, and submitted to gas-chromatographic analysis of the guests, DSC and crystal structure analysis. The result showed the composition to be: $H \cdot (0.32 \text{ 2,3-xyleneol}) \cdot (0.68 \text{ 3,5-xyleneol})$, the DSC showed both peaks of the guests, and the refinement of the structure modelled the positions of both guests successfully. A second example where two guests occupy the same site in the structure is that occurring with the host *trans*-9,10-dihydroxy-9,10-bis(*p*-*tert*-butylphenyl)-9,10-dihydroanthracene, which forms inclusion compounds with dimethylformamide, A and dimethylsulphoxide, B . The inclusion compounds are of the type $H \cdot nA \cdot (4-n) B$ such that n varies integrally from 0 to 4. The results of the competition experiments are unusual, in that the curve is not smooth, but show that the stoichiometry varies in discrete steps [29], giving rise to distinct compounds: $H \cdot 4A$, $H \cdot 3A \cdot B$, $H \cdot 2A \cdot 2B$, $H \cdot A \cdot 3B$ and $H \cdot 4B$ (Figure 10).

The stoichiometry is therefore controlled by the composition of the guest mixture. The compounds are isostructural with respect to the location of the host molecules, and the guests lie in essentially the same sites and are partially disordered. This is an important result, in that the ratio of the guests can be controlled, and this phenomenon has implications for crystal engineering. Thus, the physical and chemical properties of such compounds can be governed, and this has significance in such fields as chemical sensors, optical and electronic properties of organic crystals, as well as their thermal stabilities and kinetics of desolvation.

A more challenging task would be to synthesise inclusion compounds of the type $H \cdot n_1G_1 \cdot n_2G_2$ where G_1 and G_2 are different by virtue of size, polarity and symmetry. An example is shown schematically in Figure 11 in which the

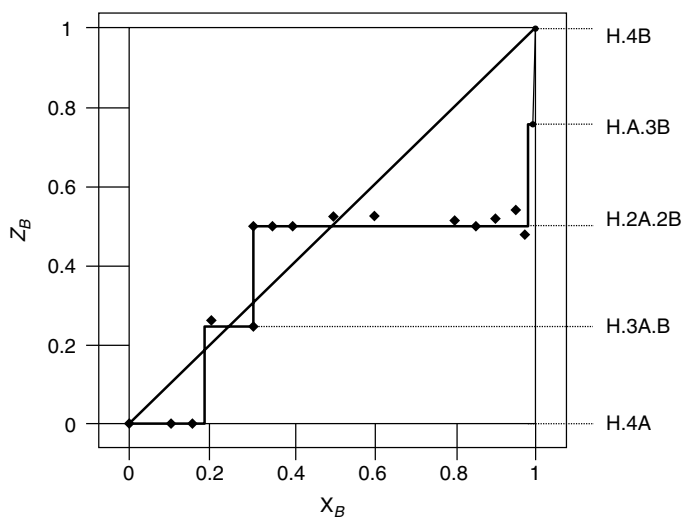


Figure 10 Results of the DMF–DMSO competition experiments. Figure reproduced from ref. 29, by permission of the Royal Society of Chemistry.

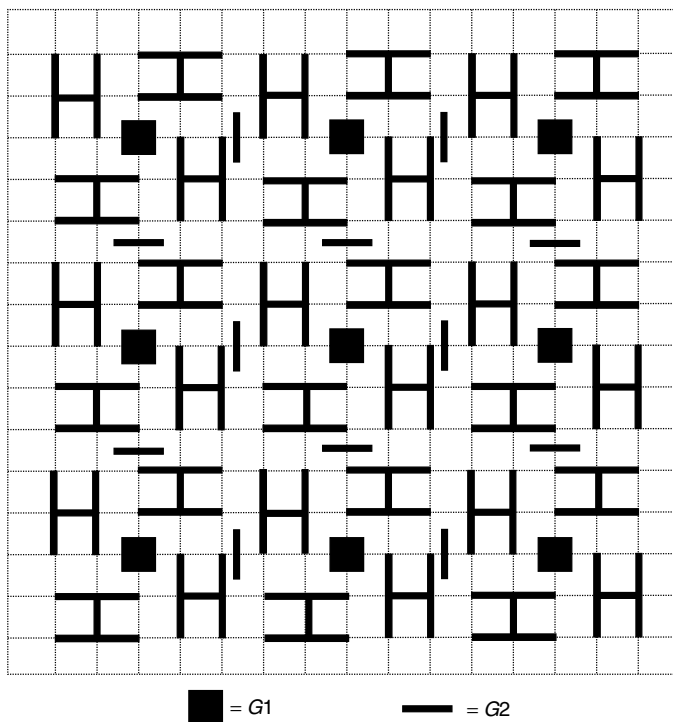


Figure 11 Schematic diagram of host *H* accommodating guests with different symmetry.

host molecules H leave spaces in the lattice which can accommodate guests with fourfold symmetry (G_1) and guests with twofold symmetry (G_2).

By varying the relative site occupancies of G_1 and G_2 , inclusion compounds with different properties would result. Some progress in this direction has been achieved [30,31], and Desiraju [32], in an article entitled 'Matching of molecular and supramolecular symmetry. An exercise in crystal engineering', has indicated the direction of future progress.

REFERENCES

1. R. M. Barrer, *Zeolites and Clay Minerals as Sorbents and Molecular Sieves*, Academic Press, London, 1978.
2. H. van Bekkum, E. M. Flanigen and J. C. Jansen (eds), *Introduction to Zeolite Science and Practice*, Elsevier, Amsterdam, 1991.
3. J. B. Nagy, P. Bodart, I. Hannus and I. Kiricsi, *Synthesis, Characterisation and Use of Zeolitic Microporous Materials*, DecaGen, Szeged, Hungary, 1998.
4. B. T. Ibragimov, S. A. Talipov and T. F. Aripov, *J. Incl. Phenom. Mol. Rec. Chem.*, **17**, 317 (1994).
5. P. Brunet, M. Simard and J. D. Wuest, *J. Am. Chem. Soc.*, **119**, 2737 (1997).
6. S. Noro, S. Kitagawa, M. Kondo and K. Seki, *Angew. Chem. Int. Ed.*, **39**, 2082 (2000).
7. S. S.-Y. Chui, S. M.-F. Lo, J. P. H. Charmant, A. G. Orpen and I. D. Williams, *Science*, **283**, 1148 (1999).
8. A. M. Pivovar, K. T. Holman and M. D. Ward, *Chem. Mater.*, **13**, 3018 (2001).
9. M. R. Caira, A. Horne, L. R. Nassimbeni and F. Toda, *J. Chem. Soc., Perkin Trans. 2*, 1717 (1997).
10. M. R. Caira, A. Horne, L. R. Nassimbeni and F. Toda, *J. Mater. Chem.*, **7**, 2145 (1997).
11. M. R. Caira, A. Horne, L. R. Nassimbeni and F. Toda, *Supramol. Chem.*, **9**, 231 (1998).
12. M. R. Caira, L. R. Nassimbeni, F. Toda and D. Vujovic, *J. Chem. Soc., Perkin Trans. 2*, 2681 (1999).
13. L. R. Nassimbeni and H. Su, *J. Chem. Soc., Perkin Trans. 2*, 1246 (2002).
14. M. R. Caira, A. Horne, L. R. Nassimbeni and F. Toda, *J. Mater. Chem.*, **8**, 1481 (1998).
15. P. Starzewski, W. Zielenkiewicz and J. Lipkowski, *J. Incl. Phenom.*, **1**, 223 (1984).
16. J. Lipkowski and J. Chajm, *Ann. Soc. Chim. Polonorum*, **51**, 1443 (1977).
17. A. Gavezzotti, *Cryst. Rev.*, **7**, 5 (1998).
18. A. Vedani and J. D. Dunitz, *J. Am. Chem. Soc.*, **107**, 7653 (1985).
19. M. R. Caira, L. R. Nassimbeni, F. Toda and D. Vujovic, *J. Am. Chem. Soc.*, **122**, 9367 (2000).
20. R. J. Davey, K. Allen, N. Blagden, W. I. Cross, H. F. Lieberman, M. J. Quayle, S. Righini, L. Setton and G. J. T. Tiddy, *CrystEngComm*, **4**, 257 (2002).
21. J. Jacques, A. Collet and S. H. Wilen, *Enantiomers, Racemates and Resolutions*, Krieger Publishing Company, Malabar, Florida, 1991.

22. S. H. Wilen and E. L. Eliel, *Tables of Resolving Agents and Optical Resolutions*, University of Notre Dame Press, Notre Dame – London, 1971.
23. F. Toda, in *Topics in Current Chemistry, Vol. 140*, ed E. Weber, Springer-Verlag, Berlin, 1987.
24. F. Toda, in *Inclusion Compounds, Vol. 4*, eds J. L. Atwood, J. E. D. Davies and D. D. MacNicol, Oxford University Press, Oxford, 1991.
25. F. Toda and Y. Tohi, *Chem. Commun.*, 1238 (1993).
26. F. Toda and H. Takumi, *Enantiomer*, **1**, 29 (1996).
27. A. N. Collins, G. N. Shelldrake and J. Crosby (eds), *Chirality in Industry II*, Wiley, Chichester, 1997.
28. M. R. Caira, L. R. Nassimbeni, D. Vujovic and F. Toda, *J. Phys. Org. Chem.*, **13**, 75 (2000).
29. M. R. Caira, T. le Roex and L. R. Nassimbeni, *Chem. Commun.*, 2128 (2001).
30. R. Thaimattam, F. Xue, J. A. R. P. Sarma, T. C. W. Mak and G. R. Desiraju, *J. Am. Chem. Soc.*, **123**, 4432 (2001).
31. N. Hayashi, K. Kuruma, Y. Mazaki, T. Imakubo and K. Kobayashi, *J. Am. Chem. Soc.*, **120**, 3799 (1998).
32. P. K. Thallapally, K. Chakraborty, A. K. Katz, L. H. Carrell, S. Sambasivarao and G. R. Desiraju, *CrystEngComm*, Paper 31 (2001).

Chapter 6

Regioselective Synthesis of Fullerene Derivatives and Separation of Isomers of the Higher Fullerenes

L. ECHEGOYEN AND M. A. HERRANZ

Clemson University, Department of Chemistry, 219 Hunter Chemistry Laboratories, Clemson, SC 29634-0973, USA

F. DIEDERICH AND C. THILGEN

Laboratorium für Organische Chemie, ETH-Hönggerberg Wolfgang-Pauli-Strasse 10, CH-8093 Zürich, Switzerland

1 INTRODUCTION

Fullerenes represent a unique family of three-dimensional building blocks that can be used as molecular scaffolding to prepare interesting structures, thus complementing the present repertoire of two-dimensional acetylenic, olefinic or benzenoid components. Of the many derivatization reactions involving C₆₀, the so-called Bingel–Hirsch reaction, first reported in 1993, is undoubtedly one of the most versatile, and consequently one of the most used for the preparation of fullerene derivatives [1,2]. Sequential double Bingel addition on the [60]fullerene core, which results in regio-isomeric product formation, is illustrated in Figure 1. Hirsch and co-workers obtained seven (1–7) out of the eight

possible bis-adduct isomers, named as *cis*-1–3, *e*, and *trans*-1–4, which could be separated by high-performance liquid chromatography (HPLC) [2]. No *cis*-1 bis-adduct was isolated, presumably due to the steric compression that would result from the close proximity of the two adducts of this isomer. The *trans*-1 derivative is almost always the least abundant, due to kinetic and statistical reasons [3,4]. The controlled sequential multiple functionalization of the carbon sphere, however, has proved to be difficult, mainly because isolation of pure higher adducts usually requires tedious chromatographic isomer separation [5]. In order to have regioisomeric control of bis- and tris-adduct formation, some of us applied the concept of tether-directed remote functionalization, initially introduced by Breslow and co-workers in a different context [6], which affords a variety of interesting addition patterns by double and triple additions [7].

The electrochemical properties of all these bis-adducts have been studied in reasonable detail, using either cyclic voltammetry (CV) or controlled potential electrolysis (CPE) [8]. Reductive electrolysis of ester-containing methanofullerenes results in the removal of the adducts in a versatile and useful reaction, initially called the retro-Bingel reaction (Figure 1). Additional work resulted in the discovery of an intramolecular electrochemically induced isomerization of C₆₀-bis-adducts. Exhaustive reduction with one electron per molecule resulted in seven regio-isomers regardless of which pure bis-adduct regioisomer was electrolyzed. Recently, it has been observed that, in addition to the malonates, electrochemical reduction of other methano-adducts can also lead to removal of the addends,

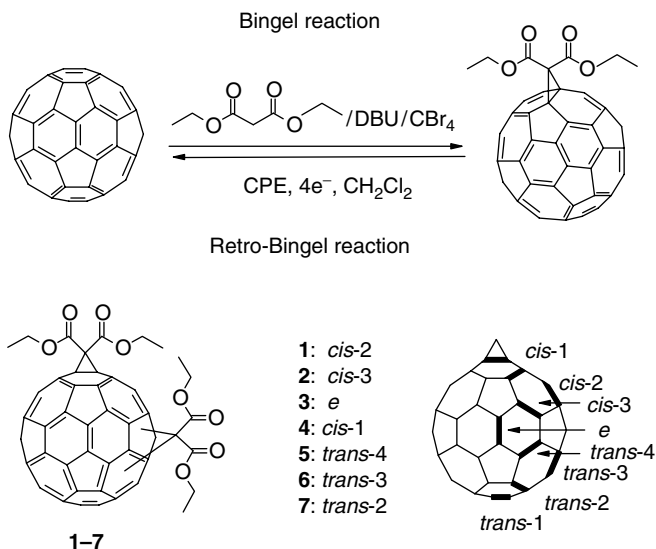


Figure 1 Bingel and retro-Bingel reactions on C₆₀. Position notation for bis-adducts of C₆₀.

and the reaction can be more generally referred to as a retro-cyclopropanation reaction [9–11]. The work described in this chapter is intended to demonstrate how the retro-cyclopropanation reaction has become a powerful tool for the separation of enantiomers and constitutional isomers of fullerenes and in concert with the isomerization reaction, serves for the preparation of methanofullerene derivatives which are not accessible otherwise.

2 REGIOSELECTIVE SYNTHESIS OF FULLERENES

The search for alternatives to the stepwise addition of new addends to a mono-, bis-, or tris-adduct of C_{60} for the preparation of highly functionalized fullerenes has been a challenge since the beginning of fullerene chemistry. Here we present the principal approaches introduced to control the regiochemistry of multiple additions to fullerenes by the use of tethered addend systems. The tethered macrocyclization method proved to be a major breakthrough and has provided relatively facile access to otherwise strongly disfavored addition patterns.

2.1 Anthracene as a Reversible Covalent Template

Prior to the development of tether-directed functionalization methods, Kräutler and co-workers developed a very elegant topochemically controlled, solid-state group-transfer synthesis [12,13] to obtain the *trans*-1 bisanthracene adduct **9** (Figure 2).

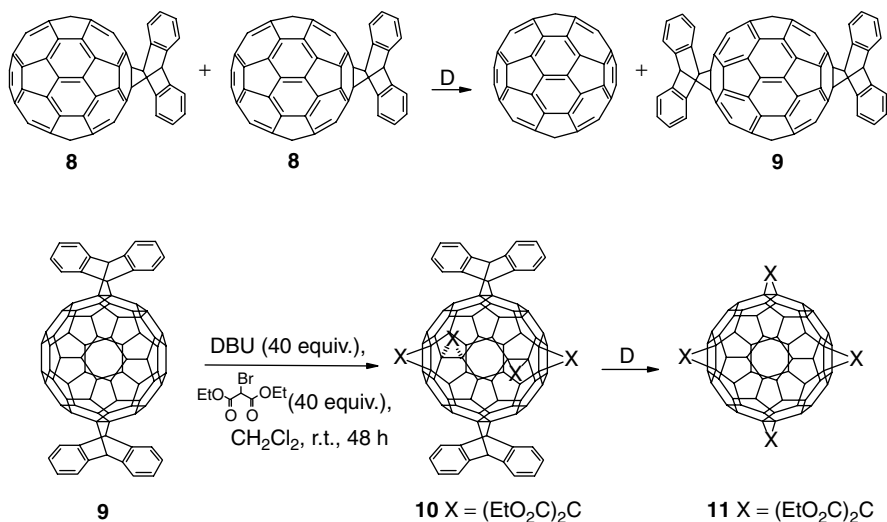


Figure 2 Topochemical solid-state synthesis of bis-adduct **9** and templated synthesis of tetrakis-adduct **11** in solution.

The regiospecific thermolysis of crystalline mono-adduct **8** gives a (1:1) mixture of C_{60} and the *trans*-1 bis-adduct **9** in 48% yield. The two anthracene addends of **9** served, in solution, to direct four bromomalonate addends regiospecifically into *e*-positions, yielding hexakis-adduct **10**. The subsequent thermal removal of the two anthracene molecules led to a tetrakis-adduct with an equatorial belt of bis[(ethoxycarbonyl)methano] addends on the carbon sphere [14], representing a valuable building block for further specific functionalization.

Other examples for the use of this template activated method include the formation of hexakis-adducts [15,16] with, for example, dendrimers featuring a fully buried fullerene core [8,17,18].

2.2 Tether-Directed Remote-Functionalization

The tether-directed remote-functionalization methodology has proved to be a very powerful synthetic tool, due to its high regio- and stereoselectivity. Since the first description of such a reaction in 1980 [6] a variety of regioselective protocols have been developed for fullerene derivatization, and these were recently reviewed [7], so this section constitutes a selective overview mainly focused on the pertinent features relevant to this chapter.

Tethers (which are usually removable) are used to provide spatial separation between addends in tether-directed remote functionalization. The addends can be identical or different, like the ones represented in Figure 3 as *A* and *RG*, where *A* is the anchor addend that is connected initially and *RG* is a secondary reactive group that is subsequently added to the fullerene. The tether structure and rigidity controls the regio- and, in the occurrence, stereochemistry of the addition pattern between *A* and *RG*.

To illustrate the utility and scope of the tether-directed remote functionalization process, one example is now presented and explained in detail. To achieve the regioselective formation of an *e* bis-adduct of C_{60} , the preformed anchor–tether–reactive group conjugate depicted in Figure 4 was attached in a sequence consisting of a Bingel reaction followed by a double Diels–Alder addition at the two *e* positions on opposite sides of the carbon sphere. The product was the orange-brown tris-adduct **12** in 60% yield with complete regioselectivity [19].

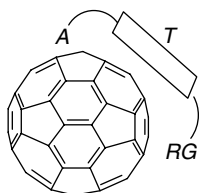


Figure 3 Tether-directed remote functionalization (*A* = anchoring point, *T* = connecting tether, *RG* = reactive group).

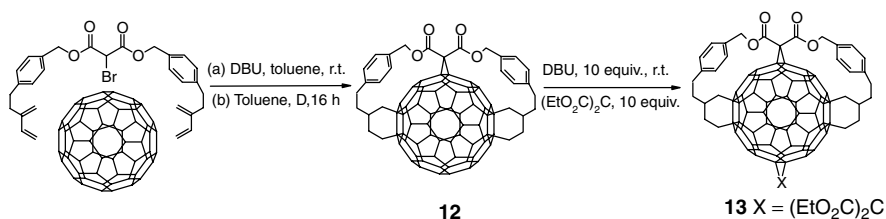


Figure 4 Tether-directed remote functionalization and *e* addition pattern.

Note that the Diels–Alder addends are in a *trans*-1 arrangement relative to each other. The C_{2v} -symmetric tris-adduct **12** can be readily prepared in multi-gram quantities, and its addition pattern cannot be accessed by stepwise, nontethered reaction sequences. Starting from tris-adduct **12**, sequential malonate additions to *e* 6–6 bonds provided novel tetrakis-(**13**), pentakis-, and, eventually, yellow-colored hexakis-adducts. The reactivity and physical properties of these higher adducts have been investigated in great detail [19–21]; also, the corresponding endohedral ^3He compounds were prepared, and their π -electron ring-current effects studied by ^3He -NMR [22].

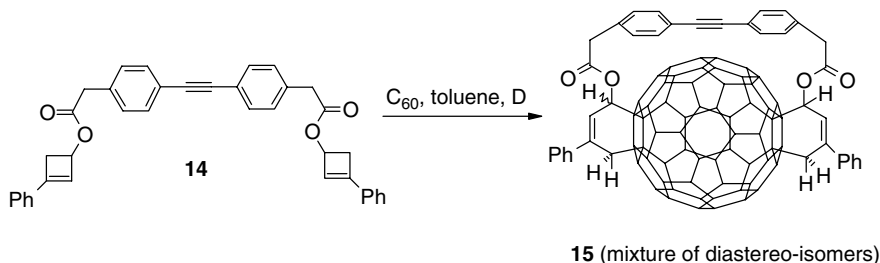


Figure 5 Preparation of the *trans*-1 bis-adduct **15**.

Using a very similar approach, the double Diels–Alder addition [23,24] of a tethered bis(buta-1,3-diene) to C_{60} has been used for the regioselective formation of *trans*-1 bis-adducts by Rubin and his group [25]. They prepared the tethered bis(cyclobutene) **14** as a mixture of stereo-isomers (Figure 5). Upon refluxing **14** with C_{60} in toluene, ring opening (cycloreversion) of the cyclobutenes occurred and the resulting 1,3-diene underwent [4 + 2] cycloaddition regioselectively to afford the *trans*-1 derivative **15** in 30% yield.

Possibly the simplest and most versatile method for the preparation of covalent bis-adducts of C_{60} with high regio- and diastereoselectivity is the macrocyclization between C_{60} and bismalonate derivatives in a double Bingel reaction [7,8,26,27]. In theory, each macrocyclic regio-isomer could form as a mixture of diastereomers, depending on how the EtOCO residues at the two methano bridge C-atoms are oriented with respect to each other (*in-in*, *in-out*,

and *out-out* stereo-isomerism) [28]. However, with the exception of the *in-out* isomers derived from 1,10-phenanthroline-2,9-dimethanol [8], *out-out* stereoisomers have been obtained exclusively until now.

Some interesting examples (**16–19**) [29–33] for the various functionalization patterns are presented in Figure 6. The Bingel macrocyclization is increasingly being exploited in the synthesis of functional supramolecular systems. For example, compound **16** has been employed for the preparation of glycodendrons of high generation [34]. The *trans*-4 crown ether (\pm)-**17** was used in the construction of C_{60} -containing catenanes [29] with an unprecedented intramolecular A–D–A–D–A stack (A = acceptor, D = donor). A porphyrin has been connected tangentially to C_{60} by double attachment to the *trans*-1 positions at the two poles of the C-sphere in conjugates such as **18** [35]. The tetraphenylporphyrin

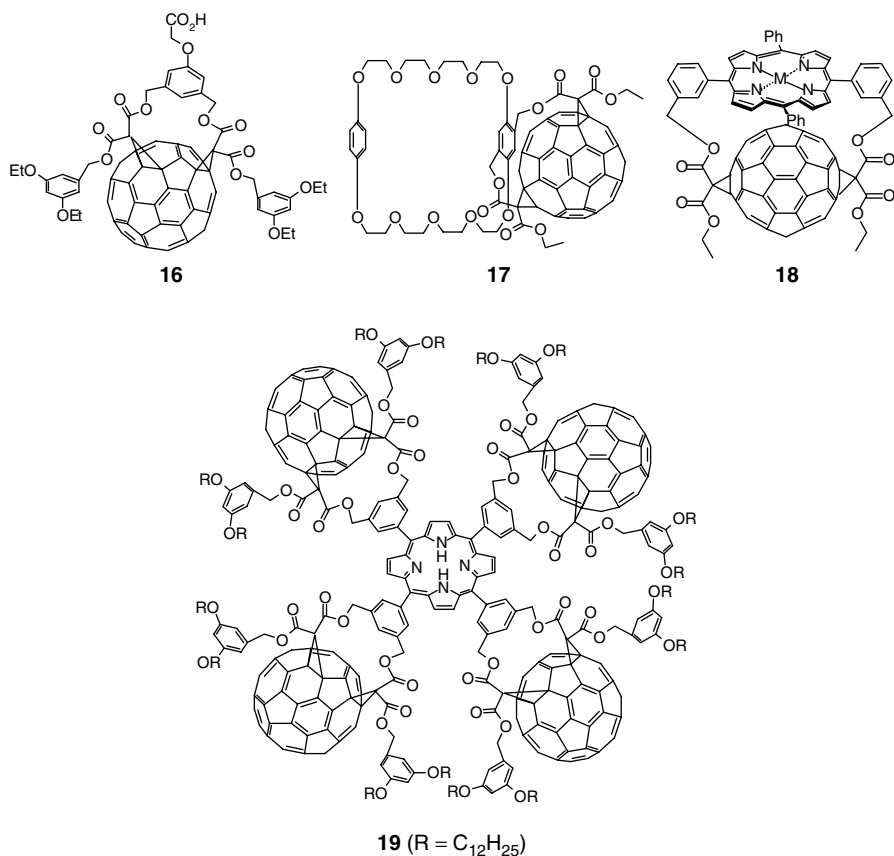


Figure 6 Representative examples of C_{60} bis-adducts directly produced by the Bingel macrocyclization reaction.

derivative **19** described by Nierengarten *et al.* [34], exhibits a strong effect on the redox properties of the porphyrin moiety. The first oxidation potential of the porphyrin ring is significantly more anodic ($AE \approx 175$ mV) than that of the corresponding free porphyrin. The shift is believed to be a consequence of the strong electron-withdrawing effect of the four fullerene subunits, which could substantially destabilize the first oxidized state of the porphyrin moiety.

A sequence of highly diastereoselective Bingel macrocyclizations, using a nonracemic tether, followed by removal of the tether via transesterification, provided an enantioselective synthesis of optically active bis-adducts in which the chirality results exclusively from the addition pattern [7,36]. Starting from (*R,R*)-**20** and (*S,S*)-**20**, which were prepared from the corresponding optically pure diols, the two enantiomeric *cis*-3 bis-adducts (*R,R*,^f*A*)-**21** and (*S,S*,^f*C*)-**21** were obtained with high diastereoselectivity (>97%) (Figure 7). In each macrocyclization, two diastereomeric *out-out cis*-3 bis-adducts are possible due to the chiral addition pattern; however, the high asymmetric induction by the optically active tether in the second intramolecular Bingel addition led to the formation of (*R,R*,^f*A*)-**21** and (*S,S*,^f*C*)-**21** only. The simple stereochemical descriptors ^f*C* and ^f*A* (*f* = fullerene, *C* = clockwise, *A* = anticlockwise) were introduced to specify the configurations of chiral fullerenes and fullerene derivatives with

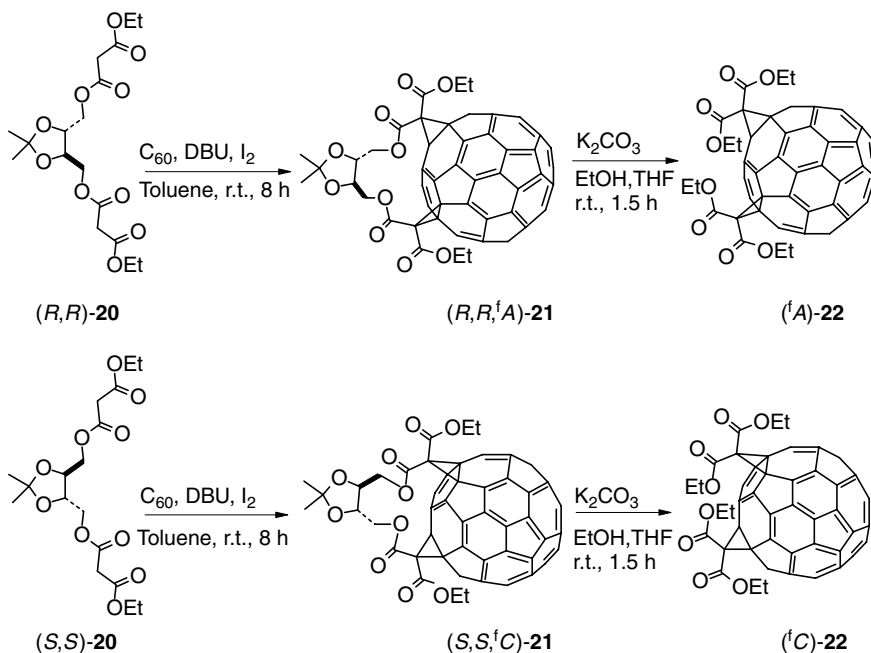


Figure 7 Enantioselective synthesis of (^f*A*)-**22** and (^f*C*)-**22** by diastereoselective tether-directed bis-cyclopropanation of C_{60} , followed by transesterification.

a chiral functionalization pattern [37]. Transesterification of $(R,R,^fA)$ -**21** and $(S,S,^fC)$ -**21** yielded the *cis*-3 tetraethyl esters (^fA) -**22** and (^fC) -**22** with an enantiomeric excess higher than 99% [(^fA) -**22**] and 97% [(^fC) -**22**] (HPLC), reflecting the enantiomeric excesses of the corresponding commercial starting diols. The absolute configurations of these optically active fullerene derivatives could be assigned from their calculated circular dichroism (CD) spectra [37]. The fact that the tethers in $(R,R,^fA)$ -**21** and $(S,S,^fC)$ -**21** could be readily removed by transesterification makes them true covalent templates.

2.3 Other Bis-functionalization Patterns

The cycloaddition of azomethine ylides to C_{60} [38] is another widely used fullerene functionalization methodology; however, it is much less selective. To study the possibility of controlling the reactivity of these dipoles, Da Ros and co-workers have carried out a systematic study based on the use of a reversible anchorage [39]. First, an anchor is attached to C_{60} with the formation of an isoxazolinofullerene (**23**). Then the azomethine ylide is generated, which attacks intramolecularly a second double bond of the same fullerene spheroid (**24a–c**) (see Figure 8). The length of the arm between the anchor and the pyrrolidine ring have been varied in order to determine its influence on regioselectivity. Since the isoxazoline ring is asymmetric, two possibilities exist: additions of the azomethine ylide on the side of the imine carbon of the isoxazoline are designated by the suffix-C and additions on the side of the oxygen are designated by the suffix-O. With relatively short tethers (three or four methylene units), only *cis*-1-C bis-adducts are obtained, characterized by relatively small distances between the imine carbon and the pyrrolidine nitrogen. With the longer pentamethylene tether, the *cis*-1-O and *cis*-3-C bis-adducts are obtained. It is remarkable that in this case no *cis*-1-C compound was observed, probably because this addition

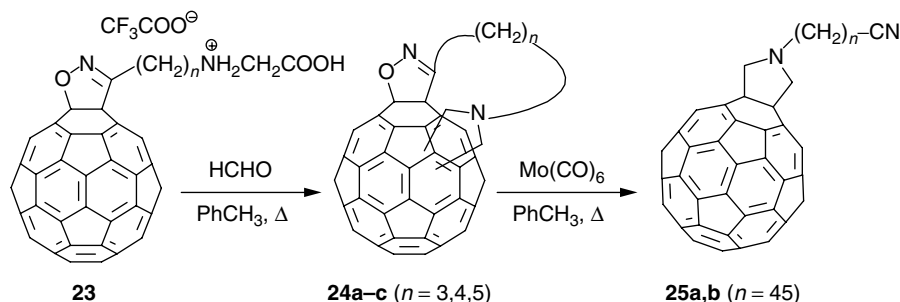


Figure 8 Tether-directed additions of azomethine ylides to fullerene C_{60} , assisted by a removable anchor.

modality requires an energetically unfavored twisting of the long methylenic chain. Eventually, the anchor is removed using reducing agents such as $\text{Mo}(\text{CO})_6$ or DIBALH, and the fulleropyrrolidines **25a–b** are obtained.

Other tethers have been employed in the search for regioselectivity in multiple additions to fullerenes. Some of these methodologies include the use of bis(*o*-quinodimethanes) connected by α, ω -dioxamethylene tethers [40], tethered nucleophilic vinylcarbenes [41] or azides [42].

An interesting templated bis-functionalization was reported by Shinkai and co-workers, who introduced two boronic acid groups regioselectively via Diels–Alder addition on to the fullerene, using saccharides as ‘imprinting’ templates (Figure 9) [43,44]. Preliminary recognition studies showed that, after cleavage of the boronate esters, the resulting fullerene-derived bis(boronic acid) shows selective binding for the sugar initially used as a template.

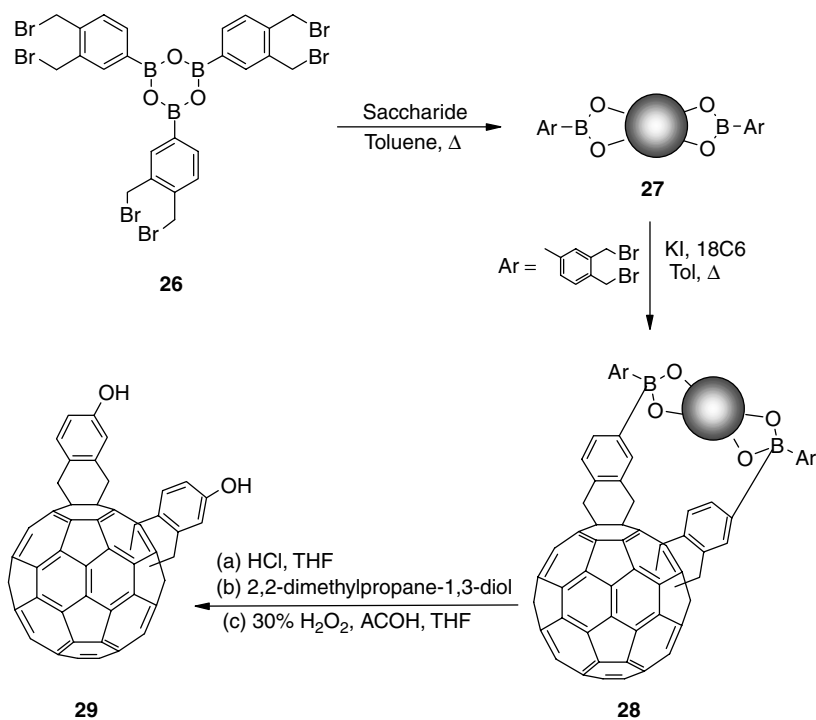


Figure 9 Regioselective bis-functionalization of C_{60} using a saccharide as an imprinting template.

2.4 Tris-adduct Formation by Tether-directed Bingel Addition

In contrast to the large number of bis-adducts generated through a tether-directed methodology, only a few examples of tris-adducts have been described [19,45,46].

In theory, bis-adducts of C_{60} derived from Bingel cyclopropanation reactions can exist as eight different regio-isomers, seven of which have been detected and isolated [2] (see Figure 1). The number of possible regio-isomers increases to 46 in the case of tris-adducts in which three of the 30 6–6 bonds are cyclopropanated [5c]. In 1997, Djojo and co-workers reported the stepwise preparation of a series of tris-adducts starting from untethered reagents, in which they obtained the *trans*-3,*trans*-3,*trans*-3 and *e,e,e* regio-isomers, together with other isomers, after tedious separation and purification [45a].

We recently reported the C_3 -symmetric [60]fullerene-cyclotrimeratrylene (CTV) tris-adducts (\pm)-**32** (with a *trans*-3,*trans*-3,*trans*-3 addition pattern) and (\pm)-**33** (with an *e,e,e* addition pattern) prepared in 11% and 9% yield, respectively, by the regio- and diastereoselective tether-directed Bingel reaction of C_{60} with the tris-malonate-appended CTV derivative (\pm)-**31** (Figure 10) [47]. This is the first example of tris-adduct formation by a one-step tether-directed Bingel addition. We demonstrated that interchromophoric interactions between the electron-rich CTV cap and the electron-attracting fullerene moiety have a profound effect on the electrochemical behavior of the C-sphere. The fullerene-centered first reduction potentials in compounds (\pm)-**32** and (\pm)-**33** are 100 mV more negative than those of their corresponding tris[bis(ethoxycarbonyl)methano][60]fullerene analogs that lack the CTV cap.

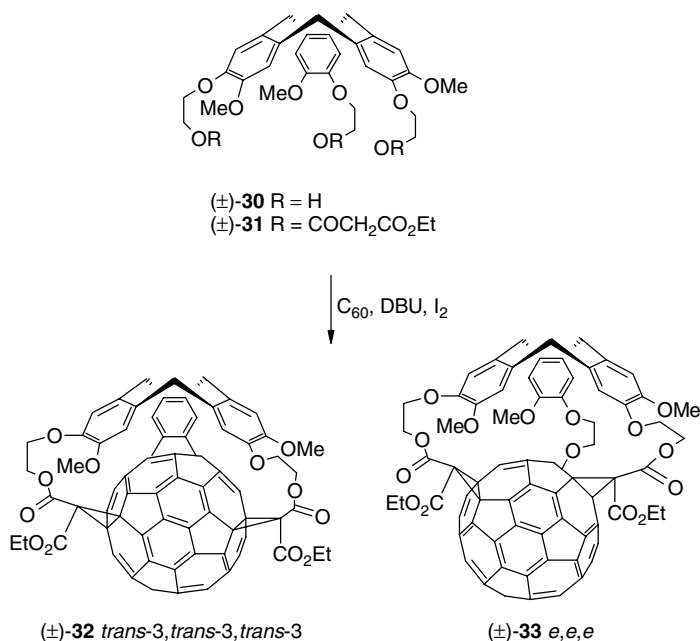


Figure 10 Regioselective one-step synthesis of topologically chiral *trans*-3,*trans*-3,*trans*-3 and *e,e,e* [60]fullerene-cyclotrimeratrylene tris-adducts.

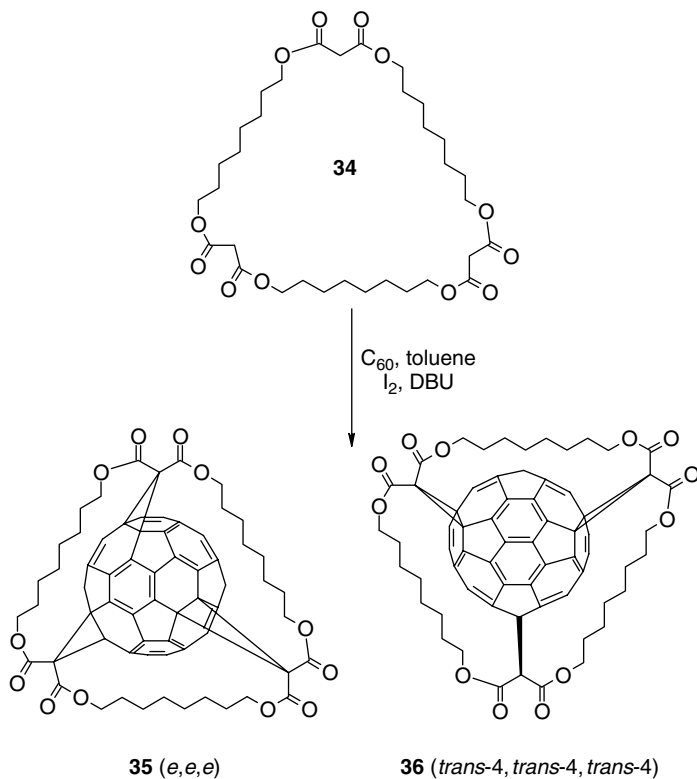


Figure 11 Synthesis of the *e,e,e* (**35**) and *trans-4,trans-4,trans-4* (**36**) tris-adducts.

A particular interest in (\pm)-**32** and (\pm)-**33** arises from the topological chirality of these molecules. A complete topology study led to the conclusion that the four possible classical stereo-isomers of the *e,e,e* regioisomer, resulting from the combination of the chiral fullerene addition pattern and the chiral CTV unit, are topologically different, and, therefore, there exist four different stereo-isomers. Interestingly, in the case of the *trans-3,trans-3,trans-3* tris-adduct, there are four classical stereo-isomers but only two stereo-isomers [48]. The introduction of topological isomerism adds another dimension to the ongoing exploration of the chirality of fullerenes and their covalent and supramolecular derivatives – an exciting field of contemporary stereochemistry [49].

Hirsch and co-workers last year introduced a new concept for the tether-directed multifunctionalization of C_{60} , with the use of cyclo-[*n*]-octylmalonates such as **34** (Figure 11) [50]. As a result of the identical spacer lengths in these macrocycles, only bis- and tris-adducts with rotational symmetry are formed. The reaction of cyclo-[3]-octylmalonate (**34**) with C_{60} leads to the *e,e,e* isomer **35** with high regioselectivity and excellent yield (94%). Additionally, 6% of

trans-4,*trans*-4,*trans*-4 tris-adduct **36** was obtained. The *trans*-3,*trans*-3,*trans*-3 tris-adduct could not be detected at all. The tris-adduct **35** can be saponified to the corresponding *e,e,e*-hexaacid by a standard procedure. Therefore, this reaction sequence provides a valuable tool for the large-scale production of water-soluble *e,e,e* hexaacid, which exhibits a high solubility in water and is a very potent anti-oxidant compound [50].

3 FULLEROCROWN ETHERS: SUPRAMOLECULAR FULLERENE CHEMISTRY

Crown ethers are excellent cation binding units extensively used in the preparation of host-guest complexes, where the guests are usually alkali or alkaline-earth metal ions [51]. The idea of attaching crown ethers to fullerenes (fullerocrowns) to affect the electrochemical behavior of the carbon sphere was developed by several groups since 1990. The group of Wilson [52] and some of us [53] reported the synthesis and properties of the first crown-ether derivatives of C₆₀. However, no substantial effects due to cation complexation on the redox properties of the fullerene sphere were observed, mainly because the required close proximity and geometric disposition of the two units for a substantial coulombic effect to be observable were not present.

In order to have the crown ring close enough and essentially tangential to the cage for maximum coulombic interaction, we used the regioselective Bingel macrocyclization of C₆₀ with a bis-malonate containing an *anti*-disubstituted dibenzo[18]crown-6 (DB18C6) tether, which yields up to 30% of the planar chiral *trans*-1 bis-adduct (\pm)-**37**, together with a small amount of (\pm)-**38** [30]. (DB18C6) was chosen as the tether, since computer modeling indicated that its dimensions and shape would be appropriate to direct the second Bingel addition of the bis-malonate to the *trans*-1 position. More interestingly, when the crown ether tether was further rigidified by K⁺-ion complexation, the yield and selectivity were greatly enhanced, and (\pm)-**37** was obtained as the only regioisomer at 50% yield. The macrocyclization, starting from a mixture of tethered bis-malonates with *anti* and *syn* bisfunctionalized DB18C6 moieties, yielded the *trans*-1 ((\pm)-**37**, 15%), *trans*-2 ((\pm)-**38**, 1.5%) and *trans*-3 ((\pm)-**39**, 20%) isomers (Figure 12).

The addition pattern of (\pm)-**37** was confirmed by transesterification with removal of the tether (Figure 13). Thus the reaction of (\pm)-**37** with Cs₂CO₃ in anhydrous hexanol/THF 1:1 provided the D_{2h} symmetric bis-adduct **45** at 34% yield. Its ¹³C-NMR spectrum displayed only nine resonances for the fullerene C-atoms, and the expected peaks for four equivalent hexyl residues. Of all possible regio-isomeric bis(dihexyl malonate) adducts of C₆₀, only the *trans*-1 compound displays this high symmetry [2].

Compound **45** was also obtained by a second route. We prepared the bis (*tert*-butyl ester) (\pm)-**42** by transforming the DB18C6 diol **40** into bis-malonate **41**,

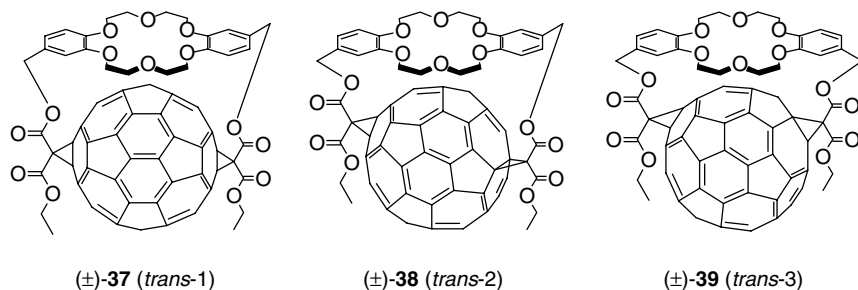


Figure 12 Cyclophane type fullerene-dibenzo[18]crown-6 conjugates with *trans*-1, *trans*-2 and *trans*-3 addition patterns.

followed by macrocyclization with C_{60} . Unfortunately, upon heating with TsOH in PhMe, compound (±)-42 was readily transformed into the tetracarboxylic acid 43. Apparently, acidic cleavage of the tethered ester groups is quite favorable due to the stabilization of the intermediately formed benzylic carbocations by the *p*-alkoxy groups. The tetracarboxylic acid 43 was directly transformed with oxalyl chloride into the intermediate tetrakis(acyl halide) 44, which then reacted with hexanol in the presence of pyridine to give 45 in a 45% total yield.

The intermediate tetrakis(acyl halide) 44 was also employed in the preparation of hexakis adducts that feature the location of all addends along an equatorial belt rather than evenly distributed over the entire carbon sphere, as in (±)-49 (Figure 14) [54]. The target compound (±)-49 was synthesized by a short route that involves the initial coupling reaction of 44 with mono-*t*-BuMe₂Si-protected 1,3-benzenedimethanol yielding 46, which was then deprotected with HF/pyridine and converted with ethyl malonyl chloride into 48. Fourfold intramolecular Bingel addition of 48 under high dilution conditions gave (±)-49, after column chromatography, as a single hexakis adduct at 10% yield.

In (±)-49 π -electron conjugation between the two free poles is maintained through two *trans*-stilbene-like bridges. As a result of this extended conjugation, the compound is red in solution, with an end absorption extending to 600 nm. This contrasts with the light-yellow color (end adsorption around 450 nm) of the hexakis adducts with a pseudo-octahedral addition pattern, in which the residual π -electron chromophore is reduced to a benzenoid 'cubic cyclophane'-type substructure [15,54].

The ionophoric properties of (±)-37 with a variety of alkaline and alkaline-earth cations have been reported, and K^+ ions were found to bind preferentially (effective complex-formation constant $\log K^{\text{eff}} = 5.4 \pm 0.2$) over the other alkali-metal ions [55].

The complex between (±)-37 and KPF_6 was characterized by X-ray crystal-structure analysis, which confirmed the close tangential orientation of the ionophore moiety with respect to the fullerene surface, which had been predicted by computer modeling (Figure 15).

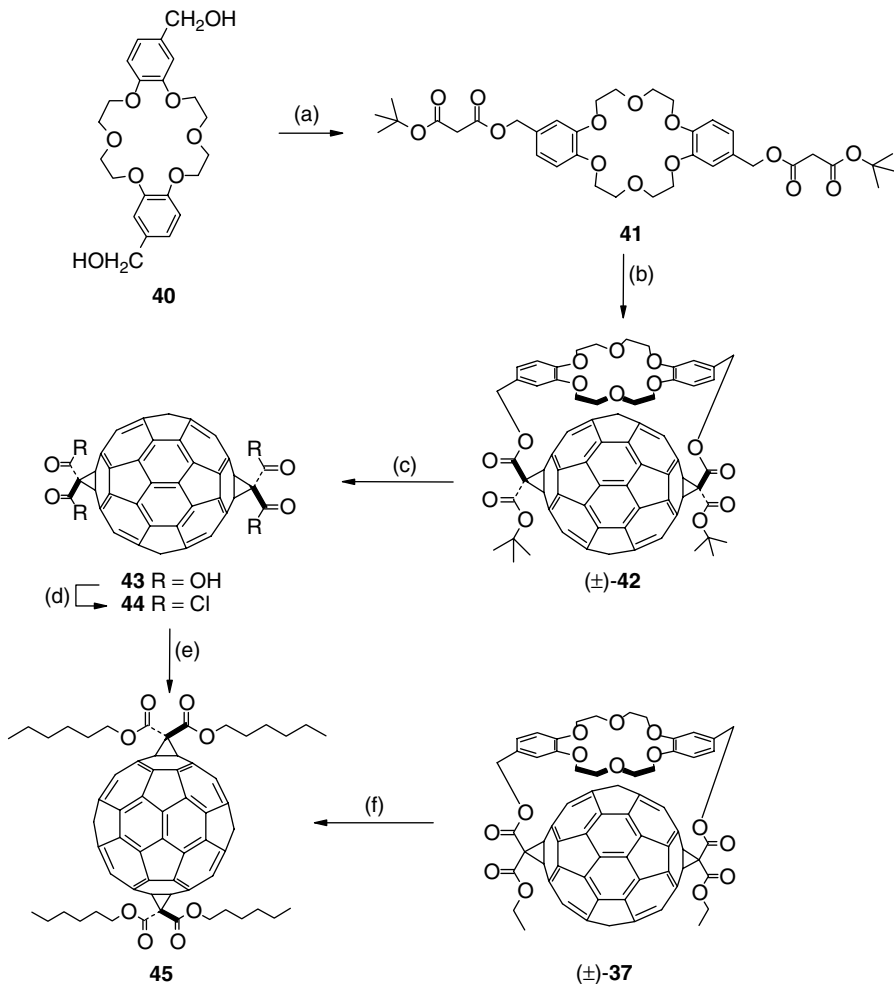


Figure 13 Preparation of **45** by transesterification. (a) $\text{ClCOCH}_2\text{CO}_2(t\text{-Bu})$, pyridine, CH_2Cl_2 , r.t., 1 h. (b) C_{60} , I_2 , DBU, KPF_6 , toluene/acetonitrile, r.t., 1 h. (c) TsOH , toluene, Δ , 12 h. (d) $(\text{COCl})_2$, CH_2Cl_2 , 40°C , 4 h. (e) Hexanol, pyridine, CH_2Cl_2 , r.t., 14 h. (f) Hexanol/THF 1:1, Cs_2CO_3 , KPF_6 , r.t., 3.5 h.

Additionally, substantial effects on the fullerene-centered reduction steps due to cation complexation by the tangential and proximal dibenzo-crown ether were observed by cyclic voltammetry (CV) for **(±)-37** [30,55] (Figure 16). The CV was recorded both in the presence of one equivalent of [2.2.2]cryptand and in the presence of ten equivalents of KPF_6 . The cryptand was added to ensure that the species observed initially was uncomplexed, since peaks corresponding with the Na^+ and K^+ complexes were observed in the FAB mass spectrum of

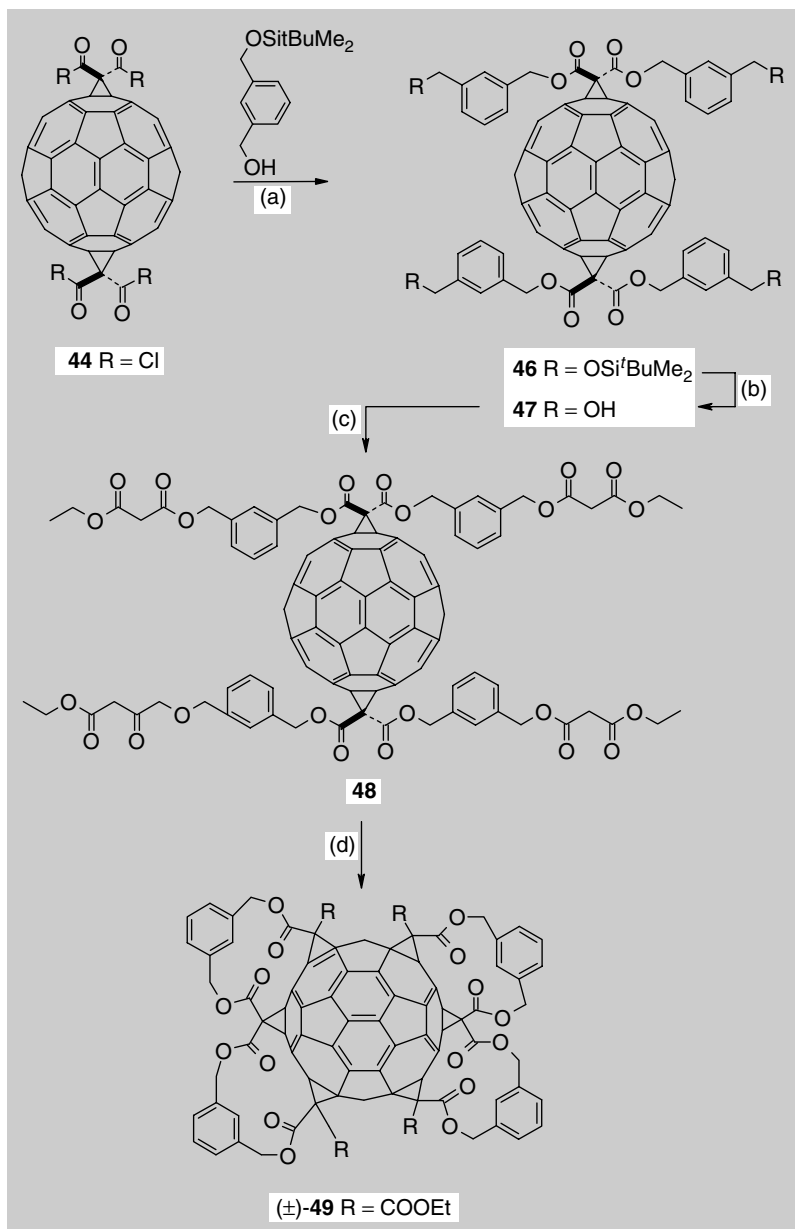


Figure 14 Synthesis of hexakis-adduct (\pm) -49. (a) Pyridine, CH_2Cl_2 , 20°C , 12 h. (b) HF-pyridine, CH_2Cl_2 , 0°C , 1 h. (c) $\text{EtO}_2\text{CCH}_2\text{COCl}$, N,N-dimethylaniline, CH_2Cl_2 , 20°C , 14 h. (d) I_2 , DBU, PhMe/Me₂SO, 20°C , 12 h.

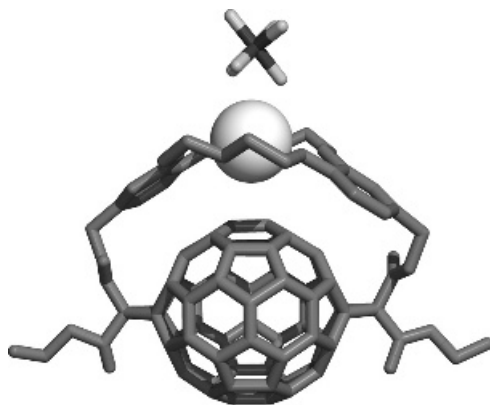


Figure 15 Graphical visualization of the X-ray crystal structure of (\pm)-**37** (reprinted with permission from Helvetica Chimica Acta [55]).

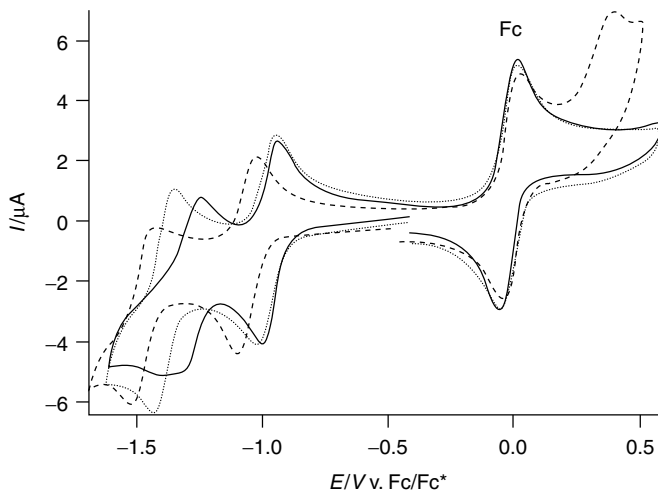


Figure 16 Cyclic voltammograms for (\pm)-**37** recorded at 100 mV s^{-1} on a glassy carbon electrode in the presence of (a) 1 equivalent of [2.2.2]cryptand (---), (b) 10 equivalents of KPF_6 (.....), and (c) 10 equivalents of $\text{Ba}(\text{CF}_3\text{SO}_3)_2$ (—) v. ferrocene as internal reference (reprinted with permission from Helvetica Chimica Acta [55]).

free (\pm)-**37**. The first fullerene-based reduction process of uncomplexed (\pm)-**37** is quasireversible ($\Delta E_{\text{pp}} = 70 \text{ mV}$) and occurs at $E_{1/2} = -1.04 \text{ V v. ferrocene (Fc)}$. The second fullerene-based reduction process is somewhat more complicated, and exhibits what appear to be two closely spaced waves. Because of these observations, we did not attempt to quantify $E_{1/2}$ for this process. The chemical irreversible oxidation observed around $+0.4 \text{ V}$ corresponds with the added cryptand.

Addition of KPF_6 results in a large anodic shift of the reduction processes, with the first one shifting to -0.95 V v. Fc. This is a shift in potential of 90 mV relative to that of the uncomplexed compound, and is attributed to the electrostatic effect of K^+ bound in close proximity to the carbon sphere. If KPF_6 is incrementally titrated into the solution containing (\pm) -**37**, it is possible to see the gradual decrease of the original first reduction wave and the growth of the one for the complex. This behavior clearly indicates the formation of a highly stable complex between K^+ and (\pm) -**37** [56]. The second redox process in the complex has $\Delta E_{\text{pp}} = 100$ mV and $E_{1/2} = -1.36$ v. Fc. Addition of ten equivalents of [2.2.2] cryptand reverses the voltammetric response to the original voltammogram observed in the absence of KPF_6 , which indicates that the K^+ binding process with (\pm) -**37** is reversible.

Very similar results were obtained from the CV studies of (\pm) -**38** and (\pm) -**39**, but the observed anodic shifts of the first redox couples upon complexation with K^+ were smaller (50 mV for (\pm) -**38** and 40 mV for (\pm) -**39**). The reduction of the anodic shift from 90 mV (in (\pm) -**37**) to 40 mV (in (\pm) -**38**) can be explained by an increasing average distance between the cation bound to the crown ether and the fullerene surface, as the addition pattern changes from *trans*-1, to *trans*-2, and to *trans*-3 [55]. Additionally, the effects of different alkali- and alkaline-earth-metal ion salts on the redox properties of (\pm) -**37** were investigated. As expected, all electrochemical data clearly demonstrate a much larger interaction between crown-ether-bound cations with the negatively charged than with the neutral fullerene core [55].

The same two-point crown attachment concept was extended to C_{70} -based systems. Prior to this work, the tether-directed bis-addition macrocyclization had not been successful on C_{70} or other higher fullerenes. Sequential, double Bingel cyclopropanation of C_{70} [57] occurs on opposing hemispheres at the most curved α -type [58] 6–6 bonds emanating from the two polar pentagons through which the C_5 symmetry axis passes (Figure 17). In a Newman-type projection looking down the C_5 axis, the two addends adopt a twelve, two, or five o'clock geometric relationship, respectively, see Figure 17. Accordingly, the kinetically controlled Bingel bis-cyclopropanation with achiral dialkyl malonates provides three constitutional isomers, two of which (two, (\pm) -**52**, and five o'clock, (\pm) -**53**) are pairs of enantiomers, in a ratio 2.8:6.8:1.0, respectively (twelve, two, and five o'clock orientation of the addends). Similar addition patterns were also obtained in other bis-functionalization reactions, with the two o'clock geometric relationship being highly favored in each case [49,58,59–62].

The application of the tether-directed remote functionalization allowed the preparation of stereo-isomeric C_{70} bis-adducts (\pm) -**55a** and (\pm) -**55b** with complete regioselectivity, featuring the kinetically disfavored five o'clock addition pattern [63], see Figure 18.

The *anti* compound **54** adds to C_{70} under modified Bingel conditions and in the presence of KPF_6 (10 eq.) to form the diastereo-isomers (\pm) -**55a** and

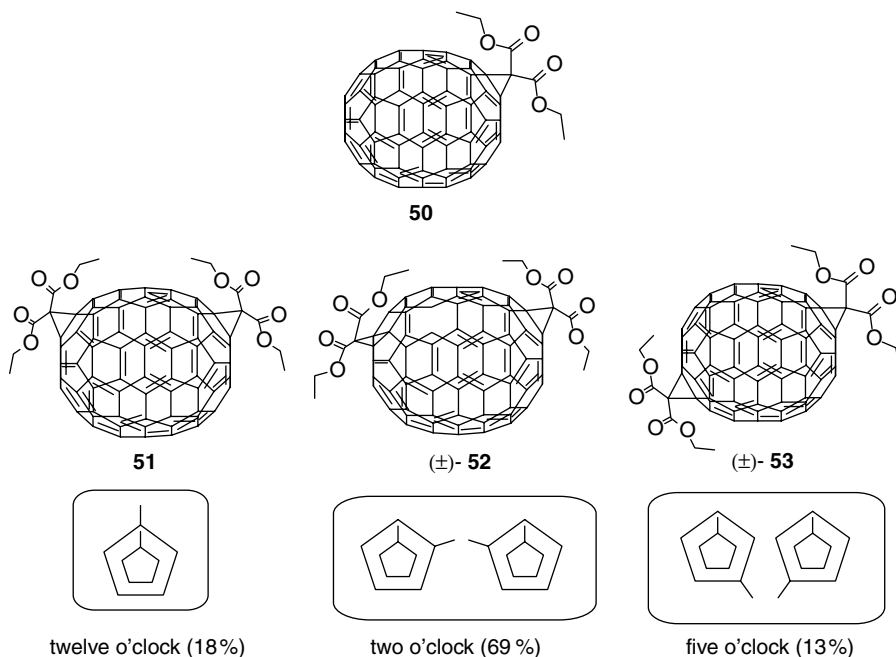


Figure 17 Mono (**50**) and regio-isomeric bis-adducts (**51**, **(±)-52** and **(±)-53**) formed by Bingel cyclopropanation of [70]fullerene. Also shown are Newman-type projections looking down the C_5 -symmetry axis of the C_{70} core on to the two polar pentagons, which show the relative orientations of the addends.

(±)-55b in a 56:44 ratio and with an overall yield of 41%. Transesterification of the crude product mixture **(±)-55a/b** (Cs_2CO_3 , THF-EtOH (1:1)) afforded only one single C_2 -symmetric bis-adduct **(±)-53**. The inherently chiral five o'clock addition pattern and the *out-out* orientation of the COOEt groups in **(±)-55a** was unequivocally established by X-ray crystallography (Figure 19) [64]. Interestingly, the crown ether moiety exists in a conformation different from the four conformations reported so far in the literature for uncomplexed DB18C6 [63]. In order to bridge the fullerene poles, it adopts an 'umbrella shaped' geometry with a distorted C_2 -symmetry (Figure 19).

The first electrochemical reduction of these constitutional isomers occurs around -1.13 V v. Fc/Fc^+ and they are anodically shifted by about 70–80 mV when complexed by either Na^+ or K^+ . The anodic shift is due to the presence of the positive charge on the bound cation, as observed previously for the C_{60} *trans*-1 crown ether analog [30,55]. Successive reductions of the fullerenocrowns are chemically irreversible, a consequence of retrocyclopropanation reactions, as will be described later in this chapter.

With the bis-malonate **56** containing a *syn*-disubstituted DB18C6 tether, the regioselectivity of the macrocyclization of C_{70} via double Bingel cyclopropanation

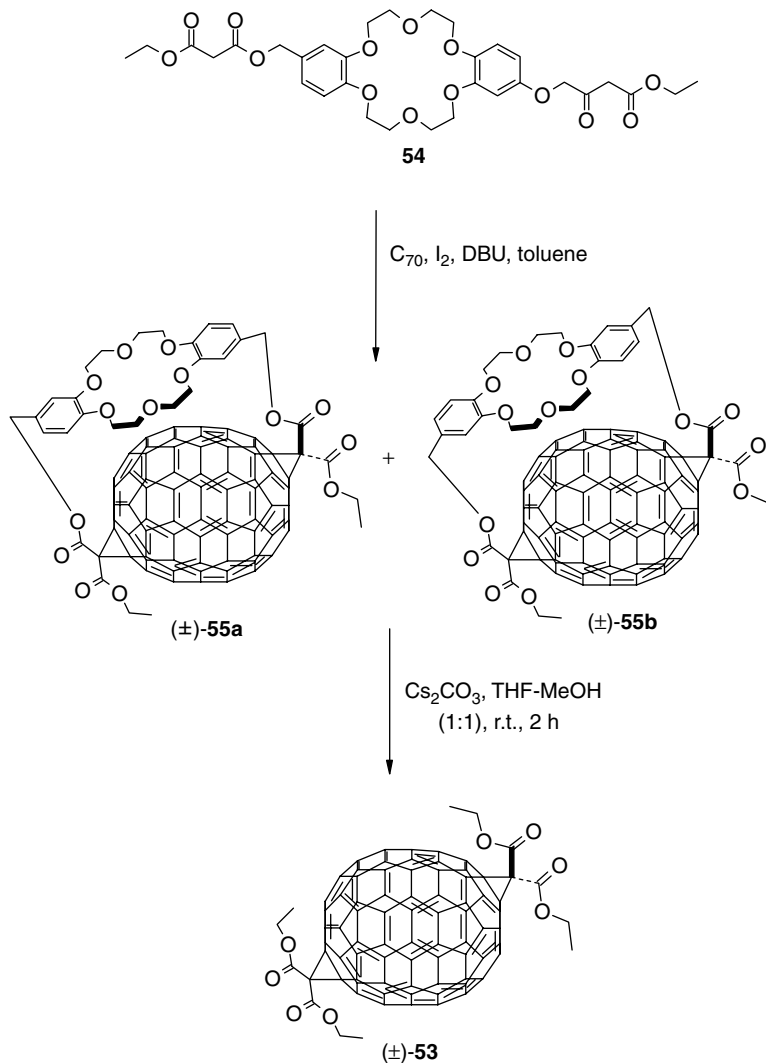


Figure 18 Tether-directed regioselective bis-functionalization of C_{70} .

changed completely, resulting in two constitutionally isomeric C_{70} crown ether conjugates in a *c.*1:1 ratio, featuring the twelve and two o'clock addition pattern, respectively [64].

More recently, bis-crown derivatives of the diastereo-isomeric fullerencrowns **55a/b** have been prepared, and their electrochemical properties have been measured as well [64,65]. It is important to note that these bis-crown compounds (**(±)-57a/b**, Figure 20), were successfully obtained at 30% yield when the five

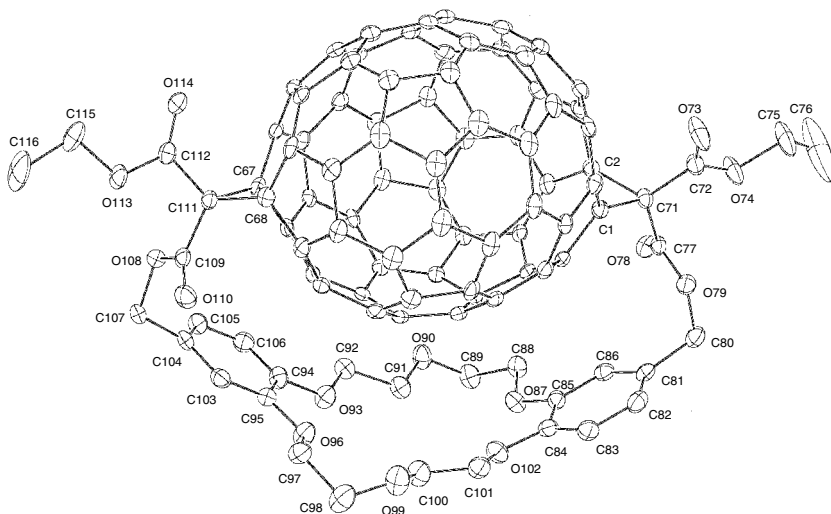


Figure 19 Crystal structure of (\pm)-**55a**. Atomic displacement parameters obtained at 233 K are drawn at a 30% probability level [63]. Reproduced by permission of the Royal Society of Chemistry.

o'clock diastereo-isomers **55a/b** were reacted with the *syn* DB-18C6 compound **56**. When reacted with the *anti* compound (**54**), an inseparable mixture of four bis-crown conjugates was obtained at 69% yield. As expected, the bis-crown compounds are more difficult to reduce than the corresponding mono-crown derivatives by about 300 mV. First reduction potentials are -1.47 and -1.44 V *v.* Fc/Fc⁺ for the two bis-crown isomers (\pm)-**57a** and (\pm)-**57b**, respectively. Addition of either Na⁺ or K⁺ results in pronounced anodic shifts, which continue until two cation equivalents are added. Further salt additions do not cause additional changes in the voltammetric properties, indicating that a 2:1 complex forms. The magnitude of the shifts is around 170 mV for both alkali cations—essentially twice the observed shifts for the corresponding mono-crown derivatives. This is strong evidence that the ion effect is purely electrostatic in nature, since the two crown rings in the bis-crown compounds are not equivalent and could have led to different electronic effects on the carbon cage.

4 RETRO-CYCLOPROPANATION REACTIONS

At the beginning of this chapter, we mentioned how the removal of di(alkoxycarbonyl)methano addends on a C₆₀ core can be achieved by electrolytic reduction to yield the parent [60]fullerene. This so-called retro-Bingel reaction was initially conducted on diethyl 1,2-methano[60]fullerene-61,61-dicarboxylate (see Figure 1) leading to > 80% yield of recovered C₆₀ after controlled potential

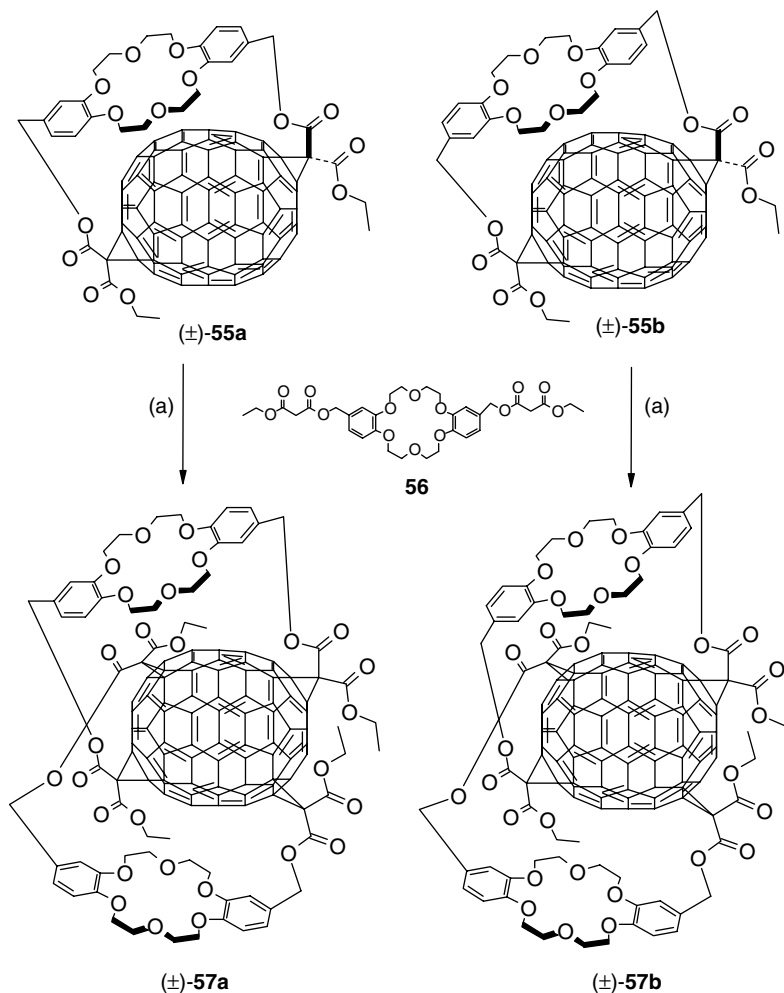


Figure 20 Synthesis of the C₇₀ bis-crown ether conjugates (±)-57a,b. (a) I₂, DBU, toluene/Me₂SO 4:1, r.t.

electrolysis (CPE) at the second reduction potential. The generality of the retro-Bingel reaction was proved by removing up to four di(alkoxycarbonyl)methano groups from a variety of fullerene derivatives [66–71]. Remarkably, it was found that, with the exception of the *cis*-2 isomer which requires only one electron, a two-electron controlled potential electrolysis (CPE) of any isomer of bis[di(ethoxycarbonyl)methano][60]fullerene results in the addends rearranging or isomerizing on the fullerene surface [69]. Using this electrolytic reaction, the product distribution is the same regardless of which bis-adduct

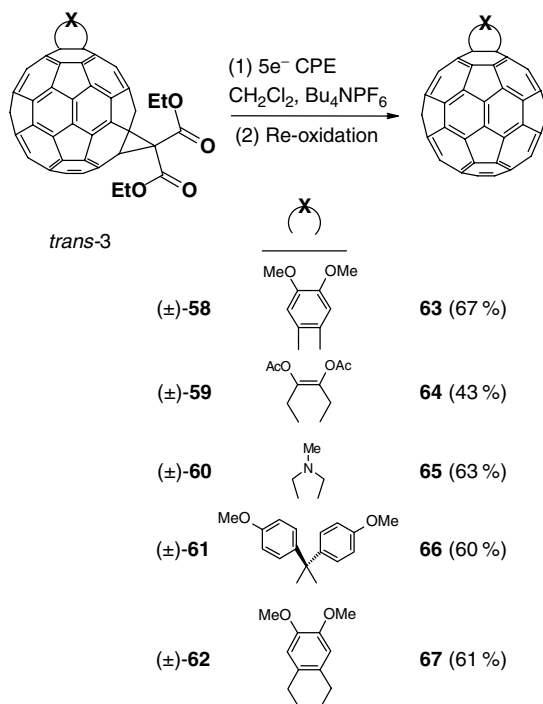


Figure 22 Selective removal of bis(ethoxycarbonyl)methano addends in mixed C_{60} -bis-adducts by the retro-Bingel reaction.

of the addends was always a di(ethoxycarbonyl)methano group and the other one ranged from a fused pyrrolidine to a bis(*p*-methoxyphenyl)methano group (58–62, Figure 22) [68]. In all cases it was shown that controlled potential electrolysis led to the selective removal of the Bingel addend, while the other one was retained. The isolated yields for these retro-Bingel (retro-cyclopropanation) reactions ranged from 43% to 67%, making them synthetically useful in the preparation, through a protective–deprotective protocol, of fullerene derivatives with the desired functionalization scheme [68].

Other methanofullerenes (not of the Bingel-type) were also found to be unstable after several reduction processes (68–70, Figure 23), [9–11] and under CPE they led to the isolation of [60]fullerene. A more recent study was conducted in THF to avoid the well-known reactivity of CH_2Cl_2 towards the polyanions of C_{60} [72] and to explore the mechanisms involved during adduct removal [9b,10]. Surprisingly, an electrochemically induced intermolecular adduct transfer was observed for the spiro-methanofullerenes studied, and the regio-isomer distribution found in THF differed significantly from that obtained when the compounds are prepared by a direct synthetic route [10]. The proposed mechanism for the formation of

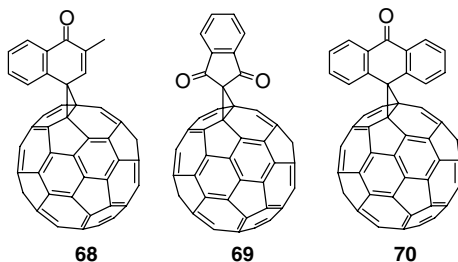


Figure 23 Representative examples of electroreduced spiromethanofullerenes.

bis-adducts during the CPE time-scale involves the presence of two distinct pathways. When the reductive electrochemistry leads to the cleavage of one of the two cyclopropane bridging bonds, the intermediate is capable of either losing the addend from the fullerene cage or of reacting with another fullerene molecule. This could lead to the formation of dimers in which the two fullerene cages share one or two addends. Using digital simulations of the cyclic voltammetric results of these spiromethanofullerenes has afforded a better understanding of the mechanistic details involved in these electroreductive reactions [73].

In fact, we have recently proved that singly bonded dimers are formed as intermediates during retro-cyclopropanation reactions [74]. For the phosphonate adduct **71**, upon electroreduction with more than two electrons/molecule, there is evidence of the reversible formation of a very stable intermediate (Figure 24, graph in grey), which is oxidized at a potential 500 mV more positive than the first fullerene-based reduction of the parent compound. On this basis, we proposed a mechanism for the retro-Bingel reaction occurring in derivative **71**. Reductive electrochemistry heterolytically opens the cyclopropane ring, leading to charge formation either in the fullerene core or in the addend, and these interconvert at equilibrium. Dimers can then form between fullerene-based radicals.

These same selective adduct removal reactions were also accomplished via chemical reduction using a Mg/Hg amalgam or a combination of Mg/18C6 [75,76].

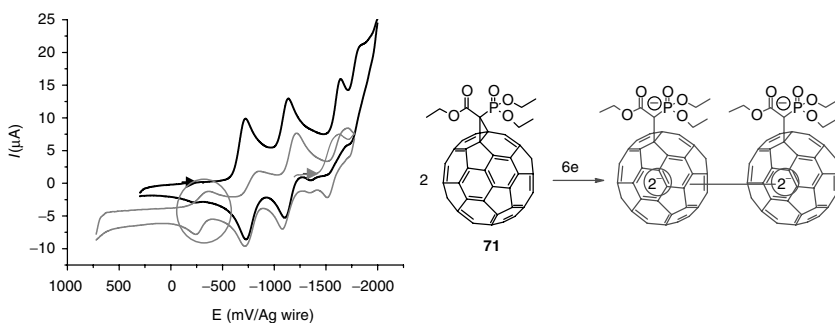


Figure 24 Formation of dimeric [60]fullerene derivatives from electroreduced **71**.

However, the chemical reduction reaction does not work efficiently for the removal of two Bingel addends, whereas the electrochemical reduction process works very efficiently. One of the most interesting examples that illustrates the difference between the chemical and electrochemical methodologies involves the cyclophane type *trans*-1 (\pm -**37**) conjugate [76]. The chemical reductive protocol fails completely with this compound, presumably due to ion complexation by the crown ether group and consequent stabilization. When the electroreductive method was used, a clean retrocyclopropanation reaction was observed (Figure 25).

The *trans*-1 bis-adduct (\pm -**37**) was subjected to CPE to its mono-anionic state, *c.* 100–150 mV after the first reduction wave. The charge transferred corresponded with one electron per molecule, and no changes were observed in the CV. When the CPE was carried out after the second reduction wave, changes in the CV indicated that a chemical transformation had taken place. After 30 min of electrolysis, reoxidation of the solution at 0 V (*v.* Ag) led to the voltammogram observed in Figure 25 (graph b) with an anodically shifted first (172 mV) and second reduction (166 mV) compared with the starting fullerenocrown. Purification and analysis of the recovered solution by column chromatography (SiO_2 , $\text{PhCH}_3/\text{AcOEt}$) yielded pure C_{60} at 70 % yield. In addition, to determine the potential effect of cation complexation on the electroreductive reaction, the CPE of (\pm -**37**) was also carried out in the presence of KPF_6 . CPE after the second reduction wave shows a two electron/molecule transfer and is fully reversible – no changes in the cyclic or OSWV voltammogram are observed. The compound was recovered at high yield following reoxidation to its neutral state. Complexation of the DB18C6 moiety in (\pm -**37**) by a metal ion seems to result in pronounced stabilization of the overall structure and inhibition of the retro-cyclopropanation reaction.

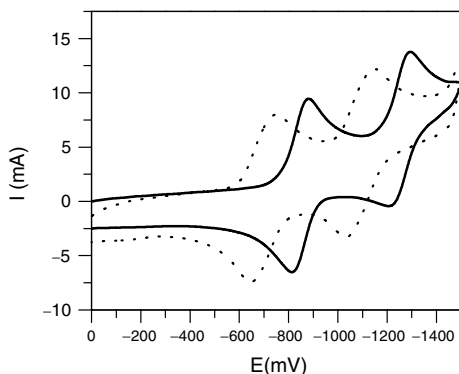


Figure 25 Cyclic voltammograms in CH_2Cl_2 (+0.1 M Bu_4NPF_6) at 100 mV s^{-1} for: (a) (—) *trans*-1 fullerene-dibenzo[18]crown-6 ((\pm)-**37**); (b) (· · ·) after 2e CPE and reoxidation. Reprinted from *Chemical Retro-cyclopropanation Reactions in Methanofullerenes: Effect of the 18-crown-6 moiety*, 1, M. A. Herranz, *et al.* 299–303, copyright 2003, with permission from Elsevier.

5 THE RETRO-CYCLOPROPANATION REACTION AS A SYNTHETIC TOOL IN THE SEPARATION, PURIFICATION AND ISOLATION OF HIGHER FULLERENE ISOMERS

In this section we present the use of the retro-cyclopropanation reactions for the synthesis of fullerene derivatives which are not available by other routes, and for the isolation of isomers and enantiomers of the higher fullerenes.

5.1 Retro-cyclopropanation Reaction in the Preparation of Optically Active C₇₆ Enantiomers

Prior to our work, Hawkins and Meyer had performed the kinetic optical resolution of the inherently chiral fullerene D₂-C₇₆ by employing the asymmetric Sharpless osmylation reaction [77]. A comparison of the circular dichroism (CD) spectra reported by Hawkins and Meyer for the C₇₆ enantiomers that they obtained [77] with those of a variety of optically active, covalent derivatives of C₇₆, prepared by ourselves [78] revealed a large, unexpected difference in the magnitude of the Cotton effects. Whereas our covalent C₇₆ derivatives displayed bands reaching $\Delta\epsilon$ values up to 250 M⁻¹ cm⁻¹, the enantiomers of the pure fullerenes reported by Hawkins and Meyer displayed bands with $\Delta\epsilon$ values up to only 32 M⁻¹ cm⁻¹ [77,79]. In order to reinvestigate the chiroptical properties of C₇₆ and to test the power and generality of the retro-Bingel reaction, we decided to prepare the pure diastereomeric mono-adducts **72** and **73**, which were previously reported [78]. The general idea was to use a chiral Bingel addend as an auxiliary, to allow separation of the diastereomers followed by removal of the addend via the retro-cyclopropanation reaction, to yield the pure enantiomers of C₇₆.

Diastereo-isomers **72** and **73** (Figure 26), were independently submitted to CPE and to subsequent purification by HPLC. The two enantiomers of C₇₆ were obtained at low yields (between 5 and 10%). So far, it has been impossible to optimize these yields, due to the limited availability of the starting diastereoisomers [70].

The CD spectra of the enantiomers of C₇₆ are shown in Figure 27. They exhibit the expected mirror-image relationship with band positions that are in full agreement with those reported by Hawkins and Meyer [77,79]. In contrast to their results, however, the Cotton effects observed in our spectra are almost a full magnitude larger than those previously reported. The $\Delta\epsilon$ values reach up to 210 M⁻¹ cm⁻¹, and are therefore much more in agreement with the values measured for optically pure C₇₆ derivatives such as **72** and **73** [79].

5.2 Retro-cyclopropanation Reaction in the Isolation of Pure C_{2v}-C₇₈ and a new C₂-symmetric Bis-adduct

A similar procedure to that described in the previous section was used to prepare pure C_{2v}-C₇₈, starting from a previously isolated tris(methano)-adduct,

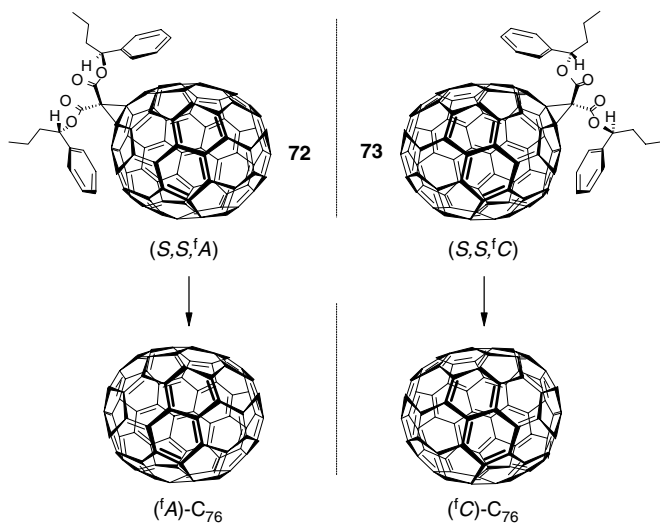


Figure 26 Electrochemical preparation of the enantiomers of C₇₆.

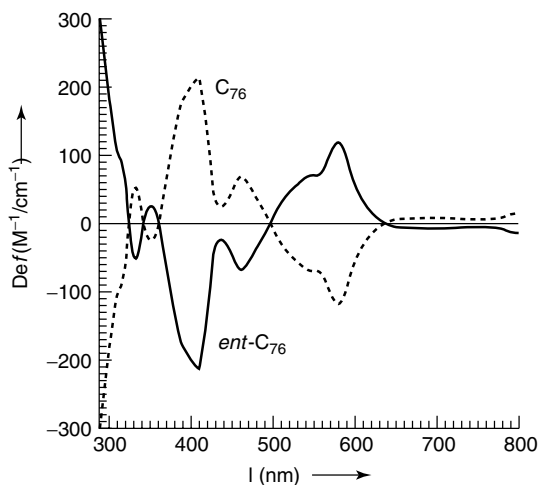


Figure 27 CD spectra of the enantiomers of C₇₆ in toluene. Reprinted from ref. [76] with permission from Wiley-VCH.

compound **74** (Figure 28) [80]. This compound was isolated using HPLC, and the symmetry of the fullerene core was determined to be C_{2v} by analysis of the ^{13}C NMR spectrum [80]. It was thus an excellent precursor to prepare C_{2v} -C₇₈ via the retro-Bingel removal of the three addends.

Although we anticipated that approximately 8e would be required for complete removal of the three adducts, we analyzed the CV of (\pm)-**74** after an initial

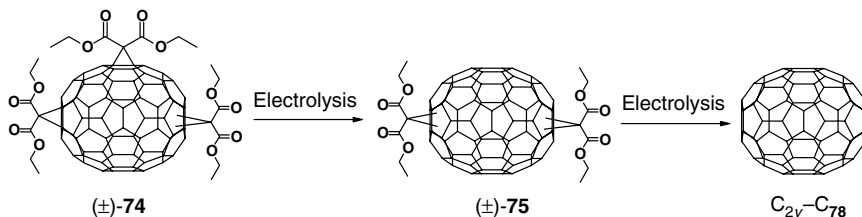


Figure 28 Formation of C₂-symmetric bis-adducts of C₇₈ from electrolysis of tris-adduct (\pm)-74.

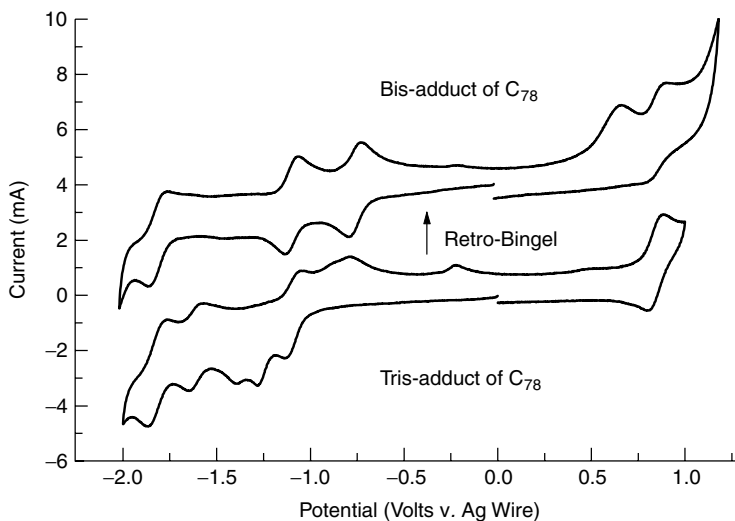


Figure 29 Cyclic voltammogram in CH₂Cl₂ (+0.1 M Bu₄NPF₆) under vacuum, scan rate 100 mV s⁻¹ for the tris-adduct (\pm)-74 and the retro-Bingel product (\pm)-75.

transfer of 3e during the CPE at -1.30 V. The observed changes in the CV were quite dramatic, as can be seen in Figure 29. Not only was C_{2v}-C₇₈ obtained, but, in addition, a bis-methano-adduct was also isolated after removal of only the first addend via the retro-cyclopropanation reaction [70]. This C₂-symmetric bis-adduct was not formed during the Bingel addition process to the C₇₈ isomers. The CV of the tris-adduct shows that only the first reduction is reversible, and it occurs at a very negative potential (Figure 29). However, three reversible couples are observed for the product bis-adduct (Figure 29). The first reduction of the bis-adduct is approximately 500 mV anodically shifted (easier to reduce) than the corresponding process for the tris-adduct. The bis-adduct was isolated at 55% yield after reoxidizing the solution at 0 V.

Partial electrolyses of other bis-adducts of C₇₈, such as D₃-C₇₈, led to CVs that are very similar to the one shown in Figure 29, and to intermediate CVs

similar to the one in Figure 29. We believe that this is the result of ‘shuffling’ or isomerization of the addends on the surface of C_{78} [67].

When complete electrolysis of (\pm)-**74** is achieved at -1.8 V *v.* Ag, followed by reoxidation at 0 V, the three addends are removed and pure C_{2v} - C_{78} can be isolated in a 31 % yield, after purification. The other isomer, D_3 - C_{78} , was obtained by HPLC separation of a mixture of C_{2v} - and D_3 - C_{78} , as previously described [81]. Having these pure isomers allowed us to examine their electrochemical behavior independently [70].

5.3 Retro-cyclopropanation Reaction in the Optical Resolution of D_2 - C_{84}

Using traditional separation methods, Shinohara and co-workers isolated and characterized a total of nine constitutional isomers of C_{84} (see reference 82 and references therein). At the present time, it appears as if six constitutional isomers of C_{84} have been characterized to date – using electrochemistry [71,82]. By far the most complete electrochemical characterization of C_{84} isomers was provided by Pénicaud and co-workers, who reported electrochemical results for D_2 (IV), D_{2d} (II), D_{2d} (I), D_2 (II), C_2 (IV), and one of the C_s isomers of C_{84} , tentatively assigned by them to C_s (V). Another C_s (specific structure not assigned) isomer and the D_{3d} and D_{6h} isomers appear also to have been isolated, but their electrochemical behavior has not been reported.

The six isomers characterized by Pénicaud and co-workers present characteristic fingerprint signatures when considering both their electrochemical and ESR responses [82]. Reasonably good agreement was found between calculated energy levels using density functional theory and the experimental redox potentials measured for these six isomers. Remarkably, the C_2 (IV) isomer exhibits a much less negative first reduction potential compared with the others. The value -0.28 V *v.* Fc/Fc⁺ is close to that of TCNQ (only 60 mV away), making it potentially useful for the preparation of charge-transfer salts. Interestingly, the C_2 (IV) and C_s (V) isomers are the only ones that exhibit a large gap between the second and third reductions, as previously reported for the otherwise uncharacterized isomer in reference 71. On this basis a C_s (V) symmetry was assigned to the isolated compound exhibiting a large potential difference between the second and third reductions. In order to isolate C_{84} isomers of importance, in the future it will be necessary to develop synthetic methods that provide larger yields.

We also introduced an alternative purification method which makes use of functionalization of the isomer mixture, followed by HPLC separation and final removal of the functional groups [71]. Since the functional group attached as an auxiliary is chiral, the method is similar to the one described above for C_{76} . It offers the advantage of not only providing pure constitutional isomers but also enantiomers – when these exist [71]. A conceptually similar approach was

recently described by Saunders and his co-workers, using dimethylantracene as a reversible derivatization agent to separate seven constitutional isomers of C_{84} in a single stage [83]. No matter which separation method was used, electrochemical characterization of the isomers has proved to be revealing [71,82].

In our approach, a C_{84} fraction of soot enriched in higher fullerenes was treated in *o*-dichlorobenzene at 20 °C with bis[(*S*)-1-phenylbutyl]-2-bromomalonate in the presence of DBU. Subsequent purification by column chromatography yielded four fractions containing, according to mass spectrometry: pure C_{84} , mono-adducts, bis-adducts, and tris-adducts, respectively. The mono-adduct and bis-adduct fractions were further separated by HPLC. The bis-adduct fraction led to six main products. The fourth and fifth fractions corresponded with C_2 -symmetric bis-adducts, which featured mirror-image CD spectra with large Cotton effects (Figure 30, top right). With the addends being chiral (stereogenic center) and enantiomerically pure, such spectra are characteristic of a pair of diastereo-isomeric C_{84} adducts, the CD spectra of which are dominated by the contributions of the enantiomeric π -chromophores of the inherently chiral fullerene cores. The UV/visible spectra of the two diastereo-isomers differ considerably from those of the identified achiral D_{2d} - C_{84} bis-adduct [71], which suggests that they are derivatives of the chiral

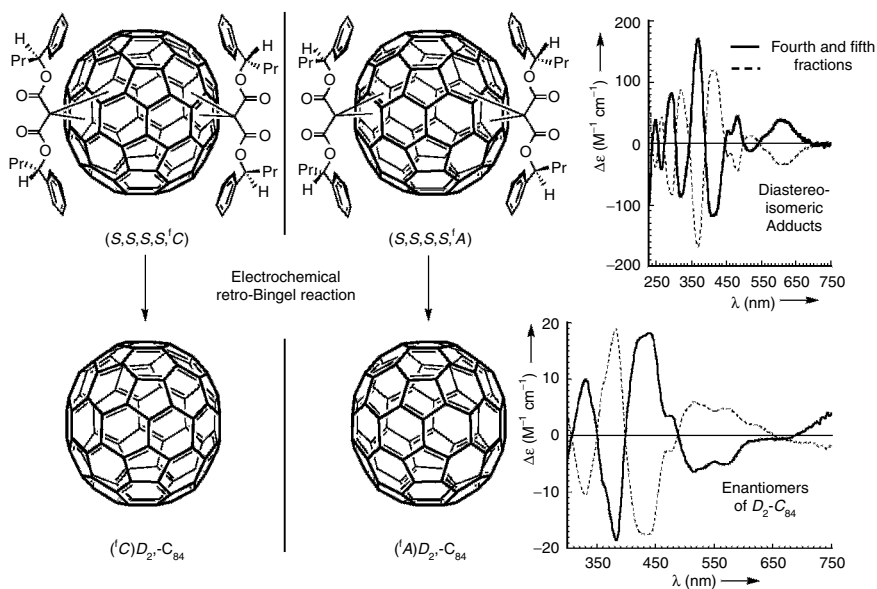


Figure 30 Preparation of the pure enantiomers of D_2 - C_{84} by a retro-Bingel reaction of the fourth and fifth fractions of the bis-adducts, and CD spectra of the diastereo-isomeric bis-adduct (top right) as well as of the fullerene enantiomers (bottom right) in CH_2Cl_2 . The absolute configurations of the fullerene spheroids reflect the structural drawings, but have not been assigned experimentally. Reprinted from ref. [71] with permission from Wiley-VCH.

fullerene D_2-C_{84} . This was clearly confirmed after the retro-Bingel reaction and the electrochemical investigations on the parent fullerene enantiomers. Controlled potential electrolysis of the separated diastereo-isomers yielded the pure enantiomers of D_2-C_{84} , and their mirror image CD spectra (Figure 30, bottom right) correspond nicely with those reported by Hawkins *et al.* for samples obtained by kinetic resolution through asymmetric osmylation [79].

Not many methano- or other adducts are removed via electrochemical reduction, offering the possibility of using Bingel addends as potential protecting–deprotecting groups for fullerene derivatization. The application of this strategy, Bingel–retro-Bingel, offers many possibilities for the preparation of regio-isomers that are not readily accessible via direct synthesis.

6 SUMMARY AND CONCLUSIONS

We have shown how templated synthesis approaches are currently revolutionizing the covalent chemistry of fullerenes. They provide elegant and imaginative protocols to produce highly selectively functionalized fullerene building blocks for three-dimensional molecular scaffolding.

The scope of the tether-directed remote functionalization has been expanded from C_{60} to the higher fullerene C_{70} , and the described reactions are completely regioselective, featuring, in the case of C_{70} , the kinetically disfavored addition pattern. The crown ether is a real template, since it can be readily removed by transesterification, giving a much-improved access to certain bis-adducts that are not accessible by the direct route. Cation-binding studies by CV reveal that cyclophane-type crown ethers derived from C_{60} and C_{70} form stable complexes with metal cations, and a perturbation of the fullerene reduction potentials occurs because the cation is tightly held close to the fullerene surface. This conclusion is of great importance for future developments of fullerene-based electrochemical ion sensors.

Finally, the wide applicability and the experimental simplicity of the retro-Bingel reaction was evidenced in the isolation of pure enantiomers of C_{76} , in the formation of methanofullerene compounds not accessible otherwise, such as (\pm) -**75**, and in the separation of constitutional isomers as well as of enantiomers of C_{84} . The retro-cyclopropanation reaction seems to be generally selective, and still needs to be exploited in the preparation of unusual derivatives with controlled regiochemistry.

ACKNOWLEDGEMENT

The authors wish to express their gratitude to the Chemistry Division of the National Science Foundation (CHE-0135786) and to the Swiss National Science Foundation for generous financial support.

REFERENCES

1. C. Bingel, *Chem. Ber.* **1993**, *28*, 1957–1959.
2. (a) A. Hirsch, I. Lamparath, H. R. Karfunkel, *Angew. Chem.* **1994**, *106*, 453–455; *Angew. Chem. Int. Ed.* **1994**, *33*, 437–438; (b) F. Djojo, A. Herzog, I. Lamparath, F. Hampel, A. Hirsch, *Chem. Eur. J.* **1996**, *2*, 1537–1547.
3. A. Hirsch, I. Lamparath, T. Grösser, H. R. Karfunkel, *J. Am. Chem. Soc.* **1994**, *116*, 9385–9386.
4. A. Hirsch, I. Lamparath, G. Schick, *Liebigs Ann.* **1996**, 1725–1734.
5. (a) F. Diederich, C. Thilgen, *Science* **1996**, *271*, 317–323; (b) S. Samal, S. K. Sahoo, *Bull. Mater. Sci.* **1997**, *20*, 141–230; (c) A. Hirsch, *Top. Curr. Chem.* **1999**, *199*, 1–65.
6. R. Breslow, *Acc. Chem. Res.* **1980**, *13*, 170–177.
7. (a) L. Isaacs, R. F. Haldimann, F. Diederich, *Angew. Chem.* **1994**, *106*, 2434–2437; *Angew. Chem. Int. Ed.* **1994**, *33*, 2339–2342; (b) F. Diederich, R. Kessinger 'Regio- and stereoselective multiple functionalization of fullerenes' Chapter 7 in *Templated Organic Synthesis*, F. Diederich and P. Stang, eds, Wiley-VCH, New York, pp. 189–218, 2000.
8. (a) C. Boudon, J.-P. Gisselbrecht, M. Gross, L. Isaacs, H. L. Anderson, R. Faust, F. Diederich, *Helv. Chim. Acta* **1995**, *78*, 1334–1344; (b) J.-F. Nierengarten, T. Habicher, R. Kessinger, F. Cardullo, F. Diederich, V. Gramlich, J.-P. Gisselbrecht, C. Boudon, M. Gross, *Helv. Chim. Acta* **1997**, *80*, 2238–2276.
9. (a) M. W. J. Beulen, L. Echegoyen, J. A. Rivera, M. A. Herranz, A. Martín-Domenech, N. Martín, *Chem. Commun.* **2000**, 917–918; (b) M. W. J. Beulen, J. A. Rivera, M. A. Herranz, A. Martín-Domenech, N. Martín, L. Echegoyen, *Chem. Commun.* **2001**, 407–408.
10. M. W. J. Beulen, J. A. Rivera, M. A. Herranz, B. Illescas, N. Martín, L. Echegoyen, *J. Org. Chem.* **2001**, *66*, 4393–4398.
11. M. W. J. Beulen, J. A. Rivera, M. A. Herranz, M. C. Díaz, B. M. Illescas, N. Martín, L. Echegoyen, *J. Mater. Chem.* **2002**, *12*, 2048–2053.
12. B. Kräutler, T. Müllen, J. Maynollo, K. Gruber, C. Kratky, P. Ochsenbein, D. Schwarzenbach, H.-B. Bürgi, *Angew. Chem.* **1996**, *108*, 1294–1296; *Angew. Chem. Int. Ed.* **1996**, *35*, 1204–1206.
13. R. Schwenninger, T. Müllen, B. Kräutler, *J. Am. Chem. Soc.* **1997**, *119*, 9317–9318.
14. F. Cardullo, L. Isaacs, F. Diederich, J.-P. Gisselbrecht, C. Boudon, M. Gross, *Chem. Commun.* **1996**, 797–799.
15. (a) I. Lamparath, C. Maichle-Mössmer, A. Hirsch, *Angew. Chem.* **1995**, *107*, 1755–1757; *Angew. Chem. Int. Ed.* **1995**, *34*, 1607–1609; (b) I. Lamparath, A. Herzog, A. Hirsch, *Tetrahedron* **1996**, *52*, 5065–5075.
16. X. Camps, H. Schönberger, A. Hirsch, *Chem. Eur. J.* **1997**, *3*, 561–567.
17. C. J. Hawker, K. L. Wooley, J. M. J. Fréchet, *J. Chem. Soc., Chem. Commun.* **1994**, 925–926.
18. M. Brettreich, A. Hirsch, *Tetrahedron Lett.* **1998**, *39*, 2731–2734.
19. L. Isaacs, F. Diederich, R. F. Haldimann, *Helv. Chim. Acta* **1997**, *80*, 317–342.
20. L. Isaacs, P. Seiler, F. Diederich, *Angew. Chem.* **1995**, *107*, 1636–1639; *Angew. Chem. Int. Ed.* **1995**, *34*, 1466–1469.
21. R. F. Haldimann, F.-G. Klärner, F. Diederich, *Chem. Commun.* **1997**, 237–238.

22. M. Rüttimann, R. F. Haldimann, L. Isaacs, F. Diederich, A. Khong, H. Jiménez-Vásquez, R. J. Cross, M. Saunders, *Chem. Eur. J.* **1997**, *3*, 1071–1076.
23. Y. Rubin, S. Khan, D. I. Freedberg, C. Yeretzyan, *J. Am. Chem. Soc.* **1993**, *115*, 344–345.
24. P. Belik, A. Gügel, J. Spickermann, K. Müllen, *Angew. Chem.* **1993**, *105*, 95–97; *Angew. Chem. Int. Ed.* **1993**, *32*, 78–80.
25. (a) Y. Rubin, *Chem. Eur. J.* **1997**, *3*, 1009–1016; (b) W. Qian, Y. Rubin, *Angew. Chem.* **1999**, *111*, 2504–2508; *Angew. Chem. Int. Ed.* **1999**, *38*, 2356–2360.
26. J.-F. Nierengarten, V. Gramlich, F. Cardullo, F. Diederich, *Angew. Chem.* **1996**, *108*, 2242–2244; *Angew. Chem. Int. Ed.* **1996**, *35*, 2101–2193.
27. J.-F. Nierengarten, A. Herrmann, R. R. Tykwinski, M. Rüttimann, F. Diederich, C. Boudon, J.-P. Gisselbrecht, M. Gross, *Helv. Chim. Acta* **1997**, *80*, 293–316.
28. R. W. Alder, S. P. East, *Chem. Rev.* **1996**, *96*, 2097–2111.
29. P. R. Ashton, F. Diederich, M. Gómez-López, J.-F. Nierengarten, J. A. Preece, F. M. Raymo, J. F. Stoddart, *Angew. Chem.* **1997**, *109*, 1611–1614; *Angew. Chem. Int. Ed.* **1997**, *36*, 1448–1451.
30. J.-P. Bourgeois, L. Echegoyen, M. Fibbioli, E. Pretsch, F. Diederich, *Angew. Chem.* **1998**, *110*, 2203–2207; *Angew. Chem. Int. Ed.* **1998**, *37*, 2118–2121.
31. E. Dietel, A. Hirsch, E. Eichorn, A. Rieker, S. Hackbarth, B. Röder, *Chem. Commun.* **1998**, 1981–1982.
32. J.-P. Bourgeois, F. Diederich, L. Echegoyen, J.-F. Nierengarten, *Helv. Chim. Acta* **1998**, *81*, 1835–1844.
33. J.-P. Bourgeois, C. R. Woods, F. Cardullo, T. Habicher, J.-F. Nierengarten, R. Gehrig, F. Diederich, *Helv. Chim. Acta* **2001**, *84*, 1207–1226.
34. J.-F. Nierengarten, C. Schall, J.-F. Nicoud, *Angew. Chem.* **1998**, *110*, 2037–2040; *Angew. Chem. Int. Ed.* **1998**, *37*, 1934–1936.
35. N. Armaroli, G. Marconi, L. Echegoyen, J.-P. Bourgeois, F. Diederich, *Chem. Eur. J.* **2000**, *6*, 1629–1645.
36. F. Diederich, R. Kessinger, *Acc. Chem. Res.* **1999**, *32*, 537–545.
37. (a) C. Thilgen, A. Herrmann, F. Diederich, *Helv. Chim. Acta* **1997**, *80*, 183–199; (b) W. H. Powell, F. Cozzi, G. P. Moss, C. Thilgen, R. J. R. Hwu, A. Yerin, *Pure Appl. Chem.* **2002**, *74*, 629–695; (c) H. Goto, N. Harada, J. Crassous, F. Diederich, *J. Chem. Soc., Perkin Trans 2* **1998**, 1719–1723; (d) R. Kessinger, C. Thilgen, T. Mordasini, F. Diederich, *Helv. Chim. Acta* **2000**, *83*, 3069–3096.
38. M. Maggini, G. Scorrano, M. Prato, *J. Am. Chem. Soc.* **1993**, *115*, 9798–9799.
39. T. Da Ros, M. Prato, V. Lucchini, *J. Org. Chem.* **2000**, *65*, 4289–4297.
40. M. Taki, S. Sugita, Y. Nakamura, E. Kasashima, E. Yashima, Y. Okamoto, J. Nishimura, *J. Am. Chem. Soc.* **1997**, *119*, 926–932.
41. (a) E. Nakamura, H. Isobe, H. Tokuyama, M. Sawamura, *Chem. Commun.* **1996**, 1747–1748; (b) H. Isobe, H. Tokuyama, M. Sawamura, E. Nakamura, *J. Org. Chem.* **1997**, *62*, 5034–5041.
42. (a) L.-L. Shiu, K.-M. Chien, T.-Y. Liu, T.-I. Lin, G.-R. Her, T.-Y. Luh, *J. Chem. Soc., Chem. Commun.* **1995**, 1159–1110; (b) C. K.-F. Shen, K.-M. Chien, C.-G. Juo, G.-R. Her, T.-Y. Luh, *J. Org. Chem.* **1996**, *61*, 9242–9244; (c) C. K.-F. Shen, H.-H. Yu, C.-G. Juo, K.-M. Chien, C.-R. Her, T.-Y. Luh, *Chem. Eur. J.* **1997**, *3*, 744–748.
43. T. Ishii, K. Nakashima, S. Shinkai, *Chem. Commun.* **1998**, 1047–1048.

44. (a) T. Ishii, K. Nakashima, S. Shinkai, K. Araki, *Tetrahedron* **1998**, *54*, 8679–8686; (b) Ishii, T., Nakashima, K., Shinkai, S., Ikeda, A. *J. Org. Chem.* **1999**, *64*, 984–990.
45. (a) F. Djojo, A. Hirsch, *Chem. Eur. J.* **1998**, *4*, 344–356; (b) T. Hamano, K. Okuda, T. Mashino, M. Hirobe, K. Arakane, A. Ryu, S. Mashiko, T. Nagano, *Chem. Commun.* **1997**, 21–22.
46. F. Cardullo, P. Seiler, L. Isaacs, J.-F. Nierengarten, R. F. Haldimann, F. Diederich, T. Mordasini-Denti, W. Thiel, C. Boudon, J.-P. Gisselbrecht, M. Gross, *Helv. Chim. Acta* **1997**, *80*, 343–371.
47. G. Rapenne, J. Crassous, A. Collet, L. Echegoyen, F. Diederich, *Chem. Commun.* **1999**, 1121–1122.
48. G. Rapenne, J. Crassous, L. E. Echegoyen, L. Echegoyen, E. Flapan, F. Diederich, *Helv. Chim. Acta* **2000**, *83*, 1209–1223.
49. (a) A. Herrmann, M. W. Rüttimann, T. Gibtner, C. Thilgen, F. Diederich, T. Mordasini, W. Thiel, *Helv. Chim. Acta* **1999**, *82*, 261–289 and references cited therein; (b) C. Thilgen, I. Gosse, F. Diederich, *Top. Stereochem.* **2003**, *23*, 1–24.
50. U. Reuther, T. Brandmüller, W. Donaubaue, F. Hampel, A. Hirsch, *Chem. Eur. J.* **2002**, *8*, 2261–2273.
51. J.-M. Lehn, *Supramolecular Chemistry*, VCH, Weinheim, **1995**.
52. (a) S. R. Wilson, Y. Wu, *J. Am. Chem. Soc.* **1993**, *115*, 10334–10337; (b) S. R. Wilson, Y. Wu, *J. Chem. Soc., Chem. Commun.* **1993**, 784–786.
53. F. Diederich, U. Jonas, V. Gramlich, A. Herrmann, H. Ringsdorf, C. Thilgen, *Helv. Chim. Acta* **1993**, *76*, 2445–2453.
54. C. R. Woods, J.-P. Bourgeois, P. Seiler and F. Diederich, *Angew. Chem.* **2000**, *112*, 3971–3974; C. R. Woods, J.-P. Bourgeois, P. Seiler, F. Diederich, *Angew. Chem. Int. Ed.* **2000**, *39*, 3813–3816.
55. J.-P. Bourgeois, P. Seiler, M. Fibbioli, E. Pretsch, F. Diederich, L. Echegoyen, *Helv. Chim. Acta* **1999**, *82*, 1572–1595.
56. S. R. Miller, D. A. Gustowski, Z. Chen, G. W. Gokel, L. Echegoyen, A. E. Kaifer, *Anal. Chem.* **1988**, *60*, 2021–2024.
57. C. Bingel, H. Schiffer, *Liebigs Ann. Chem.* **1995**, 1551–1553.
58. A. Herrmann, M. Rüttimann, C. Thilgen, F. Diederich, *Helv. Chim. Acta* **1995**, *78*, 1673–1704.
59. X. Zhang, C. C. Foote, *J. Am. Chem. Soc.* **1995**, *117*, 4271–4275.
60. (a) A. L. Balch, J. W. Lee, M. M. Olmstead, *Angew. Chem.* **1992**, *104*, 1400–1402; *Angew. Chem. Int. Ed.* **1992**, *31*, 1356–1358; (b) A. L. Balch, L. Hao and M. M. Olmstead, *Angew. Chem.* **1996**, *108*, 211–213; A. L. Balch, L. Hao, M. M. Olmstead, *Angew. Chem. Int. Ed.* **1996**, *35*, 188–190.
61. H. P. Spielmann, G.-W. Wang, M. S. Meier, B. R. Weedon, *J. Org. Chem.* **1998**, *63*, 9865–9871.
62. C. Thilgen, F. Diederich, *Top. Curr. Chem.* **1998**, *199*, 135–171.
63. M. J. van Eis, R. J. Alvarado, L. Echegoyen, P. Seiler, F. Diederich, *Chem. Commun.* **2000**, 1859–1860.
64. M. J. van Eis, P. Seiler, L. A. Muslinkina, M. Badertscher, E. Pretsch, F. Diederich, R. J. Alvarado, L. Echegoyen, I. Pérez-Núñez, *Helv. Chim. Acta* **2002**, *85*, 2009–2055.
65. M. J. van Eis, I. Pérez-Núñez, L. A. Muslinkina, R. J. Alvarado, E. Pretsch, L. Echegoyen, F. Diederich, *J. Chem. Soc., Perkin Trans. 2* **2001**, 1890–1892.

66. R. Kessinger, J. Crassous, A. Herrmann, M. Rüttimann, L. Echegoyen, F. Diederich, *Angew. Chem.* **1998**, *110*, 2022–2025; *Angew. Chem. Int. Ed.* **1998**, *37*, 1919–1922.
67. R. Kessinger, M. Gómez-López, C. Boudon, J.-P. Gisselbrecht, M. Gross, L. Echegoyen, F. Diederich, *J. Am. Chem. Soc.* **1998**, *120*, 8545–8546.
68. (a) N. S. Fender, B. Nuber, D. I. Schuster, S. R. Wilson, L. Echegoyen, *J. Chem. Soc., Perkin Trans. 2* **2000**, 1924–1928; (b) R. Kessinger, N. S. Fender, L. E. Echegoyen, C. Thilgen, L. Echegoyen, F. Diederich, *Chem. Eur. J.* **2000**, *6*, 2184–2192.
69. L. E. Echegoyen, F. D. Djojo, A. Hirsch, L. Echegoyen, *J. Org. Chem.* **2000**, *65*, 4994–5000.
70. C. Boudon, J.-P. Gisselbrecht, M. Gross, A. Herrmann, M. Rüttimann, J. Crassous, F. Cardullo, L. Echegoyen, F. Diederich, *J. Am. Chem. Soc.* **1998**, *120*, 7860–7868.
71. J. Crassous, J. Rivera, N. S. Fender, L. Shu, L. Echegoyen, C. Thilgen, A. Herrmann and F. Diederich, *Angew. Chem.* **1999**, *38*, 1716–1721; *Angew. Chem. Int. Ed.* **1999**, *38*, 1613–1617.
72. M. W. J. Beulen, L. Echegoyen, *Chem. Commun.* **2000**, 1065–1066.
73. M. Carano, L. Echegoyen, *Chem. Eur. J.* **2003**, *9*, 1974–1981.
74. M. Oçafraïn, M. A. Herranz, L. Marx, C. Thilgen, F. Diederich, L. Echegoyen, *Chem. Eur. J.* **2003**, *9*, 4811–4819.
75. N. N. P. Moonen, C. Thilgen, L. Echegoyen, F. Diederich, *Chem. Commun.* **2000**, 335–336.
76. M. A. Herranz, J. A. Rivera, R. J. Alvarado, N. Martín, C. Thilgen, F. Diederich, L. Echegoyen, *J. Supramol. Chem.* **2003** (volume date 2001), *1*, 299–303.
77. J. M. Hawkins, A. Meyer, *Science* **1993**, *260*, 1918–1920.
78. A. Herrmann, F. Diederich, *Helv. Chim. Acta* **1996**, *79*, 1741–1756.
79. J. M. Hawkins, M. Nambu, A. Meyer, *J. Am. Chem. Soc.* **1994**, *116*, 7642–7645.
80. A. Herrmann, F. Diederich, *J. Chem. Soc., Perkin Trans. 2* **1997**, 1679–1684.
81. F. Diederich, R. L. Whetten, C. Thilgen, R. Ettl, I. Chao, M. M. Alvarez, *Science* **1991**, *254*, 1768–1770.
82. M. Inakuma, H. Shinohara, *J. Phys. Chem. B* **2000**, *104*, 7595–7599.
83. G.-W. Wang, M. Saunders, A. Khong, R. J. Cross, *J. Am. Chem. Soc.* **2000**, *122*, 3216–3217.

Chapter 7

Selective Reactions in Inclusion Crystals

ZOFIA URBANCZYK-LIPKOWSKA

*Institute of Organic Chemistry, Polish Academy of Sciences,
01-224 Warsaw, Poland*

FUMIO TODA

*Department of Chemistry, Okayama University of Science, Ridaicho 1-1,
Okayama 700-0005, Japan*

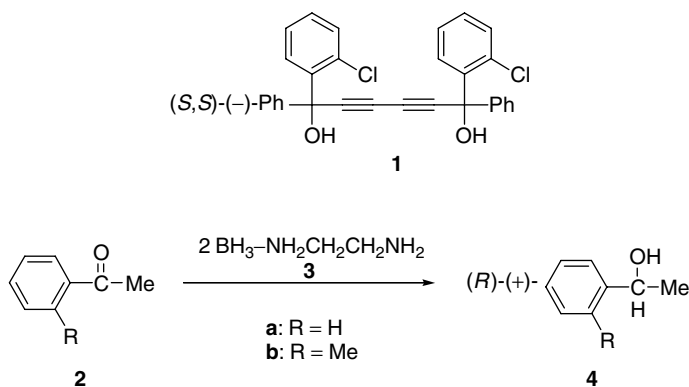
1 INTRODUCTION

When chemical reactions are carried out in inclusion complexes, reactions can proceed selectively due to template control effects caused by the host compound. In some cases, reaction occurs only in the inclusion complex, but not in solution, since molecules can be arranged in the appropriate positions for reaction in an inclusion crystal. When an optically active host compound is used, enantioselective reactions can be accomplished. For some time we have been studying such selective reactions in inclusion complex crystals in the solid state. However, these reactions have already been published in the book 'Organic Solid State Reactions' [1]. In this present chapter, some representative topics and some recent new results of selective thermochemical and photochemical reactions in inclusion crystals are briefly summarized.

2 ENANTIOSELECTIVE THERMOCHEMICAL REACTIONS IN INCLUSION CRYSTALS

2.1 Reduction of Ketones

When a mixture of powdered ketone and NaBH_4 is kept at room temperature, reduction of the ketone occurs to give the corresponding alcohol [2]. When the reaction is carried out in inclusion crystals containing a chiral host compound, the optically active alcohol can be obtained by enantio-control of the reaction by the chiral host. For example, treatment of inclusion crystals of acetophenone (**2a**) or *o*-methylacetophenone (**2b**) and (*S,S*)-(-)-1,6-bis(*o*-chlorophenyl)-1,6-diphenylhexa-2,4-diyne-1,6-diol (**1**) [3] with powdered BH_3 -ethylenediamine complex (**3**) in the solid state gave **4a** of 44 % ee (96 % yield) or **4b** of 59 % ee (57 % yield), respectively [4].

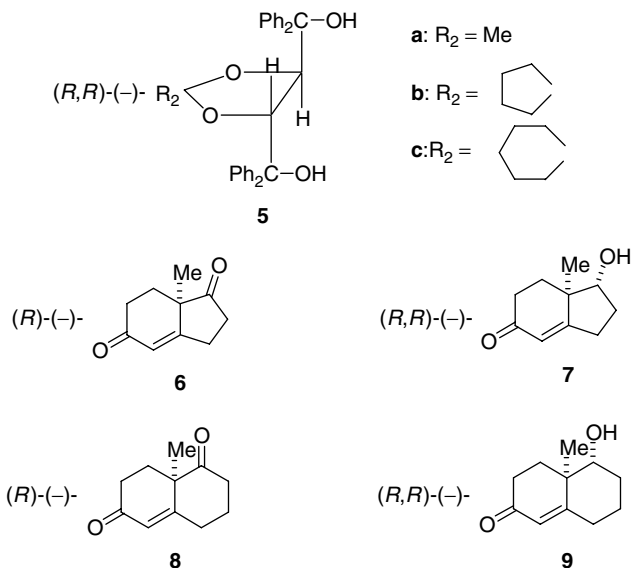


Scheme 1

First, treatment of *rac*-**6** with (*R,R*)-(-)-*trans*-4,5-bis(hydroxydiphenylmethyl)-2,2-dimethyl-1,3-dioxacyclopentane (**5a**) [5] resulted in selective formation of a 1:1 inclusion complex of **5a** with (*R*)-(-)-**6** [5,6]. Second, further treatment of this complex with NaBH_4 in the solid state gave (*R,R*)-(-)-**7** of 100 % ee (54 % yield) [2]. Since the hydride attacks the carbonyl carbon at the 7-position from the side opposite the methyl group, **6** should give **7** of 100 % ee, as was found. The enone carbonyl of **6** is not attacked, since it is masked by forming a hydrogen bond with the hydroxyl group of **5a** [7]. Similar treatment of the 1:1 inclusion complex of **5a** and **8** with NaBH_4 gave (*R,R*)-(-)-**9** of 100 % ee in 53 % yield [2].

2.2 Michael Addition Reactions

Highly enantioselective Michael addition reactions of 2-mercaptopyridine (**11**) to 2-cyclohexenone (**10**) have been accomplished by treatment of the 1:1 inclusion



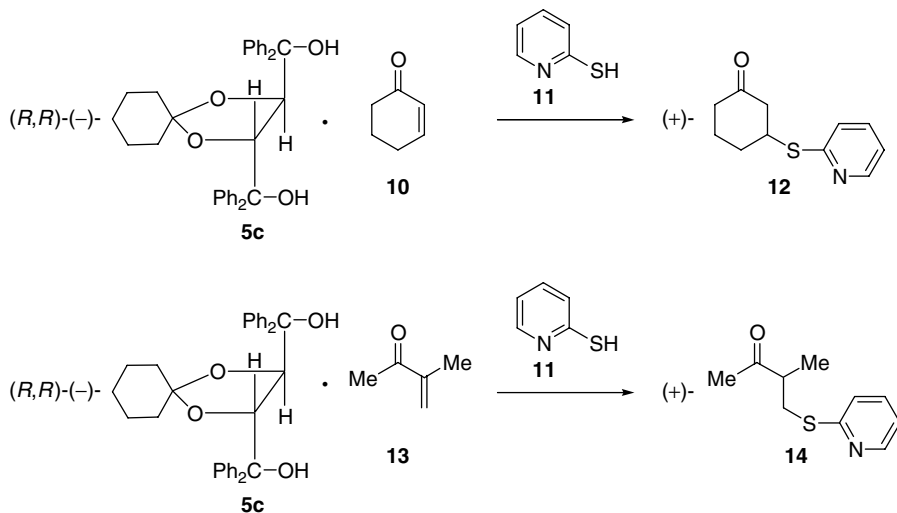
Scheme 2

complex of **10** and **5c** with **11** in the solid state. For example, when a mixture of the powdered 1:1 inclusion complex of **10** with **5c**, **11** and a catalytic amount of benzyltrimethylammonium hydroxide was bombarded with ultrasound at room temperature for 1 h, the addition product **12** of 80 % ee was obtained in 51 % yield [8].

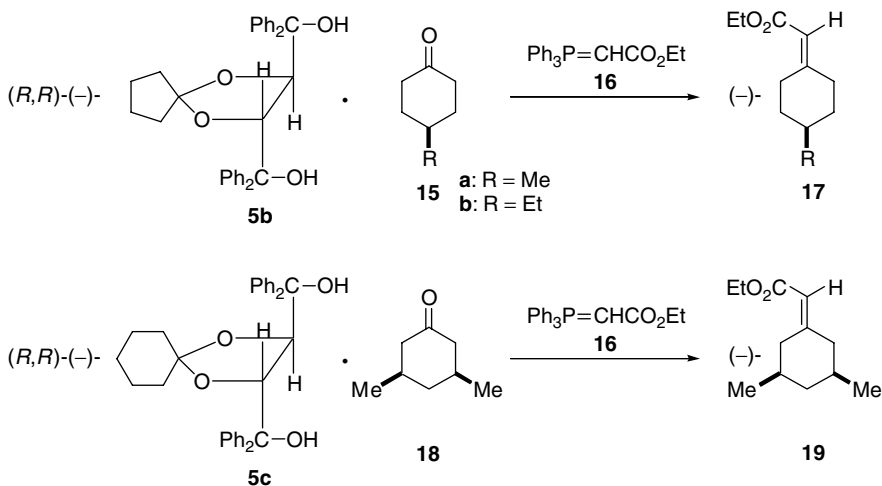
Similar treatment of the 1:1 inclusion complex of 3-methyl-3-buten-2-one (**13**) and **5c** with **11** gave the addition product **14** of 49 % ee in 76 % yield [8].

2.3 Wittig Reactions

Wittig reactions of cyclohexanone derivatives in their inclusion compounds with the chiral host **5** gave optically active reaction products. For example, when a mixture of finely powdered 1:1 inclusion compound of **5b** with 4-methyl-(**15a**) or 4-ethylcyclohexanone (**15b**) and phosphorane (**16**) was kept at 70 °C, the Wittig reaction in the solid state was completed within 4 h. To the reaction mixture was added diethyl ether–petroleum ether (1:1), and then the precipitated triphenylphosphine oxide was removed by filtration. The crude product left after evaporation of solvent from the filtrate was distilled *in vacuo* to give (-)-4-methyl- (**17a**) of 42 % ee (73 % yield) or (-)-4-ethyl-1-(carboethoxymethylene)cyclohexane (**17b**) of 45 % ee (57 % yield), respectively [9]. Similar reaction of the 1:1 inclusion compound of **5c** and *cis*-3,5-dimethylcyclohexanone (**18**) with **16** gave **19** of 57 % ee in 58 % yield [9].



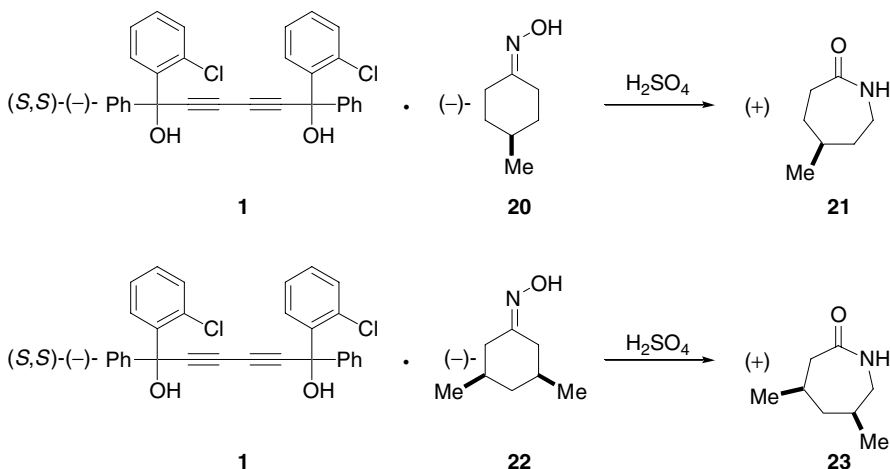
Scheme 3



Scheme 4

2.4 Beckmann Rearrangement

When a solution of *rac*-4-methyl-1-(hydroxyimino)cyclohexane (**20**) and **1** in diethyl ether–petroleum ether was kept at room temperature, a 1:1 inclusion compound of *(-)*-**20** of 79% ee and **1** was obtained as colorless needles by an enantioselective inclusion complexation. Heating of the inclusion compound

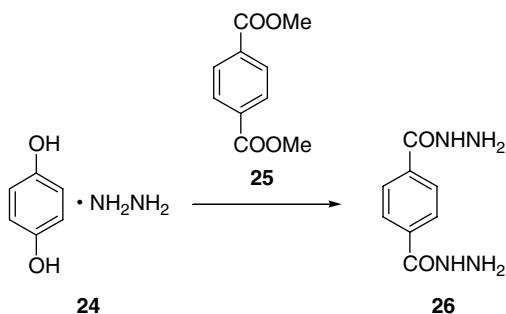


Scheme 5

with concentrated H_2SO_4 gave the Beckmann rearrangement product, (-)-5-methyl- ϵ -caprolactam (**21**) of 80 % ee [10]. Similar treatment of the 1:1 inclusion compound of **1** and (+)-**22** of 59 % ee, prepared by an enantioselective inclusion complexation process between **1** and *rac*-**22**, gave (+)-**23** of 59 % ee [10].

2.5 Aminolysis

The inclusion complex of an unstable reactant or reagent is sometimes useful in organic synthesis in the solid state. For example, very reactive anhydrous hydrazine can be trapped as a 1:1 inclusion complex with hydroquinone (**24**). This 1:1 inclusion compound (**24**) is a stable white powder that can easily be prepared by mixing aqueous hydrazine with powdered hydroquinone. Compound **24** is



Scheme 6

useful as an aminolysis reagent. For example, a mixture of powdered dimethyl terephthalate (**25**) and **24** was kept at 100–125 °C for 25 h under N₂. To the reaction mixture was added MeOH, and the almost pure dihydrazide **26** was obtained simply by filtration in 88 % yield [11].

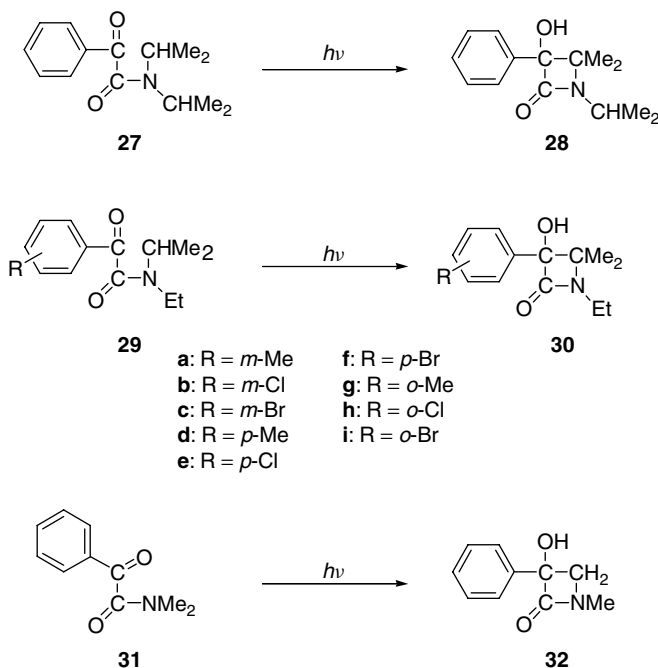
3 ENANTIOSELECTIVE PHOTOCHEMICAL REACTIONS

Since photochemical reactions in inclusion compounds have been described in one chapter of the previous book [1], enantioselective β -lactam formation reactions are summarized in this present chapter as a typical application of the inclusion technique for enantioselective photosynthesis. In addition, as a representative enantioselective single-crystal-to-single-crystal photoreaction, the photodimerization reactions of coumarin and thiocoumarin in their inclusion compound with a chiral host are also described. Furthermore, a host-catalyzed photodimerization reaction of chalcone and 2-pyridone in the solid state is also added to this chapter as a unique example of the application of inclusion techniques to selective photoreaction.

3.1 β -Lactam Formation Reactions

3.1.1 *By photocyclization reactions of α -oxoamides*

The oxoamide (**27**), which has two isopropyl groups on its nitrogen atom, forms chiral crystals in which the achiral **27** molecules are arranged in a chiral form [12]. Photoirradiation of the chiral crystals in the solid state gave the almost optically pure β -lactam derivative (**28**) in quantitative yield [12]. This is an enantioselective reaction which can be accomplished without using any chiral source, and is termed an absolute asymmetric synthesis. In the case of the oxoamides **29** which have one isopropyl and one ethyl group, some form chiral crystals and some do not. For example, **29** with *m*-substituents such as **29a**, **29b** and **29c** form chiral crystals which upon irradiation for 5–10 h gave **30a** of 91 % ee (63 % yield), **30b** of 100 % ee (75 % yield), or **30c** of 96 % ee (97 % yield), respectively [13]. However, **29** with *p*-substituents such as **29d**, **29e** and **29f** form racemic crystals which upon irradiation gave *rac*-**30d** (60 % yield), *rac*-**30e** (50 % yield), or *rac*-**30f** (65 % yield), respectively. In contrast, the oxoamides with *o*-substituents such as **29g** formed chiral crystals, which upon irradiation for 10 h gave optically active **30g** of 92 % ee in 54 % yield, but **29h** and **29i** formed racemic crystals and their irradiation for 24 h gave *rac*-**30h** (42 % yield) or *rac*-**30i** (48 % yield), respectively. For the formation of chiral crystals, the presence of an isopropyl group is clearly important. The mechanism of chiral crystal formation was studied by X-ray structural analysis of the chiral crystal derived from **27** [14]. Therefore,



Scheme 7

it is reasonable that the oxoamide **31** which has two methyl groups will not form chiral crystals, and hence its irradiation gives *rac*-**32**.

Even for oxoamides that do not form their own chiral crystals, enantioselective photocyclization to the corresponding optically active β -lactam can be accomplished by applying inclusion techniques involving a chiral host. For example, irradiation of the 1:1 inclusion complex of **1** with **31** gave (–)-**32** of 100% ee in quantitative yield [15]. X-ray crystal structure analysis showed that the achiral molecules of **31** are arranged in a chiral form through construction of a chiral hydrogen-bonded cycle as depicted in Figure 1 [15]. Since the host **1** is recovered unchanged and can be used again, this method is economical. By application of this method to other oxoamides that do not form their own chiral crystals, various enantioselective β -lactam synthetic routes have been developed [16].

3.1.2 By photocyclization of 2-pyridones

Optically pure β -lactam derivatives can also be prepared by an enantioselective photocyclization reaction of 2-pyridone in its inclusion complex with a chiral host. For example, irradiation of the 1:1 inclusion complex of **1** and 4-methoxy-*N*-methyl-2-pyridone (**33**) in the solid state gave (–)-**34** of 100% ee

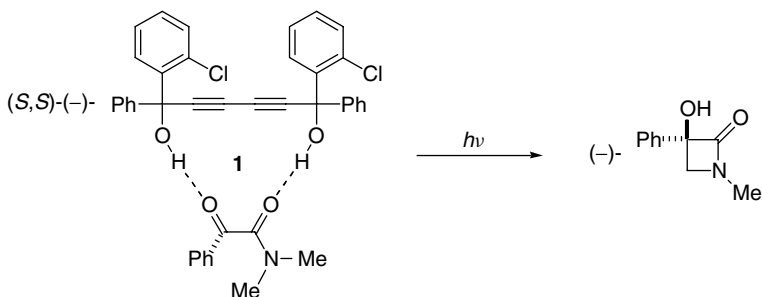
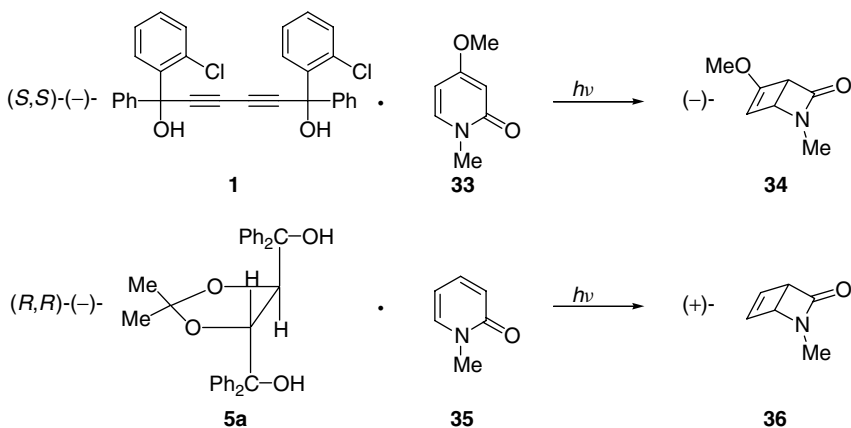


Figure 1 Enantioselective photocyclization reactions of **31** in a 1:1 inclusion compound with **1**.



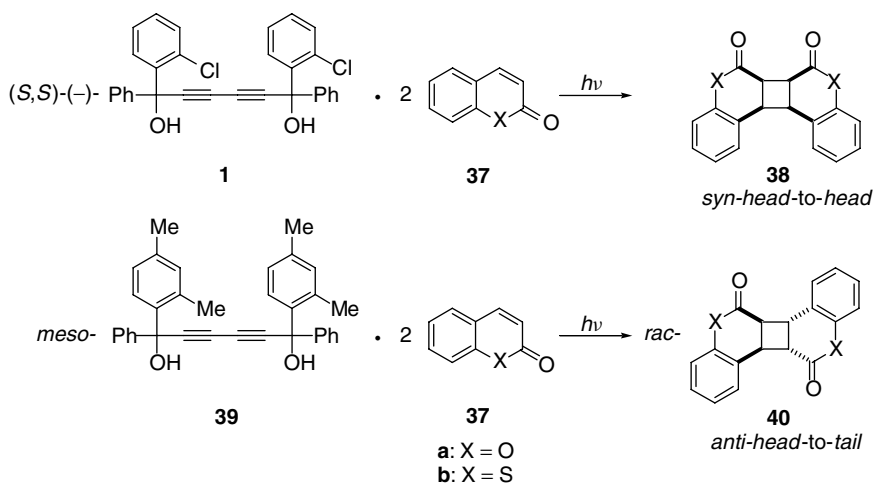
Scheme 8

in 97% yield [17]. Similar irradiation of the 1:1 inclusion complex of **5a** and *N*-methyl-2-pyridone (**35**) gave (+)-**36** of 100% ee in 93% yield [17]. This enantioselective synthetic method can be modified by using various other chiral host compounds [18].

3.2 Single-Crystal to Single-Crystal Photodimerization of Coumarin and Thiocoumarin

The steric course of the photodimerization reactions of coumarin (**37a**) and thiocoumarin (**37b**) succeeded in being controlled almost perfectly by carrying out the reaction in inclusion complexes using various host compounds. Furthermore, enantioselective dimerization reactions of **37a** and **37b** were found to proceed through a single-crystal to single-crystal process.

Irradiation of the 1:2 inclusion complexes of **1** with **37a** or **37b** for 4–5 h gave *syn*-head-to-head dimers **38a** (75 % yield) or **38b** (74 % yield), respectively [19,20]. When the 1:2 inclusion complexes of *meso*-1,6-bis(2,4-dimethylphenyl)-1,6-diphenylhexa-2,4-diyne-1,6-diol (**39**) with **37a** or **37b** were irradiated in the solid state, the corresponding *rac*-*anti*-head-to-tail dimers **40a** (94 % yield) or **40b** (69 % yield), respectively, were obtained [19,20]. In contrast, irradiation for 1 h of the 1:1 inclusion complex of **5a** and **37a** gave the (–)-*anti*-head-to-head dimer (**41a**) of 96 % ee in 96 % yield [19,20]. Similarly, a 2 h irradiation of the 1:1 inclusion complex of **5b** and **37b** gave the (+)-*anti*-head-to-head dimer (**41b**) of 100 % ee in 73 % yield [20]. These two enantioselective reactions from **37** to **41** were found to proceed by means of a single-crystal to single-crystal



Scheme 9

conversion. The mechanism of the enantioselective single-crystal to single-crystal photodimerization reactions has been clarified by X-ray crystal structural studies [20]. These interesting results are summarized, together with similar findings, in review articles [21,22].

3.3 Host-catalyzed Photodimerization Reactions

Irradiation of the powdered 1:2 inclusion complex of 1,1,6,6-tetraphenylhexa-2,4-diyne-1,6-diol (**42**) [23] and chalcone (**43**) for 1 h gave the *syn*-head-to-tail dimer (**44**) in 82% yield [24]. X-ray analysis of the 1:2 inclusion complex of **42** and **43** showed that two **43** molecules are arranged through hydrogen-bond formation with the hydroxyl groups of **42**, as depicted in Figure 2 [25]. This manner of molecular arrangement is ideal for yielding the dimer **44** by photoreaction.

In 1987, we discovered an interesting molecular reorganization process in the solid state [26]. By mixing powdered host and powdered guest compounds using a pestle and mortar, their inclusion crystals were formed very easily. By a combination of this molecular reorganization and photoreaction in the solid state, very interesting host-catalyzed photodimerization reactions could be designed.

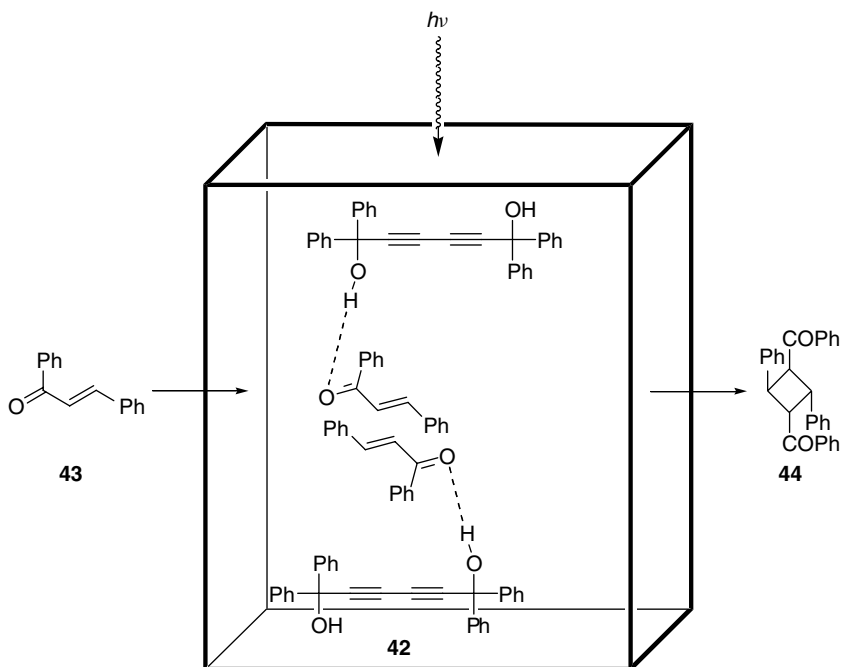
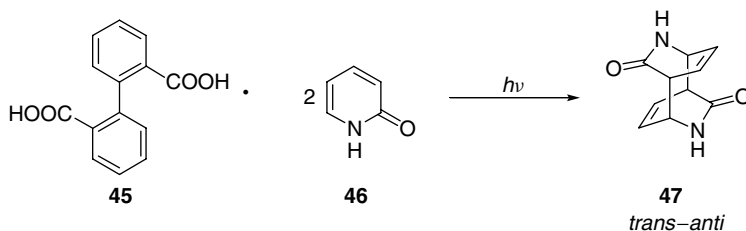


Figure 2 Host-catalyzed photodimerization reaction of **43** in the solid state.

For example, irradiation of a 1:4 mixture of powdered **42** and **43** for 72 h, with occasional grinding using a pestle and mortar, gave **44** in 87 % yield. This result shows that the host **42** was used twice as a catalyst. This is illustrated in Figure 2. By mixing **42** and **43**, their 1:2 complex is formed by molecular movement, and then irradiation gives **44** with release of **42**. On further mixing, recovered **42** and excess **43** form a new complex that upon irradiation again gives **44**.

Photodimerization of 2-pyridone (**46**) in the presence of the 2, 2'-biphenyldicarboxylic acid host (**45**) also proceeded via a catalytic process. First, irradiation of the 1:2 inclusion complex of **46** and **45** in the solid state gave the *trans-anti* dimer (**47**) in 92 % yield [27]. The mechanism of this stereoselective photoreaction was investigated through X-ray analysis of this complex. In the complex, two **46** molecules are arranged in ideal positions for yielding **47** by dimerization [27]. Secondly, a catalytic dimerization reaction of **46** was carried out. Photoirradiation for 20 h of a 1:4 mixture of powdered **45** and **46** under occasional mixing in the solid state gave **47** in 81 % yield. These data clearly show that molecules of **45** worked twice as a catalyst. Namely, the mixing of **45** and **46** produces their inclusion complex and its irradiation gives **47** and **45**. By further mixing, excess **46** is included with **45** to give their complex, which, upon continued irradiation, forms **47** [27,28].



Scheme 10

REFERENCES

1. K. Tanaka and F. Toda in 'Organic Solid State Reactions' ed. by F. Toda, Kluwer, Dordrecht, The Netherlands, **2002**, pp. 1–46 (thermal reactions) and pp. 109–158 (photoreactions).
2. F. Toda, K. Kiyoshige and M. Yagi, *Angew. Chem. Int. Ed. Engl.*, **1989**, 28, 320.
3. F. Toda, K. Tanaka, T. Omata, K. Nakamura and T. Oshima, *J. Am. Chem. Soc.*, **1983**, 105, 5151.
4. F. Toda and K. Mori, *J. Chem. Soc., Chem. Commun.*, **1989**, 1245.
5. F. Toda and K. Tanaka, *Tetrahedron Lett.*, **1988**, 29, 551.
6. D. Seebach, A. K. Beck, R. Imwinkelried, S. Roggo and A. Wonnacott, *Helv. Chim. Acta*, **1987**, 70, 954.
7. D. R. Bond, S. A. Bourne, L. R. Nassimbeni and F. Toda, *J. Cryst. Spect. Res.*, **1989**, 19, 809.

8. F. Toda, K. Tanaka and J. Sato, *Tetrahedron Asymm.*, **1993**, 4, 1771.
9. F. Toda and H. Akai, *J. Org. Chem.*, **1990**, 55, 3446.
10. F. Toda and H. Akai, *J. Org. Chem.*, **1990**, 55, 4973.
11. F. Toda, S. Hyoda, K. Okada and K. Hirotsu, *J. Chem. Soc., Chem. Commun.*, **1995**, 1531.
12. F. Toda, M. Yagi and S. Soda, *J. Chem. Soc., Chem. Commun.*, **1987**, 1413.
13. F. Toda and H. Miyamoto, *J. Chem. Soc., Perkin Trans. 1*, **1993**, 1129.
14. A. Sekine, K. Hori, Y. Ohashi, M. Yagi and F. Toda, *J. Am. Chem. Soc.*, **1989**, 111, 697.
15. M. Kaftory, K. Tanaka and F. Toda, *J. Org. Chem.*, **1988**, 53, 4393.
16. F. Toda, K. Tanaka and M. Yagi, *Tetrahedron*, **1987**, 43, 1493.
17. F. Toda and K. Tanaka, *Tetrahedron Lett.*, **1988**, 4299.
18. K. Tanaka, R. Nagahiro and Z. Urbanczyk-Lipkowska, *Chem. Lett.*, **2001**, 3, 1567.
19. K. Tanaka and F. Toda, *J. Chem. Soc., Perkin Trans. 1*, **1992**, 943.
20. K. Tanaka, F. Toda, E. Mochizuki, M. Yasui, Y. Kai, I. Miyahara and K. Hirotsu, *Angew. Chem. Int. Ed. Engl.*, **1999**, 38, 3523.
21. F. Toda, *Aust. J. Chem.*, **2001**, 54, 573.
22. F. Toda, *CrystEngComm*, **2002**, 4, 215.
23. F. Toda and K. Akagi, *Tetrahedron Lett.*, **1968**, 3695.
24. K. Tanaka and F. Toda, *J. Chem. Soc., Chem. Commun.*, **1983**, 593.
25. M. Kaftory, K. Tanaka and F. Toda, *J. Org. Chem.*, **1985**, 50, 2154.
26. F. Toda, K. Tanaka and A. Sekikawa, *J. Chem. Soc., Chem. Commun.*, **1987**, 279.
27. M. Yagi, S. Hirano, S. Toyota, F. Toda, P. Giastas and I. Mavridis, *Heterocycles*, **2003**, 59, 735.
28. F. Toda, *Acc. Chem. Res.*, **1995**, 28, 480.

Chapter 8

Supramolecular Control of Reactivity in the Solid State Using Linear Templates

LEONARD R. MACGILLIVRAY

Department of Chemistry, University of Iowa, Iowa City, IA 52242-1294, USA

1 INTRODUCTION

Devices that pick and position individual atoms and molecules for chemical reaction are anticipated to have widespread applications in chemical synthesis and materials science [1,2]. Such devices, or assemblers [1], are expected to combine the diversity of synthetic organic chemistry (e.g. natural product synthesis), which is chiefly realized at the atomic level, with the ability of human engineers to fabricate objects using mechanical devices (e.g. robotic welders), which is chiefly realized at the macroscopic level, for the development of a universal molecular manufacturing scheme (Figure 1) [1]. Owing to superior stereo- and regiocontrol of chemical synthesis promised by an assembler, molecular manufacturing via molecular assemblers may provide access to products and processes not available by standard synthetic methods. Strong, lightweight materials with applications in transportation, or processes that eliminate chemical waste, are possible [3]. Despite this realization, however, a synthetic system that enables such general ‘pick-and-place’ control of matter, either at the atomic- or nanometer-scale level, has not been realized [1–5].

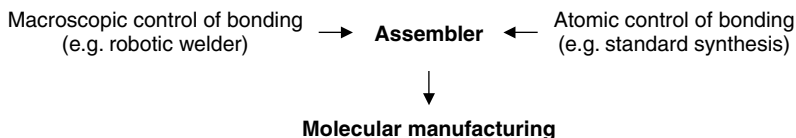


Figure 1 Molecular manufacturing provided by an assembler.

2 OVERVIEW

It is with these ideas in mind that we provide here an account of work performed in our laboratory [6–12] that focuses upon employing rigid bifunctional molecules, in the form of linear reaction templates [13], as assemblers for directing chemical reactivity in the solid state. In particular, upon identifying the ability of linear templates to orient molecules by way of hydrogen bonds in organic solids for reaction, we have demonstrated an ability of linear templates to enable, in a similar way to standard solution-based organic synthesis, molecular synthesis by design [14]. The method, which is inspired by Nature, has enabled the identification of molecules yet to be synthesized that therefore may be considered targets of linear templates in assembler-based chemistry.

3 THE ASSEMBLER AND LINEAR TEMPLATES

For the synthetic chemist [14], the synthetic behavior of an assembler is akin to a molecule that functions as a template (Figure 2) [13]. The ‘pick-and-place’ paradigm evoked by an assembler [1] suggests a molecule that grabs and positions two molecules for a reaction that leads to a covalent bond. Moreover, such structure behavior is reminiscent of a linear template, a ditopic molecule that juxtaposes, by way of molecular recognition and self-assembly [5], two molecules linearly to achieve a particular linking of atoms.

3.1 Linear Templates in Chemistry

Although chemists have designed molecules that function as linear templates, the concept of the assembler goes beyond the synthetic abilities of linear templates

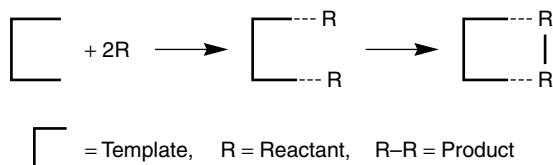


Figure 2 Synthetic behavior of a linear template.

designed to date. Whereas macroscopic devices that function as assemblers (e.g. robotic welders) build objects using mechanical or thermal energy, molecules that function as linear templates employ intermolecular forces (e.g. hydrogen bonds) based on chemical energy to achieve a similar synthesis [13]. Such forces are of comparable strength to entropy and solvent effects in solution, which can disrupt the interaction between the template and its reactants, making the system inefficient.

Kelly observed entropy and solvent effects in the first synthetic system that operates as a linear template (Figure 3a) [15]. Specifically, a bifunctional molecule based on a 1,3-disubstituted benzene was found to organize two molecules in apolar media, by way of a $N-H \cdots N$ and $N-H \cdots O$ forces, for a regiocontrolled S_N2 reaction. The reaction occurred six times faster than the same reaction without the template. The enhanced rate, however, was significantly less than an analogous intramolecular process. This was attributed, in part, to entropic effects

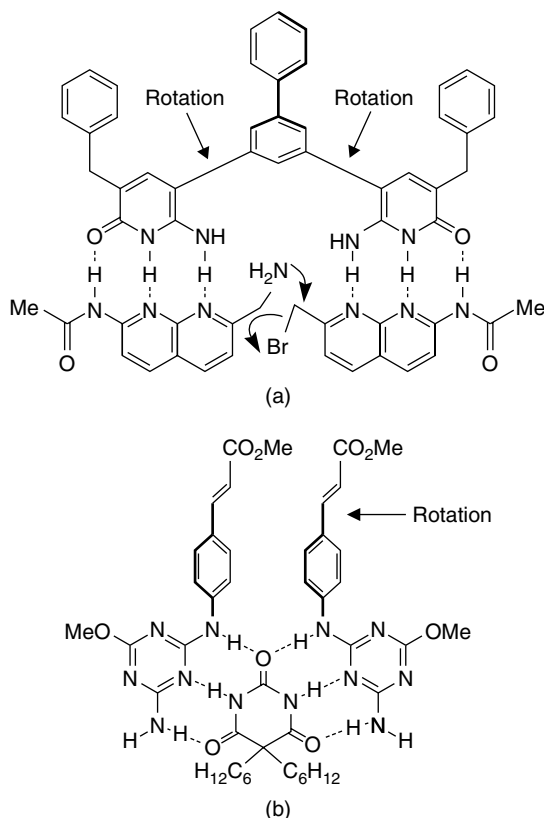


Figure 3 Artificial linear templates that operate in the liquid phase: (a) linear template of Kelly and (b) linear template of Bassani.

involving free rotation about carbon–carbon (C–C) linkages of the template that produced nonproductive conformers.

Since the work of Kelly, there have been very few reports that focus upon applications of synthetic linear templates to chemical synthesis. Most recent studies have focused on systems that self-replicate [13]. A synthetic system based on a barbituric acid has been shown to organize two cinnamates in apolar media, by way of N–H···N and N–H···O forces, for a regiocontrolled [2 + 2] ultraviolet-(UV) induced cycloaddition reaction (Figure 3b) [16]. Similar to the system of Kelly, a mixture of products was attributed to free rotation about C–C bonds of the reactants.

3.2 A Linear Template in Biology

Although synthetic devices that enable general pick-and-place control of atoms and molecules have yet to be realized, Nature employs such a system. In particular, deoxyribonucleic acid (DNA) exhibits the manufacturing capabilities required of an assembler [17].

Specifically, DNA functions as a linear template by juxtaposing two molecules to react by way of hydrogen bonds. The phosphate backbone provides a scaffold that enables two covalently attached nucleotides oriented orthogonal to the backbone to organize two bases (e.g. adenine–thymine) by way of hydrogen bonds for stereo- and regiocontrolled S_N2 P–O bond formation (Figure 4). An enzyme known as a polymerase mediates the reaction. Indeed, the system of hydrogen bonds and base pairing of DNA has evolved such that the structure of DNA, consistent with the idea of an assembler, manufactures a wide range of products (e.g. proteins) with specific properties (e.g. host–guest) and applications (e.g. delivery). The information that codes for the structure and function of the products is stored linearly, as a sequence of bases, within the template, while the applications of the products are typically realized by an ability of the products to assemble with either themselves, or additional chemical species, to form larger, functional structures (e.g. viruses) [2]. The larger structures, in the form of (macro)molecular assemblies, are usually of nanometer-scale dimensions [1].

4 TEMPLATE-DIRECTED SOLID-STATE ORGANIC SYNTHESIS

To enable linear templates to be used as general devices for building molecules, we have identified an ability of rigid bifunctional molecules to serve as linear templates in the organized environment of the solid state [6–12]. The templates operate by assembling two complementary molecules by way of hydrogen bonds for a UV-induced [2 + 2] cycloaddition reaction [18]. By using the solid state as a medium for reaction, we have been able to circumvent the structure effects of

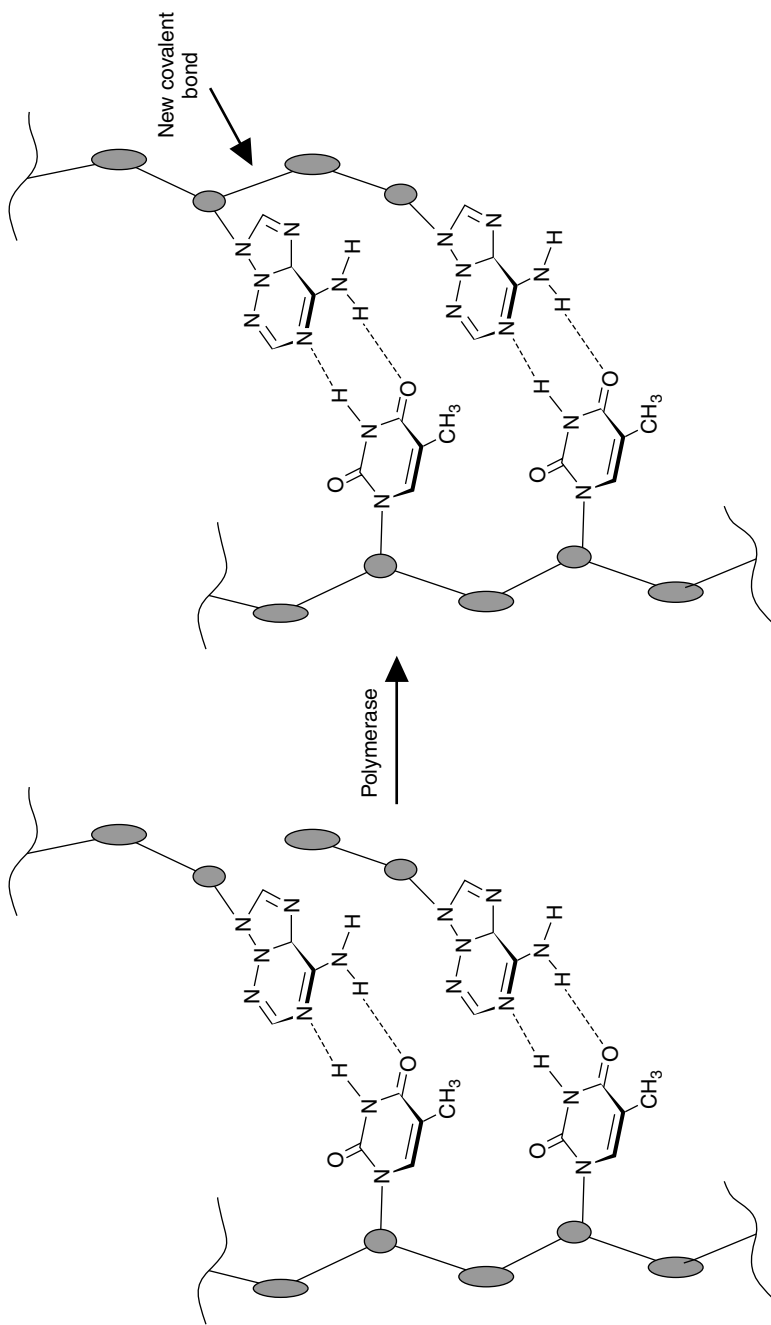


Figure 4 DNA as a linear template.

entropy and solvent that have made linear templates less effective in the liquid phase [15,16], such that linear templates may be used to assemble and construct molecules by design.

4.1 The Solid-state [2 + 2] Cycloaddition Reaction

For a [2 + 2] cycloaddition reaction to occur in the solid state, two C=C bonds should conform to geometry criteria outlined by Schmidt [18]. Specifically, following crystal structure studies involving cinnamic acid, Schmidt has revealed that two C=C bonds should be aligned parallel and separated by $<4.2 \text{ \AA}$ (Figure 5). Such criteria place the four *p*-orbitals of two C=C bonds in close enough proximity and proper orientation to react. Schmidt has also demonstrated that the photodimerization is highly regioselective, such that the stereochemical relationship of the reactants is preserved within the cyclobutane products. The geometry criteria and stereochemical relationship of the reactants to the products make up the 'topochemical postulates'. Thus, UV-irradiation of crystalline α -*trans*-cinnamic acid – a polymorph of cinnamic acid wherein two C=C bonds conform to the geometry criteria of the topochemical postulates and the olefins are arranged head-to-tail (ht) – produces α -truxinic acid, while irradiation of β -*trans*-cinnamic acid – wherein two C=C bonds conform to the geometry criteria of the topochemical postulates and the olefins are arranged head-to-head (hh) – produces β -truxinic acid. Indeed, there now exists a wealth of crystallographic data supporting the topochemical postulates of Schmidt. These data makes the solid-state [2 + 2] photodimerization a good starting point for studies involving linear template chemistry.

4.2 Selection of a Linear Template and Reactants

To develop a system of linear templates to control the [2 + 2] cycloaddition in the solid state, we turned to crystal structure studies involving a bis(resorcinol) anthracene [19,20]. In particular, it had been shown that co-crystallization of a 1,8-bis(resorcinol)anthracene with anthraquinone yielded a one-dimensional (1-D) hydrogen-bonded polymer wherein each resorcinol unit of the anthracene organized, by way of O–H \cdots O hydrogen bonds, two quinones in a face-to-face

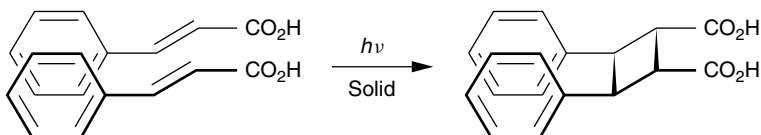


Figure 5 Solid-state photoreaction of β -cinnamic acid to produce β -truxinic acid.

stacked arrangement (Figure 6) [19]. In the arrangement, the aromatic rings of the quinones stacked at a separation distance of approximately 4.0 Å, a distance comparable with the distance criterion of Schmidt for photodimerization in a solid. Thus, from this study, we anticipated that resorcinol, or a derivative, could serve as a linear template in the solid state. Such a molecule could, in principle, be employed to assemble, by way of hydrogen bonds, two complementary olefins within a discrete solid-state molecular assembly wherein the reactants are preorganized for a UV-induced [2 + 2] cycloaddition reaction.

With linear templates based on resorcinol established, the reactants would be required to serve as hydrogen-bond acceptors. In such a context, structure studies involving pyridines had revealed the ability of pyridyl groups to serve as hydrogen-bond acceptors in the solid state and adopt an orthogonal twist with respect to a resorcinol [21]. Consequently, as a starting point, *trans*-1,2-bis(4-pyridyl)ethylene (4,4'-bpe), which is photostable as a neat crystalline solid [22], was chosen as the reactant (Figure 7). The stilbene possessed the structural features necessary to enable the molecule to serve as a reactant of a linear template based on resorcinol:hydrogen bond acceptors sites, in the form of two pyridyl units, and a C=C bond.

Thus, it was anticipated that co-crystallization of resorcinol with 4,4'-bpe would yield a four-component molecular assembly, 2(resorcinol)·2(4,4'-bpe), held together by four O–H···N hydrogen bonds (Figure 8). The C=C bonds of the assembly would be arranged in a parallel fashion and separated by approximately 4.0 Å. UV-irradiation of the crystalline solid would produce, stereospecifically, *rc**tt*-tetrakis(4-pyridyl)cyclobutane (4,4'-tpcb).

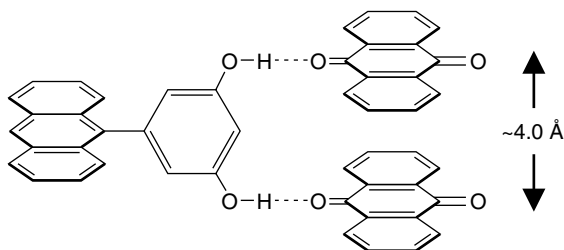


Figure 6 Schematic showing the face-to-face stacking of anthraquinone achieved by a 1,8-bis(resorcinol)anthracene.

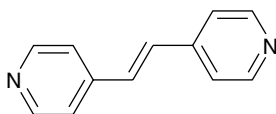


Figure 7 Schematic representation of *trans*-1,2-bis(4-pyridyl)ethylene.

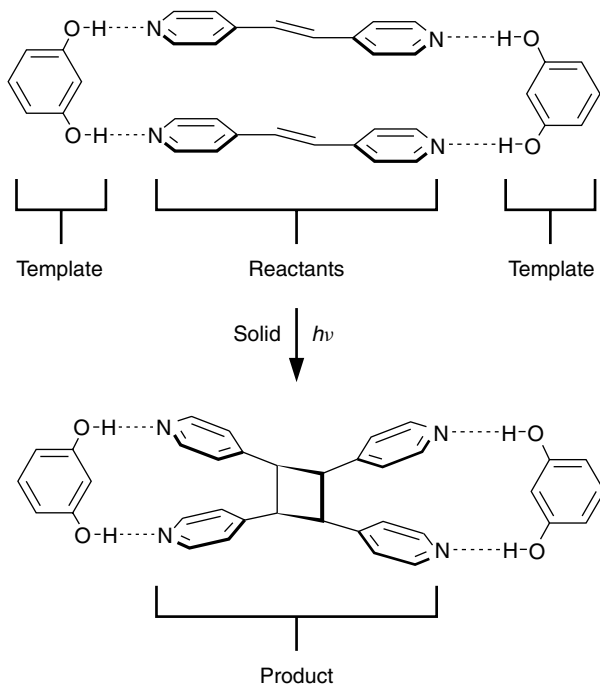


Figure 8 Schematic representation of the photoactive assembly 2(resorcinol)·2(4,4'-bpe).

4.3 Resorcinol as a Linear Template

The product of the co-crystallization of resorcinol with 4,4'-bpe is shown in Figure 9. As anticipated, the components assembled to form a discrete four-component complex, 2(resorcinol)·2(4,4'-bpe), held together by four O–H...N hydrogen bonds [7]. In this arrangement, the four pyridyl units of the two stilbenes were stacked and twisted approximately orthogonal to the diol, such that the two C=C bonds were oriented parallel and separated by 3.65 Å, an ideal position for a [2 + 2] cycloaddition reaction. Irradiation of the solid with broadband UV radiation (Hg lamp) produced the anticipated photoproduct, 4,4'-tpcb, in quantitative yield. Single-crystal X-ray analysis confirmed the structure of the product, where it was determined that the product assembles with the template to form a three-component complex, 2(resorcinol)·2(4,4'-bpe), held together by four O–H...N hydrogen bonds (Figure 10). The template-directed solid-state reaction was also carried out on a gram scale, where the diol and cyclobutane product were separated by way of a liquid-phase extraction.

Thus, by employing resorcinol to juxtapose, by way of hydrogen bonds, two bipyridines within a solid-state molecular assembly for reaction, the diol served

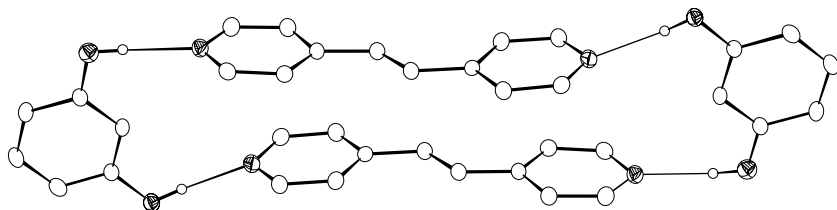


Figure 9 ORTEP perspective of the four-component assembly 2(resorcinol)·2(4,4'-bpe).

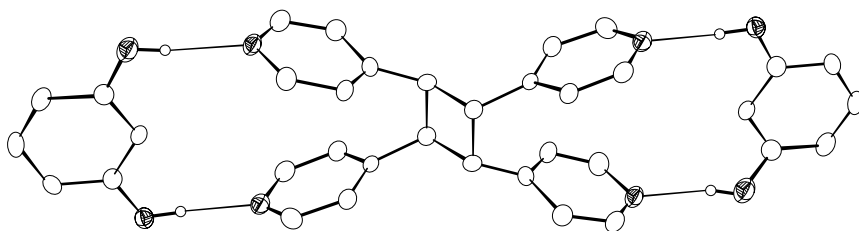


Figure 10 ORTEP perspective of the three-component assembly 2(resorcinol)·(4,4'-tpcb).

as a linear template [13], demonstrating basic synthetic behavior of an assembler [1].

4.4 Role of the Solid State

It is important to emphasize the role of the solid state in providing a medium for the formation of the molecular assembly 2(resorcinol)·2(4,4'-bpe). Indeed, that 2(resorcinol)·2(4,4'-bpe) is stabilized by weak forces (i.e. hydrogen bonds) comparable in strength to structure effects of solvent and entropy of the liquid phase [13] means that the components of 2(resorcinol)·2(4,4'-bpe) may assemble in solution to produce multiple equilibria involving individual molecules and undesirable (photostable) complexes. In effect, the solid state was used to sequester [23] 2(resorcinol)·2(4,4'-bpe) from the liquid phase, facilitating the formation of the desired photoactive complex and construction of the cyclobutane product.

4.5 Tolerance of the Assembly Process

To expand the scope of products accessible using linear templates, and thereby enable linear templates to begin to fulfill the design principles of assemblers,

we anticipated that it would be necessary to determine the tolerance [24] of the assembly process to structural and chemical changes to the templates and reactants. Such modifications, for example, could introduce functionalities (e.g. lone pairs) that interfere with the interaction between the template and reactants. In the ideal case, the template would interact preferentially with the reactants despite such structural changes to the templates and/or reactants. Moreover, with basic knowledge of structural and chemical changes tolerated by the assembly process, the designed synthesis of molecules, which may be less available or completely inaccessible using standard solution-based synthesis, could be realized.

4.5.1 Modifying the template

We have determined that the assembly process is tolerant to substituents placed along the periphery of the template [7]. In particular, derivatives of resorcinol with substituents unable to disrupt the hydrogen bonds between the templates and reactants (e.g. $-R$, $-OR$) have been found to serve as templates. Thus, co-crystallization of 5-methoxyresorcinol (5-OMe-res) with 4,4'-bpe produced the four-component complex, $2(5\text{-OMe-res})\cdot 2(4,4'\text{-bpe})$, with two olefins aligned parallel and separated by 3.66 Å. UV-irradiation of the solid with broadband UV-radiation produced 4,4'-tpcb in quantitative yield.

4.5.1.1 A new linear template

In addition to resorcinol, we have determined that 1,8-naphthalenedicarboxylic acid (1,8-nap) can serve as a template [8]. Similar to $2(\text{resorcinol})\cdot 2(4,4'\text{-bpe})$, co-crystallization of 1,8-nap with 4,4'-bpe produced the four-component assembly, $2(1,8\text{-nap})\cdot 2(4,4'\text{-bpe})$, held together by four $\text{O-H}\cdots\text{N}$ hydrogen bonds (Figure 11). In this arrangement, the two carboxylic acid groups, each of which was twisted out of the plane of the naphthalene unit, positioned the reactants for reaction, the two $\text{C}=\text{C}$ bonds being aligned parallel and separated by 3.73 Å. UV-irradiation of the solid using broadband UV radiation produced 4,4'-tpcb in quantitative yield.

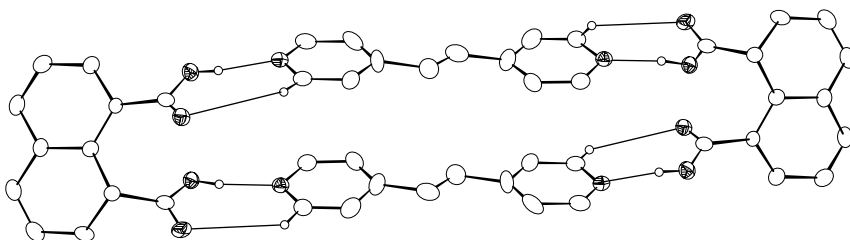


Figure 11 ORTEP perspective of the four-component assembly $2(1,8\text{-nap})\cdot 2(4,4'\text{-bpe})$.

4.5.2 Modifying the reactants

In principle, the reactants may be modified by changing the number and/or position of the hydrogen bond acceptors sites, as well as by adding (or removing) functional groups. In this context, we have determined that the assembly process is tolerant to changes to both the number and position of the acceptor sites. A study involving the addition of alkyl groups to a hydrogen-bond acceptor substrate has also been conducted.

4.5.2.1 Number of hydrogen-bond acceptor sites

The minimalist molecules that may be organized by a linear template within a molecular assembly for reaction are molecules with a single hydrogen-bond acceptor site. Thus, a single template may organize two stilbazoles in a 'head-to-head' arrangement for a regiocontrolled photodimerization that produces a head-to-head cyclobutane product.

Similar to 2(resorcinol)-2(4,4'-bpe), co-crystallization of resorcinol with 4-chlorostilbazole (4-Cl-sbz) produced the three-component assembly, (resorcinol)·2(4-Cl-sbz), held together by three O–H···N hydrogen bonds [9]. Cl···Cl interactions also formed between the complexes, such that nearest-neighbor assemblies constituted six-component complexes held together by Cl···Cl and O–H···N forces (Figure 12a). The assemblies packed in the solid to form linear stacks. As a consequence of these forces, the olefins of the 'super-assembly' were organized

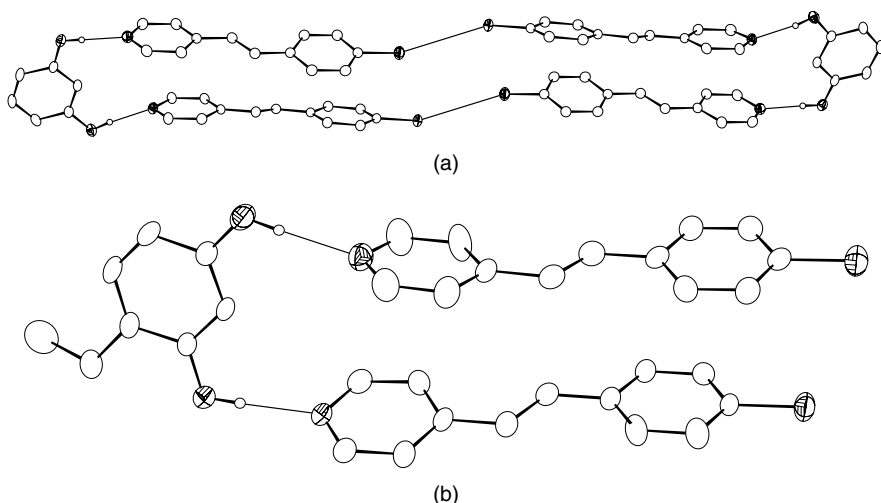


Figure 12 ORTEP perspective of the three-component assemblies: (a) (resorcinol)·2(4-Cl-sbz) and (b) (4-ethylresorcinol)·2(4-Cl-sbz).

such that the C=C bonds lie in close proximity, the two C=C bonds being separated by 3.98 Å. Unlike 2(resorcinol)·2(4,4'-bpe), however, the olefins of the complex adopted an antiparallel orientation, which was expected to render the C=C bonds photostable.

Although the olefins of (resorcinol)·2(4-Cl-sbz) were misaligned, the stilbazoles were photoactive. UV irradiation of a crystalline sample of (resorcinol)·2(4-Cl-sbz) using 350 nm radiation produced *rac*-1,2-bis(4-pyridyl)-3,4-bis(4-chlorophenyl)cyclobutane (4-Cl-dpcb) in quantitative yield. The generation of 4-Cl-dpcb was attributed to the reactant undergoing a pedal-like change in conformation in the solid [25] that enabled the C=C bonds to adopt a parallel orientation suitable to form the cyclobutane ring.

That the C=C bonds of 4-Cl-sbz were misaligned within (resorcinol)·2(4-Cl-sbz) prompted us to devise an alternative strategy to achieve olefin alignment. Although the olefins were photoactive, such a strategy might be useful to achieve reaction involving reactive sites of an assembly that are misaligned and photostable [26]. To achieve olefin alignment, substituents were attached to the template. It was reasoned that such a change to the shape of the template would alter the crystal-packing environment of the hydrogen-bonded complex and, therefore, the reactants. Owing to the specific packing demands of the template, and the ready ability of C=C bonds of *trans*-stilbenes to adopt either parallel or nonparallel orientations in solids [27], such a change could result in olefin alignment. In effect, such switching of the template would exploit the sensitivity of crystal packing to molecular structure, enabling the approach to increase the likelihood of achieving olefin alignment.

Thus, co-crystallization of 4-ethylresorcinol (4-Et-res) with 4-Cl-sbz produced the three-component assembly, (4-Et-res)·2(4-Cl-sbz), held together by three O-H···N hydrogen bonds (Figure 12b). Unlike (resorcinol)·2(4-Cl-sbz); however, the C=C bonds of the complex, which were separated by 3.92 Å, were aligned parallel, the assemblies packing in a herringbone motif. UV irradiation of the crystalline solid produced the targeted product, 4-Cl-dpcb, in near-quantitative yield.

4.5.1.2 Position of the hydrogen-bond acceptor site

In addition to changes to the number of hydrogen-bond acceptor sites, we have determined that the assembly process is tolerant to changes to the positions of the acceptor sites. Such changes to the positions of the hydrogen-bond acceptor sites were expected to require the templates to assemble so as to occupy different positions along the peripheries of the reactants.

Co-crystallization of 1,8-nap with 2,2'-bpe, for example, produced the discrete four-component assembly, 2(1,8-nap)·2(2,2'-bpe), held together by four O-H···N hydrogen bonds (Figure 13a) [8]. The C=C bonds of the complex

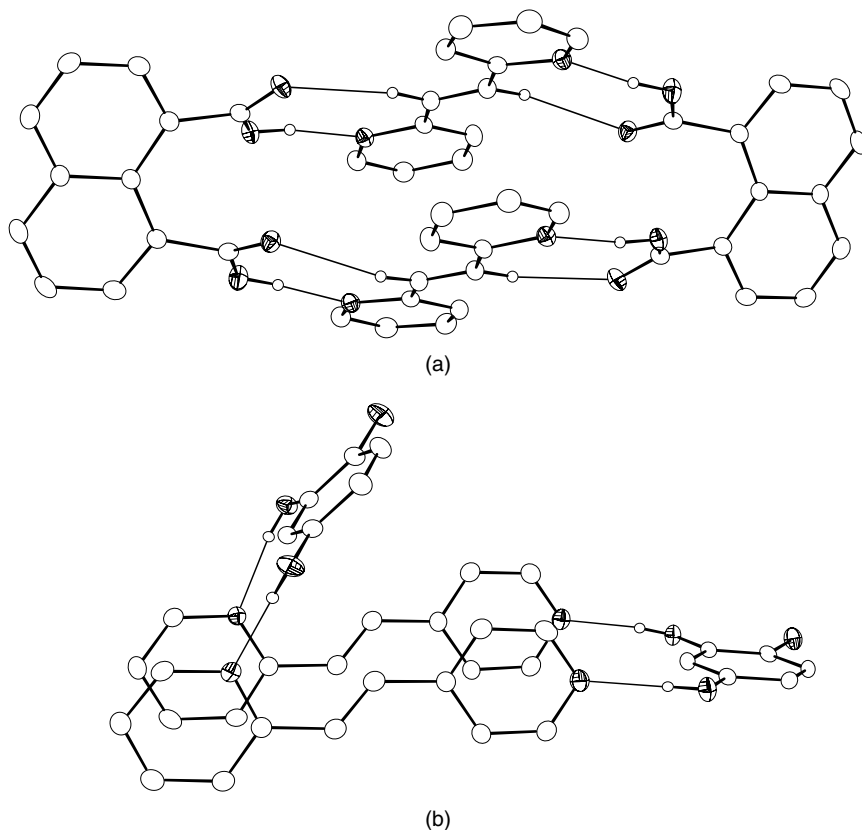


Figure 13 ORTEP perspective of assemblies based on different hydrogen-bond acceptor sites: (a) 2(1,8-nap)·2(2, 2'-bpe) and (b) 2(4-Cl-res)·2(2,4-bpe).

were organized parallel and separated by 3.91 Å. In contrast to 2(1,8-nap)·2(4,4'-bpe), each template assembled in close proximity to each C=C bond. UV-irradiation of the solid with broadband UV-radiation produced 2,2-tpcb in quantitative yield.

The ability of a linear template to orient two identical pyridyl units in a face-to-face stacked arrangement suggested that a linear template might be used to assemble two unsymmetrical reactants for a head-to-head photodimerization. Since different combinations of hydrogen-bond acceptor sites may be employed for the reaction (i.e. *trans*-1-(*n*-pyridyl)-2-(*m*-pyridyl)ethylene (where $n, m = 2, 3, \text{ or } 4$; $n \neq m$)), a general means to establish regiocontrol of the cycloaddition could be achieved.

Thus, co-crystallization of 4-Cl-res with 2,4-bpe produced the four-component assembly 2(4-Cl-res)·2(2,4-bpe) (Figure 13b) [10]. The bipyridine was organized

within the assembly in a head-to-head fashion – each diol interacting with either a 2-pyridyl or 4-pyridyl unit. The C=C bonds were aligned parallel and separated by 3.89 Å. UV-irradiation of the solid using broadband UV radiation produced the head–head photoproduct 2,4-tpcb-hh in quantitative yield. Similar to 2(4-Cl-res)-2(2,4-bpe), co-crystallization of 1,8-nap with 3,4-bpe produced the four-component assembly, 2(1,8-nap)·2(3,4-bpe), wherein the two olefins were organized head-to-head [11]. The two C=C bonds were aligned parallel and separated by 3.58 Å. UV-irradiation of 2(1,8-nap)·2(3,4-bpe) produced the head-to-head cycloproduct, 3,4-tpcb-hh, in quantitative yield.

4.5.2.3 Functional groups

Our first investigation to determine tolerance of the assembly process to functional groups has involved methylene linkages. That the assembly process is tolerant to methylene linkages is illustrated by three assemblies involving 1,2-bis(4-pyridyl)ethane (4,4'-bipyeth) as a hydrogen-bond acceptor substrate.

Specifically, co-crystallization of resorcinol with 4,4'-bipyeth produced, in contrast to 2(resorcinol)·2(4,4'-bpe), an infinite 1-D polymer, (resorcinol)·(4,4'-bipyeth) [12]. In this arrangement, the resorcinol unit adopted a conformation wherein the hydroxyl groups lie divergent. Similar to neat crystalline 4,4'-bipyeth, the ethane moiety and pyridyl units of the bipyridine were twisted approximately orthogonal (Figure 14). Notably, the closest N(bipyridine)⋯C–H(resorcinol) separations of the 1-D array involved the 4- and 6-positions of the diol. Thus, the flexibility of the methylene groups, as realized by the twisting of the ethane moiety, enabled the diol and bipyridine to form the infinite array, largely prohibiting the components from forming the targeted discrete structure.

That 4,4'-bipyeth and resorcinol assembled to form a 1-D array prompted us to develop an alternative strategy to produce the targeted discrete complex. Stacking of methylene groups in the solid state was established [28], while the known flexibility of 4,4'-bipyeth [29] suggested that the bipyridine could be forced to adopt a planar conformation suitable for discrete assembly formation. Moreover, it was reasoned that substituents in the 4- and/or 6-positions of a resorcinol might enable the diol to direct stacking of 4,4'-bipyeth within a discrete complex (Figure 15). In addition to making a 1-D assembly energetically unfavorable by sterically protecting each ‘side’ of the diol [30], the positioning of the substituents near the hydroxyl groups would promote the diol to adopt a convergent conformation.

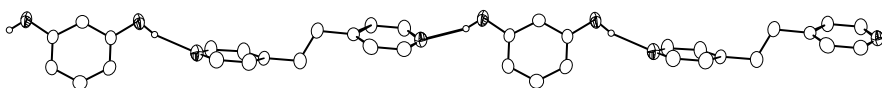


Figure 14 ORTEP perspective of the infinite 1-D assembly (resorcinol)·(4,4'-bipyeth).

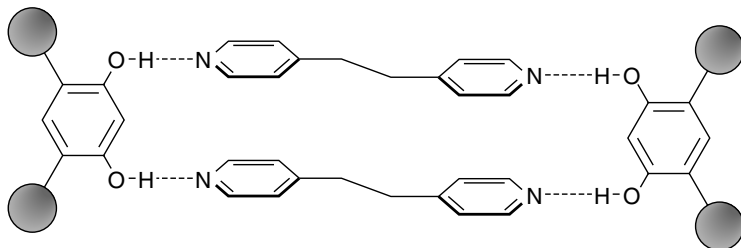


Figure 15 Schematic representation of a discrete assembly achieved using a derivatized resorcinol assembler.

In effect, the substituents would largely preorganize [5] a resorcinol unit to form the targeted discrete structure.

As anticipated, co-crystallization of either 4-Cl-res or 4,6-dichlororesorcinol (4,6-di-Cl-res) with 4,4'-bipyeth produced the four-component complex, 2(4-Cl-res)·2(4,4'-bipyeth) and 2(4,6-di-Cl-res)·2(4,4'-bipyeth), respectively – each held together by four O–H···N hydrogen bonds. The bipyridines were stacked alongside each resorcinol unit, such that the methylene linkages were aligned and separated by 4.13 Å. In contrast to (resorcinol)·(4,4'-bipyeth), the bipyridines adopted an approximate planar conformation, wherein the ethane moiety and pyridyl units were twisted toward co-planarity (Figure 16). Thus, in addition to promoting the formation of the discrete complex, the substituents of each diol affected the conformation of the bipyridine [12].

4.6 Target-Oriented Synthesis

The tolerance of the assembly process to structural changes to the templates and reactants demonstrated that linear templates could be used as reliable tools for directing the formation of covalent bonds. Moreover, that the templates assembled along the peripheries of the hydrogen-bonded assemblies suggested to us that linear templates might be used to synthesize molecules of varying size (e.g. lengthening) and shape (e.g. bending), since the assembly process would permit the templates to adapt to the sizes and shapes of the corresponding reactants. Notably, an increase in size of the reactants could be accompanied by the attachment of additional reactive sites (i.e. C=C bonds) to the reactants. Indeed, such an ability to dictate the size and shape of molecular products using linear templates would be reminiscent of those synthetic flexibilities of standard solution-based organic synthesis where such synthetic ‘freedoms’ are utilized to create molecular targets [14]. An ability to conduct target-oriented syntheses using linear templates would, in effect, enable the templates to serve as general assemblers for constructing molecules [1,2].

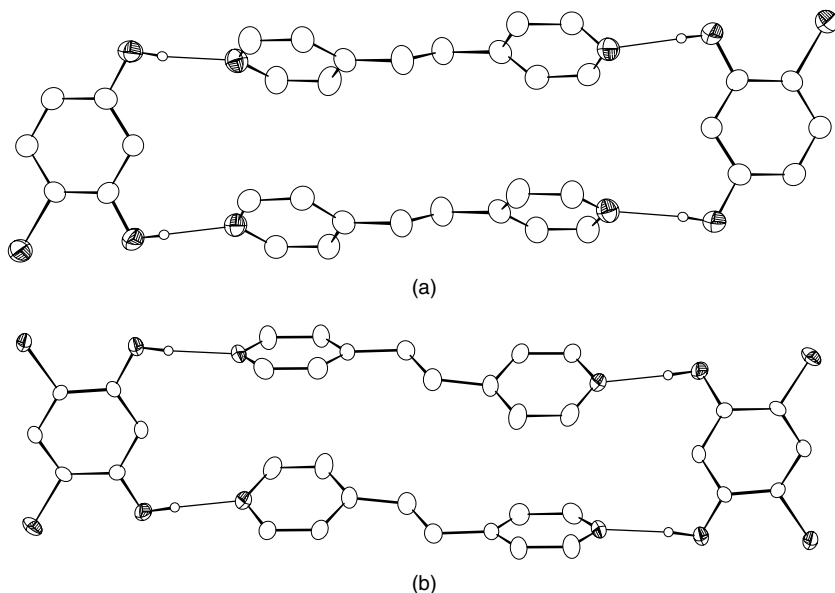


Figure 16 ORTEP perspectives of the discrete assemblies: (a) $2(4\text{-Cl-res})\cdot 2(4,4'\text{-bipyeth})$ and (b) $2(4,6\text{-di-Cl-res})\cdot 2(4,4'\text{-bipyeth})$.

4.6.1 Construction of a cyclophane

To employ a linear template as an assembler to construct a molecule, we focused upon a [2.2]paracyclophane as a target (Figure 17). The molecule is a member of a general class of layered aromatic compounds that have gained much interest owing to the ability of such molecules to provide challenging targets in organic chemistry and find applications in areas ranging from synthetic chemistry (e.g. catalysis) to materials science (e.g. optical materials) [31]. Specifically, we anticipated that co-crystallization of a resorcinol, or a 1,8-nap, with the lengthened diolefin 1,4-bis[2-(4-pyridyl)ethenyl]benzene (1,4-bpeb) would produce a four-component assembly, $2(\text{resorcinol})\cdot 2(1,4\text{-bpeb})$, with two olefins positioned for photoreaction. UV-irradiation of the crystalline solid would give a tricyclic product with an inner cyclic core reminiscent of a [2.2]paracyclophane. The periphery of the product would, in effect, possess an imprint of the template along the exterior of the molecule [7]. Notably, the related *ortho*- and *meta*-cyclophanes, each of which would be based on a bent reactant, could also serve as targets. The method would provide a novel entry to cyclic molecules, where low yields often requiring high-dilution conditions (i.e. large batches of solvent) are common in solution [32].

The product of the co-crystallization of 1,4-bpeb with 5-methoxyresorcinol (5-OMe-res) is shown in Figure 18 [7]. As anticipated, the components assembled

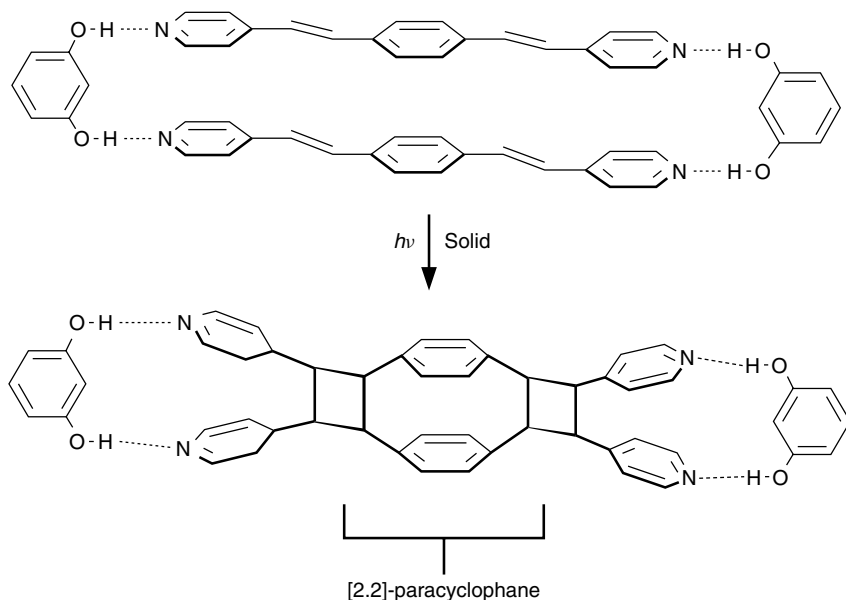


Figure 17 Schematic representation illustrating the construction of a [2.2]paracyclophane.

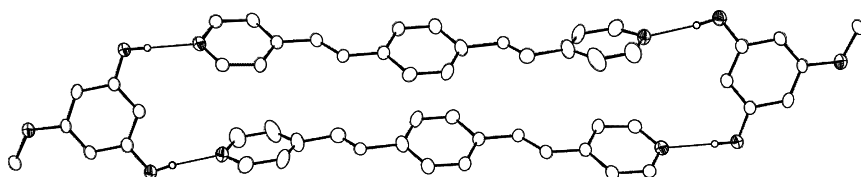


Figure 18 ORTEP perspective of the four-component assembly 2(5-OMe-res)-2(1,4-bpeb).

to form a discrete four-component complex, 2(5-OMe-res)·2(1,4-bpeb), held together by four O–H···N hydrogen bonds. In this arrangement, the olefins of 1,4-bpeb, one of which was disordered across two positions (occupancies: 70:30), were aligned within the assembly such that the olefin of the major site conformed to the geometry criteria of the topochemical postulates with the ordered olefin, the two C=C bonds being separated by 3.70 Å. UV-irradiation of 2(5-OMe-res)·2(1,4-bpeb) produced the targeted [2.2]paracyclophane, along with a monocyclized dimer and indefinable products, in 60% yield. The structure of the photoproduct, achieved using 4-benzoylresorcinol as a template, has been confirmed by way of single-crystal X-ray diffraction [33]. Thus, by adapting to the size of a lengthened reactant, the template served as an assembler [1], enabling the regio- and stereocontrolled construction of a lengthened cyclophane target.

5 CONCLUSIONS

Linear templates afford chemists an ability to organize, by way of noncovalent forces, reactive molecules to form covalent bonds. By systematically modifying the reactants, linear templates may be used to construct molecular targets. Consequently, rather than simply serving to organize two reactive sites, linear templates serve as assemblers able to manufacture molecules. In the present case, the solid state has provided a medium to organize reactants using linear templates wherein the templates operate by way of hydrogen bonds.

Although linear templates can be used to construct molecular targets, the full benefits of the supramolecular approach will most likely be realized with further expansion of the method. Additional templates and reactions, as well as products of increasing complexity, are possible. That the targets of the templates are available in good yields also means that the molecules, akin to the synthesis paradigm of DNA [17], could be used in various applications. Initial studies have demonstrated that the products serve as building blocks of metal–organic hosts [10,34]. That the targets are synthesized in a solvent-free medium also means that organic solvents for critical covalent-bond-making processes are eliminated, suggesting benefits to green chemistry [35]. The molecule-by-molecule construction principles achieved using the templates also make the method a possible approach for constructing molecular objects, or nanostructures [36].

Interplay involving a variety of areas may bring such possibilities closer to reality [36].

ACKNOWLEDGEMENTS

LRM is grateful to the National Science Foundation (CAREER Award, DMR-0133138) and the University of Iowa for support of this work. Acknowledgement is also made to the Donors of The Petroleum Research Fund, administered by the American Chemical Society and the Research Corporation (Research Innovation Award) for partial support of the research. It is with pride and pleasure that LRM thanks the talented co-workers whose names appear in the references below.

REFERENCES

1. Drexler, K. E. Machine-Phase Technology. *Sci. Amer.* **2001**, 285, 74–75.
2. Whitesides, G. M. The Once and Future Nanomachine. *Sci. Amer.* **2001**, 285, 78–83.
3. Drexler, K. E. Molecular Engineering: an Approach to the Development of General Capabilities for Molecular Manipulation. *Proc. Natl. Acad. Sci. USA* **1981**, 78, 5275–5278.
4. Dagani, R. Building From the Bottom Up. *Chem. and Eng. News.* **2000**, 78, 25–44.

5. Fyfe, M. C. T.; Stoddart, J. F. Synthetic Supramolecular Chemistry. *Acc. Chem. Res.* **1997**, *30*, 393–401.
6. MacGillivray, L. R. From Engineering Crystals to Engineering Molecules: Emergent Consequences of Controlling Reactivity in the Solid State Using Linear Templates. *Cryst. Eng. Commun.* **2002**, *4*, 37–42.
7. MacGillivray, L. R.; Reid, J. L.; Ripmeester, J. A. Supramolecular Control of Reactivity in the Solid State Using Linear Molecular Templates. *J. Am. Chem. Soc.* **2000**, *122*, 7817–7818.
8. Papaefstathiou, G. S.; Kipp, A. J.; MacGillivray, L. R. Exploiting Modularity in Template-Controlled Synthesis: a New Linear Template to Direct Reactivity Within Discrete Hydrogen-Bonded Molecular Assemblies in the Solid State. *Chem. Commun.* **2001**, 2432–2433.
9. MacGillivray, L. R.; Reid, J. L.; Ripmeester, J. A.; Papaefstathiou, G. S. Toward a Reactant Library in Template-Directed Solid-State Organic Synthesis: Reactivity Involving a Mono-Functional Reactant Based on a Stilbazole. *Indust. Eng. Chem. Res.* **2002**, *41*, 4494.
10. Hamilton, T. D.; Papaefstathiou, G. S.; MacGillivray, L. R. A Polyhedral Host Constructed Using a Linear Template. *J. Am. Chem. Soc.* **2002**, *124*, 11 606–11 607.
11. Varshney, D. B.; Papaefstathiou, G. S.; MacGillivray, L. R. Site-Directed Regio-controlled Synthesis of a ‘Head-to-Head’ Photodimer Via a Single-Crystal-to-Single-Crystal Transformation Involving a Linear Template. *Chem. Commun.* **2002**, 1964–1965.
12. Papaefstathiou, G. S.; MacGillivray, L. R. Discrete Versus Infinite Molecular Self-Assembly: Control in Crystalline Hydrogen-Bonded Assemblies based on Resorcinol. *Org. Lett.* **2001**, *3*, 3835–3838.
13. Anderson, S.; Anderson, H. L. In *Templated Organic Synthesis*; Diederich, F.; Stang, P. J., (eds) Wiley-VCH, New York, pp. 1–38, **2000**.
14. Nicolau, K. C.; Yue, E. W.; Oshima, T. New Roads to Molecular Complexity. In *The New Chemistry*; Hall, N., (ed.), Cambridge University Press, New York, pp. 168–198, **2000**.
15. Kelly, T. R.; Zhao, C.; Bridger, G. J. A Bisubstrate Reaction Template. *J. Am. Chem. Soc.* **1989**, *111*, 3744–3745.
16. Bassani, D. M.; Darcos, V.; Mahony, S.; Desvergne, J.-P. Supramolecular Catalysis of Olefin [2 + 2] Photodimerization. *J. Am. Chem. Soc.* **2000**, *122*, 8795–8796.
17. Stryer, L. In *Biochemistry*; W. H. Freeman, New York, **1988**.
18. Schmidt, G. M. J. Photodimerization in the Solid State. *Pure Appl. Chem.* **1971**, *27*, 647–678.
19. Aoyama, Y.; Endo, K.; Anzai, T.; Yamaguchi, Y.; Sawaki, T.; Kobayashi, K.; Kanehisa, N.; Hashimoto, H.; Kai, Y.; Masuda, Y. Crystal Engineering of Stacked Aromatic Columns. Three-Dimensional Control of the Alignment of Orthogonal Aromatic Triads and Guest Quinones via Self-Assembly of Hydrogen-Bonded Networks. *J. Am. Chem. Soc.* **1996**, *118*, 5562–5571.
20. For conceptually similar approaches, see: (a) Ito, Y.; Borecka, B.; Trotter, J.; Scheffer, J. R. Control of Solid-State Photodimerization of *trans*-Cinnamic Acid by Double Salt Formation with Diamines. *Tetrahedron Lett.* **1995**, *36*, 6083–6086; (b) Amirsakis, D. G.; Garcia-Garibay, M. A.; Rowan, S. J.; Stoddart, J. F.; White, A. J. P.; Williams, D. J. Host–Guest Chemistry Aids and Abets a Stereospecific Photodimerization in the

- Solid State. *Angew. Chem., Int. Ed. Engl.* **2001**, *40*, 4256–4261; (c) Zitt, H.; Dix, I.; Hopt, H.; Jones, P. G. 4,15-Diamino[2.2]paracyclophane, a Reusable Template for Topochemical Reaction Control in Solution. *Eur. J. Org. Chem.* **2002**, 2298–2307.
21. MacGillivray, L. R.; Atwood, J. L. Rational Design of Multi-Component Resorcin[4]arenes and Control of Their Alignment in the Solid State. *J. Am. Chem. Soc.* **1997**, *119*, 6931–6932.
 22. Vansant, J.; Toppet, S.; Smets, G.; Declercq, J. P.; Germain, G.; Van Meerssche, M. Azastilbenes. 2. Photodimerization. *J. Org. Chem.* **1980**, *45*, 1565–1573.
 23. Lawrence, D. S.; Jiang, T.; Levett, M. Self-Assembling Supramolecular Complexes. *Chem. Rev.* **1995**, *95*, 2229–2260.
 24. For a discussion on the importance of tolerance to functional groups in organometallic-based synthesis, see: Trnka, T. M.; Grubbs, R. H. The Development of $L_2X_2Ru=CHR$ Olefin Metathesis Catalysts: an Organometallic Success Story. *Acc. Chem. Res.* **2001**, *34*, 18–29.
 25. Ohba, S.; Hosomi, H.; Ito, Y. In Situ X-ray Observation of Pedal-like Conformational Change and Dimerization of *trans*-Cinnamamide in Cocrystals with Phthalic Acid. *J. Am. Chem. Soc.* **2001**, *123*, 6349–6352.
 26. Murthy, G. S.; Arjunan, P.; Venkatesan, K.; Ramamurthy, V. Consequences of Lattice Relaxability in Solid State Photodimerizations. *Tetrahedron* **1987**, *43*, 1225–1240.
 27. Galli, S.; Mercandelli, P.; Sironi, A. Molecular Mechanics in Crystalline Media: the Case of (E)-Stilbenes. *J. Amer. Chem. Soc.* **1999**, *121*, 3767.
 28. Menger, F. M.; Lee, J.-J.; Hagen, K. S. Molecular Laminates. Three Distinct Crystal Packing Modes. *J. Am. Chem. Soc.* **1991**, *113*, 4017–4019.
 29. Hennigar, T. L.; MacQuarrie, D. C.; Losier, P.; Rogers, R. D.; Zaworotko, M. J. Supramolecular Isomerism in Coordination Polymers: Conformational Freedom of Ligands in $[Co(NO_3)_2(1,2\text{-bis}(4\text{-pyridyl)ethane})_{1.5}]_n$. *Angew. Chem., Int. Ed. Engl.* **1997**, *36*, 972–973.
 30. Whitesides, G. M.; Simanek, E. E.; Mathias, J. P.; Seto, C. T.; Chin, D. N.; Mammen, M.; Gordon, D. M. Noncovalent Synthesis: Using Physical-Organic Chemistry to Make Aggregates. *Acc. Chem. Res.* **1995**, *28*, 37–44.
 31. Cram, D. J.; Cram, J. M. Cyclophane Chemistry: Bent and Battered Benzene Rings. *Acc. Chem. Res.* **1971**, *4*, 204–213.
 32. Dietrich, B.; Viout, P.; Lehn, J.-M. *Macrocyclic Chemistry*. Wiley-VCH, New York, **1993**.
 33. Frišèia, T.; MacGillivray, L. R., Template Switching: A Supramolecular Strategy for the Quantitative, Gram-Scale Construction of a Molecular Target in the Solid State. *Chem. Commun.* **2003**, 1306–1307.
 34. Papaefstathiou, G. S.; MacGillivray, L. R. An Inverted Metal-Organic Framework with Compartmentalized Cavities Constructed by Using an Organic Bridging Unit Derived from the Solid State. *Angew. Chem., Int. Ed. Engl.* **2002**, *41*, 2070–2073.
 35. Anastas, P. T.; Warner, J. C. *Green Chemistry: Theory and Practice*. Oxford University Press, New York, **1998**.
 36. Hecht, S. Welding, Organizing, and Planting Organic Molecules on Substrate Surfaces—Promising Approaches Towards Nanoarchitectonics From the Bottom Up. *Angew. Chem., Int. Ed. Engl.* **2003**, *42*, 24–26.

Chapter 9

Development of a New Biocide as an Inclusion Complex

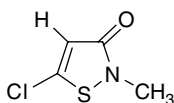
MINORU YAGI, AYAKO SEKIKAWA AND TETSUYA AOKI

Kurita Water Industries Ltd, 4–7 Nishi-Shinjuku 3-Chome, Shinjuku-ku, Tokyo 160–8383, Japan

1 INTRODUCTION

In water systems such as those of the cooling-water units of various factory plants and buildings or the pulp and paper industries, the slime (a viscid film made up of organisms as well as inorganic waste) [1] composed of various bacteria and fungi adheres to the surface of ducts or lines, causing various problems, such as reducing the efficiency of heat exchange as well as the production efficiency.

To prevent the problems caused by slime formation, various microbicides (slime-controlling agents) can be used. Of these, 5-chloro-2-methyl-4-isothiazoline-3-one (Cl-MIT; **1**) is the most widely used as a slime-controlling agent, a bactericide, an algicide or a fungicide, for various industrial water systems such as those in cooling-water units or papermills, as it has an excellent microbicidal activity. [2]



5-Chloro-2-methyl-4-isothiazoline-3-one
(Cl-MIT)

Table 1 Composition of KATHON WT^a.

Ingredient	(wt %)
Cl-MIT	10.4
MIT	3.6
MgCl ₂	9.0
MgNO ₃	16.0
Impurities	1.0
Water	60.0
Total	100.0

^aKATHON WT is a commercialized biocide product created by Rohm and Haas Ltd.

Although KATHON WT (Table 1) is marketed as an industrial slime-controlling agent containing Cl-MIT, extreme care is necessary when handling this chemical, because KATHON WT is extremely irritating to exposed skin. Also, since Cl-MIT decomposes extremely easily, a large amount of Mg salts have to be added to stabilize it. Therefore KATHON WT cannot be used to treat latex and emulsion products, which will coagulate with Mg salts.

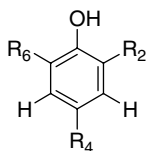
As a way of overcoming the problems mentioned above, we first created an inclusion complex that was extremely effective in stabilizing Cl-MIT and reducing its irritant properties. [3] However, despite being able to develop the production process commercially, the initial host compound was a halide which was complicated to produce, so it was necessary to develop a new host compound that is less hazardous to the environment and is easy to manufacture. With this aim, we investigated the new hosts that form inclusion complexes with Cl-MIT, using various nonhalide phenol or carboxylic acid compounds which are easily available commercially. We found out that ten types of compound form inclusion complexes with Cl-MIT. We then evaluated the performance of these inclusion complexes, and consequently it became clear that 4,4'-ethylidenebisphenol is the most efficient host. Also, we succeeded in commercially producing a new biocide complex.

The results of these investigations are reported in Section 2, together with details of these inclusion complexes and the advantages of the new functional biocide.

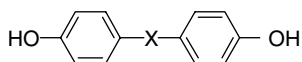
2 RESULTS AND DISCUSSION

2.1 Investigation of the New Host

As a result of investigating the nonhalide phenol and carboxylic acid compounds as potential new hosts, it was found out that three types of phenol compound and seven types of carboxylic acid compound will form inclusion complexes with Cl-MIT (Tables 2–4).

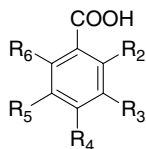
**Table 2** Inclusion complexation of Cl-MIT by phenol host compounds.

Number	Host			Complex	
	R ₂	R ₄	R ₆	Host:guest	Number
2	H	CH ₃	H	n ^a	17
3	H	CH ₂ CH ₃	H	n	
4	H	CH(CH ₃) ₂	H	n	
5	H	C(CH ₃) ₃	H	n	
6	C(CH ₃) ₃	CH ₃	H	n	
7	C(CH ₃) ₃	CH ₂ CH ₃	H	n	
8	C(CH ₃) ₃	C(CH ₃) ₃	H	2:1	
9	C(CH ₃) ₃	C(CH ₃) ₃	C(CH ₃) ₃	n	
10	C(CH ₃) ₃	H	C(CH ₃) ₃	n	
11	OH	CH ₃	H	n	
12	OH	CH ₂ CH ₃	H	n	
13	OH	C(CH ₃) ₃	H	n	
14	OH	COOCH ₃	OH	1:1	
15	OH	COOH	OH	n	
16	H	COOCH ₃	H	n	

^aNo complexation occurred.**Table 3** Inclusion complexation of Cl-MIT by bisphenol host compounds.

Number	Host	Complex	
	X	Host:guest	Number
19	None	n ^a	23
20	CH ₂	n	
21	CH(CH ₃)	1:1	
22	C(CH ₃) ₂	n	

^aNo complexation occurred.

**Table 4** Inclusion complexation of Cl-MIT by benzoic acid host compounds.

Number	Host					Complex	
	R ₂	R ₃	R ₄	R ₅	R ₆	Host:guest	Number
24	OH	H	H	H	H	n ^a	
25	OH	OH	H	H	H	n	
26	OH	H	OH	H	H	n	
27	OH	H	H	OH	H	1:1	36
28	OH	H	H	H	OH	3:2	37
29	H	OH	OH	H	H	1:1	38
30	H	OH	H	OH	H	n	
31	COOH	H	H	H	H	n	
32	H	COOH	H	H	H	n	
33	H	H	COOH	H	H	n	
34	COOH	H	COOH	H	H	3:1	39
35	COOH	H	COOH	COOH	H	2:1	40

^aNo complexation occurred.

Inclusion complexes were prepared by crystallization of Cl-MIT and host compounds from methanol. When alkyl phenol compounds (**2–10**) were used as hosts, a 2:1 complex (**17**) of 2,4-di-*tert*-butylphenol (**8**) and Cl-MIT (**1**) was obtained (Table 2). However, other similarly structured phenol compounds (**2–7,9,10**) failed to yield inclusion complexes. For example, when a *tert*-butyl group from **8** was exchanged for a methyl group (**6**) or an ethyl group (**7**), no inclusion complex was obtained, so it is obvious that even a slight difference in structure influences whether or not an inclusion complex is formed.

Also, when catechol and pyrogallol compounds (**11–15**) were used as hosts, a 1:1 complex (**18**) of gallic acid methyl ester (**14**) and Cl-MIT (**1**) was obtained. However, inclusion complexes were not obtained with other compounds. In particular, it was not possible to obtain an inclusion complex with gallic acid (**15**), and it was found that the difference in structure between the ester and the carboxyl group influences the formation of the inclusion complex. Therefore, we used 4-hydroxybenzoic acid methyl ester (**16**) as a host to examine the effects of the ester structure. However, again no inclusion complex was produced. Thus, predicting the molecular structure of a host capable of forming an inclusion complex with Cl-MIT is fraught with difficulty.

In order to understand why the ester **14** forms an inclusion complex, we analyzed the crystal structure of **18**. (See Figure 1). [4] One of the three OH groups

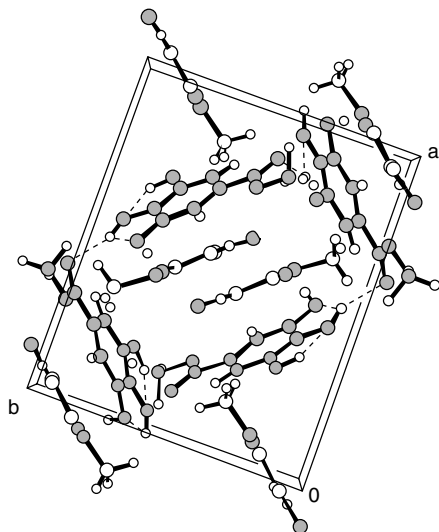


Figure 1 Crystal structure of the 1:1 complex (**18**) of **14** with Cl-MIT.

in **14** forms a hydrogen bond $\text{O-H} \cdots \text{O}$ with the carbonyl group of **1**. The $\text{O} \cdots \text{O}$ distance is 2.671 Å. Another OH group in **14** participates in an intermolecular hydrogen bond with the carbonyl group of a neighboring molecule (**14**). The host (**14**) forms quadrilateral channels with these hydrogen bonds, and Cl-MIT molecules are trapped in the channels. This appears to be the reason why **14** forms an inclusion complex with Cl-MIT, as the channels are the correct size to fit the Cl-MIT structure.

Furthermore, in the inclusion complexation when bisphenol compounds (**19–22**) were used as hosts, a 1:1 complex (**23**) of 4,4'-ethylidenebisphenol (**21**) with Cl-MIT (**1**) was obtained (Table 3). However, inclusion complexes were not obtained with the other similarly structured bisphenol compounds (**19,20,22**).

In order to understand why **21** can form an inclusion complex, we carried out a crystal structure analysis of **23**. The crystal structure of **23** is shown in Figure 2. [4] One of the two OH groups of the host molecule makes a hydrogen bond: $\text{O-H} \cdots \text{O}$ with the oxygen atom of another OH group of the neighboring host molecule, to form a linear chain. Another OH group of the host molecule connects with the carbonyl group of the guest molecule by forming another hydrogen bond: $\text{O-H} \cdots \text{O}$. The $\text{O} \cdots \text{O}$ distance here is 2.627 Å. However, we were unable to explain clearly why **21** forms an inclusion complex. Nevertheless, it seems that the structure of **21** is asymmetric compared with the other bisphenols (**19,20,22**), and this influences the formation of the inclusion complex. For example, we believe that since the ethylidene chain of **21** lacks the additional methyl group as compared with the propylidene chain of **22**, it is easy for a guest molecule to occupy the free space.

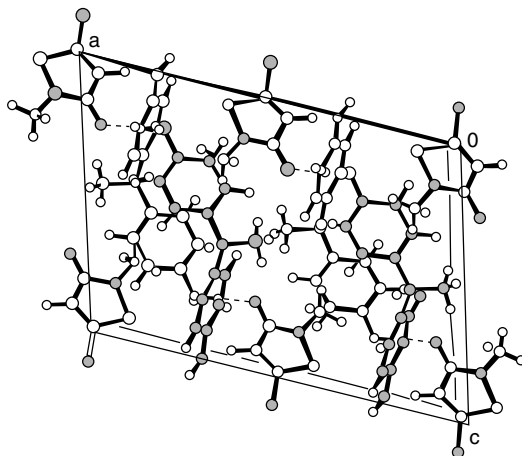


Figure 2 Crystal structure of the 1:1 complex (**23**) of **21** with Cl-MIT.

Next, when hydroxybenzoic acid compounds (**24–30**) were used as hosts, a 1:1 complex (**36**) of 2,5-dihydroxybenzoic acid (**27**) with Cl-MIT (**1**), a 3:2 complex (**37**) of 2,6-dihydroxybenzoic acid (**28**) with **1**, and a 1:1 complex (**38**) of 3,4-dihydroxybenzoic acid (**29**) with **1** were obtained (Table 4).

Also, when benzene polycarboxylic acid compounds (**31–35**) were used, a 3:1 complex (**39**) of trimellitic acid (**34**) with **1**, and a 2:1 complex (**40**) of pyromellitic acid (**35**) with **1** were obtained (Table 4). Although the inclusion complexes were not obtained with the other similarly structured compounds (**31–33**), it was shown that as the number of carboxyl groups of the host increases, the inclusion complexation becomes easier.

Furthermore, when aliphatic dicarboxylic acid compounds (**41–46**) were used as hosts, a 1:1 complex (**47**) of oxalic acid (**41**) with **1**, and a 1:2 complex (**48**) of acetylenedicarboxylic acid (**42**) with **1** were obtained (Table 5). Although the

Table 5 Inclusion complexation of Cl-MIT by aliphatic dicarboxylic acid host compounds.

Host		Complex	
Number	X	Host:guest	Number
41	None	1:1	47
42	C \equiv C	1:2	48
43	CH=CH(<i>cis</i>)	n ^a	
44	CH=CH(<i>trans</i>)	n	
45	CH ₂	n	
46	CH ₂ CH ₂	n	

^aNo complexation occurred.

inclusion complexes were not formed with other similarly structured compounds (**43–46**), our data appear to show that straight-chain dicarboxylic acids facilitate the inclusion of Cl-MIT. However, we could not clearly explain the reason why **41** and **42** are able to include Cl-MIT. X-ray crystal structural analyses of these complexes are in progress.

As the aforementioned results indicate, it is difficult to predict the molecular structure of a suitable host for Cl-MIT, so it is necessary to employ a degree of trial and error. However, it becomes easier to design the host molecule if the crystal structure and stability of the inclusion complex are predictable.

2.2 Characterization of Cl-MIT Inclusion Complexes

We studied Cl-MIT inclusion complexes, with a view to evaluating their thermal stability and the degree to which they release Cl-MIT into water. As a result, it was clear that the inclusion complex (**23**) with 4,4'-ethylidenebisphenol (**21**) is the most efficient complex for commercial use. The experimental method is detailed below.

First, the thermal stability of Cl-MIT in the inclusion complexes was evaluated at 40° C for two months. The fraction of Cl-MIT remaining in the complexes was measured using HPLC, and it was found that Cl-MIT in the complexes was more stable than the pure Cl-MIT (Figures 3–5). Leaving aside complexes **18,37** and **47** the other complexed Cl-MIT remained stable for two months. So it was clear that it is possible to prevent the decomposition of Cl-MIT by creating inclusion complexes rather than adding Mg salts as stabilizers.

Next, we evaluated the profile of Cl-MIT release from the inclusion complexes into water. The inclusion complex was dispersed in 1 liter of water, so that when

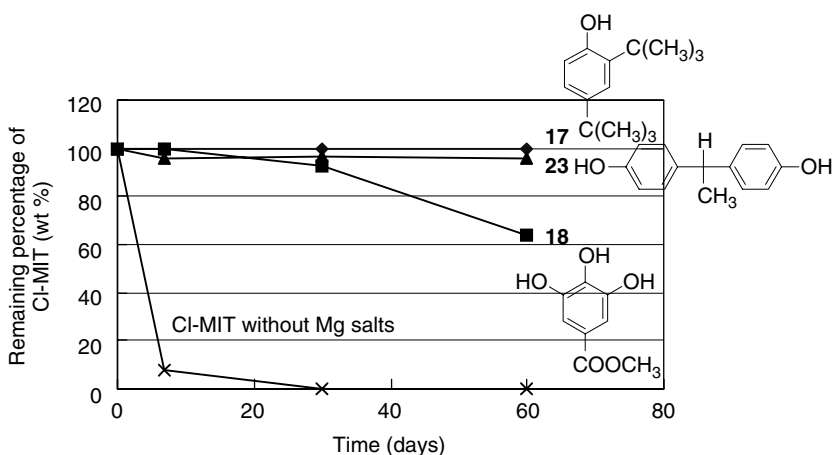


Figure 3 Thermal stability of Cl-MIT in the inclusion complexes – 1(40°C).

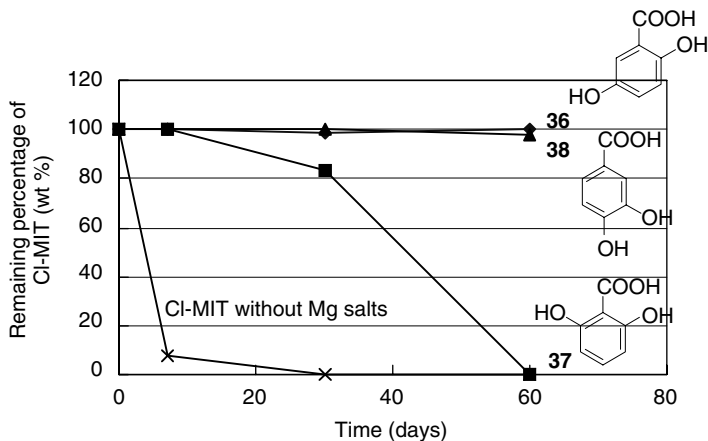


Figure 4 Thermal stability of CI-MIT in the inclusion complexes – 2(40 °C).

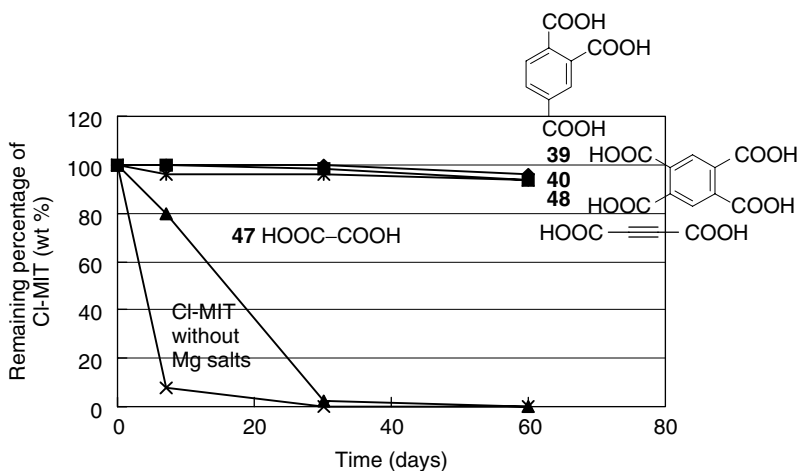


Figure 5 Thermal stability of CI-MIT in the inclusion complexes – 3(40 °C).

all the CI-MIT in the complex was released, the concentration of CI-MIT becomes 3000 mg/L^{-1} . Measurements were continued for a month at 25°C . The CI-MIT concentration of the water filtered with a 0.45 micrometer filter was measured using HPLC, and it was found out that the CI-MIT concentration for complex (23) with 4,4'-ethylidenebisphenol (21) is the lowest, at about 330 mg L^{-1} (Figure 6). From these results, we judge that the aforementioned complex is the most suitable for our purposes.

The reason why the inclusion complex (23) outperforms the other complexes may be explained by differences in crystal structure. For example, CI-MIT in

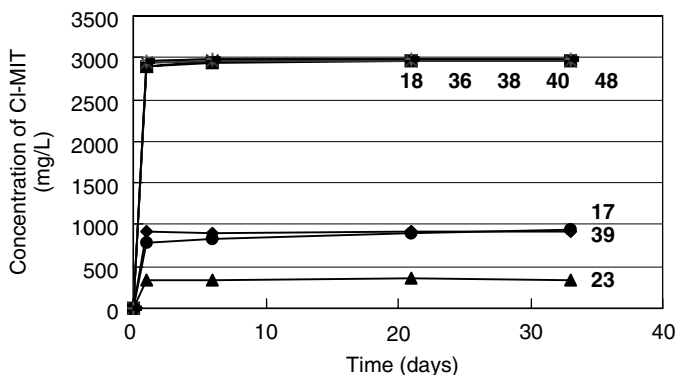


Figure 6 Release profile of Cl-MIT from the inclusion complexes, into water (25 °C).

complex (**23**) is more thermally stable and more slowly released into water than that in complex (**18**) with gallic acid methyl ester (**14**). Therefore we decided to compare the crystal structure of complexes (**23**) and (**18**). Consequently, the hydrogen bond between the host and the guest in the former complex is stronger than that in the latter complex, since the O...O distances are 2.627 and 2.671 Å for the former and latter complexes, respectively (Figures 2 and 3). It seems that this is a reason why the former complex performs better than the latter one.

2.3 Industrial Manufacture and Characteristics of the New Biocide

First, the industrial manufacturing method for the inclusion complex (**23**; FIB-CIDE-K58) of Cl-MIT with 4,4'-ethylidenebisphenol was investigated. As a result, FIB-CIDE-K58 has been manufactured using the process shown in Figure 7 obviating the addition of Mg salts [5].

In addition, a new type of new biocide (designated FIB-CIDE-KF), this time a water-based flowable product in which the inclusion complex (FIB-CIDE-K58) has been ground into fine particles of 10 μm or less, in an aqueous solvent, has been manufactured using the process shown in Figure 8 [6].

The degree of skin irritation caused by FIB-CIDE-K58 was evaluated using the Draize method [7], i.e. by applying the product to the skin of rabbits. (The primary irritation index (PII) uses a scale of 0 to 8, where a high value indicates severe irritation.) Consequently, the PII for FIB-CIDE-K58 containing 36 wt % of Cl-MIT was 0.7, with a descriptive rating of 'slight irritation' (Table 6). On the other hand the PII for KATHON-WT containing 10 wt % of Cl-MIT was 8.0, with a descriptive rating of 'severe irritation'. Thus it was found that inclusion complexation is extremely effective in reducing of the amount of skin irritation caused by Cl-MIT. We believe that the host compound prevents Cl-MIT from directly touching the skin.

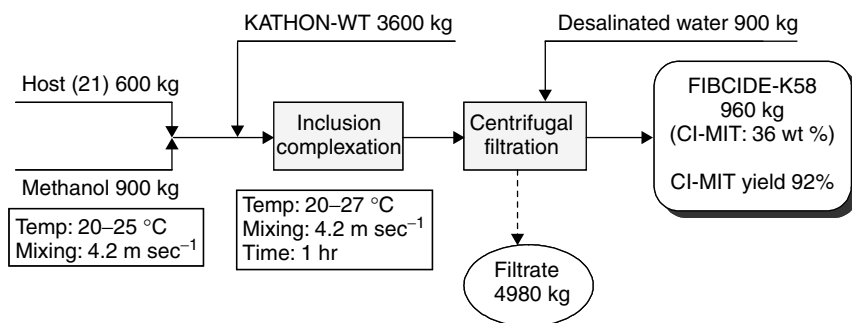
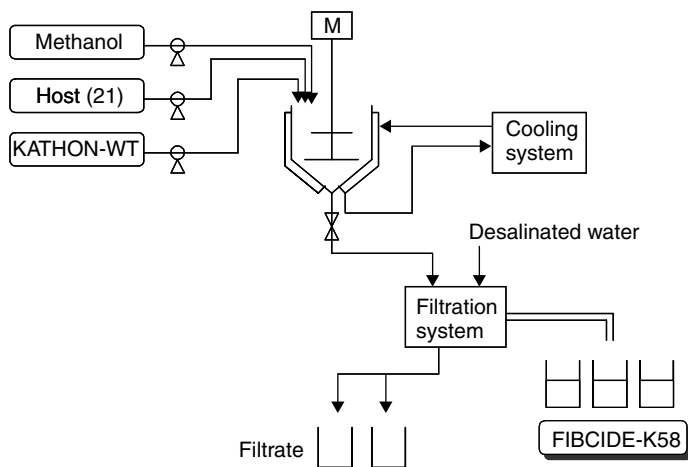


Figure 7 Manufacturing process for FIBCID-K58.

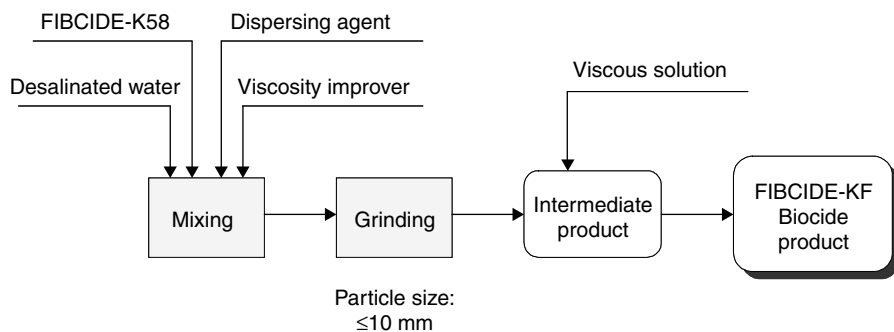


Figure 8 Manufacturing process for FIBCID-KF.

Table 6 Skin irritation data for FIBCIDE-K58 (using the Draize method)^a.

Test sample	Concentration ratio of Cl-MIT(wt %)	Primary irritation index (PII)	Dermal irritation toxicity categories
FIBCIDE-K58	36	0.7 (Slight irritation)	Slight: 0–2 Moderate: 2–5 Severe: 5–8
KATHON WT	10	8.0	

^aDose administration: 0.5 g per site.

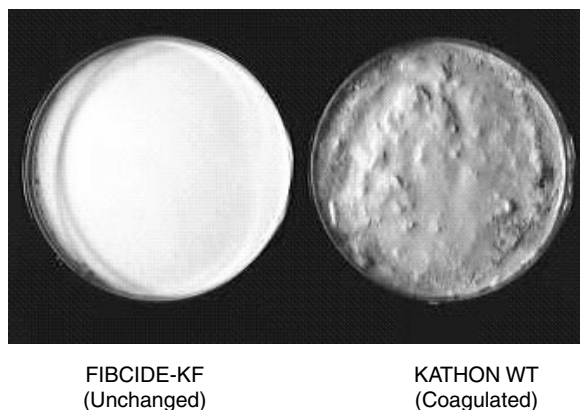


Figure 9 Influence of biocide on a coating material for printer paper. (The concentration of the biocide is 150 mg/L in the form Cl-MIT.).

Next, FIBCIDE-KF containing Cl-MIT (3 wt %) was tested as an additive to a coating material for printer paper. The coating material was unaffected by the addition of FIBCIDE-KF, but coagulation occurred when KATHON WT was added instead (Figure 9). Since KATHON-WT contains Mg salts, whereas FIBCIDE-KF does not, it is thought that this was the cause of the problems with coagulation.

From the aforementioned results, we believe that the new biocide FIBCIDE-KF could be widely applied in the field of latex and emulsion products.

Further to these results, the microbicidal activities of FIBCIDE-KF and KATHON WT were evaluated. The minimum inhibitory concentrations (MIC) for *Pseudomonas aeruginosa*, *Pseudomonas putida*, *Bacillus subtilis* and *Microbacterium* sp. are identical for both compounds, so the microbicidal effect has not diminished (Figure 10). It appears that the biocidal effects are similar because the Cl-MIT in the inclusion complex is released into water, as shown in Figure 6.

It should be noted that the new biocide has an excellent microbicidal activity against *Legionella pneumophila* in cooling-water systems. [8]

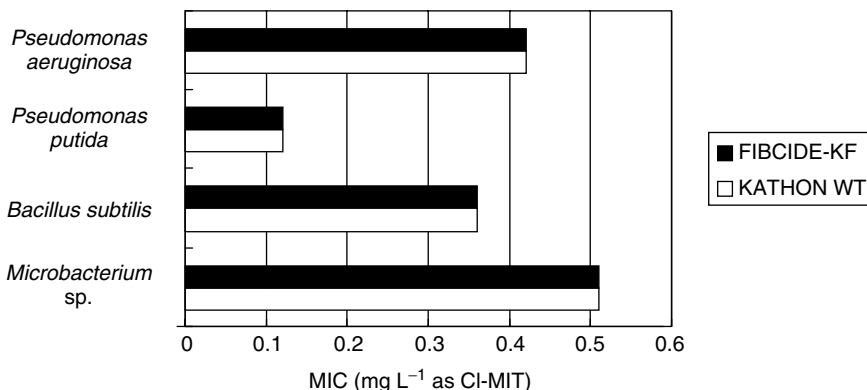


Figure 10 Microbicidal effect of FIBCID-KF (30 °C, pH 7.0, 48 h).

2.4 Experimental Method

All IR spectra were measured using an FT-IR spectrometer, JASCO FT/IR-420. All concentrations of Cl-MIT were measured by HPLC, using a column (0.6 cm × 15 cm), packed with YMC PAC ODS-A. Some 20 vol. % aqueous solution of acetonitrile was used as solvent (flow rate: 1.0 ml min⁻¹, detection: UV spectrophotometer 273 nm). All melting points were measured with the sample packed in a capillary tube.

2.4.1 Preparation of Cl-MIT (1)

Cl-MIT was prepared by extraction from KATHON WT. KATHON WT (500 mL) was extracted with chloroform (2 × 100 mL). The chloroform solution was washed with water, dried (Na₂SO₄) and evaporated to give an extract of Cl-MIT. The purity of Cl-MIT in the extract was measured by HPLC.

2.4.2 Preparation of inclusion complexes of Cl-MIT (1)

Inclusion complexes of Cl-MIT (**1**) were prepared by crystallization of hosts and **1** from methanol solution. The IR spectra and the content of **1** in these complexes were measured by IR spectrometry and HPLC, respectively. The host–guest ratio of each complex was determined from the content of **1**.

2.4.3 Thermal stability of Cl-MIT in the inclusion complex

Each inclusion complex (particle size: 0.5 mm or less) was kept at 40 °C for two months. A test sample was removed at each pre-determined time, and the

17	H:G (8:1) = 2:1	m.p.48–54 °C
	IR (Nujol) v_{\max} : 3350, 1658, 1620 and 1600 cm^{-1}	
18	H:G (14:1) = 1:1	m.p.118–121 °C
	IR (Nujol) v_{\max} : 3420, 3330, 3200, 1678, 1624 and 1608 cm^{-1}	
23	H:G (21:1) = 1:1	m.p.111–115 °C
	IR (Nujol) v_{\max} : 3300, 1645, 1620 and 1580 cm^{-1}	
36	H:G (27:1) = 1:1	m.p. not clear
	IR (Nujol) v_{\max} : 3270, 3110, 1670, 1645, 1622 and 1608 cm^{-1}	
37	H:G (28:1) = 3:2	m.p. not clear
	IR (Nujol) v_{\max} : 3320, 1670 and 1635 cm^{-1}	
38	H:G (29:1) = 1:1	m.p. not clear
	IR (Nujol) v_{\max} : 3430, 3200–2200, 1680, 1630 and 1605 cm^{-1}	
39	H:G (34:1) = 3:1	m.p. not clear
	IR (Nujol) v_{\max} : 3400–2000, 1695 and 1590 cm^{-1}	
40	H:G (35:1) = 2:1	m.p. not clear
	IR (Nujol) v_{\max} : 3520, 3400, 3300–2100 and 1705 cm^{-1}	
47	H:G (41:1) = 1:1	m.p.101–108 °C
	IR (Nujol) v_{\max} : 3470, 3200–2100, 1750 and 1720 cm^{-1}	
48	H:G (42:1) = 1:2	m.p.117–120 °C
	IR (Nujol) v_{\max} : 3200–2100, 1695 cm^{-1}	

content of **1** in the complex was measured using HPLC. The remaining fraction of Cl-MIT in each complex was calculated by the content and the initial content.

2.4.4 Release profile of Cl-MIT from the inclusion complex into water

The inclusion complex (particle size: 0.5 μm or less) was dispersed in 1 liter of water, so that when all the Cl-MIT in the complex is released into water, the concentration of Cl-MIT in the water becomes 3000 mg L^{-1} . The sample was then allowed to stand at 25 °C for a month. Part of the sample was filtered using a 0.45 μm filter, and the concentration of Cl-MIT in the sample was measured using HPLC.

2.4.5 Skin irritation tests

The extent of the skin irritation caused the sample was evaluated using the Draize method [7] on the skin of rabbits. Each animal was tested on a patch of unbroken skin. Each test area was treated with 0.5 g of the test substance. The test areas were covered for four hours. Inspections of the test areas for signs of erythema

added 1×10^7 CFU ml⁻¹. The biocide was added to this culture medium at a predetermined concentration, and cultivated at 30 °C for 48 hours. It was concluded that there had been an increase in the bacterial population in the culture medium when it became cloudy, and the minimum concentration at which the solution remained clear was designated as the minimum inhibitory concentration.

REFERENCES

1. Heukelekian H., *Sewage and Ind. Wastes*, **27**, 1391 (1955).
2. Law, A. B., Donnelly, T. W. and Lashen, E. S., *Prodotto Chimico and Aerosol Selezione*, **28**, 27 (1987).
McCoy, W. F., Ridge, J. E. and Lashen, E. S., *Materials Performance*, **25**, 9 (1986).
McCoy, W. F., Wireman, J. W. and Lashen, E. S., *J. Indust. Microbiol.*, **1**, 49 (1986).
3. Toda, F., Okamoto, M. and Mochizuki, F., *United States Patent*, US 4644021 (1987).
Sugi, H., Sekikawa, A. and Takahashi, R., *United States Patent*, US 5036087 (1991).
Yagi, M. and Toda, F., *United States Patent*, US 5091400 (1992).
4. (a) Sekine, A., Mitsumori, T., Uekusa, H., Ohashi, Y. and Yagi, M., *Analytical Science; X-ray Structure Analysis Online*, **19**, x47 2003, in press. (b) Sekine, A., Jomoto, K., Uekusa, H., Ohashi, Y. and Yagi, M., *Analytical Science; X-ray Structure Analysis Online*, **19**, x45 (2003), in press.
5. Yagi, M., Nakane K. and Hiyane, Y., *Jpn. Kokai Tokkyo Koho*, JP 07101890 (1995).
Yagi, M., Sekikawa, A. and Nakane, K., *Jpn. Kokai Tokkyo Koho*, JP 0892015 (1996).
6. Yagi, M., Nakane, K. and Takahashi, M., *Jpn. Kokai Tokkyo Koho*, JP 08259410 (1996).
7. Draize, J. H., Woodward, G. and Calvery, H. O., *J. Pharmacol. Exp. Ther.*, **82**, 377 (1944).
8. Aoki, T., Sekikawa, A. and Yagi, M., *Reito*, **72**, 848 (1997).

Cumulative Author Index

This index comprises the names of contributors to Volumes 1–8 of **Perspectives in Supramolecular Chemistry**

- Akashi, Ken-ichirou, *Observation of a Variety of Giant Vesicles under an Optical Microscope*, **6**, 45; *see also* Miyata, Hidetake, **6**, 319.
- Akazome, Motohiro, *see* Ogura, Katsuyuki, **8**, 61.
- Alargova, Rossitsa, G., *see* Bivas, Isak, **6**, 207.
- Albrecht, Anne-Marie, *see* Dannenmuller, Olivier, **6**, 385.
- Angelova, Miglena, I., *Liposome Electroformation*, **6**, 27; *see also* Kinnunen, Paavo, K., **6**, 273.
- Aoki, Tetsuya, *see* Yagi, Minoru, **8**, 205.
- Arakawa, Kenji, *see* Dannenmuller, Olivier, **6**, 385.
- Atwood, Jerry L., *Very Large Supramolecular Capsules Based on Hydrogen Bonding*, **7**, 153.
- Bacri, Jean-Claude, *see* Sandre, Olivier, **6**, 169.
- Barawkar, Dinesh, A. *see* Ganesh, Krishna N., **3**, 263.
- Barbour, Leonard, J., *see* Atwood, Jerry L., **7**, 153.
- Bassereau, Patricia, *see* Manneville, Jean-Baptiste, **6**, 351.
- Beginn, Uwe, *Supramolecular Structures with Macromolecules*, **4**, 89.
- Bell, Ian M., *see* Hilvert, Donald, **1**, 73.
- Benkovic, S. J., *Macrocycles and Antibodies as Catalysts*, **1**, 149.
- Bernard, Anne-Laure, *see* Guedeau-Boudeville, Marie-Alice, **6**, 341.
- Biradha, Kumar, *Layered Materials by Design: 2D Coordination Polymeric Networks Containing Large Cavities/Channels*, **7**, 211.
- Bishop, Roger *Enantiomer Ordering and Separation During Molecular Inclusion*, **8**, 33.
- Bivas, Isak, *Free Energy of a Fluctuating Vesicle. Influence of the Fluctuations on the Laplace Law*, **6**, 93; *see also* *Mechanical Properties of Lipid Bilayers Containing Grafted Lipids*, **6**, 207.
- Blanc, Sylvie, *see* Dannenmuller, Olivier, **6**, 385.
- Bothorel, Pierre, *see* Bivas, Isak, **6**, 207.
- Bowden, Ned, *see* Issacs, Lyle, **4**, 1.

- Bradley, Jean-Claude, *see* Guedeau-Boudeville, Marie-Alice, **6**, 341.
- Bradshaw, Jerald, S., *see* Izatt, Reed, M., **4**, 225.
- Braga, Dario, *Polymorphism, Crystal Transformations and Gas-Solid Reactions*, **7**, 325.
- Brammer, Lee, *Hydrogen Bonds in Inorganic Chemistry: Application to Crystal Design*, **7**, 1.
- Bruce, Duncan, W., *Metallomesogens – Supramolecular Organization of Metal Complexes in Fluid Phases*, **5**, 285.
- Bruening, Ronald, L., *see* Izatt, Reed, M., **4**, 225.
- Burkholder, Eric, *see* Finn, Robert, C., **7**, 241.
- Camuil, Valérie, *see* Sandre, Olivier, **6**, 169.
- Cebers, Andrejs, *see* Sandre, Olivier, **6**, 169.
- Chambron, Jean-Claude, *Rotaxanes: From Random to Transition Metal-templated Threading of Rings at the Molecular Level*, **5**, 225.
- Chandaroy, Parthapratim, *see* Hui, Sek Wen, **6**, 231.
- Chang, Ning-Leh, *see* Davis, Raymond E., **2**, 63.
- Chin, Donovan, N., *see* Issacs, Lyle, **4**, 1.
- Collinson, Simon, *see* Bruce, Duncan, W., **5**, 285.
- Cramer, Friedrich, *Emil Fischer's Lock-and-Key Hypothesis after 100 Years – Towards a Supracellular Chemistry*, **1**, 1.
- Czarnik, Anthony, W., *Chemosensors: Synthetic Receptors in Analytical Sensing Applications*, **4**, 177.
- Dance, Ian, *Supramolecular Organic Chemistry*, **2**, 137.
- Dannenmuller, Olivier, *Membrane Properties of Archaeal Phospholipids: Effects of Macrocyclization*, **6**, 385.
- Davis, Raymond E., *Molecular Shape as a Design Criterion in Crystal Engineering*, **2**, 63.
- De Cian, André, *see* Martz, Julien, **7**, 177.
- Decurtins, Silvio, *see* Pilkington, Melanie, **7**, 275.
- Demleitner, Bernhard, *see* Saalfrank, Rolf, W., **5**, 1.
- Desiraju, Gautam R., *Crystal Engineering and Molecular Recognition – Twin Facets of Supramolecular Chemistry*, **2**, 31.
- Diederich, F., *see* Echegoyen, L., **8**, 137.
- Dietrich, Christian, *see* Dimova, Rumiana, **6**, 221.
- Dimova, Rumiana, *Motion of Particles Attached to Giant Vesicles: Falling Ball Viscosimetry and Elasticity Measurements on Lipid Membranes*, **6**, 221.
- Döbereiner, Hans-Günther, *Fluctuating Vesicle Shapes*, **6**, 149; *see also* Xu, Liyu, **6**, 181; Petrov, Peter G., **6**, 335.
- Doi, Toshifusa, *see* Imai, Masanao, **6**, 361.
- Dunnitz, Jack D., *Thoughts on Crystals as Supermolecules*, **2**, 1.
- Echegoyen, L., *Regioselective Synthesis of Fullerene Derivatives and Separation of Isomers of the Higher Fullerenes*, **8**, 137.
- Eguchi, Tadashi, *see* Dannenmuller, Olivier, **6**, 385.
- Fabbrizzi, Luigi, *Fluorescent Sensors for and with Transition Metals*, **5**, 93.
- Fagan, Paul J., *Molecular Engineering of Crystals by Electrostatic Templating*, **2**, 107.
- Finn, Robert, C., *The Construction of One-, Two-, and Three-Dimensional Organic-Inorganic Hybrid Materials*

- from *Molecular Building Blocks*, **7**, 241.
- Fischer, Aline, *Formation of Giant Vesicles from Different Kinds of Lipids Using the Electrothermal Method*, **6**, 37; *see also* Oberholzer, Thomas, **6**, 285.
- Fredricks, John R., *Metal Template Control of Self-Assembly in Supramolecular Chemistry*, **3**, 1.
- Fujita, Makota, *see* Biradha, Kumar, **7**, 211.
- Ganesh, Krishna N., *Synthetic Control of DNA Triplex Structure Through Chemical Modifications*, **3**, 263.
- Gangl, Susanne, *Molecular Organization on Giant Unilamellar Vesicles*, **6**, 379.
- Gerbeaud, Claire, *see* Méléard, Philippe, **6**, 185.
- Glusker, Jenny P., *The Protein as a Supermolecule: The Architecture of a $(\beta\alpha)_8$ Barrel*, **2**, 235.
- Goto, Ayako, *Dynamic Aspects of Fatty Acid Vesicles: pH-induced Vesicle–Micelle Transition and Dilution-induced Formation of Giant Vesicles*, **6**, 261.
- Goto, Rensuke, *see* Goto, Ayako, **6**, 261.
- Graf, Ernest, *see* Martz, Julien, **7**, 177.
- Grepioni, Fabrizia, *see* Braga, Dario, **7**, 325.
- Guedeau-Boudeville, Marie-Alice, *Changes in the Morphology of Giant Vesicles Under Various Physico-chemical Stresses*, **6**, 341.
- Hamilton, Andrew, D., *see* Fredricks, John R., **3**, 1.
- Hanessian, Stephen, *see* Saladino, Raffaele, **7**, 77.
- Herranz, M.A., *see* Echegoyen, L., **8**, 137.
- Hosseini, Mir Wais, *see* Martz, Julien, **7**, 177.
- Helfrich, Wolfgang, *Bending Elasticity of Fluid Membranes*, **6**, 51; *see also* Klösigen, Beate, **6**, 243; *see also* Thimmel, Johannes, **6**, 253.
- Hilvert, Donald, *New Biocatalysts via Chemical Modifications*, **1**, 73.
- Holopainen, Juha, M. *see* Kinnunen, Paavo, K., **6**, 273.
- Horovitz, Ammon, *see* Katchalski-Katzir, Ephraim, **1**, 25.
- Hui, Sek Wen, *Control of Fusion Between Giant Vesicles*, **6**, 231.
- Imae, Toyoko, *see* Goto, Ayako, **6**, 261.
- Imai, Masanao, *Entrapment of Proteins in Soybean Phosphatidycholine Vesicles*, **6**, 361.
- Issacs, Lyle, *Self-Assembling Systems on Scales from Nanometers to Millimeters: Design and Discovery*, **4**, 1.
- Itoh, Horoyasu, *see* Akashi, Ken-ichirou, **6**, 45.
- Izatt, Reed, M., *Ion Separations in Membrane and Solid Phase Extraction Systems*, **4**, 225.
- Jerga, Agoston, *see* Atwood, Jerry L., **7**, 153.
- Jullien, Ludovic, *see* Guedeau-Boudeville, Marie-Alice, **6**, 341.
- Kakinuma, Katsumi, *See*, Dannenmuller, Olivier, **6**, 385.
- Katchalski-Katzir, Ephraim, *Molecular recognition in Biology: Models for Analysis of Protein–Ligand Interactions*, **1**, 25.
- Kim, Kimoon, *Self-Assembly of Interlocked Structures with Cucurbituril Metal Ions and Metal Complexes*, **5**, 371.
- Kinnunen, Paavo, K., *Giant Liposomes as Model Biomembranes for Roles of Lipids in Cellular Signalling*, **6**, 273.

- Kinosita, Kazuhiko, Jr., *see* Akashi, Kenichirou, **6**, 45; *see also* Miyata, Hidetake, **6**, 319.
- Klein Gebbink, Robertus, J.M., *see* Meijer, Michel, D., **7**, 375.
- Klöggen, Beate, *Membrane Roughness and Dispersive Phase as Effects of Higher-order Bending in Fluid Membranes*, **6**, 243; *see also* Thimmel, Johannes, **6**, 253.
- Köhler, Gottfried, *see* Gangl, Susanne, **6**, 379.
- Krishnamohan Sharma, C.V., *see* Desiraju, Gautam, R., **2**, 31.
- Kuboi, Ryoichi, *see* Shimanouchi, Toshinori, **6**, 369.
- Kuhn, Hans, *A Model of the Origin of Life and Perspectives in Supramolecular Engineering*, **1**, 247.
- Kumar, Vijayanti, A. *see* Ganesh, Krishna N., **3**, 263.
- Lahav, Meir, *Lock-and-Key Processes at Crystalline Interfaces: Relevance to the Spontaneous Generation of Chirality*, **1**, 173.
- Lancet, Doron, *see* Katchalski-Katzir, Ephraim, **1**, 25.
- Lasic, Danilo, D. *Giant Vesicles: A Historical Introduction*, **6**, 11.
- Lehn, Jean-Marie, *Perspectives in Supramolecular Chemistry – From the Lock-and-Key Image to the Information Paradigm*, **1**, 307.
- Leiserowitz, Leslie, *see* Lahav, Meir, **1**, 173.
- Lévy, Daniel, *see* Manneville, Jean-Baptiste, **6**, 351.
- Licchelli, Maurizio, *see* Fabbrizzi, Luigi, **5**, 93.
- Lugtenberg, Ronny J.W., *Selective Ion Recognition with Durable Sensors*, **4**, 193.
- Luisi, Pier Luigi, *Why Giant Vesicles?*, **6**, 3; *see also* Fischer, Aline, **6**, 37.
- Lukas, Arno, *see* Gangl, Susanne, **6**, 379.
- MacGillivray, Leonard R., *Supramolecular Control of Reactivity in the Solid State Using Linear Templates*, **8**, 185.
- Maitra, Uday, *A Survey of Supramolecular Chemistry (1993–1994)*, **3**, 41.
- Manneville, Jan-Baptiste, *Magnification of Shape Fluctuations of Active Giant Unilamellar Vesicles*, **6**, 351.
- Marriott, Gerard, *see* Miyata, Hidetake, **6**, 319.
- Martz, Julien, *Molecular Tectonics: Molecular Networks Based on Inclusion Processes*, **7**, 177.
- Mayer, Bernd, *see* Gangl, Susanne, **6**, 379.
- Mayrhofer, Peter, *see* Gangl, Susanne, **6**, 379.
- Meijer, E.W., *see* van Genderen, Marcel H.P., **4**, 47.
- Meijer, Michel, D., *Solid–Gas Interactions Between Small Gaseous Molecules and Transition Metals in the Solid State. Toward Sensor Applications*, **7**, 375.
- Méléard, Philippe, *Electromechanical Properties of Model Membranes and Giant Vesicle Deformations*, **6**, 185; *see also* Bivas, Isak, **6**, 207.
- Ménager, Christine, *see* Sandre, Olivier, **6**, 169.
- Mitov, Marin, D., *see* Méléard, Philippe, **6**, 185; *see also* Bivas, Isak, **6**, 207.
- Miyata, Hidetake, *see* Akashi, Kenichirou, **6**, 45; *see also* *Cell deformation Mechanisms Studied with Actin-containing Giant Vesicles, a Cell-mimicking System.*, **6**, 319.
- Miyata, Mikiji, *see* Yoswathananont, Nungruethai, **8**, 87.
- Mody, Tarak, D., *Porphyrim- and Expanded Porphyrim-Based Diagnostic and Therapeutic Agents*, **4**, 245.
- Möller, Martin, *see* Beginn, Uwe, **4**, 89.
- Momenteau, Michel., *Models of Hemoprotein Active Sites*, **3**, 155.

- Nagayama, Kazuhito, *see* Imai, Masanao, **6**, 361.
- Nakano, Kazunori, *see* Yoswathananont, Nungruethai, **8**, 87.
- Nakatani, Yoichi, *see* Dannenmuller, Olivier, **6**, 385.
- Nassimbeni, Luigi R., *Physicochemical Studies of Separation of Isomers by Supramolecular Systems*, **8**, 123
- Needham, David, *Use of Micropipet Manipulation Techniques to Measure the Properties of Giant Lipid Vesicles*, **6**, 103.
- Nishiyama, Shuji, *see* Miyata, Hidetake, **6**, 319.
- Nomura, Shin-ichirou, *Giant Phospholipid Vesicles Entrapping Giant DNA*, **6**, 313.
- Oberholzer, Thomas, *see*, Fischer, Aline, **6**, 37; *see also* *Microinjection of Macromolecules in Giant Vesicles Prepared by Electroformation*, **6**, 285.
- Ogura, Katsuyuki, *Molecular Recognition of Crystalline Dipeptides and Its Application to Separation*, **8**, 61.
- Ohki, Kazuo, *see* Miyata, Hidetake, **6**, 319.
- Osaki, Nobukazu, *see* Imai, Masanao, **6**, 361.
- Ourisson, Guy, *see* Dannenmuller, Olivier, **6**, 385.
- Pallavicini, Piersandro, *see* Fabbrizzi, Luigi, **5**, 93.
- Parodi, Luisa, *see* Fabbrizzi, Luigi, **5**, 93.
- Perkins, Meghan, *see* Hui, Sek Wen, **6**, 231.
- Petrov, Peter G., *Light-Induced Shape Transitions of Giant Vesicles*, **6**, 335.
- Pilkington, Melanie, *A Rational Approach for the Self-Assembly of Molecular Building Blocks in the Field of Molecule-Based Magnetism*, **7**, 275.
- Popovitz-Biro, Ronit, *see* Lahav, Meir, **1**, 173.
- Pott, Tanja, *see* Méléard, Philippe, **6**, 185.
- Poulligny, Bernard, *see* Dimova, Rumiana, **6**, 221.
- Prost, Jacques, *see* Manneville, Jean-Baptiste, **6**, 351.
- Prost, Jérôme, *see* Sandre, Olivier, **6**, 169.
- Provent, Christophe, *The Chirality of Polynuclear Transition Metal Complexes*, **5**, 135.
- Rapp, Gert, *see* Thimmel, Johannes, **6**, 253.
- Real, José Antonio, *Bistability in Iron (II) Spin-Crossover Systems: A Supramolecular Function*, **5**, 53.
- Rebek Jr, Julius, *see* Wintner, Edward A., **3**, 225.
- Reinhoudt, D.N., *see* Lugtenberg, R.J.W., **4**, 193.
- Rünzler, Dominik, *see* Gangl, Susanne, **6**, 379.
- Saalfrank, Rolf, W., *Ligand and Metal Control of Self-Assembly in Supramolecular Chemistry*, **5**, 1.
- Sada, Kazuki, *see* Yoswathananont, Nungruethai, **8**, 87.
- Saladino, Raffaele, *Molecular Recognition and Self-Assembly Between Amines and Alcohols (Supraminols)*, **7**, 77.
- Sandre, Olivier, *Oblate-Prolate Transition of Ellipsoidal Magnetoliposomes: Experiments showing an Anisotropic Spontaneous Curvature*, **6**, 169.
- Scrimin, Paolo., *Control of Reactivity in Aggregates of Amphiphilic Molecules*, **3**, 101.
- Seifert, Udo, *Giant Vesicles: a Theoretical Perspective*, **6**, 71.
- Sekikawa, Ayako, *see* Yagi, Minoru, **8**, 205.
- Sessler, Jonathan, L., *see* Mody, Tarak, D., **4**, 245.
- Shimanouchi, Toshinori, *Study on Stress-mediated Behavior and Preparation of Giant Vesicles*, **6**, 369.

- Singh, Alok, *see* Guedeau-Boudeville, Marie-Alice, **6**, 341.
- Smithrud, D.B., *see* Benkovic, S.J., **1**, 149.
- Stark, Susaane, *see* Gangle, Susanne, **6**, 379.
- Suzuki, Akihiro, *see* Goto, Ayako, **6**, 261.
- Taglietti, Angelo, *see* Fabbrizzi, Luigi, **5**, 93.
- Tanaka, Hikaru, *see* Imai, Masanao, **6**, 361.
- Thilgen, C., *see* Echegoyen, L., **8**, 137.
- Thimmel, Johannes, *Swelling and Separation of DOPC Multilayer Systems*, **6**, 253.
- Thurner, Caroline, *see* Gangl, Susanne, **6**, 379.
- Toda, Fumio *see* Urbanczyk-Lipkowska, **8**, 1; *see also* **8**, 173.
- Umakoshi, Hiroshi, *see* Shimanouchi, Toshinori, **6**, 369.
- Urbanczyk-Lipkowska, Zofia, *Inclusion Complexation as a Tool in Resolution of Racemates and Separation of Isomers*, **8**, 1; *see also* *Selective Reactions in Inclusion Crystals*, **8**, 173.
- van Genderen, Marcel H.P., *Dendritic Architectures*, **4**, 47.
- van Koten, Gerard, *see* Meijer, Michel, D., **7**, 375.
- Vitkova, Victoria, *see* Bivas, Isak, **6**, 207
- Vlassov, V.V., *Oligonucleotides: Superspecific Ligands for Targeting Nucleic Acids and Proteins and Development of Molecular Devices*, **1**, 89.
- Walde, Peter, *see* Fischer, Aline, **6**, 37; *see also* Goto, Ayako, **6**, 261; *Enzymatic Reactions in Giant Vesicles*, **6**, 297.
- Ward, Michael, D., *see* Fagan, Paul J., **2**, 107.
- Waser, Jürg, *see* Kuhn, Hans, **1**, 247.
- Weissbuch, Isabelle, *see* Lahav, Meir, **1**, 173.
- Whitesell, James, K., *see* Davis, Raymond E., **2**, 63.
- Whitesides, George, M., *see* Issacs, Lyle, **4**, 1.
- Williams, Alan, F., *see* Provent, Christophe, **5**, 135.
- Winpenny, Richard E.P., *Design and Serendipity in the Synthesis of Polymetallic Complexes of the 3d-Metals*, **5**, 193.
- Winterhalter, Mathias, *see* Bivas, Isak, **6**, 207.
- Wintner, Edward A., *Recent Developments in the Design of Self-Replicating Systems*, **3**, 225.
- Wong, Man-Shing, *see* Davis, Raymond E., **2**, 63.
- Xia, Younan., *see* Issacs, Lyle **4**, 1.
- Xu, Liyu, *Micromanipulation of Tubular Vesicles*, **6**, 181.
- Yagi, Minoru, *Development of a New Biocide as an Inclusion Complex*, **8**, 205.
- Yamazaki, Koiji, *see* Goto, Ayako, **6**, 261.
- Yoon, Juyong, *see* Czarnik, Anthony, W., **4**, 177.
- Yoshikawa, Kenichi, *see* Nomura, Shinichirou, **6**, 313.
- Yoshioka, Hisashi, *see* Goto, Ayako, **6**, 261.
- Yoswathananont, Nungruethai, *Separation of Isomers and Enantiomers by Bile Acid Derivatives*, **8**, 87.
- Zhelev, Doncho, *see* Needham, David, **6**, 103.
- Zubieta, Jon, A., *see* Finn, Robert, C., **7**, 241.

Cumulative Title Index

This index comprises the titles and authors of all chapters appearing in Volumes 1–8 of **Perspectives in Supramolecular Chemistry**

- A Model of the Origin of Life and Perspectives in Supramolecular Engineering (*Kuhn and Waser*) **1**, 247.
- A Rational Approach for the Self-Assembly of Molecular Building Blocks in the Field of Molecule-Based Magnetism (*Melanie Pilkington and Silvio Decurtins*) **7**, 275.
- A Survey of Supramolecular Chemistry (1993–1994) (*Maitra*) **3**, 41.
- Bending Elasticity of Fluid Membranes (*Helfrich*) **6**, 51.
- Bistability in Iron (II) Spin-Crossover Systems: A Supramolecular Function (*Real*) **5**, 53.
- Cell Deformation Mechanisms Studied with Actin-containing Giant Vesicles, a Cell-mimicking System (*Miyata, Ohki, Marriott, Nishiyama, Akashi and Kinoshita*) **6**, 319.
- Changes in the Morphology of Giant Vesicles Under Various Physico-chemical Stresses (*Guedeau-Boudeville, Bernard, Bradley, Singh and Jullien*) **6**, 341.
- Chemosensors: Synthetic Receptors in Analytical Sensing Applications (*Czarnik and Yoon*) **4**, 177.
- Control of Fusion Between Giant Vesicles (*Hui, Perkins and Chandaroy*) **6**, 231.
- Control of Reactivity in Aggregates of Amphiphilic Molecules (*Scrimm*) **3**, 101.
- Crystal Engineering and Molecular Recognition – Twin Facets of Supramolecular Chemistry (*Desiraju and Krishnamoran Sharma*) **2**, 31.
- Dendritic Architectures (*van Genderen and Meijer*) **4**, 47.
- Design and Serendipity in the Synthesis of Polymetallic Complexes of the 3d-Metals (*Winpenny*) **5**, 193.
- Development of a New Biocide as an Inclusion Complex (*Yagi, Sekikawa and Aoki*) **8**, 205.

- Dynamic Aspects of Fatty Acid Vesicles: pH-induced Vesicle-Micelle Transition and Dilution-induced Formation of Giant Vesicles (*Goto, Suzuki, Yoshioka, Goto, Imae, Yamazaki and Walde*) **6**, 261.
- Emil Fischer's Lock-and-Key Hypothesis after 100 Years—Towards a Supracellular Chemistry (*Cramer*) **1**, 1.
- Enantiomer Ordering and Separation During Molecular Inclusion (*Bishop*) **8**, 33.
- Entrapment of Proteins in Soybean Phosphatidylcholine Vesicles (*Imai, Nagayama, Tanaka, Osaki and Doi*) **6**, 361.
- Enzymatic Reactions in Giant Vesicles (*Walde*) **6**, 297.
- Fluorescent Sensors for and with Transition Metals (*Fabrizzi, Licchelli, Pallavicini, Parodi and Taglietti*) **5**, 93.
- Formation of Giant Vesicles from Different Kinds of Lipids Using the Electroformation Method (*Fischer, Luisi, Oberholzer and Walde*) **6**, 37.
- Free Energy of a Fluctuating Vesicle. Influence of the Fluctuations on the Laplace Law (*Bivas*) **6**, 93.
- Giant Liposomes as Model Biomembranes for Roles of Lipids in Cellular Signalling (*Kimmunen, Holopainen and Angelova*) **6**, 273.
- Giant Phospholipid Vesicles Entrapping Giant DNA (*Nomura and Yoshikawa*) **6**, 313.
- Giant Vesicles: A Historical Introduction (*Lasic*) **6**, 11.
- Giant Vesicles: a Theoretical Perspective (*Seifert*) **6**, 71.
- Hydrogen Bonds in Inorganic Chemistry: Application to Crystal Design (*Lee Brammer*) **7**, 1.
- Inclusion Complexation as a Tool in Resolution of Racemates and Separation of Isomers (*Urbanczyk-Lipkowska and Toda*) **8**, 1.
- Ion Separations in Membrane and Solid Phase Extraction Systems (*Izatt, Bradshaw and Bruening*) **4**, 225.
- Layered Materials by Design: 2D Coordination Polymeric Networks Containing Large Cavities/Channels (*Kumar Biradha and Makoto Fujita*) **7**, 211.
- Ligand and Metal Control of Self-Assembly in Supramolecular Chemistry (*Saalfrank and Demleitner*) **5**, 1.
- Light-induced Shape Transitions of Giant Vesicles (*Petrov and Döbereiner*) **6**, 335.
- Liposome Electroformation (*Angelova*) **6**, 27.
- Lock-and-Key Processes at Crystalline Interfaces: Relevance to the Spontaneous Generation of Chirality (*Weissbuch, Popovitz-Biro, Leiserowitz and Lahav*) **1**, 173.
- Macrocycles and Antibodies as Catalysts (*Smithrud and Benkovic*) **1**, 149.
- Magnification of Shape Fluctuations of Active Giant Unilamellar Vesicles (*Manneville, Bassereau, Lévy and Prost*) **6**, 351.
- Membrane Properties of Archaeal Phospholipids: Effects of Macrocyclization (*Dannemuller, Nakatani, Ourisson, Arakawa, Eguchi, Kakinuma, Blanc and Albrecht*) **6**, 385.

- Membrane Roughness and Dispersive Phase as Effects of Higher-order Bending in Fluid Membranes (*Klöggen and Helfrich*) **6**, 243.
- Metallomesogens – Supramolecular Organization of Metal Complexes in Fluid Phase (*Collison and Bruce*) **5**, 285.
- Metal Template Control of Self-Assembly in Supramolecular Chemistry (*Fredericks and Hamilton*) **3**, 1.
- Microinjection of Macromolecules in Giant Vesicles Prepared by Electroformation (*Oberholzer and Fischer*) **6**, 285.
- Models of Hemoprotein Active Sites (*Momenteau*) **3**, 155.
- Molecular Engineering of Crystals by Electrostatic Templating (*Fagan and Ward*) **2**, 107.
- Molecular Organization on Giant Unilamellar Vesicles (*Gangl, Stark, Mayrhofer, Rünzler, Thurner, Lukas, Mayer and Köhler*) **6**, 379.
- Molecular Recognition and Self-Assembly Between Amines and Alcohols (Supraminols) (*Raffaele Saladino and Stephen Hanessian*) **7**, 77.
- Molecular Recognition in Biology: Models for Analysis of Protein–Ligand Interactions (*Lancet, Horovitz and Katchalski-Katzir*) **1**, 25.
- Molecular Recognition of Crystalline Dipeptides and Its Application to Separation (*Ogura and Akazome*) **8**, 61.
- Molecular Shape as a Design Criterion in Crystal Engineering (*Davis, Whitesell, Wong and Chang*) **2**, 63.
- Molecular Tectonics: Molecular Networks Based on Inclusion Processes (*Julien Martz, Ernest Graf, André De Cian and Mir Wais Hosseini*) **7**, 177.
- Motion of Particles Attached to Giant Vesicles: Falling Ball Viscosimetry and Elasticity Measurements on Lipid Membranes (*Dimova, Dietrich and Pouligny*) **6**, 221.
- New Biocatalysts via Chemical Modifications (*Bell and Hilvert*) **1**, 73.
- Observation of a Variety of Giant Vesicles under an Optical Microscope (*Akashi, Kinoshita, Miyata, and Itoh*) **6**, 45.
- Oligonucleotides: Superspecific Ligand for Targeting Nucleic Acids and Proteins and Development of Molecular Devices (*Vlassov*) **1**, 89.
- Perspectives in Supramolecular Chemistry – From the Lock-and-Key Image to the Information Paradigm (*Lehn*) **1**, 307.
- Physicochemical Studies of Separation of Isomers by Supramolecular Systems (*Nassimbeni*) **8**, 123.
- Polymorphism, Crystal Transformations and Gas–Solid Reactions (*Dario Braga and Fabrizia Grepioni*) **7**, 325.
- Porphyrin- and Expanded Porphyrin-Based Diagnostic and Therapeutic Agents (*Mody and Sessler*) **4**, 245.
- Recent Developments in the Design of Self-Replicating Systems (*Wintner and Rebek Jr*) **3**, 225.
- Regioselective Synthesis of Fullerene Derivatives and Separation of Isomers of the Higher Fullerenes (*Echegoyen, Herranz, Diederich, and Thilgen*) **8**, 137.
- Rotaxanes: From Random to Transition Metal-Templated Threading of Rings at the Molecular Level (*Chambron*) **5**, 225.
- Selective Ion Recognition with Durable Sensors (*Lugtenberg and Reinhoudt*) **4**, 193.

- Selective Reactions in Inclusion Crystals (*Urbanczyk-Lipkowska and Toda*) **8**, 173.
- Self-Assembling Systems on Scales from Nanometers to Millimeters: Design and Discovery (*Issacs, Chin, Bowden, Xia and Whitesides*) **4**, 1.
- Self-Assembly of Interlocked Structures with Cucurbituril Metal Ions and Metal Complexes (*Kim*) **5**, 371.
- Separation of Isomers and Enantiomers by Bile Acid Derivatives (*Yoswathananont, Miyata, Nakano and Sada*) **8**, 87.
- Solid–Gas Interactions Between Small Gaseous Molecules and Transition Metals in the Solid State. Toward Sensor Applications (*Michel D. Meijer, Robertus J. M. Klein Gebbink and Gerard van Koten*) **7**, 375.
- Study on Stress-mediated Behavior and Preparation of Giant Vesicles (*Shimanouchi, Umakoshi and Kuboi*) **6**, 369.
- Supramolecular Control of Reactivity in the Solid State Using Linear Templates (*MacGillivray*) **8**, 185.
- Supramolecular Structures with Macromolecules (*Beginn and Möller*) **4**, 89.
- Swelling and Separation of DOPC Multilayer Systems (*Thimmel, Klösger, Helfrich and Rapp*) **6**, 253.
- Synthetic Control of DNA Triplex Structure Through Chemical Modifications (*Ganesh, Kumar and Barawkar*) **3**, 263.
- The Chirality of Polynuclear Transition Metal Complexes (*Provent and Williams*) **5**, 135.
- The Construction of One-, Two- and Three-Dimensional Organic–Inorganic Hybrid Materials from Molecular Building Blocks (*Robert C. Finn, Eric Burkholder and Jon A. Zubieta*) **7**, 241.
- The Protein as a Supermolecule: The Architecture of a ($\beta\alpha$)₈ Barrel (*Glusker*) **2**, 235.
- Thoughts on Crystals as Supermolecules (*Dunitz*) **2**, 1.
- Very Large Supramolecular Capsules Based on Hydrogen Bonding (*Jerry L. Atwood, Leonard J. Barbour and Agoston Jerga*) **7**, 153.
- Why Giant Vesicles? (*Luisi*) **6**, 3.

Index

Note: Figures and Tables are indicated by *italic page numbers*

- acetone, inclusion compounds with bile acid derivatives, *93, 94, 96*
acetylacetone, keto–enol equilibrium, *26–27*
3-acetylcyclohex-2-enol, resolution of, *16*
acetylene alcohol compounds, inclusion complexation using, *4, 20, 21, 22*
achiral host molecules, *34*
achiral inclusion structures, formation of, *35–36*
acrylonitrile, inclusion compounds with bile acid derivatives, *99, 101*
alcohols
 inclusion compounds with bile acid derivatives, *90, 93*
 optical resolution of, *6–9, 114–115*
algicide, *205*
alkyl phenyl sulfoxides, chiral recognition of, *72–77*
alkylaryl sulfoxides, resolution of, *12, 63, 116*
4-allyl-1,2-diethoxybenzene, in inclusion compounds, *79, 79*
allylic alcohols, in inclusion compounds, *65–67, 81*
amides
 cyclic, resolution of, *116*
 inclusion complexation procedure using, *8*
amines, resolution of, *19*
aminobenzonitrile isomers, separation of, *22, 129*
3-amino-1-*tert*-butylazetid-2-one, resolution of, *18*
aminolysis, in inclusion compounds, *177–178*
anthracene, as template for synthesis of fullerenes, *139–140*
anthraquinone, photodimerization of, *190–191*
apocholic acid (ACA), *94*
 inclusion compounds, *89, 92, 94*
assemblers (in molecular manufacturing), *185, 186*
atom–atom potentials, lattice energies evaluated from, *128–129*
atropisomeric host molecules, *34, 36*
azoles, tautomers, stabilization of, *25–26*
azomethine ylides, addition to fullerenes, *144*

bactericide, *205*
barbituric acid-based template, *187, 188*
Beckmann rearrangement, in inclusion compounds, *176–177*

- benzenediol isomers, separation of, 23
- benzenes, monosubstituted, selective enclathration of cholic acid with, 109–110, 109, 111
- benzyl methyl sulfoxide, in inclusion compounds, 73, 75–77, 77
- N*-benzylcinchonidium chloride, resolution using, 9
- 4-benzylresorcinol, as template, 201
- bi-aryl compounds, resolution of, 9–10
- bile acid derivatives
- acid derivatives, 88
 - crystal structures, 90
 - inclusion compounds, 90, 92, 93, 94
 - alcohol derivatives, 88
 - crystal structures, 90
 - inclusion compounds, 90, 95
 - amide derivatives, 88
 - crystal structures, 90
 - inclusion compounds, 90, 93, 94–95, 115
 - assembly process, 91
 - bis(homobile) acids, 88
 - inclusion compounds, 97, 115
 - crystal structures, 90
 - 3-epible acids, 88
 - inclusion compounds, 97, 115
 - ester derivatives, 88
 - inclusion compounds, 96
 - hydrogen-bonding networks, 91
 - inclusion behavior, and modification of molecular structure, 90
 - inclusion mechanisms, 98–106
 - guest exchanges by recrystallization and intercalation, 106
 - packing coefficients of host cavities, 102–105
 - polymorphism, 98–102 - isomer separation by, 106–114
 - listed, 88
 - molecular structure, 89, 89
 - norobile acids, 88, 96
 - inclusion compounds, 96–97, 96
 - polymorphism, 98–102
 - salt derivatives, 97
 - inclusion compounds, 97
- binaphthol, inclusion compounds, 126–127
- binaphthyl compounds, resolution of, 9–10
- Bingel–Hirsch reaction, 137
- Bingel macrocyclizations, 141, 142, 148
- Bingel reaction, 138
- biocides, 205
- as inclusion complexes, 206–219
- biphenyl compounds, resolution of, 9–10
- 2,2'-biphenyldicarboxylic acid, 183
- (*S,S*)-(-)-1,6-bis(*o*-chlorophenyl)-1,6-diphenylhexa-2,4-diyne-1,6-diol, 174, 177, 180
- bis(homobile) acids, 88
- crystal structures, 97, 98
 - hydrogen bonding in, 98
 - inclusion compounds, 97, 98
- (*R,R*)-(-)-*trans*-bis(hydroxydiphenylmethyl)-1,4-dioxaspiro[4.5]decane, 5, 6
- (*R,R*)-(-)-*trans*-2,3-bis(hydroxydiphenylmethyl)-1,4-dioxaspiro[4.4]nonane, 9
- (*R,R*)-(-)-*trans*-4,5-bis(hydroxydiphenylmethyl)-2,2-dimethyl-1,3-dioxacyclopentane, 174
- 1,1-bis(4-hydroxyphenyl)cyclohexane, inclusion compounds, 126, 127, 131–132
- bis[2-(methylsulfinyl)benzyl] ether, 74
- bis(naphthol), 36
- 1,2-bis(4-pyridyl)ethane, in template-directed reactions, 198–199, 200
- 1,4-bis[2-(4-pyridyl)ethenyl]benzene, in template-directed reactions, 200–201
- trans*-1,2-bis(pyridyl)ethylenes, in template-directed reactions, 191–194, 196–198
- 1,8-bis(resorcinol)anthracene, as template, 190–191
- capillary electrophoresis, 3
- cavities
- attachment of chiral conformers in, 116
 - in bile acid inclusion compounds, 111, 114
 - in dipeptide inclusion compounds, 70, 71, 77, 81

- packing coefficients, 102–103
 - in cholic acid inclusion compounds with aliphatic alcohol guests, 105
 - in cholic acid inclusion compounds with aromatic guests, 103–105
- centrosymmetric enantiomer ordering, 37–43
- chalcone, photodimerization of, 182–183
- channel compounds, 6, 89
 - see also* tubulate inclusion compounds
- chenodeoxycholamide (CDCAM), 88
 - hydrate, 90, 95
- chenodeoxycholic acid (CDCA), 88, 90
- chiral recognition in, 118
 - hydrogen bonding in, 91
 - inclusion compounds, 89, 93, 94
- chiral chromatography, 3
- chiral crystal lattice packing, 37
- chiral discrimination, solvent-dependent, 13, 15–17
- chiral host molecules
 - racemic mixtures, 36–56
 - formation of unresolved structures, 37–47
 - self-resolution of enantiomeric crystals containing both enantiomeric molecules, 53–56
 - self-resolution of enantiomeric molecules, 47–52
- chiral inclusion structures, formation of, 34–35
- chiral recognition
 - in bile acid inclusion compounds, 116–119
 - dynamic, in bile acid inclusion compounds, 116
 - factors affecting, 116
 - four-location model, 117, 119
 - α -hydroxy esters, 70–72
 - steric visualization of inclusion spaces, 116
 - sulfoxides, 72–77
 - three-attachment model, 117, 118
- chiral resolution, 130, 131
- chiral steroidal molecules, hierarchical structures generated by, 117–119
- chirality
 - in biological systems, 1
 - of fullerene derivatives, 147
 - meaning of term, 2
- 5-chloro-2-methyl-4-isothiazoline-3-one, 205
 - inclusion complex with 2,4-di-*tert*-butylphenol, 207, 208
- inclusion complex with 4,4'-ethylidenebisphenol, 207, 209
 - crystal structure, 210
 - manufacture of, 213, 214
 - release profile in water, 213
 - thermal stability, 211
 - see also* FIBCID-K58
- inclusion complex with gallic acid methyl ester, 207, 208–209, 209, 211
- inclusion complexes, 206–219
 - with aliphatic dicarboxylic acid compounds, 210–211, 210
 - with benzene polycarboxylic acid compounds, 208, 210, 212
 - with bisphenol host compounds, 207, 209, 210
 - experimental methods for characterization, 216–219
 - with hydroxybenzoic acid compounds, 208, 210
 - with phenol host compounds, 207, 208–209, 209
 - physicochemical data, 217
 - preparation method, 216
 - release profiles in water, 211–212, 213
 - thermal stability, 211, 211–212
 - in industrial product, 206
- 2-chlorooctane, resolution of, 35
- (*R*)-2-chlorophenyl methyl sulfoxide, in inclusion compounds, 73, 74, 76
- 4-chlorostilbazole, template-directed reactions, 195–196
- cholamide (CAM), 88
 - hydrogen bonding in, 91
 - inclusion compounds, 90, 93, 95, 102, 102
 - optical resolution of alcohols by, 115

- cholesterol, 88
- cholic acid (CA), 88
- enantioresolution by, 116
 - hydrogen bonding in, 91
 - inclusion compounds, 89, 90, 92, 93, 94, 98–101, 102
 - competitive recrystallization of, 106–109
 - dynamic chiral recognition in, 116
 - guest-dependent polymorphism, 98–100
 - packing coefficients of cavities, 103–105
 - selective enclathration mechanism, 108–113
- cinnamic acid, photodimerization of, 190
- circular dichroism spectra
- bile acid inclusion compounds, 116
 - fullerene derivatives, 144, 162, 163
- competition experiments, 125–127
- mixed-guests systems, 131–134
- competitive recrystallization
- cholic acid inclusion compounds, 106–109
 - separation factor, 107
 - listed for various cholic acid inclusion compounds, 108
- conglomerate (of enantiomers), 2, 37
- controlled potential electrolysis (CPE)
- fullerene bis-adducts, 138, 161
 - and retro-Bingel reaction, 157, 158
- coumarin, photodimerization of, 180–182
- resol isomers, separation of, 24
- resol ethers, 148
- fullerene derivatives, 148–156
- crystal engineering, absence of theory, 61
- crystal structure polymorphism, 100
- cyclic voltammetry (CV), fullerene derivatives, 138, 150, 161, 163–165
- [2 + 2] cycloaddition reaction, template-directed solid-state, 190
- cyclo-[3]-octylmalonates, fullerene derivatives synthesized using, 147–148
- cyclophane-type fullerene-dibenzo[18] crown-6 conjugates, 148, 149
- cyclophanes, template-directed synthesis of, 200–201
- cyclotrimeratrylene (CTV) tris-adducts of fullerene, 146
- dehydrocholic acid, optical resolution by, 116
- deoxycholamide (DCAM), 88
- inclusion compounds, 90, 91, 93, 94–95
- deoxycholic acid (DCA), 88
- chiral recognition in, 118
 - hydrogen bonding in, 91
 - inclusion compounds, 88–89, 90, 92
 - optical resolution by, 115
 - selective enclathration by, 113, 114
- deoxyribonucleic acid (DNA), as linear template, 188, 189
- Dianin's compound, 41
- inclusion compounds, 41–42
- diastereo-isomeric crystallization, 3
- 2,4-di-*tert*-butylphenol, inclusion compound with Cl-MIT biocide, 207, 208
- Diels–Alder additions, fullerene derivatives synthesized by, 140, 141
- 1,2-diethoxybenzene, 79, 79
- differential scanning calorimetry, 127–128
- dihydrobenzoic acids, inclusion compounds with Cl-MIT biocide, 208, 210, 212, 213
- (*S*)-dihydro-3-hydroxy-4,4-dimethyl-2(3H)-furanone, in inclusion compounds, 71
- trans*-9,10-dihydroxy-9,10-bis(*p*-*tert*-butylphenyl)-9,10-dihydroanthracene, inclusion compounds, 132
- 3 α ,24-dihydroxy-5 β -cholane (LCA diol), 88
- inclusion compounds, 90, 95
- 2,2'-dihydroxy-1,1'-dinaphthyl inclusion complexes with, 23–24, 26
- resolution of, 8–9
- 1,3-diketones, keto–enol equilibrium, 26–27
- 1,2-dimethoxybenzene, in inclusion compounds, 78, 79, 79

- 1,2-dimethoxyethane, in inclusion compounds, 67, 68, 78, 79, 80
- 5,6-dimethoxyindane, in inclusion compounds, 79, 79
- 3,5-dimethylcyclohexanone isomers, separation of, 22
- dimethylformamide/dimethylsulfoxide competition experiment, 132, 133
- 1,4-diol-containing dimeric hosts, optical resolution using, 12–17
- dipeptides, 62–63
molecular recognition of, 63–69
- diphenylhydroxymethyl grouping, steric hindrance, 5
- diphthalimide, resolution of, 18–19
- diquinoline compounds, lattice inclusion hosts formed by, 37–41
- dynamic chiral recognition, in bile acid inclusion compounds, 116
- edge-to-face (EF) interactions, 40, 63, 78
- ellipsoidal clathrate structure, 44–45, 46, 57–58
- enantiomeric crystals, 37
self-resolution of, 53–56
- enantiomeric resolution
by inclusion complexation, 6–20, 62–63, 114–116, 130
see also optical resolution
- enantiomeric self-resolution, on crystallisation, 47–50
- enantiomer(s)
meaning of term, 2
separation of *see* chiral recognition; optical resolution
- enantiopure host molecules, 56–58
- enantiopure materials, demand for, 1
- 3-epibile acids, 88
crystal structures, 98
hydrogen bonding in, 98
inclusion compounds, 97, 98
optical resolution of alcohols by, 115
- epoxides, resolution of, 8–9, 116
- ethers, in inclusion compounds, 64–65, 65, 77–80
- 1-ethoxy-2-methoxybenzene, in inclusion compounds, 79, 79
- ethylene glycol
inclusion compounds with bile acid derivatives, 93
see also poly(ethylene glycol)s
- (S)-ethyl lactate, in inclusion compounds, 71
- 4,4'-ethylidenebisphenol, inclusion compound with Cl-MIT biocide, 207, 209
- 4-ethylresorcinol, template-directed reactions, 196
- FIBCID-K58
manufacture of, 213, 214
skin irritation data, 213, 215
see also 5-chloro-2-methyl-4-isothiazoline-3-one, inclusion complex with 4,4'-ethylidenebisphenol
- FIBCID-KF
manufacture of, 213, 214
microbial activities, 215, 216
as paper coating additive, 215
- fullerene derivatives
bis-adducts, 138, 139, 141–145
dimers, 160
hexakis-adducts, 139, 140, 149, 151
regioselective synthesis of, 139–148
anthracene used as template, 139–140
bis-functionalization methodology, 144–145
by tether-directed remote functionalization, 140–144
tris-adduct formation, 145–148
retro-cyclopropanation reactions, 156–161
tetrakis-adducts, 139
tris-adducts, 141, 145–148
- fullerene-cyclotrimeratrylene tris-adducts, 146
- fullerene-dibenzo[18]crown-6 conjugates, 149
cyclic voltammetry, 150, 152, 153
reduction processes, 152–153
synthesis of, 148

- fullerenes, 137
 C₆₀, regioselective synthesis of, 139–148
 C₇₆ enantiomers, preparation of, 162
 C₇₈, isolation of, 162–165
 C₈₄, resolution of, 165–167
 fullerenocrown ethers, 148–156
 C₆₀-based systems, 148–153
 C₇₀-based systems, 153–156
 C₇₀ bis-crown ether conjugates, 155–156, 157
 fulleropyrrolidines, 144, 145
 fungicide, 205
- Gabriel synthesis, reaction intermediates, optical resolution of, 17–19
 gallic acid methyl ester, inclusion compound with CI-MIT biocide, 207, 208–209, 209, 211, 213
 gossypol, 34, 34, 36
- helical tubuland diols, 45, 47, 49
 hepta(ethylene glycol) dimethyl ether, in inclusion compound, 81
 hydrazine–hydroquinone inclusion compound, 177–178
 hydrogen-bonding networks, bile acid derivatives, 91
 α -hydroxy esters, chiral recognition of, 70–72
 4-hydroxycyclopent-2-enone, resolution of, 15
- imidazole tautomers, 25–26
 imides, resolution of, 17–19
 inclusion complexation
 of biocide (CI-MIT), 206–211
 chiral recognition mechanisms, 5, 15
 factors affecting, 4–5
 isomers separated by, 20–24
 molecular basis, 4–6
 resolution of enantiomers by, 6–20, 70–77
 tautomeric forms stabilized by, 25–27
see also lattice inclusion compounds
- inclusion crystals
 enantioselective photochemical reactions, 178–183
 enantioselective thermochemical reactions, 174–178
 inclusion phenomena, 3–4
 factors affecting, 4
 inclusion spaces, steric visualization of, 116
 intercalation, bile acid derivative inclusion compounds, 106
 isomers
 separation of, 123
 by bile acid derivative inclusion compounds, 106–114
 by selective inclusion, 20–24, 123–125
 1-isopropoxy-2-methoxybenzene, in inclusion compounds, 79, 79
 isopropyl phenyl sulfoxide, in inclusion compounds, 63, 64, 72, 73, 74
- KATHON WT (slime-controlling agent), 206
 compared with FIBICIDE-K58/
 FIBICIDE-KF, 213, 215, 215, 216
see also 5-chloro-2-methyl-4-isothiazoline-3-one
 keto–enol tautomerism, 26–27
 ketones
 cyclic, resolution of, 116
 reduction of, in inclusion compounds, 174
- key-and-lock mechanism (molecular recognition), 102–103
 β -lactam formation reactions, 178–180
 lactones, resolution of, 116
 lattice energies, as measure of thermal stability, 127–130
 lattice inclusion compounds
 achiral structures, 35–36
 atropisomeric hosts, 36
 chiral structures, 34–35
 packing coefficients of cavities, 103
see also inclusion complexation
- linear templates
 in biology, 188

- in chemistry, 186–188
 - examples, 187
 - see also template. . .
- lithocholamide (LCAM), 88
 - hydrogen bonding in, 91
 - inclusion compounds, 90, 95, 117
 - optical resolution of alcohols by, 115
- lithocholic acid (LCA), 88, 89, 90, 91, 94
- lutidines, in inclusion compounds, 21, 126, 129

- McCabe–Thiele plots, 130, 131
- methacrylonitrile, inclusion compounds
 - with bile acid derivatives, 101
- methallyl alcohol, in inclusion compounds, 66, 71
- methanol, in inclusion compounds, 66
- 5-methoxyresorcinol, as template, 200–201
- methylbenzaldehyde isomers, separation of, 20–21
- methyl chenodeoxycholate (MCDC), 88, 96
- methyl cholate (MC), 88
 - inclusion compounds, 96
- methyl deoxycholate (MDC), 88
 - inclusion compounds, 96
- (*S*)-methyl α -hydroxy- β,β -dimethylbutyrate, in inclusion compounds, 72
- (*S*)-methyl α -hydroxyhexanoate, in inclusion compounds, 71
- (*S*)-methyl α -hydroxy- β -methylbutyrate, in inclusion compounds, 72
- (*S*)-methyl α -hydroxy- γ -methylpentanoate, in inclusion compounds, 71
- (*S*)-methyl α -hydroxypentanoate, in inclusion compounds, 71
- methylimidazole tautomers, 26
- (*S*)-methyl lactate, in inclusion compounds, 70–71, 70
- methyl lithocholate (LMC), 88, 96
- methyl methacrylate, selective enclathration of cholic acid with, 109, 111, 113
- methyl phenyl sulfoxide, in inclusion compounds, 73, 74, 75
- 2-methylpiperidine, resolution of, 15
- methylpyrazole tautomers, 25
- Michael addition reactions, in inclusion compounds, 174–175, 176
- microbial activity, minimum inhibitory concentrations
 - experimental method, 218–219
 - FIBCID-K58 compared with KATHON WT biocide, 215, 216
- mixtures of resolving agents, optical resolution using, 19–20
- molecular manufacturing, 185, 186
 - see also templates
- molecular pens, 43, 44, 53, 54, 55

- 1,8-naphthalenedicarboxylic acid, as template, 194, 196–197, 200
- (*R*)-(1-naphthyl)glycyl-(*R*)-phenylglycine, 62
 - inclusion structures formed by, 64–72
 - with ethers, 65, 68, 77–80
 - with α -hydroxy esters, 70–72
 - with poly(ethylene glycol) dimethyl ethers, 80–83
- natural compounds
 - separation from natural sources, 21
 - as templates, 188, 189
 - see also gossypol
- norbile acids, 88, 96
 - hydrogen bonding in, 96
 - inclusion compounds, 93, 96–97, 96
 - optical resolution of alcohols by, 115
- nordeoxycholic acid (NDCA), 88
 - inclusion compounds, 93, 96, 97, 117

- offset face-to-face (OFF) interactions, 40, 43
- omeprazole, resolution of, 10
- optical activity, meaning of term, 2
- optical resolution, 130
 - of alcohols, 6–8, 114–115
 - of alkylaryl sulfoxides, 12, 63, 116
 - of bi-aryl compounds, 9–10
 - by bile acid derivatives, 114–116
 - of cyclic ketones, 116
 - by 1,4-diol-containing dimeric hosts, 12–17

- optical resolution (*continued*)
 of epoxides, 8–9, 116
 of [C84]fullerene isomers, 165–167
 of lactones, 116
 meaning of term, 2
 by mixtures of resolving agents, 19–20
 of P-chiral phosphorus compounds,
 10–12
 by peptides, 62
 of reaction intermediates, 17–19
 by retro-cyclopropanation reaction,
 165–167
 α -oxamides, photocyclization of, 178–179
- [2.2]paracyclophane, template-directed
 synthesis of, 200–201
- penannular inclusion compounds, 43, 53
- 1-phenylethanol, resolution of, 7
- (*R*)-phenylglycyl-(*R*)-phenylglycine, 62
 inclusion structures formed by, 62, 64,
 75–77
 with ethers, 78–80
 with sulfoxides, 63–64, 72–77
- phosphine oxides, resolution of, 10, 11, 12
- phosphorus compounds, P-chiral,
 resolution of, 10–12
- photochemical reactions, in inclusion
 crystals, 178–183
- photocyclization reactions, 178–180
 oxamides, 178–179
 2-pyridones, 179–180
- photodimerization reactions, 180–183
 coumarin and thiocoumarin, 180–182
 host-catalyzed, 182–183
- π -halogen dimer (PHD) interaction, 38,
 39, 41
- ‘pick-and-place’ technology, 185, 186
 in Nature, 188
- poly(ethylene glycol) dimethyl ethers, in
 inclusion compounds, 80–83
- poly(ethylene glycols), in inclusion
 compounds, 81
- polymers, tailor-made, 3
- polymorphism
 bile acid derivatives, 98–102
 guest-dependent, 98–100
 with identical guests, 100–102
- porphyrin derivatives, fullerene
 derivatives, 142–143
- powdered host compounds, inclusion
 complexation using, 6–9, 12, 23,
 182–183
- proteins, dipeptides in, 62–63
- pseudopolymorphism, 101–102
- 2-pyridones
 photocyclization of, 179–180
 photodimerization of, 183
- pyromellitic acid, inclusion compound
 with Cl-MIT biocide, 208, 210, 212,
 213
- racemate(s)
 meaning of term, 2
 resolution of, by inclusion
 complexation, 5–20
- reaction intermediates, optical resolution
 of, by inclusion complexation,
 17–19
- recrystallization
 bile acid derivative inclusion
 compounds, 106
 competitive, cholic acid inclusion
 compounds, 106–109
- resolution *see* optical resolution
- resorcinol and derivatives, as templates,
 190–193, 195–196, 197–199,
 200–201
- retro-Bingel reaction, 138
- retro-cyclopropanation reactions
 fullerene derivatives, 138–139,
 156–161
 isolation of higher fullerenes using,
 162–165
 optical resolution of higher fullerenes
 using, 165–167
 synthesis of higher fullerenes by, 162
- saccharides, as templates, 145
- selective enclathration
 of cholic acid
 with monosubstituted benzenes,
 109–110
 with xylene isomers, 110–112

- selective inclusion, separation of isomers
by, 20–24, 123–125
- selectivity profiles, 126, 127
- selenoxides, alkylaryl-substituted,
resolution of, 12
- self-resolution
enantiomeric crystals, 53–56
enantiomeric molecules, 47–52
- sheet structures, 61–62
‘antiparallel’ mode, 65–67, 69
of bile acid derivative inclusion
compounds, 91, 92
of dipeptide inclusion compounds,
62, 64, 65, 66, 67, 68,
70, 72
‘extended antiparallel’ mode, 67,
69
‘parallel’ mode, 65, 67, 69
structural variations, 69, 92
‘water-buried’ sheet, 67, 69
- single-crystal-to-single-crystal
photodimerization, 180–182
- skin irritation tests
Draize method scoring, 218
experimental method, 217–218
FIBCID-K58 compared with
KANTHON WT biocide, 215,
218
- slime formation, 205
prevention of, 205–206
- solvent-dependent chiral discrimination,
13, 15–17, 51–52
- spiromethanofullerenes, electroreduced,
159–160, 160
- staircase structures, 37–38, 38, 39
- steric visualization of inclusion spaces,
116
- stilbazole derivatives, template-directed
reactions, 195–196
- trans*-stilbenes, template-directed
reactions, 191–194, 196–198
- sulfoxides
alkylaryl-substituted
chiral recognition of, 72–77
resolution of, 12, 63, 116
see also isopropyl phenyl
sulfoxide
- taddols, 5
- tartaric acid derivatives, chiral host
compounds prepared from, 5, 7, 8,
19
- tautomeric forms, stabilization of, by
inclusion complexation, 25–27
- template-activated synthesis, of fullerene
derivatives, 139–140
- template-directed solid-state organic
synthesis, 188–201
[2 + 2] cycloaddition reaction, 190
modification of reactants, 195–199
functional groups, 198–199
number of hydrogen-bond acceptor
sites, 195–196
position of hydrogen-bond acceptor
site, 196–198
modification of template, 194
resorcinol as linear template, 192–
193
role of solid state, 193
selection of template and reactants,
190–192
target-oriented synthesis, 199–201
- template(s)
anthracene as, 139–140
barbituric acid-based, 187, 188
DNA as, 188, 189
1,8-naphthalenedicarboxylic acid as,
194, 196–197
resorcinol and derivatives as, 190–
193, 195–196, 197–199, 200–
201
saccharides as, 145
- tether-directed remote functionalization
C₇₀-fullerocrown ethers synthesized by,
140–144
fullerene derivatives synthesized by,
140–144
- tetrahydrofuran (THF), in inclusion
compounds, 64–65, 65, 77–78
- 3 α ,7 α ,12 α ,24-tetrahydroxy-5 β -cholane
(CAetraol), 88, 90
- 1,1,6,6-tetraphenylhexa-2,4-diyne-1,6-diol,
inclusion compounds, 4, 20, 21, 22,
129, 182–183
- thermal gravimetry, 127–128

- thermal stability
 Cl-MIT (biocide) inclusion compounds, 211–212
 experimental method, 216–217
- thermochemical reactions, in inclusion crystals, 174–178
- thiocoumarin, photodimerization of, 180–182
- thiourea, 34
 chiral inclusion structures based on, 35–36
- topochemical postulates, 190, 191, 201
- transesterification, fullerenocrown ethers synthesized by, 148, 150
- 1,2,3-triazole tautomers, 25
- 1,2,4-triazole tautomers, 25
- 3 α ,7 α ,24-trihydroxy-5 β -cholane (CDCAtriol), 88
 inclusion compounds, 90, 95
- 3 α ,12 α ,24-trihydroxy-5 β -cholane (DCAtriol), 88
 inclusion compounds, 90, 95
- trimellitic acid, inclusion compound with Cl-MIT biocide, 208, 210, 212, 213
- tris[bis(ethoxycarbonyl)methano][C60] fullerene, 146
- truxinic acid, 190
- tubulate inclusion compounds, 34–36, 49–50, 49, 51, 56, 57, 58
 see also channel compounds
- urea, 34
 chiral inclusion structures based on, 35
- urea–poly(tetrahydrofuran) inclusion compounds, 83
- Wittig reactions, in inclusion compounds, 175, 176
- xylene isomers
 boiling points, 123
 selective enclathration of cholic acid with, 109, 110–112

With kind thanks to Paul Nash for creation of this index.